Aston University

Some parts of this thesis may have been removed for copyright restrictions.

If you have discovered material in AURA which is unlawful e.g. breaches copyright, (either yours or that of a third party) or any other law, including but not limited to those relating to patent, trademark, confidentiality, data protection, obscenity, defamation, libel, then please read our Takedown Policy and contact the service immediately

CHLORIDE RESISTANCE AND DURABILITY OF CEMENT PASTE AND CONCRETE CONTAINING METAKAOLIN

GAVIN ALEX CHADBOURN

Doctor of Philosophy

THE UNIVERSITY OF ASTON IN BIRMINGHAM

July 1997

This copy of the thesis has been supplied on condition that anyone who consults it is understood to recognise that its copyright rests with its author and that no quotation from the thesis and no information derived from it may be published without proper acknowledgement.

THE UNIVERSITY OF ASTON IN BIRMINGHAM

Chloride Resistance and Durability of Cement Paste and Concrete Containing Metakaolin.

Gavin Alex CHADBOURN **Doctor of Philosophy 1997**

SYNOPSIS

Metakaolin (MK), a calcined clay, was included as a partial cement replacement material, at up to 20% by weight of binder, in cement pastes and concrete, and its influence on the resistance to chloride ingress investigated. Reductions in effective chloride diffusion coefficients through hardened cement paste were obtained for binary blends and by combining OPC, MK and a second cement replacement material of pulverised fuel ash or ground granulated blast furnace slag. Steady state oxygen diffusion measurements through hardened cement pastes measured using an electrochemical cell showed that the interaction between charged species and the pore surfaces is a major factor in determining chloride diffusion rate.

Rheology of the binder, particularly at high MK replacement levels, was found to have a dramatic influence on the diffusion performance of cement pastes. It was concluded that plasticising admixtures are essential for adequate dispersion of MK in cement pastes.

Chloride concentration profile analysis of the concrete cylinders, exposed to sodium chloride solution for one year, was employed to obtain apparent chloride diffusion coefficients for concrete specimens. MK was found to reduce the depth of chloride penetration into concrete when compared with that of unblended mixes.

Corrosion rate and corrosion potential measurements were taken on steel bars embedded in concrete exposed to a saline environment under conditions of cyclic wetting and drying. The initiation time for corrosion was found to be significantly longer for MK blended mixes than for plain OPC systems.

The aggregate-paste interfacial zone of MK blended systems was investigated by steady state diffusion of chloride ions through mortar containing glass beads as model aggregate. For the model aggregate specimens tested the work confirmed the hypothesis that properties of the bulk paste are the controlling factors in ionic diffusion through mortar.

KEY WORDS: Blended Pastes, Oxygen Diffusion, Interfacial Zone, Rheology, Reinforcement Corrosion.

To my Family

ACKNOWLEDGEMENTS

The author is deeply indebted to Professor C L Page under whose supervision this research project was conducted, and whose knowledge, expertise, guidance and support are greatly appreciated.

Thanks are also due to ECC International who provided funding through a case award for this project, and in particular Dr Tom Jones, Jacek Kostuch and Tony Asbridge, who made me welcome during my placement in Cornwall.

The technical staff in the Civil Engineering Department are thanked, in particular Messrs C J Thompson, P Green and W Curtis for their assistance with laboratory work.

I wish to thank my friends and colleagues G Abdelaziz, M Ismail, Drs P Edmunds, D Greene, G Sergi, R Walker and R Sibbick, for their stimulating discussions, humour, motivation and assistance during the course of this project.

I am particularly grateful to my friends and colleagues Drs G Seneviratne and V T Ngala for their effort and patience in reading through this thesis.

Last but not least the author wishes to express his appreciation to his family who have supported and encouraged him in all his endeavours.

LIST OF CONTENTS

LIST OF TABLES

LIST OF FIGURES

CHAPTER ONE

1. INTRODUCTION

1.1. FIELD OF INVESTIGATION

The use of cementitious materials for construction can be traced back to ancient times, and has gradually developed over the centuries. There is evidence that the Egyptians used a lime based cement in the construction of the Great Pyramid at Giza in 2500 BC (Stanley 1979). However it was the Greeks and Romans who have been credited with developing concrete. Calcined lime was mixed with water and crushed rock, which reacted with carbon dioxide in the atmosphere to form a concrete. A disadvantage of lime concretes is that they do not harden under water.

Almost by accident the Romans discovered that by mixing lime concrete with a volcanic ash, from a source near the village of Pozzuoli in Italy, a stronger material that hardens under water can be produced (Neville 1995). Similar properties to those of pozzolanic cements, as they became known, could be obtained by adding finely ground burnt clay tiles which contain reactive silica and alumina to lime. Concrete structures such as the Pantheon in Rome built by the Romans 2000 years ago, and still standing, are a testament to the durability of concrete.

Cement as we recognise it today was invented by Joseph Aspdin in 1824 who heated a mixture of finely divided clay and limestone until carbon dioxide was driven off, although the temperature was not high enough to cause clinkering which is necessary for the formation of strongly cementitious compounds (Neville 1995). Portland cement, so named due to its resemblance in colour to Portland stone, has subsequently become the most widely used construction material in the world.

Modern cement is manufactured from limestone or chalk and, silica and alumina containing materials, such as shale and clay. The raw materials are ground and mixed together and heated in a rotary kiln at 1400^{o}C such that they fuse and form a clinker. The resultant Portland cement essentially consists of calcium silicates and aluminates which are finely ground together with gypsum, which is added to prevent flash set on hydration. Cement is the binding component of concrete, which when mixed with water, sand and coarse aggregate reacts to form a hardened mass.

In the main concrete is durable and its exceptional compressive load bearing capacity, along with the relative abundance of the raw materials necessary for its manufacture, has led to its position as the pre-eminent construction material. However concrete is comparatively brittle

in tension necessitating the inclusion of steel reinforcing bars to carry tensile loads. The first person accredited with reinforcing concrete with steel in 1854 was a Newcastle builder William Wilkinson (Stanley 1979). However the presence of steel in concrete can lead to problems with durability.

1.2 DEGRADATION OF CONCRETE STRUCTURES

In the early 1970's it became obvious that many reinforced concrete structures, particularly highway bridges, were deteriorating due to the corrosion of embedded steel, and would thus not last their intended service lives. The scale of the problem was highlighted by several reports, in particular the Federal Highway Administration disclosed that one in six bridges in the US were deficient (Engineering News Record 1977).

Generally concrete offers good physical and chemical protection to embedded steel. The highly alkaline environment of the hydrated cement matrix induces the formation of a thin continuous passive ferric oxide film on the surface of the steel and ensures its electrochemical stability. A layer of calcium hydroxide is formed on the surface of steel cast in OPC paste which may act as a physical barrier to chloride penetration and as a hydroxyl ion replenisher at potential corrosion sites (Page 1975). The amount of calcium hydroxide in the cement matrix may also have a direct influence on the ability of embedded steel to resist corrosion. Pozzolanic additives react with calcium hydroxide, removing the ability of the cement matrix to buffer the alkali concentration of the pore fluid and possibly reducing the ability of the concrete to repair corrosion sites.

Corrosion of steel embedded in concrete can occur in two ways. Loss of alkalinity in the pore solution, which causes a decrease in the stability of the passive film, and subsequent depassivation of the steel, or attack by aggressive ions which causes localised disruption of the passive film and pitting corrosion. The expansive nature of the corrosion products leads to cracking of the concrete cover, rust staining and subsequent spalling. This exposes more steel to the environment further promoting the corrosion process. In addition the loss of load bearing cross sectional area will ultimately have a catastrophic effect on the structure (Woodward and Williams 1988). By far the most common cause of corrosion is attack of the steel by chloride ions.

Wallbank (1989) highlighted that nearly one third of highway bridges in the UK are in need of repair, the main cause of problems being chloride attack. The cost of repairs was estimated at £620m over 10 years. Realisation that corrosion of structures was a consequence of chloride ions led to chloride containing admixtures, such as calcium chloride accelerating compounds, being banned in 1977. However sodium chloride in the

form of rock salt is still widely used as a deicer on highways throughout the world (New Civil Engineer 1991).

In addition to problems associated with the highway network construction is taking place in ever more severe environments. Structures such as oil rigs in the North Sea, and the Dartford crossing founded in estuarine conditions are exposed to high levels of chloride ions so perhaps the most aggressive environment in terms of chloride attack is the marine splash zone (Nagano and Naito 1985, Bamforth 1994, 1996). Structures sited in these highly aggressive environments are not as easily repaired or protected from corrosion as a highway structure, so the concrete employed must be capable of preventing corrosion by limiting chloride ingress throughout the life of the structure.

1.3 PREVENTION OF PREMATURE DETERIORATION

A number of solutions to the problem of embedded steel corrosion are in use today. These range from electrochemical techniques such as cathodic protection, desalination and realkalization to the application of an extra physical barrier by impregnating the concrete with polymers and surface coatings. Galvanised or epoxy coated reinforcing steel, supercover concrete and inhibitors have been used to extend the service life of structures although each method has its drawbacks not least increased cost making most of these protection methods unattractive. Ideally the solution would be to maximise the protective properties of the cement, to produce a concrete that it is capable of resisting the ingress of deleterious agents without the need for maintenance over the service life of the structure.

It is generally agreed that the inclusion of mineral additives such as Pulverised Fuel Ash (PFA), Blast Furnace Slag (BFS) and Silica Fume (SF) can lead to improvements in resistance to chloride penetration associated with changes in the pore structure of the hardened cement paste (Gjørv and Vennesland 1979, Page et al 1981, Li and Roy 1986). However there are drawbacks associated with the use of these blending materials.

BFS, PFA and SF are industrial waste-products and so their composition and quality are not controlled during production. PFA is produced from the burnt residue of coal used in power stations. Consequently its carbon and sulphate content varies according to the source of the coal, degree to which it was burnt, and type of power station. This is particularly noticeable in the colour variation between PFA batches which can vary from pale brown to dark grey, depending on carbon content. A high proportion of coarse PFA particles and carbon content have a detrimental effect on pozzolanic reactivity and subsequent strength and durability. Similarly blast furnace slag (BFS), the by-product of iron manufacture, suffers from compositional variation which can have detrimental effects on the properties of concrete. At

the very least differences in composition will alter aesthetics of the concrete as well as strength gain and durability.

Metakaolin (MK) is a relatively new mineral additive in modern concrete, although burnt clays have been utilised since ancient times. The use of calcined clays as pozzolanic cements can be traced back to ancient Roman times. Even today their use continues in countries such as India where they are known as Surkhi and Egypt as Homra (Cook 1986). These materials are usually made by pulverizing reject fired clay bricks and tiles, resulting in a pozzolan with extremely variable reactivity.

1.4 METAKAOLIN AS A PARTIAL CEMENT REPLACEMENT

Metakaolin is not a waste-product, but is specifically manufactured for use in concrete, and as such is much purer than other cement replacements. Consequently the composition of MK is carefully controlled to produce a product with consistent colour, fineness and reactivity characteristics.

Metakaolin is manufactured from china clay containing a high percentage of kaolin, and very little impurity. By calcining the clay at a temperature of 800^{o}C to drive off the water of crystallisation a non-crystalline material made up of approximately 60% alumina and 40% silica is formed. The amorphous alumina and silica readily react with calcium hydroxide at room temperatures to produce cementing products. As metakaolin contains very little calcium oxide it has no hydraulic properties on its own.

Work by Murat (1983a,b) and Murat et al (1985a,b,c) has shown that metakaolin reacts with calcium hydroxide to produce CSH gel and other hydrates with cementing qualities. Their work has tended to concentrate on the use of metakaolins manufactured from clays of low to medium kaolin quality and content, with the aim of producing low cost concrete in third world countries. These concretes contain no OPC and are generally of low strength due to the low quality of the feed clays. However this work highlighted the importance of kaolin content of the feed clay on strength and presumably durability of concrete. Walters and Jones (1991) found that if the feed clay contained more than 90% wt kaolin up to 10% MK could be substituted for OPC in concrete without reducing 28 day strength.

In contrast to PFA, BFS and SF concrete there is little published literature on the use of MK concrete in structural or civil engineering applications. One of the first uses of a MK concrete on a large scale was in the construction of four dams in Brazil during the 1960's. Seven million cubic metres of concrete were poured, utilising a locally won clay that was calcined prior to incorporation in concrete (Saad et al 1982). The calcined clay was included as supplementary blending material at replacement levels of up to 30% (by wt), to reduce

the heat of hydration in mass concrete pours and prevent thermal cracking. It was subsequently found that the calcined clay suppressed alkali silica reaction caused by inclusion of reactive aggregates.

Asbridge et al (1996) have reported the successful use of MK concrete in practical situations. Mixes incorporating up to 15% MK as a cement replacement have been laid in applications such as a marine slipway and bases to acid storage tanks, although the authors noted it was too soon to assess the relative performance of the concrete. Other workers have obtained compressive strengths of up to 110 N/mm^2 for MK concrete with the added benefits of reduced bleeding and improved pumpability (New Civil Engineer 1996). Consequently as the benefits of MK concrete become known and its use increases, it may well become a competitor to SF, particularly in the UK.

1.5 SCOPE OF PRESENT INVESTIGATION

The main objective of this research programme was to investigate the effect of metakaolin, as a partial cement replacement, with a view to assessing its potential in the manufacture of high durability concrete. By comparing rates of diffusion of chloride ions through OPC pastes with those containing MK, BFS or PFA blending materials, information regarding the formulation of binders for concretes exposed to high levels of chloride can be obtained.

The diffusion properties of MK systems have given promising results in studies by Larbi (1991) and Coleman (1997). However as yet no work has been carried out to quantitatively compare the diffusion properties of MK systems with that of OPC and other more common blending materials.

In order to understand the factors influencing diffusion in cement systems, oxygen diffusion was studied. The similar size and diffusion rates of dissolved oxygen and chloride ions in dilute electrolytes means that any difference in their diffusivities in cement paste could be attributed to the interaction between the pore walls and the charge carried by the chloride ion.

By measuring transport properties of the binder alone, only an indication of the likely performance of concrete can be obtained. Since practical situations will utilise reinforced concrete, the corrosion resistance of steel embedded in MK concrete exposed to a highly aggressive saline environment was compared to that of more common blended concretes containing PFA and BFS. The exposure regime simulated the splash zone of marine structures, which is acknowledged to be the most severe in terms of corrosion risk (Lambert et al 1991, Liam et al 1992, Bamforth 1994).

The microstructure of concretes and mortars can be categorised into aggregate, bulk paste and interfacial zone paste. Several workers have highlighted the presence of a permeable region around aggregate particles that may form a percolation path through the concrete element (Barnes et al 1978, Diamond 1987, Scrivener et al 1988, Garboczi 1990). Work by Larbi (1991) has indicated that MK reduces the thickness of the interfacial zone, although he postulates that improvements in diffusion characteristics are largely due to improvements in the bulk paste. The present study aims to investigate this hypothesis.

An intrinsic part of producing a durable concrete is being able to manufacture, place and compact the mix to reach its maximum strength and minimum voids content. Thus the rheological properties of MK blended systems were investigated. MK consists of small particles of the order 2 μm, much smaller than the average cement particle which is around 100 μm in diameter. Combined with its platey shape MK has a high surface area to volume ratio, which results in a very cohesive mix. Traditional workability tests such as the slump test, underestimate the insitu workability of MK mixes, as a direct consequence of its cohesiveness (Asbridge 1996). Factors controlling workability and ways it could be improved were studied.

1.6 THESIS PLAN

The thesis is divided into nine chapters. Following this introduction, chapter two describes the materials and standard experimental techniques used throughout the study. The next six chapters contain the experimental work. Each starts with a literature review of the topic, followed by experimental procedure, results and discussion, and at the end of each chapter a summary of the conclusions.

Chapter three describes the hydration of OPC systems containing MK as a partial cement replacement, and investigates the microstructure of the resultant paste using two techniques, water desorption and mercury intrusion porosimetry. Differential thermal analysis was used to establish the products formed through MK hydration.

Chapter four details an investigation on the steady state chloride diffusion through hardened cement pastes containing different replacement levels of MK. Ternary blends containing OPC, MK and PFA or BFS were also investigated with the aim of assessing the feasibility of producing a binder with very high resistance to chloride ingress. By combining MK with a cement replacement material of lower cost, concrete containing MK may be more accessible for standard applications.

An investigation into the diffusion of dissolved oxygen through different binders is described in chapter five. Measurement of oxygen diffusion has been developed by several

workers at Aston University (Page and Lambert 1987, Yu and Page 1991, Ngala et al 1995) and the oxygen diffusivities obtained are compared with results from steady state chloride diffusion to elucidate the effects of charged species and pore surface interactions, providing greater understanding of the mechanisms involved in mass transport.

Steady state diffusion through model mortars as first reported by Page and Ngala (1997) is detailed in chapter six. Glass beads were used as model aggregate so that an approximation to Maxwell theory of diffusion through a periodic composite can be made.

Chapter seven is divided into two parts. Part 1 is a non-steady state investigation of chloride diffusion into concrete of differing binder type. Analysis of the concrete at consecutive depths enables the production of a chloride concentration profile and comparison of resistance to chloride ingress. This investigation provided information on the likely behaviour of concrete insitu, taking into account interfacial zones as well as properties of the bulk matrix.

Part 2 investigated different binder types on the corrosion resistance of steel embedded in concrete exposed to a highly corrosive environment. A wetting and drying regime was employed to maximise chloride penetration rate and ensure enough oxygen and water was present to promote corrosion.

Chapter eight describes an investigation using two point workability tests on MK pastes and mortars to establish a true measure of workability. The controlling parameter of MK workability was established and ways of improving concrete handling and performance are investigated.

Finally Chapter 9 contains general discussions and conclusions drawn from the whole investigation followed by recommendations for further research.

CHAPTER 2

2. MATERIALS AND EXPERIMENTAL TECHNIQUES

2.1 INTRODUCTION

This chapter describes the materials used, the preparation of specimens and the standard analytical techniques employed in this investigation.

2.2 MATERIALS

Throughout this project the same batches of materials were used to ensure uniformity and enable direct comparisons to be made. The ordinary portland cement (OPC), metakaolin (MK), pulverized-fuel ash (PFA) and ground granulated blast furnace slag (BFS) were each supplied in single batches and stored in airtight plastic drums until required.

Where pozzolanic additives were used they were included as a partial cement replacement on a weight basis. For example a 20% MK paste contained 80% OPC and 20% MK by weight of total binder.

Chemicals used in this work were lab reagent grade, except where standards were made up for calibration purposes when analytical reagents were used.

2.2.1 Ordinary Portland Cement

Portland cement is manufactured by mixing together clay and limestone or chalk, and heating in a rotary kiln at 1450°C until the material sinters and partially fuses into balls known as clinker. Once cool the clinker is ground together with gypsum to form a fine powder of Ordinary Portland Cement (OPC), the major constituents of which are listed in Table 2.1, together with their cement chemists notation. An estimation of the proportions of constituent compounds in a cement can be made from the percentages of the oxides present using the Bogue equations (Neville 1995). By varying the relative amounts of these main constituents the characteristics of the concrete can be drastically altered. Corish (1994) surveyed the composition of cements over the past 30 years and found that C_3S content had increased at the expense of C_2S and C_3A, with an accompanying increase in 7 and 28 day compressive strengths of concretes. In a review of coastal exposure trials Bamforth (1993) found that OPC concrete produced in 1929 performed better, in terms of depth of chloride penetration, than modern OPC concretes. He attributed the difference to a higher C_2S/C_3S ratio in earlier cements which in general had correspondingly lower compressive strengths. Thus it can be deduced that compressive strength is not a reliable indicator of durability performance.

In the presence of water the constituents of cement react to form various hydrates (refer to equations 2.1 to 2.4). The reaction of pure C_3A with water is very violent and would lead to flash set, but for the presence of gypsum. As can be seen one of the major products is calcium hydroxide. Approximately 20 grams of calcium hydroxide is produced from every 100 grams of OPC, and so will have a significant effect on the performance of cement systems.

$$2C_3S + 6H \rightarrow C_3S_2H_3 + 3CH \qquad \text{Eqn. 2.1}$$

$$2C_2S + 4H \rightarrow C_3S_2H_3 + CH \qquad \text{Eqn. 2.2}$$

$$C_4AF + 2CH + 10H \rightarrow C_3AH_6 + C_3FH_6 \qquad \text{Eqn. 2.3}$$

$$C_3A + 6H \rightarrow C_3AH_6 \qquad \text{Eqn. 2.4}$$

The cement used in this work was ordinary portland cement, or type I (ASTM description). The OPC was supplied by Blue Circle Ltd and complied with BS 12:1991, and ENV 197 - 1:1992. Its chemical analysis and Bogue composition are shown in Tables 2.2 and 2.3 respectively.

2.2.2 Cement Replacements and Additives

Pozzolanic additives are included in cement systems for engineering and economic reasons. Improvements in the performance and properties of a concrete can be realised, as can a reduction in the cost of the concrete due to reductions in the quantity of OPC used (Dhir and Byars 1993, Bamforth 1996). Improvements in durability are a direct consequence of a refining of the pore structure by secondary hydrates, such as CSH gel, which segment pores and slow the ingress of aggressive agents (Page et al 1981, Li and Roy 1986). The consumption of lime in the pozzolanic reaction reduces the alkali concentration in the pore fluid which is believed to reduce the risk of alkali-silica reaction (Hobbs 1982).

A pozzolan as described in ASTM 618-94a is, "a siliceous or siliceous and aluminous material which in itself possesses little or no cementitious value but will, in finely divided form and in the presence of moisture, chemically react with calcium hydroxide at ordinary temperatures to form compounds possessing cementitious properties." For a pozzolan to be effective it must be in a finely divided form with a consequent high surface area so that silica can readily combine with calcium hydroxide. In addition the silica must also be amorphous or glassy because crystalline silica has a low reactivity. Materials such as MK and PFA are pozzolans, whereas BFS, which possess cementing properties of its own, is termed a latent hydraulic binder.

2.2.2.1 Metakaolin

The metakaolin (MK) used in this project was supplied by ECC International Ltd., under the trade name PoleStar 505. Pale pink in appearance, it is manufactured by the calcination of kaolin at 650°C, which drives off the water of crystallisation and activates the siliceous and aluminous phases. The resultant amorphous structure is pozzolanic in nature, yielding products which exhibit cementing properties. MK contains very little CaO and so has no cementing properties of its own.

Metakaolin particles are of the order 1-10 μm in size with a high surface area, in contrast to ordinary cement particles which are of the order of 100μm, giving MK a very high pozzolanic reactivity. The chemical analysis and physical properties of the MK used throughout this investigation are shown in Tables 2.2 and 2.4 respectively.

2.2.2.2 Pulverized-Fuel Ash

Pulverised fuel ash (PFA) is a by-product of coal fired electricity generating stations, and is the most common of all pozzolans. Finely ground coal is injected into the furnace of a power station, where its carbonaceous content is instantaneously burnt, leaving a molten residue of mostly alumina and silica which rapidly cools into fine spherical particles as they exit the furnace with the exhaust gases. Before the exhaust gases can be discharged into the atmosphere the PFA is removed and collected by electrostatic precipitators.

The rapid cooling of the molten ash, while in suspension, causes the PFA to form glassy hollow spheres with a diameter between 1μm and 100μm. These properties tend to enhance the workability of the concrete by acting as "ball bearings" which lubricate surface interactions, and by improving dispersion and particle packing (Tattersall 1991, Dhir 1986). Consequently addition of PFA to a mix can enable a decrease in the water content for constant workability. Typically PFA is used as cement replacement with 25 to 30% of the total weight of binder being PFA. However inclusion of PFA tends to result in delayed strength gain, although long term strength is unaffected. To counter this effect PFA concretes often have higher binder contents than comparable OPC mixes. An advantage of the slower rate of hydration is a lower heat evolution reducing the likelihood of thermal strains developing and cracking in mass concrete applications.

The composition of pulverized-fuel ashes varies widely between sources depending on the composition of the coal and the type of power station. A general distinction is made between low-calcium ashes (Class F) derived from bituminous coals and high-calcium ashes (Class C) from sub-bituminous and lignite coals. Impurities such as carbon can adversely effect workability, while high SO_3, MgO and alkali contents can lead to expansive reactions

and eventual deterioration of the concrete. Hence limits are placed on the composition of PFA, for use in concrete by BS 3892 : part 1 :1993.

The PFA used in this project complied with BS 3892 : part 1 :1993, and was supplied by Boral Ltd. Its chemical composition is listed in Table 2.2.

2.2.2.3 Blast Furnace Slag

Blast furnace slag (BFS) is a waste-product of iron smelting, and is composed of the residue of iron ore, coke and limestone. To be used in cement, the slag left after the iron has been removed has to be quenched, so that it solidifies as glass, preventing crystallisation. This rapid cooling by water also results in fragmentation of the material into granular form. Essentially slag has the same main constituents as Portland cement, namely calcium oxide, silica and alumina, although in different proportions and so exhibits hydraulicity. The rate of this process is much slower than the hydration of OPC, but by using an activator such as gypsum or calcium hydroxide the reaction rate can be increased.

The BFS used in this work was supplied by Frodingham Ltd., and its chemical composition is listed in Table 2.2.

2.2.2.4 Plasticizers

The plasticizer and two superplasticizers used in this project were supplied by Fosroc Ltd., under the trade names P211, Conplast C430 and M1. Plasticizing admixtures are generally based on one of three materials and each of the products used represented a generic type of plasticizer, P211 being a lignosulphonate, C430 a sulphonated naphthalene formaldehyde condensate, and M1 a sulphonated melamine formaldehyde condensate. All plasticizing admixtures complied with BS 5075:1982.

2.2.3 Mild Steel

The bright mild steel used in the corrosion work had the composition shown in Table 2.5. Steel bars were cut, trimmed to length on a lathe, tapped and sand blasted to remove any rust and surface coatings. This was immediately followed by degreasing with acetone, before the bars were wiped with tissue paper and placed in a desiccator containing silica gel, where they remained for one week to enable the formation of a uniform air-formed oxide film on the surface of the bar. To ensure that corrosion only occurred as a consequence of chloride penetration through the top surface of the concrete, the ends of the bar were coated first with a layer of cement slurry, and then overlaid with a coating of epoxy sealant called sealocrete, a method first used by Lambert et al (1991) and found to prevent crevice corrosion. The cement slurry consisted of a 50:50 styrene-butadiene rubber latex and OPC mix, to ensure an alkaline environment around the bar which promoted the stability of the

passive film as well as reducing the risk of crevice corrosion. The epoxy sealant provided an impervious layer to prevent chloride attack of the surface of the steel. The length of the coating was such that the shortest distance between the exposed steel and the exterior was through the upper surface of the slab.

2.2.4 Aggregate

The aggregate used was a Trent Valley river terrace quartzite, used as a standard aggregate at Aston University. The aggregate was classified as uncrushed for mix design purposes, with a maximum particle size of 10 mm. The sand used was crushed aggregate and corresponded to sand grading zone 3 in BS 882. Both the coarse and fine aggregate had a continuous grading.

2.2.5 Glass Beads

Glass beads, supplied by English Glass Ltd., were used as aggregate in model mortars. The beads had a specific gravity of 2.95, with a diameter between 0.927 and 1.292 mm. At least 80% of the beads had a diameter between 1.010 and 1.275 mm.

2.3 EXPERIMENTAL TECHNIQUES

2.3.1 Preparation of Paste Specimens

All paste specimens were prepared from OPC that had been passed through a 150 μm sieve, to remove any large agglomerations and ensure a homogenous mix was formed, by reducing the incidence of large unhydrated cement grains. PFA and BFS were sieved in a similar fashion, although MK was not as it tended to cake on the sieve and not pass through. In order to disperse the MK in the cement paste, and break up any agglomerates the MK was mixed with water and superplasticizer to form a slurry.

The mix water was weighed out together with the superplasticizer and dispersed in the bowl of a table-mounted Hobart mixer. MK was gradually added to the water while continuously mixing. Once all the MK had been added the slurry was mixed for a further 2 minutes to ensure full dispersion. OPC was gradually added, and the paste mixed for a further 5 minutes. In the case of blends containing BFS or PFA, the additive was dry mixed with the OPC using a steel blade until evenly dispersed, before being added to the MK slurry.

Prior to placing in cylindrical PVC moulds, 49 mm in diameter by 75 mm in height, the paste was given a final mix by hand using a metal blade to ensure homogeneity. An external vibrator was used to compact the pastes until bubbles ceased to appear on the sample surface. The resultant "foamy" layer was removed and replaced with fresh paste before the specimen was given a final vibration, and a polythene sheet placed on the surface of the

paste to prevent air being forced into the specimen when the container was sealed with an air-tight cap. To minimise segregation the cylinders were rotated end over end at 8 r.p.m. for 24 hours, at room temperature, before being transferred to a curing room at 22°C for 1 week

The specimens were demoulded at 7 days, to allow sufficient strength gain and prevent damage to the young pastes, then placed under 0.035M NaOH solution at 22°C for 11 weeks. By using 0.035M NaOH solution, which has approximately the same pH as saturated calcium hydroxide solution, leaching is prevented and hydration promoted, so that uniform specimens are produced. Saturated calcium hydroxide solution was not used as it may participate in the pozzolanic reaction and also block pores.

After curing, discs 2.5 to 3 mm thick, were cut from the central regions of the cylinders for diffusion experiments using a Cambridge micro-slice diamond wheel saw and distilled water as a lubricant. Prior to mounting in a diffusion cell, the discs were lightly ground on 400 grade emery paper to remove any surface burrs and ensure a watertight seal with the gasket.

2.3.2 Preparation of Concrete Specimens

Concrete mixes are usually designed for a target workability and 28 day compressive strength. Dhir et al (1993) have used constant strength to compare concrete durability performance, on the basis that concrete is generally specified by strength. The drawback with this is that in order to obtain similar 28 day compressive strengths, water/binder (w/b) ratios and cementitious contents have to be altered. Since durability is highly sensitive to changes in these parameters, any difference in performance may be masked.

Mixes in the present investigation were designed using the procedure outlined by Teychenné et al (1975), for an OPC concrete with a target compressive strength of 40 N/mm^2 and a slump of 75 mm. Pozzolanic concretes used the same mix design, with the weight of any pozzolan added replacing an equal weight of Portland cement. Thus the cementitious material or binder content remained constant, enabling any changes in the performance of the concretes to be attributed solely to the composition of the binder.

Owing to the varied slump characteristics of each mix the target slump of 75 mm was achieved by adding different quantities of superplasticizer. This enabled similar degrees of compaction between mixes for a constant water content.

Concrete specimens were prepared in accordance with BS1881:part1. All the aggregate and half the mix water were placed in a pan mixer, mixed for one minute, and left to stand for

10 minutes to enable the aggregate to absorb water. The water absorption of the sand and coarse aggregate was calculated and found to be between 1.5 and 1% wt. respectively. This extra water requirement was included with the mix water. Superplasticisers were blended with the remaining mix water before being added to the pan mixer along with the OPC. If pozzolanic additives were used they were preblended with the OPC prior to addition to the mix.

Once all the constituents had been added mixing was continued for 10 minutes. The concrete was then slump tested and placed, in several layers, in moulds and compacted on a vibrating table. The specimens were transferred to a curing room at 22°C, (covered with polythene to prevent evaporation and plastic shrinkage), where they remained for 24 hours before being demoulded.

2.3.3 Bulk Density Measurements

Bulk density measurements were made on all cement paste discs prior to inclusion in diffusion experiments as a check on the uniformity of samples between batches, and to monitor any variation that arose during manufacture and curing. Cement paste discs were weighed under water (W_1), wiped with tissue paper, and then reweighed in a saturated surface dry condition in air (W_2). From Archimedes' principle the bulk density was calculated as follows:

$$\text{Bulk Density} = \frac{\text{Weight in Air}}{\text{Weight loss under water}} = \frac{W_2}{W_2 - W_1} \qquad \text{Eqn. 2.5}$$

2.3.4 Desorption Measurements

Porosity measurements were made on cement paste discs after measuring bulk density and then slowly drying the saturated specimen to constant weight, in a controlled environment of known relative humidity. The slow drying, which usually takes 6 weeks, is less likely to induce damage to the pore structure associated with more severe water extraction techniques. At a given relative humidity the weight loss can be attributed to pores empty of water, which can be directly related to a pore volume knowing the density of water to be $1 g/cm^3$. The relative humidity is controlled using saturated salt solutions in a vacuum desiccator. Saturated barium chloride produces a relative humidity of 90.7% at 25°C (Young 1967). This corresponds to pores greater than 30 nm in diameter being empty of pore water (Parrott 1992, Ngala et al 1995). All pores smaller than this will still be saturated. By weighing the disc once it has reached constant weight at 90.7% R.H. (W_3), a measure of the coarse capillary porosity can be obtained.

$$\text{Coarse Capillary Porosity (\%)} = \frac{W_2 - W_3}{W_2 - W_1} \times 100 \qquad \text{Eqn. 2.6}$$

Total porosity was measured by drying the specimen at 105°C for 24 hours, and weighing the disc after it had cooled down (W_4) in a desiccator. The procedure was repeated to ensure the disc had reached constant weight.

$$\text{Total Porosity (\%)} = \frac{W_2 - W_4}{W_2 - W_1} \times 100 \qquad \text{Eqn. 2.7}$$

2.3.5 Chloride Ion Analysis

Chloride ion concentrations for steady state diffusion were determined by colorimetric analysis using a method described by Vogel (1961). By mixing chloride ions with mercury thiocynate and iron ions a red/brown complex is formed, the intensity of colour being related to the original chloride ion concentration by equation 2.8.

$$2Cl^- + Hg(SCN)_2 + 2Fe^{3+} \rightarrow HgCl_2 + 2Fe(SCN)^{2+} \qquad \text{Eqn 2.8}$$

100 µl aliquots of the solution to be tested were diluted by a factor of 100 times by making the sample volume up to 10 ml with deionised water. 2 ml of 0.25M ferric ammonium sulphate in 9M nitric acid, and 2 ml of saturated mercuric thiocynate in ethanol were added to the chloride solution and agitated. The solution was left for 10 minutes for the colour to develop and then analysed using a Jenway 6105 U.V./Vis spectrophotometer. The absorption of light at a wavelength of 460 nm is directly related to the chloride concentration. From the calibration curve shown in Figure 2.1 the chloride ion concentration was estimated for a given value of absorption.

2.3.6 Total Chloride Content

The method used for total chloride extraction from concrete was based on that described in BS 8110.

The concrete sample was ground with a pestle and mortar to pass a 150 µm sieve and dried at 105°C for 12 hours. Five grammes of powdered sample were weighed into a glass beaker, to which was added 100 ml of 10% nitric acid. The mixture was agitated, covered with a watch glass and boiled using a Bunsen burner for 10 minutes. The suspension was removed from the Bunsen flame and kept warm on a hot plate for a further 15 minutes, before being allowed to cool and filtered into a 500 ml standard flask. The glass beaker and watch glass were rinsed with deionised water, and the washings filtered into the standard flask. Finally boiling water was passed through the filtered residue to wash through any last

trace of chloride ions. The solution was then made up to 500 ml with deionised water and analysed for chloride content.

Titration using silver nitrate was employed to ascertain the chloride content. This method was used in preference to the colorimetric technique as it is more accurate at the higher chloride concentrations being investigated. The colorimetric technique is very accurate for determining low chloride concentrations, but is insensitive at higher concentrations necessitating massive dilution of the filtrate and thus incurring errors. Absorption readings are also sensitive to contamination with suspended particles, necessitating much more efficient filtering than is required for the titration method.

10 or 20 ml aliquots, depending on the chloride concentration of the sample, were taken from the 500 ml flask and analysed using a Radiometer autoburette ABU91 and titration manager. Silver nitrate reacts with chloride ions to precipitate silver chloride. The volume of silver nitrate at which silver chloride ceases to be precipitated was measured by monitoring the potential of the solution, against a potassium sulphate reference electrode, enabling the chloride content to be calculated.

2.3.7 Differential Thermal Analysis

A Stanton Redcroft 673-4 differential thermal analyser was used to identify the constituent materials in cement samples. Cement paste samples were ground to pass a 150 μm sieve and dried in a vacuum desiccator over silica gel. A small amount was then placed in a rhodium-platinum crucible seated on a thermocouple in the furnace which was heated to 950°C at a rate of 10°C per minute. The temperature of the sample was monitored against that of a thermally inert reference material, in this case calcined alumina. Any thermal change between the sample and the reference, due to decomposition, was plotted on a chart recorder, as furnace temperature against differential temperature. These endothermic and exothermic variations were correlated with thermal changes in known compounds and the composition of the sample determined.

2.3.8 Mercury Intrusion Porosimetry (MIP)

MIP is a commonly used technique for determining the pore-size distribution of concrete and cement pastes. The information obtained is usually represented as a curve of cumulative pore volume versus pore size.

The technique entails pre-drying the sample of any pore water, and high pressure intrusion with mercury. The volume of mercury intruded at a given pressure can be correlated to the volume of pores at an equivalent diameter by the Washburn equation.

$$d = -\frac{4\gamma\cos\theta}{P} \qquad \text{Eqn. 2.9}$$

d	Equivalent pore diameter
γ	Surface tension of mercury
θ	Contact angle of mercury and pore walls
P	Pressure at which a given volume of mercury intrudes the pore system

Before the specimen can be intruded with mercury, all the pore water must be removed which causes disruption to the pore structure. As the sample is dried surface tension forces, exerted by the water meniscus as it withdraws, cause the collapse of the pore structure. Oven drying has been proved to inflict the most severe damage, while solvent replacement with propan-2-ol causes much less damage due to the lower surface tension of the alcohol (Feldman 1984, Marsh et al 1983, Day and Marsh 1988).

Cement paste specimens for drying were broken into pieces approximately 5 mm square, and submerged in propan-2-ol. Removal of the pore water was improved by vibrating the samples in an ultrasonic bath. The alcohol was then replaced with fresh propan-2-ol and the procedure repeated at least twice or until the solvent ceased to become cloudy. Samples were stored under alcohol for one week to ensure full solvent exchange until required for testing.

Prior to intrusion the propan-2-ol was filtered off and the sample surface dried using a cold air blower. This was followed by evacuation for 24 hours to remove any remaining solvent.

There are several assumptions inherent in the use of MIP. Pores are assumed to be cylindrical, interconnected and accessible from the exterior of the sample. This is an oversimplification, as pores are not all accessible from the exterior or cylindrical. The latter point does not account for ink-bottle pores, whose entry diameter is smaller than the majority of the pore. This is of particular importance in blended cements where secondary hydration products block pores. On intrusion, volume behind these blockages is attributed to the pressure required to break through the hydrate, giving an overestimate of the volume of fine pores.

An appropriate contact angle must also be assumed as contact angle changes with pressure. Generally a value in the range 130 to 115° is taken depending on the cement type and drying procedure. In this work a constant value of 117°, as used by Diamond (1970), was adopted. Since the data obtained is used comparatively any errors incurred by this assumption are considered unimportant.

2.3.9 Linear Polarisation

Linear polarisation is a non-destructive technique used to measure the corrosion rate of steel embedded in cement or concrete. The method, developed by Stern and Geary (1957) and Stern (1958), involves polarising the steel bar a few millivolts (ΔE) either side of its rest potential (Ecorr) and measuring the current density (ΔI). The polarisation resistance can then be calculated using the Stern-Geary equation shown below:

$$R_p = \frac{\Delta E}{\Delta I} = \frac{\beta_a \beta_c}{2.3 I_{corr}(\beta_a + \beta_c)} \qquad \text{Eqn. 2.10}$$

where β_a and β_c are anodic and cathodic Tafel constants.

For steel in concrete systems the Tafel constants are assumed to be constant giving a simplified Stern-Geary equation (Eqn.2.11). Andrade (1978) found that for steel in concrete Tafel constants of 0.12 volts/decade, which give a value of 26 mV for B in equation 2.11, produce corrosion rates similar to those obtained by gravimetric weight loss methods.

$$I_{corr} = \frac{B}{R_p \times Area} \qquad \text{Eqn. 2.11}$$

An AMEL 551 potentiostat was used to take the linear polarisation measurements. The method required a second embedded steel bar to act as a counter electrode. First the rest potential of the test bar was determined. Positive feedback was used to compensate for the IR drop across the concrete between the surface and test bar. The potential was shifted manually 20 mV above the rest potential and the resultant current recorded after 60 seconds, by which time it had reached a near constant value. The potential was returned to the rest value for a minute to allow stabilisation. The procedure was repeated for a potential shift 20 mV below the rest potential, the current recorded after 60 seconds, and ΔI taken as the average of the modulus of the two readings. Values of Icorr greater than 0.1 $\mu A/cm^2$ are indicative of significant corrosion activity.

Name of Compound	Oxide Composition	Abbreviation
Tricalcium silicate	$3CaO.SiO_2$	C_3S
Dicalcium silicate	$2CaO.SiO_2$	C_2S
Tricalcium aluminate	$3CaO.Al_2O_3$	C_3A
Tetracalcium aluminoferrite	$3CaO.Al_2O_3.Fe_2O_3$	C_4AF

$CaO = C$, $SiO_2 = S$, $Al_2O_3 = A$, $Fe_2O_3 = F$, $H_2O = H$

Table 2.1 Main constituent compounds of Portland cement.

	OPC	PFA	BFS	MK
SiO2	20.3	48.2	35.51	51.8
Al_2O_3	5.44	32.2	12.59	42.3
Fe_2O_3	2.8	8.02	0.58	2.99
CaO	63.7	1.45	40.09	0.08
MgO	1.44	0.66	9.11	0.13
SO_3	2.9	0.52	0.15	-
K_2O	0.77	2.85	-	0.61
Na_2O	0.09	0.98	0.24	0.01
TiO_2	-	0.79	0.70	0.81
MnO	-	-	0.48	-
LOI	0.94	3.84	0.91	1.3

Table 2.2 Chemical analysis of cement and blending materials.

C_3S	56.15
C_2S	15.92
C_3A	9.68
C_4AF	8.51

Table 2.3 Bogue analysis of Ordinary Portland Cement.

Pozzolanic Reactivity* (mg $Ca(OH)_2/g$) * Chapelle Test	1050 ±100
Surface Area (m^2/g)	14.6
Particle Size Distribution +300 mesh (%max) +10 μm (% max) -2 μm (% max)	 0.05 15 40
Colour Bulk Density	Pale Pink 0.4

Table 2.4 Physical properties of MK (PoleStar 505). (Information supplied by ECCI).

C	Si	Mn	P	S	Cr	Mo	Ni
0.16	0.17	0.77	0.019	0.034	0.09	0.02	0.10

Table 2.5 Analysis of mild steel.

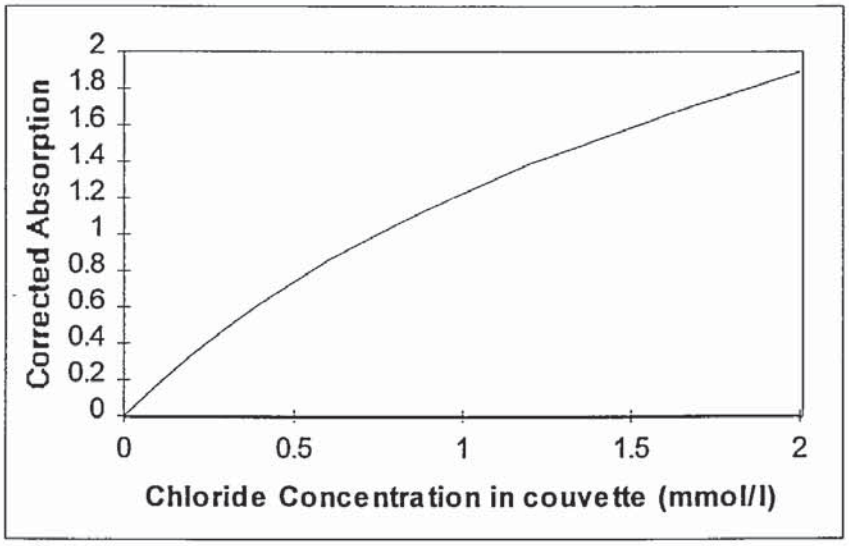

Figure 2.1 Chloride ion calibration curve for Jenway spectrophotometer.

CHAPTER 3

3. MICROSTRUCTURE OF CEMENT PASTE CONTAINING METAKAOLIN

3.1 INTRODUCTION

The microstructure of hardened cement pastes (HCP) has a major influence on the physical properties of the concrete such as strength, creep, shrinkage, diffusivity and permeability (Powers 1958, Sereda et al 1980, Nyame and Illston 1981, Parrott 1987). Consequently an understanding of the pore structure would give an insight into the mechanisms controlling service life performance of concrete. Deterioration of concrete structures occurs as a direct result of the diffusion and penetration of deleterious species into the cementitious material, which takes place through the pore fluid or porous structure. Therefore the penetration of aggressive agents depends on the pore structure and porosity of the matrix. In addition to the pore geometry considerations, the hydrates present react with penetrating species such as chloride ions and carbon dioxide, influencing durability.

It is believed that porosity, and in particular capillary porosity, influences diffusivity (Page et al 1981). Factors such as pore geometry, interconnectivity of the pores and surface interactions between the cement paste and the diffusing species influence transport processes (Li and Roy 1986, Yu and Page 1991, Ngala et al 1995). A logical step in the production of high durability cementitious materials would be lower porosities and pore sizes so as to effect lower diffusion rates. A detailed description of the pore size distribution of a paste is unlikely to be sufficient for property prediction. some measure of pore connectivity will be required for prediction of diffusion and permeability while mechanical properties of the solid phases and their bonds may be needed for prediction of strength and deformation.

The work described in the present study details the early age hydration and long term effects on the pore structure of cement pastes containing PoleStar 505 when used as a partial cement replacement, with the aim of evaluating its potential in the production of high durability concrete. Water desorption from saturated cement paste specimens and mercury intrusion porosimetry (MIP) were utilised to analyse the pore structures of HCP containing MK. The pore structure of ternary blended pastes were also studied to investigate whether the use of slow and fast reacting pozzolans in combination could produce significant improvements in the pore structure of cement systems with consequent reductions in diffusivity. Differential thermal analysis was employed to study the consumption of calcium hydroxide and hence the progress and extent of the pozzolanic reaction.

3.2 LITERATURE REVIEW

3.2.2 Microstructural Models of Hardened Cement Paste

The structure of hardened cement paste consists of poorly crystallised hydrates referred to collectively as gel, crystals of calcium hydroxide, unhydrated cement grains, and the voids formed from the remnants of water filled space. At water/cement ratios greater than 0.35 the volume of cement gel is insufficient to fill all the original water space within a paste specimen, even after complete hydration. The resulting unfilled voids are called capillary pores. In addition within the CSH gel itself there are interstitial spaces known as gel pores, which make up 28% of the total gel volume (Powers and Brownyard 1946).

Capillary porosity depends on water/cement ratio of the mix and degree of hydration, porosity being reduced with decreasing w/c ratio and continuing hydration. Production of the dense mass of cement gel reduces capillary pore sizes and volume reducing the continuity of the capillary pore system, provided the w/c ratio does not exceed 0.7 (Powers 1958). Interconnected capillary pores are a dominant factor influencing the durability performance of concrete. As hydration proceeds the initially continuous capillary pore system becomes segmented as gel is precipitated in the pore space. Consequently the capillary pores become interconnected via gel pores, the degree of segmentation being a function of w/c ratio and maturity. It is thought that improvements in durability as a result of using cement replacement materials, are caused by segmentation of the pore structure by secondary hydrates (Marsh et al 1985).

Gel pores are interconnected interstitial spaces between gel particles which are needle plate and foil shaped. The pores are typically 2-3 nm in diameter (1 order of magnitude greater than the size of a water molecule). This idea of pore structure was first proposed by Powers and Brownyard (1946).

The Powers model of pore structure is now considered as over simplistic. Young (1988) postulated that pastes contain a continuous distribution of pores classified by their behaviour with water (Figure 3.1). Micropores and the smaller meso pores are considered to form the intrinsic porosity of the gel. Water in these pores is strongly adsorbed and involved in structural bonding. In the larger meso pores and smaller macro pores the water present acts as bulk water.

The Feldman-Sereda model (1970) involves a more complex view of the role of water than is recognised by the Powers model (Figure 3.2). C-S-H structure is presented as an irregular array of single layers which may come together randomly to create interlayer spaces. Bonding between the layers is considered to be through solid-solid contacts which are

visualised as bonds whose strength lies between Van der Waals and ionic covalent. Water that enters the interlayer spaces is a part of the structure and contributes to the rigidity of the system. Most of this water can only be removed from the system by drying at a relative humidity less than 10%.

Chloride ions affect cement paste in a physical and chemical manner. The interaction of the chloride ion with HCP leads to the formation of Friedel's salt $C_3A.CaCl_2.10H_2O$ (Midgley and Illston 1980, 1984, Hoffman 1984). Diffusion may be retarded by reaction with the ion, fixing it within the system without further detriment to the existing structure or by creating a physical structure that retards the penetration of the ion.

It has been emphasised that a lower porosity and finer pore structure would lead to lower diffusion coefficients in hardened cement pastes. When considering the diffusion of charged species the interaction between the ion and pore wall will be greatly influenced by a charge on the pore wall. The exact nature of this charge is not critical since pore fluid consists of both positive and negative ions, which depending on the nature of the charge will be attracted to the pore wall. Resulting in the charged pore appearing "smaller" than the real pore size. The decrease in pore size due to charge on the surface is related to the zeta potential of a solid surface in contact with a liquid. This will be discussed in greater detail in Chapter 5. CSH gel pores, due to their small size are thought to be rendered impermeable to charged species due to surface charge effects (Page et al 1981, Li and Roy 1986, Yu and Page 1991, Ngala et al 1995).

3.2.3 Influence of Blending Materials on Microstructure

Blending materials such as PFA and BFS are known to reduce porosity and interconnectivity of the capillary pore system by the production and subsequent deposition of secondary hydrates mainly CSH gel in pore spaces which segment the pore network (Li and Rot 1986). CSH gel is thought to be impermeable to chloride ions due to double layer affects. Hence the production of CSH gel after the majority of hydration has occurred would appear to be advantageous. MK is a relatively new and untried pozzolan, which has a fast reaction rate with calcium hydroxide. Consequently it may not be as efficient as slower reacting blending materials.

3.2.3.1 Metakaolin

Cement replacements such as pulverised fuel ash (PFA), blast furnace slag (BFS) and silica fume (SF) are in common use today. They are incorporated as partial cement replacements for their beneficial effect on durability. In addition these compounds are by-products of other industries, and consequently are cheaper than OPC, reducing the overall cost of the concrete. The reactive constituents of pozzolans are amorphous silica and alumina phases.

PFA, for instance, contains approximately 80% silica and alumina. Metakaolin is a relatively new purpose-made pozzolan, which has a reactive alumina and silica content of more than 90% by weight. One would therefore expect it to be a highly reactive and efficient pozzolan which will not suffer the contamination problems common with other types of cement replacements.

Some workers have investigated the reactions between various calcined clays and calcium hydroxide, and identified pozzolanic behaviour (Murat 1983 a,b, Glasser and co-workers 1990, 1993, 1995). Limited work has been carried out on the use of metakaolin as a cement replacement, and in particular PoleStar 505 used in this investigation (Bredy et al 1989, Sabir et al 1996, Coleman and Page 1997, Wild and co-workers 1996, 1997). The reactivity and composition of the pozzolanic hydrates are governed by the composition of the feed clay, and calcining temperature among other factors (Murat 1983b, He et al 1995).

3.2.3.2 Hydration of Metakaolin

Kaolin clays heated to 450-800°C lose water causing considerable disorganisation of the structure and the formation of a poorly crystallised transition phase, designated metakaolin ($Al_2Si_2O_7$ or AS_2). Overheating causes crystallisation and the formation of mullite, noticeable by a reduction in reactivity (He et al 1995).

A limited amount of work has been published on the hydration and pore structure of OPC/MK blended systems although Glasser et al (1990, 1993,1995) have investigated reactions between calcined clays and lime, and Murat (1983 a,b) and Ambroise et al (1985 a,b) in a series of papers, investigated the potential of several clays and laterites for use in third world countries as cheap cementing materials. The clays and laterites investigated were locally won materials, activated in a fixed bed kiln at 750-800°C prior to mixing with lime. Various factors were examined such as MK/CH ratio, w/b, and curing conditions and their effect on strength monitored. Examination of the mixtures by D.T.A. and X-ray diffraction indicated that the following reactions had taken place.

$$\underset{\text{Metakaolin}}{AS_2} + 6CH + 9H \rightarrow \underset{\substack{\text{Tetracalcium}\\ \text{aluminate hydrate}}}{C_4AH_{13}} + 2CSH \qquad \text{Eqn 3.1}$$

$$AS_2 + 3CH + 6H \rightarrow \underset{\text{Hydrated Gehlenite}}{C_2ASH_8} + 2CSH \qquad \text{Eqn 3.2}$$

These reactions are similar to those reported by Turriziani (1964) who studied the reactions of natural pozzolans of volcanic origin when used as cement replacements. The hydrated gehlenite produced was found to be unstable at temperatures over 50°C, forming hydrogarnet. The CSH produced differed from that produced by plain OPC in its C:S ratio.

Metakaolin is manufactured from naturally occurring minerals and as a result not all metakaolins are the same, but are dependent on the feed clay. Murat (1983b) highlighted the effect of using raw kaolinites of differing mineralogy on hydration reactions. Factors ranging from crystallinity, purity and grain size had a marked effect on the compressive strength and the hydrates formed, with higher and purer the kaolin contents producing higher compressive strengths (Murat 1985b).

Glasser and co-workers (1990,1993,1995) have investigated reactions between metakaolin and calcium hydroxide. They found the reactions to be temperature dependent. At 20°C the initial reaction products are C_2ASH_8, CSH and C_4AH_{13}. As hydration progresses the metastable C_4AH_{13} gradually disappears until after 90 days none is present. The authors did not state what was formed in its place but it is likely to be hydrogarnet. Mixtures cured at 55°C, in an attempt to accelerate the kinetics of hydration, produced hydrogarnet (C_3AH_6) and CSH. No hydrated gehlenite was found. It should be noted that these products are similar to those formed in the hydration of high alumina cement. At low temperature and water/cement ratios HAC hydrates to form CAH_{10} and C_2AH_8. These are metastable and under warm, moist conditions form cubic hydrogarnet C_3AH_6. Since the metastable products are hexagonal and change to cubic hydrogarnet, there is a resultant increase in porosity, accompanied by a reduction in strength.

3.2.4 Effect of Metakaolin on Physical Properties

Bredy et al (1989) carried out an investigation into the effect on microstructure and porosity of MK blended cements. D.T.A. and XRD indicated that MK reduces calcium hydroxide content and contributes to the formation of hydrated gehlenite. Notably, no mention was made of tetracalcium aluminate hydrate being present. Mercury Intrusion Porosimetry results infer that MK addition causes a more discontinuous and finer pore structure than plain OPC pastes. The authors stated that they would expect an increase in durability for MK blended pastes. Replacement levels of 10% resulted in optimum compressive strength, with higher doses improving porosity.

Chapelle tests (Kostuch et al 1993) showed MK to be the most reactive pozzolan when compared with more common cement replacement materials (Table 3.1). Coleman (1997) showed that MK reacts with calcium hydroxide within days of mixing, forming hydrated gehlenite. At 36 days all the lime had been consumed at the 20% replacement level,

suggesting that there is a possibility that owing to the rapid reaction rate MK may not be as effective at pore blocking as other pozzolans. Instead of secondary hydrates being deposited to segment pores, the larger volume of CSH gel would be expected to reduce capillary porosity, without reducing connectivity as much as might be expected.

Bijen and Larbi (1990) suggested that the inclusion of MK in mortars improved the homogeneity of the mix by preventing settlement of cement and aggregate particles and the migration of water to the surface.

Zhang and Malhotra (1995) investigated the use of MK in concrete and compared its performance to OPC and silica fume (SF) concrete. The fine particle size of MK was resulted in good finishing qualities of the concrete, although this necessitated the use of a sulphonated naphthalene formaldehyde condensate superplasticizer to improve workability. High initial hydration temperatures (55^{o}C) were noted for the MK concrete, indicative of a high reactivity, resulting in a higher 28 day compressive strength than OPC, and higher strength gain than SF concrete. MK concrete had a lower drying shrinkage, higher splitting-tensile and flexural strengths, and modulus of elasticity, compared with the control and SF concretes.

3.2.5 Microstructural Analysis

There are a number of experimental techniques available for the analysis of the microstructure and pore structure of HCP. Nitrogen adsorption, low temperature calorimetry, SEM, SAX and desorption have been used to assess pore structure, although none cover such a wide range of pore sizes or are as convenient as MIP.

However, it is known that mercury intrusion porosimetry (MIP), does not give a true indication of the pore system. Therefore controlled desorption of water from saturated specimens will be used in conjunction with MIP to ascertain the pore content of a sample and enable comparison of the data obtained.

By analysing the composition of the chemical phases in a sample, the progress of hydration reactions can be followed. Differential thermal analysis (D.T.A.) was used in this work to assess the progress of the pozzolanic reaction and identify the products formed.

3.2.5.1 Mercury Intrusion Porosimetry (MIP)

Winslow and Diamond (1970) pioneered the use of MIP in examining the pore structure of cement pastes and concrete. From their investigation of OPC pastes they described what they termed "missing pore volume", or pores too fine to be intruded at the pressures encountered using MIP. Using higher pressures Diamond (1971) later attributed this volume

to encapsulated pores inaccessible to MIP. The author postulated that pore volume isolated from the outside, would not differ in make-up from portions of the paste readily accessible. If this is the case pore size distributions obtained by MIP should be representative of the sample. The technique has subsequently become the predominant method for porosity analysis.

There are a number of assumptions and drawbacks associated with MIP that limit the validity of the information obtained, such that "true" pore size distributions are extremely difficult to obtain. During the intrusion process, mercury is forced into a specimen from the surface towards the central regions. The pressure is incrementally increased enabling smaller and smaller pores to be intruded. Not only does this damage the specimen, but an implicit assumption is that the pore sizes in the system gradually diminish from the surface towards the centre, enabling full access to all the porosity. In practice there are constrictions that limit entry to the interior pore volume, a phenomenon known as "ink-bottle" pores. As mercury intrudes the sample, the matrix is damaged. In the case of blended cements, the pozzolanic hydration products are thought to be precipitated in large pores, reducing interconnectivity and forming a discontinuous pore structure. On intrusion these blockages are broken, revealing previously hidden pore volume which is apportioned to small pore diameters. This results in an overly refined structure than is actually the case. The model also assumes that all pores are cylindrical enabling pore size to be expressed conveniently as a diameter. In reality the pores in hardened cement paste are irregular with only the larger macropores, that is those larger than about 100 nm, being approximately spherical. Other factors such as contact angle and surface tension will shift the intrusion curve horizontally giving a finer or coarser pore size distribution, although the shape will remain unchanged.

Cook and Hover (1993) reviewed the use of MIP for obtaining pore size distributions for cement pastes and highlighted the effect of corrections and assumptions on data. In general the corrections applied only affected the results of very small pores (<0.001μm), and would not drastically alter the results shown in this work. Although it is accepted that MIP does not give true pore size distributions, it is still a useful technique for obtaining comparative data.

An important concept in MIP is threshold diameter, defined as the largest pore diameter at which significant intruded pore volume is detected. This equates to the largest pore diameter that is continuous throughout the specimen, and through which mercury penetrates the bulk of the sample. Zheng and Winslow (1995) showed that threshold diameter showed a close correlation with permeability. It is likely that fluid flow and permeability are controlled by pore entry sizes, so one might expect some aspect of an intrusion based analysis technique to correlate with a pastes permeability. It should be noted that surface charge effects also

influence mass transport, and it is not purely a geometric dependency. The formation of a hysteresis loop on intrusion, extrusion and reintrusion of mercury was used to divide the pore size distribution into two sub-distributions. The pore size distribution obtained from the first intrusion was termed irreversible, while the second intrusion curve represents that part of the pore system that can be irreversibly intruded. The authors showed that the irreversible pore size distribution represents the most accessible part of the pore system, and correlates well with chloride permeability as measured by the AASHTO test.

Goto and Roy (1981) and Nyame and Illston (1981) have also correlated MIP results with permeability. They concluded that the volume of pores greater than 0.1 μm is important in the determination of permeability.

A major difficulty with MIP and most techniques used to examine the pore structure of hardened cement pastes is that the water residing in the pores has to be removed in order to obtain the measurement. Unfortunately removal of water may lead to changes in the microstructure of the material.

Several papers (Moukwa and Aitchin 1988, Marsh et al 1983, Feldman 1984) have been written on the damage caused to the pore structure when water is removed by commonly used sample preparation techniques, such as oven drying and solvent replacement. In a paper comparing the effects of each method Marsh et al (1983) found specimen preparation was critical to the results obtained by MIP. Oven drying resulted in severe disruption of the pore structure particularly for pores below 0.008 μm. Disruption was primarily attributed to the effects of high surface tension forces exerted by the receding water menisci, and the removal of some chemically bound water (Day and Marsh 1988). By replacing the pore water with a solvent, which is subsequently removed, surface tension forces within the pore structure are reduced. Work by Feldman and Beaudoin (1991) showed that solvent replacement with isopropanol followed by evacuation and heating produced the least amount of stresses and consequent damage to the material. Although they stated actual pore size distributions could not be obtained due to the sensitivity of cement paste to stresses, they indicated that the technique was useful for monitoring relative pore structures. Studies by Day (1981) and Feldman and Beaudoin (1991) using methanol as the replacement solvent concluded it reacts with calcium hydroxide, altering the structure and causing an increase in threshold diameter.

Despite all its limitations MIP is still a useful technique for obtaining pore size distribution information. The wide range of pore sizes detectable and the lack of alternatives in terms of its simplicity and convenience mean that it is valid as a comparative technique.

3.2.5.2 DESORPTION

Drying of a cement paste sample causes disruption to the structure. A process that can reduce drying stresses and eliminate the damage caused by intrusion will give a more accurate indication of porosity and pore structure. Drying the sample gently, by controlling the ambient relative humidity (R.H.), reduces the stresses on the cement matrix induced by surface tension forces. If a disc of cement paste is weighed in a saturated state and after it has reached equilibrium in a controlled R.H., any weight loss can be attributed to empty pore volume. Since 1 cm^3 of water weighs 1 gram, the pore volume can be calculated. The technique has been successfully used by Parrott (1992) and Ngala et al (1995) to obtain values of coarse capillary porosity (>30 nm) and total porosity. The advantage of the technique is that it is relatively gentle on the pore structure, as the drying takes place slowly, the stresses induced by water menisci are small. However drying to constant weight takes a long time, depending on sample size and porosity.

3.3 EXPERIMENTAL PROCEDURE

Cement paste cylinders were prepared as described in section 2.2. The specimens were demoulded after 3 days and the first samples taken. The top 10 mm of the cylinder was discarded as not being representative, and samples taken from the central regions of the cylinder. The remainder of the cylinder was placed in a curing room at 22°C in a controlled environment of 100% R.H. Further samples were taken at 7, 14, 31 and 56 days.

In order to freeze hydration, samples for MIP analysis were submerged under isopropanol. Samples for DTA were left overnight in a vacuum desiccator to remove any pore water. They were then ground to pass a 150μm sieve, and stored in a vacuum desiccator until tested.

All well-cured pastes were prepared as described in section 2, demoulded after 7 days and stored under 0.035M NaOH for 3 months. They were then prepared as above.

3.3.1 Mercury Intrusion Porosimetry (MIP)

The specimens were fractured into pieces roughly 3 mm square. Approximately 3 grams were immersed under isopropanol, placed in an ultrasonic bath and vibrated for 5 minutes to aid thorough penetration of the solvent into the sample. As the pore water in the sample was replaced with solvent the solution became cloudy. The propanol was decanted off, replaced and the sample returned to the ultrasonic bath. This procedure was repeated until the solvent ceased to become cloudy. The sample was then stored under fresh propanol for 1 week, or until required for testing. Immediately prior to testing, the alcohol was decanted off, and the sample surface dried by directing cold air over the specimen, using a blower. The sample

was finally placed under vacuum for 24 hours before being placed in the porosimeter for testing.

3.3.2 Desorption

Specimens for desorption measurements were cut from cylinders stored under 0.035 M NaOH solution for 90 days. Discs, approximately 3 mm thick were cut from the central regions of the cylinders using a Cambridge Research Micro slice, and deionised water as a lubricant. Once cut, the discs were cleaned with deionised water and, to ensure the discs were fully saturated, placed in a vacuum under 0.035 M NaOH. Each disc was then weighed under water, and then in air in a saturated surface dry condition. Hence from Archimedes' principle the bulk density could be calculated. The discs were stored in a vacuum desiccator whose internal relative humidity was controlled by a saturated salt solution. Saturated Barium Chloride solution was used to keep the R.H. at 90.7% at 25°C, such that at equilibrium pores greater than 30 nm in diameter would be empty, with all pores smaller than this remaining saturated. The discs were periodically weighed until they reached constant weight. Where upon they were dried at 105°C to enable total porosity to be calculated.

3.4 RESULTS AND DISCUSSION

3.4.1. Effect of MK on Pore Size Distribution of Well Cured Hardened Cement Paste.

Figure 3.3 shows a summary of the results obtained from mercury intrusion porosimetry on OPC and OPC/MK blended pastes of water/binder ratio 0.5. The data is presented relative to the OPC control paste, to compare the influence of MK on pore structure. Capillary porosity is taken as the volume of pores greater than 0.1 μm in diameter, and threshold diameter was measured as described by Winslow and Diamond (1970). All pastes were cured under 0.035 M sodium hydroxide solution at 22°C for 3 months, to promote full hydration so that the long term effects of MK on pore structure could be elucidated, as well as enabling reproducibility.

Partial replacement of OPC with MK reduces the total and capillary porosities as well as the threshold diameter of hardened cement paste, compared to a plain unblended OPC paste. Even at 5% replacement the pore structure is more refined than a comparable OPC paste, although significant reductions in threshold diameter only occur in pastes containing 10% MK or above. Threshold diameter is the pore size at which significant intrusion into the body of the sample takes place, and has been identified as being an important parameter controlling mass transport properties (Zheng and Diamond 1995).

3.4.2 Early Age Hydration of Cement Pastes

Figures 3.4 to 3.6 show the pore structure development with age of OPC and MK blended pastes cured at 100% relative humidity at 22°C.

The plots show that partial replacement of OPC with MK reduces the total porosity and pore threshold diameter of hardened cement pastes. Significantly these improvements can be detected after only 7 days of hydration. The early reduction in the threshold diameter of the 20% MK paste may be a consequence of the high pozzolanic reactivity of MK, resulting from the consumption of calcium hydroxide as soon as it is evolved and the production of pozzolanic hydrates. A more likely explanation is that this is a manifestation of the filler effect. Inert fillers such as finely ground calcium carbonate have been incorporated in cements for their beneficial effects on density, permeability, bleeding and cracking. In addition they are thought to have a catalytic effect on the hydration of Portland cement, by fostering nucleation and densifying the cement paste (Neville 1995). MK being a very small particle in relation to OPC could be acting as nucleation sites, accelerating hydration and promoting homogeneity.

Pastes containing 10% MK have slightly lower total porosities and pore threshold diameters than 20% MK pastes, possibly due to an excess of MK in the 20% paste for complete pozzolanic reaction. Improvements in the pore structure of 20% MK pastes are likely to occur after prolonged curing when full hydration liberates the maximum amount of lime. Comparing the 20% MK data from the early age hydration (! to 56 days) with that of well cured pastes (100 days wet cure) indicates that as with most blended mixes containing a large amount of cement replacement material full benefits are not obtained unless the material is well cured over an extended period.

At 56 days all OPC and MK pastes have similar total and capillary pore volumes. If pore blocking was taking place in MK pastes one might expect much greater volumes at small pore diameters and lower capillary porosity than the OPC pastes due to the ink-bottle effect. Day and Marsh (1988) found that intrusion curves for fly ash pastes tend to become convex towards the radius axis below 10 nm supporting the conclusion that the pozzolanic reaction blocks pores, or encapsulates areas of porosity. The intrusion of mercury at high pressures breaks through the blockages, filling the pores behind, which are assigned smaller pore radii than they might actually possess.

A possible explanation of the similar nature of the mercury intrusion data for MK and OPC pastes is that significant pore segmentation does not occur. The pozzolanic reaction starts almost immediately and proceeds rapidly, with the secondary hydrates reducing total porosity, but not being located to segment the capillary pore network. BFS and PFA are

known to react more slowly than MK, and as a consequence their hydrates are deposited in the capillary pore space created by OPC hydration. Consequently although MK pastes may have less total and capillary porosity than other pozzolanic cements due to the volume of hydrates produced, the system is likely to be more continuous. The reduction in threshold diameter of both 20% and 10% MK pastes diminishes after 14 days hydration, while in contrast the threshold diameter of the OPC paste continues to change significantly at 56 days.

3.4.3 Influence of Water/Binder Ratio on Well Cured Cement Pastes

Figures 3.7 and 3.8 show the intrusion curves for OPC and 20% MK pastes cured under 0.035 M sodium hydroxide solution at 22°C for 3 months. As water/binder ratio decreases total porosity decreases and the curves move to the left, indicating a refining of the pore structure. The pore distributions for the 20% MK paste show a large difference between 0.5 and 0.65 water/binder ratios, but the difference between the 0.4 and 0.5 water/binder ratio pastes is comparatively small. For the OPC paste 0.5 and 0.65 are similar with 0.4 paste having significantly less total porosity and a much more refined structure.

Powers (1958) proposed that water/cement ratios lower than 0.38 resulted in segmentation of the capillary pore system by gel in OPC pastes. Above this w/c ratio the capillary pore system was thought to be continuous. The intrusion curves indicate that encapsulation occurs at a higher w/c ratio for 20% MK pastes than for OPC pastes. For full hydration OPC pastes need a theoretical w/c ratio of approximately 0.25. Any extra water present will result in the formation of pores. From the soichiometry of metakaolin hydration shown equations 3.1 and 3.2 it can be seen that the full hydration of 1 mole (222 grams) of MK requires between 9 and 6 moles of water (162 or 108 grams). This is equivalent to a water/binder ratio of between 0.49 and 0.7. Figure 3.7 also reveals that most of the pore volume for 20% MK pastes of w/b less than 0.5 is found in pores less than 0.01μm in size, and is therefore likely to give improvements in permeability.

The higher water demand for full hydration of MK blended cements raises the question of self desiccation, which can affect low water/binder ratio and high MK mixes. As hydration progresses, water is consumed, and if water cannot be replaced quickly enough from external sources or there is none available, the internal relative humidity will be lowered. This may lead to internal stresses which could have implications on strength and other physical properties.

3.4.4 Desorption

The capillary and total porosities of OPC and MK blended pastes, determined by desorption are shown in Figures 3.9 and 3.10. In general MK pastes have lower capillary porosities

than those of corresponding OPC pastes. Conversely OPC pastes have slightly less total porosities than MK blended pastes. This is in contrast to MIP data. A possible explanation for this discrepancy could be that MIP cannot penetrate all the gel pores, giving an artificially low total porosity.

The results show that although MK pastes have a higher total porosity, most of these pores are less than 30 nm in diameter in agreement with the MIP data. Water/binder ratio appears to have only a small effect on coarse capillary porosity for MK pastes, with only a slight increase in volume between 0.4 and 0.65 water/binder ratio specimens.

3.4.5 D.T.A. Thermograms

The DTA thermograms (Figures 3.11 to 3.14) show the progression of hydration reactions up to 31 days for cement pastes of w/c 0.5 containing 0, 10 and 20% MK. The samples were cured at 100% R.H. in a curing room at 22°C. Appendix 1 lists the characteristic temperature changes for several compounds, with the source reference.

All thermograms show the presence of C-S-H gel and calcium hydroxide, which are products of OPC hydration. In the more mature MK pastes a definite peak can be seen at the corresponding position for gehlenite hydrate. The occurrence of gehlenite hydrate was difficult to detect, especially at early ages, due to its proximity on the thermogram to C-S-H gel and ettringite. Work by Murat (1983 a,b) and Glasser et al (1990, 1995) on MK/lime systems indicated that as well as gehlenite hydrate, CSH gel and tetracalcium aluminate hydrate are formed. CSH gel was almost certainly produced, although it was difficult to differentiate between that formed through OPC hydration and that formed in the presence of MK. However a significant factor is the reduction in height and broadening of the CSH gel peak for MK paste, as hydration proceeds. This may be a result of the incorporation into CSH gel of components of the MK, which have a slightly different composition to that formed by OPC. No trace of tetracalcium aluminate hydrate or hydrogarnet could be found in any of the MK pastes.

Thermo-gravimetric analysis was used to obtain quantitative information on compounds present in the cement samples. The results are summarised in Table 3.2. The results are given as weight loss in sample at the characteristic temperature for the compound, and thus do not represent the actual quantities of material present but provide a comparative means of analysis of the composition of cement pastes. Although OPC paste does not contain any gehlenite hydrate, a weight loss is still noted at the characteristic temperature, and is effectively a background reading

After 3 days hydration the three samples do not differ significantly in the quantities of hydrate measured. No hydrated gehlenite is detected in any of the samples. At 7 days the 10% MK paste shows a reduction in the quantity of calcium hydroxide and an increase in the CSH and gehlenite hydrate contents indicating that the pozzolanic reaction is underway. Notably the results for the 20% MK paste at 7 days are similar to those for OPC suggesting that the pozzolanic reactions is retarded in this paste. The results at 14 days show that the pozzolanic reaction is underway with each blended paste containing less than half the lime found in the corresponding OPC paste. The calcium hydroxide has been consumed in the production of gehlenite hydrate and extra CSH gel. At 31 days the quantities of hydrate in both MK pastes have not altered significantly from those at 14 days suggesting that no further pozzolanic reaction has taken place. In contrast they have increased significantly for OPC, with seven and ten times as much calcium hydroxide as in 10 and 20% MK pastes respectively.

At 31 days, calcium hydroxide is still present in the 20% MK paste, even though theoretically this is sufficient MK present to consume all the lime produced by OPC hydration. Even if thermograms were taken for much more mature pastes, it is unlikely that all the lime will have been consumed since dispersion will play an important part.

The pozzolanic reaction in both blended pastes appears to have slowed down after 14 days with most of the reacting taking place between 7 and 14 days. This may not be very beneficial for pore blocking since the results also show that plain OPC paste is still reacting at 31 days hydration.

All traces confirm that the pozzolanic reaction between MK and lime occurs early in the hydration process, with a large proportion of lime being consumed by 28 days. The thermograms suggest that the pozzolanic reaction appears to tail off after 14 days. However MIP data on samples cured for 100 days indicate that the pozzolanic reaction continues to affect significant improvements in pore structure, all be it at a possibly slower rate. The rapid development of the pore structure at an early age in MK blended pastes may in fact inhibit further reaction by hindering diffusion of calcium and hydroxide ions to MK particles.

3.5 CONCLUSIONS

The D.T.A. results generally agree with work carried out by Glasser et al (1990, 1995) into MK/lime systems. A pozzolanic reaction is occurring, resulting in the consumption of calcium hydroxide and the production of gehlenite hydrate. However no hydrogarnet was found to be present.

Inclusion of MK in cement improves the pore structure of the hardened cement paste by reducing capillary porosity and threshold diameter. These improvements were noticeable after only 3 days hydration.

Implications of this fast and efficient pozzolanic reaction are numerous. A reduced calcium hydroxide content would be expected to promote resistance to acid attack and durability in a number of environments. In addition the early reaction of the pozzolan and the formation of CSH gel may prevent low compressive strength development associated with other cement replacement materials.

Aston University

Illustration removed for copyright restrictions

Figure 3.1 Pore size classification for cement pastes (Young 1988)

Aston University

Illustration removed for copyright restrictions

Figure 3.2 Schematic presentation of the Feldman-Sereda model (After Oberholster 1986).

Aston University

Illustration removed for copyright restrictions

Table 3.1 Chapelle test results for various pozzolans (Kostuch et al 1993).

		% Weight Loss		
Age (Days)	% MK (by wt binder)	CSH gel	C_2ASH_8	CH
3	0	0.739	1.122	0.576
3	10	0.875	1.230	0.367
3	20	0.719	1.166	0.620
7	0	0.739	1.122	0.566
7	10	0.876	1.230	0.224
7	20	0.719	1.166	0.620
14	0	0.727	1.872	1.640
14	10	0.969	2.193	0.790
14	20	1.0134	2.504	0.597
31	0	1.055	1.925	5.258
31	10	1.074	2.455	0.764
31	20	1.072	4.3718	0.537

Table 3.2 Thermo-gravimetric results for hydrated cement pastes.

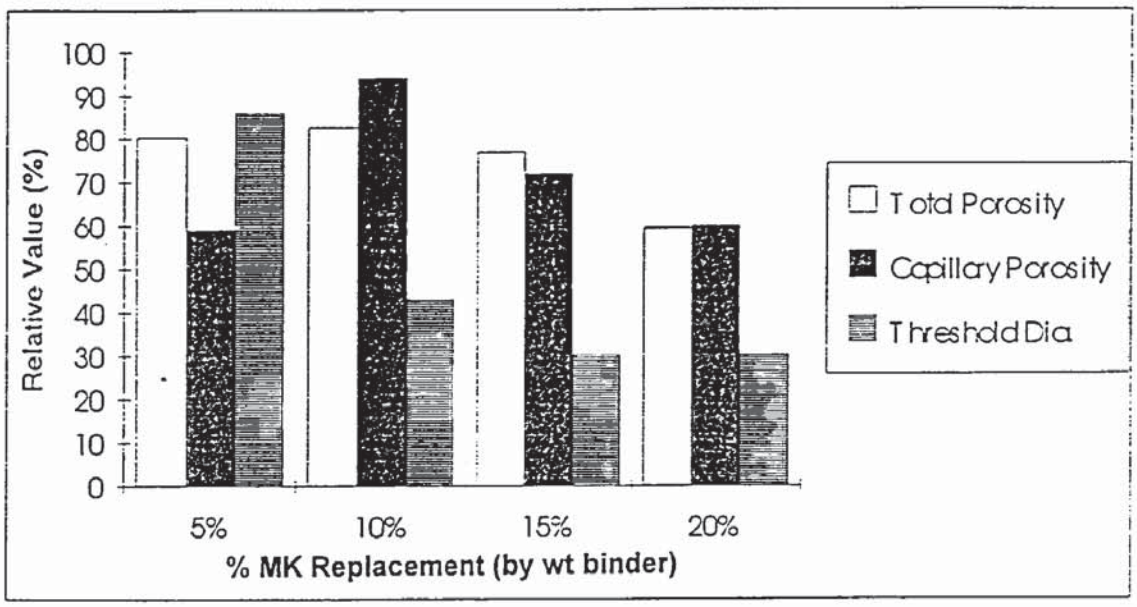

Figure 3.3 Effect of MK replacement level on pore structure.

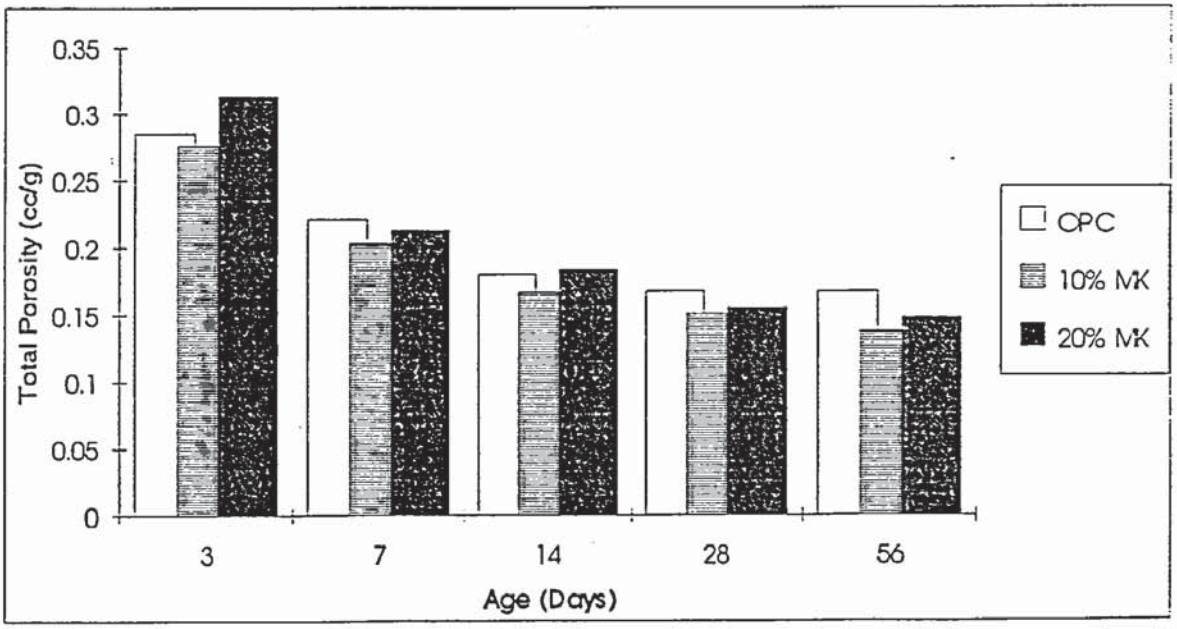

Figure 3.4 Variation of total porosity with age for OPC and MK blended pastes.

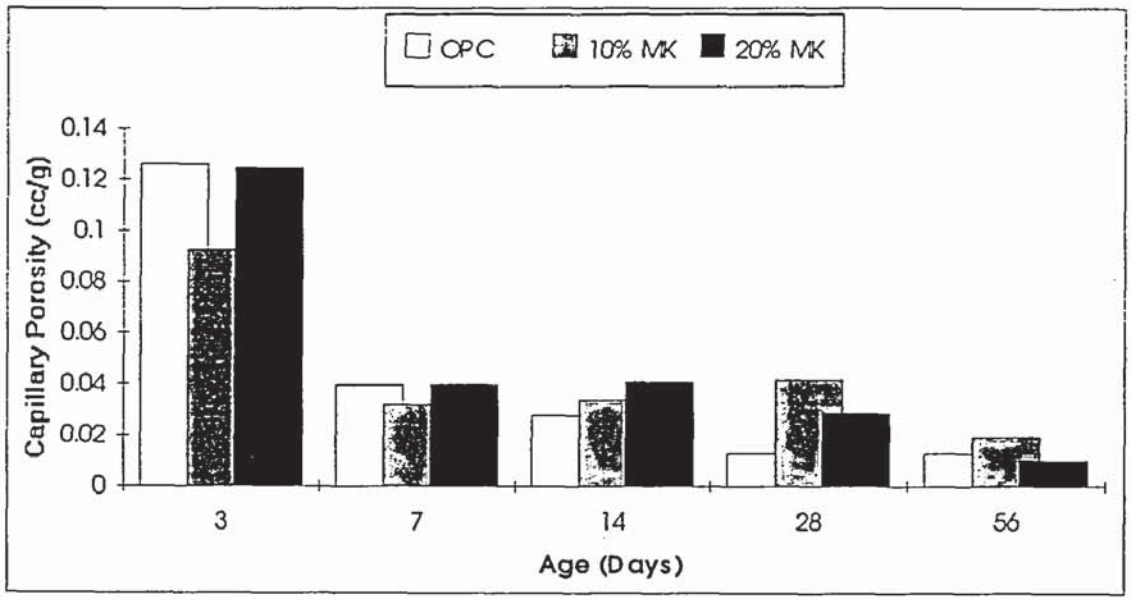

Figure 3.5 Variation of capillary porosity with age for OPC and MK blended pastes.

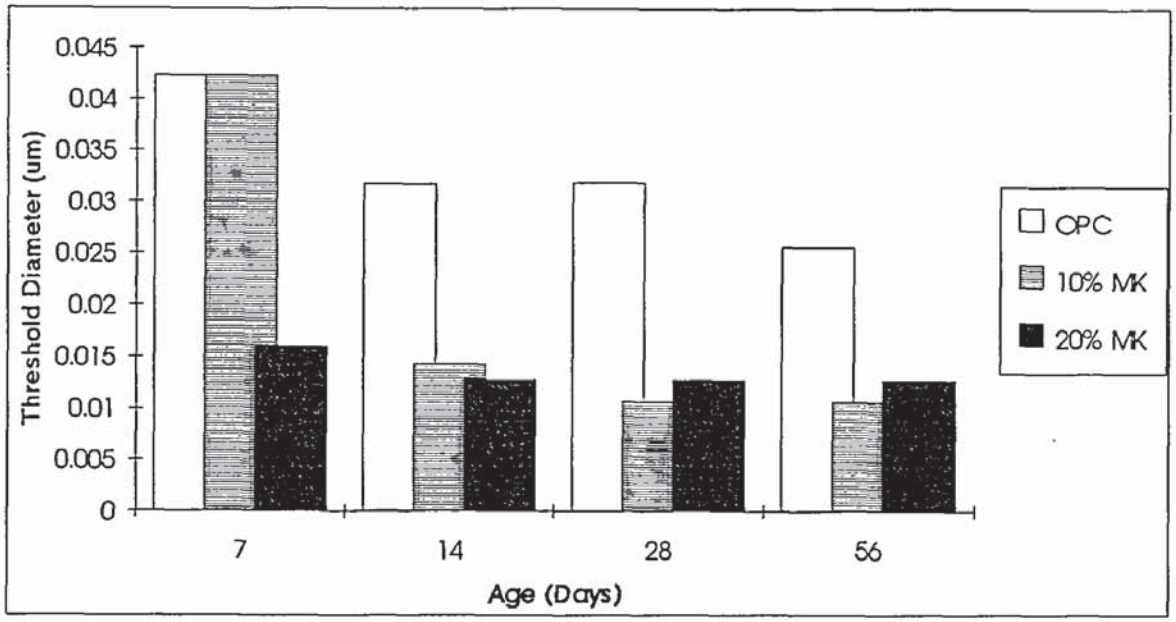

Figure 3.6 Variation of threshold diameter with age for OPC and MK blended pastes.

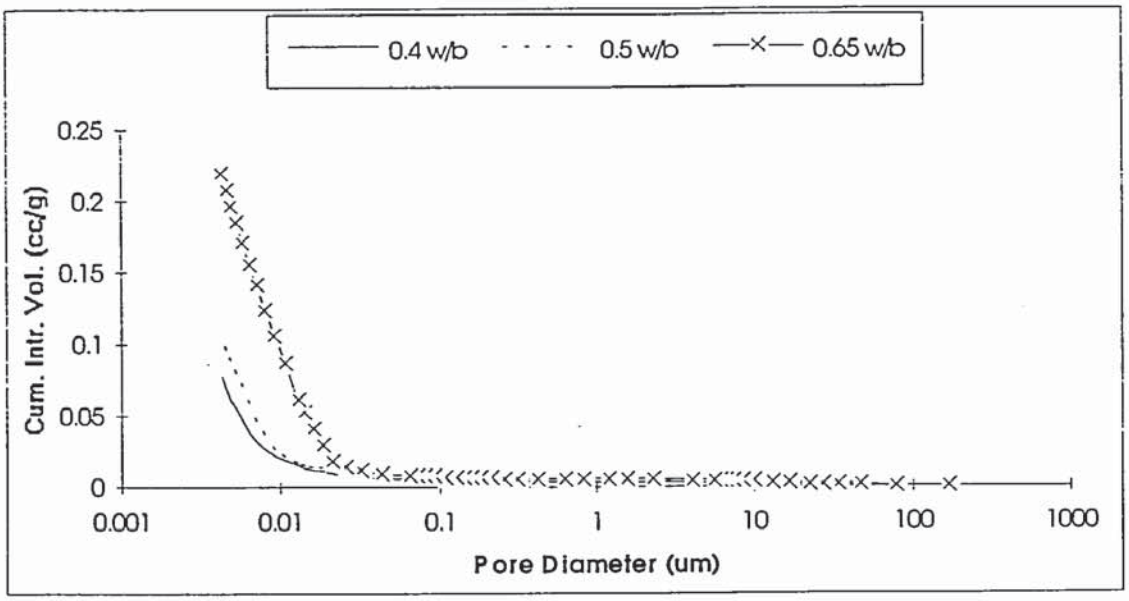

Figure 3.7 Pore size distribution curves for 20% MK blended pastes.

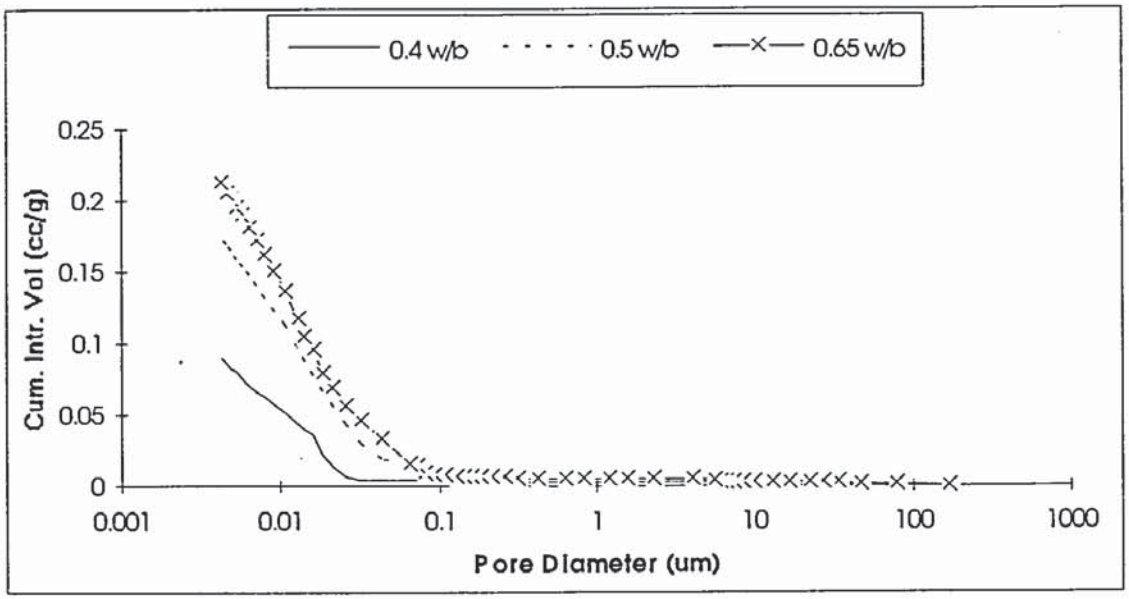

Figure 3.8 Pore size distribution curves for OPC pastes.

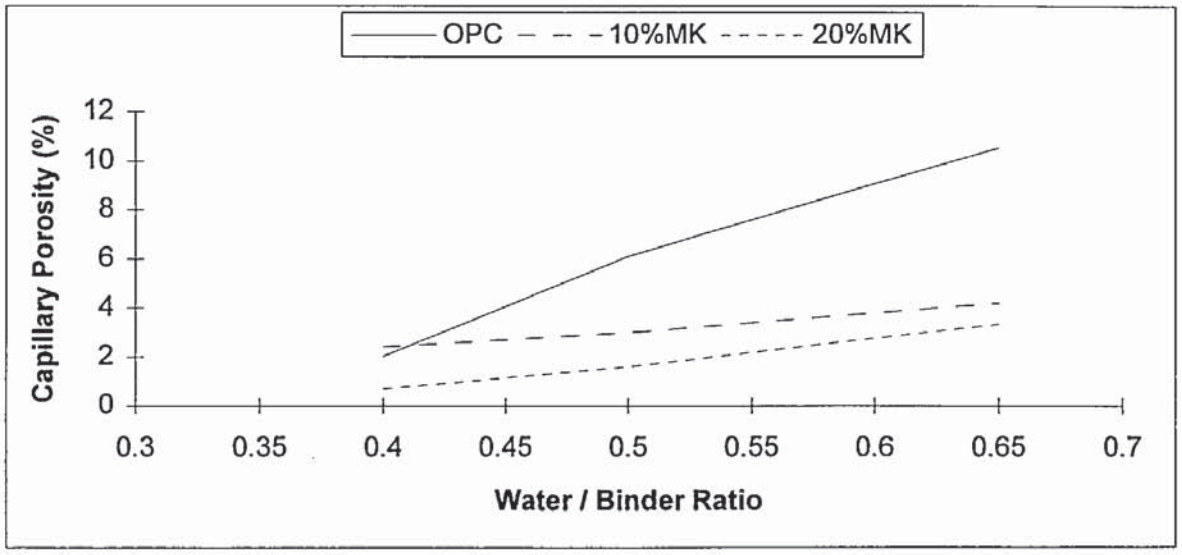

Figure 3.9 Coarse capillary porosity obtained by water desorption.

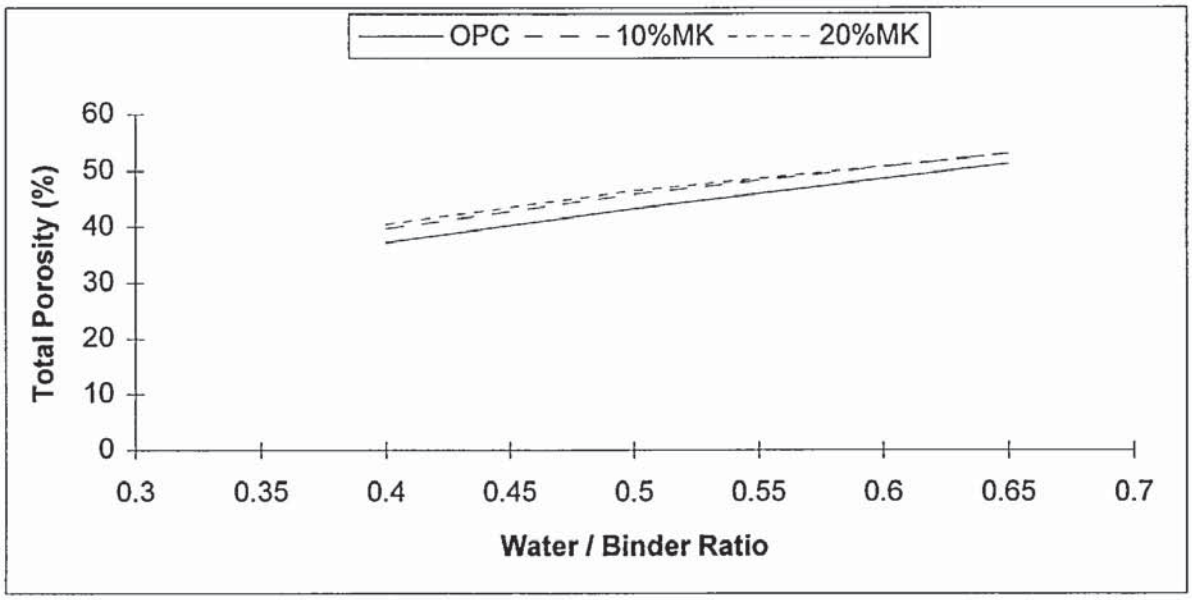

Figure 3.10 Total porosity obtained by water desorption.

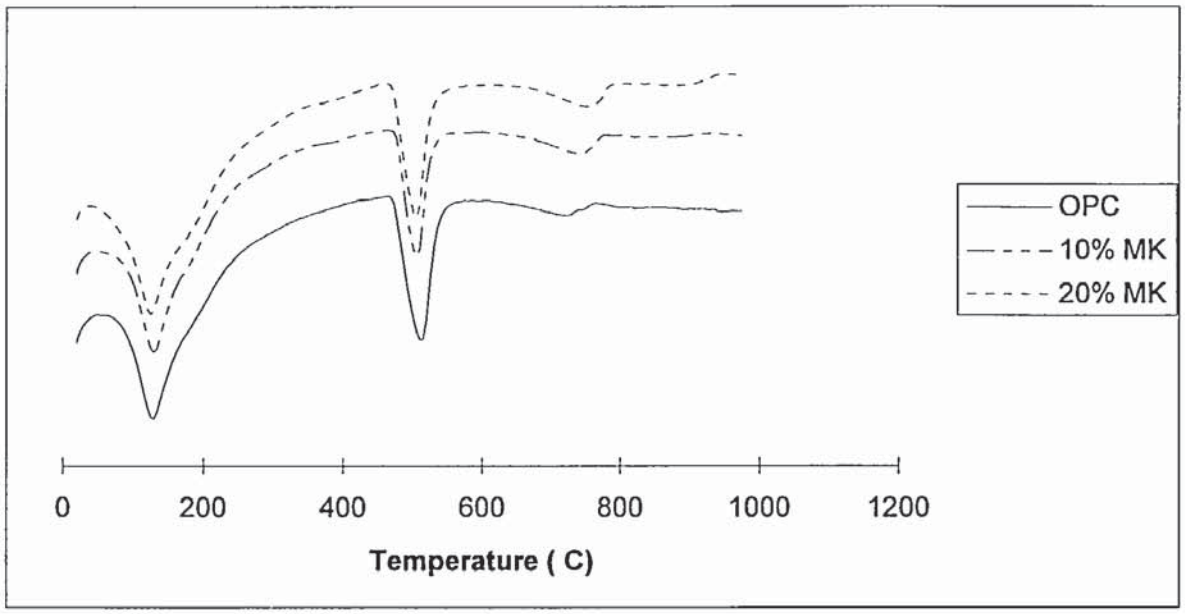

Figure 3.11 D.T.A. thermograms for 3 day old pastes.

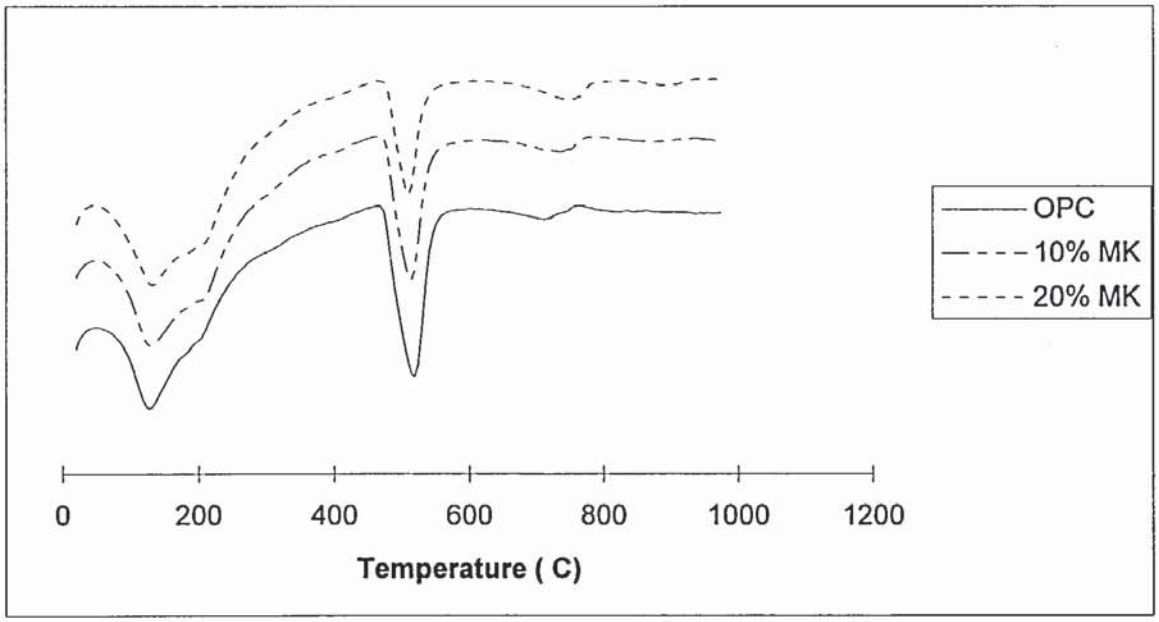

Figure 3.12 D.T.A. thermograms for 7 day old pastes.

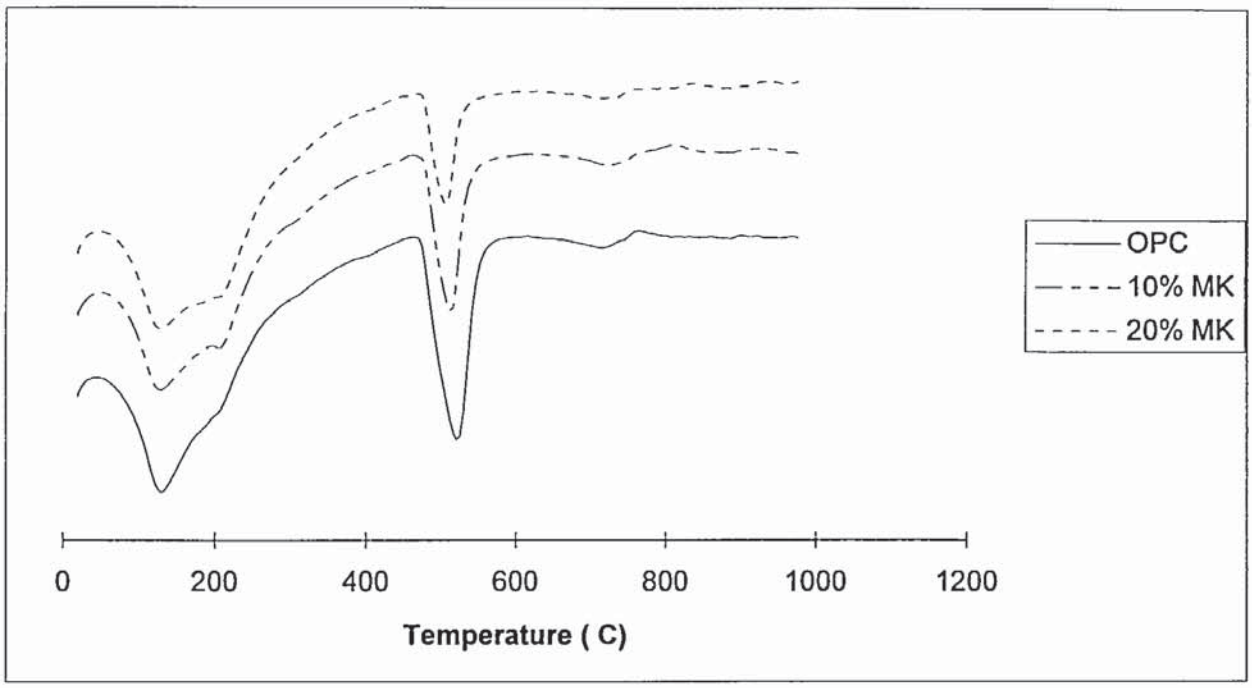

Figure 3.13 D.T.A. thermograms for 14 day old pastes.

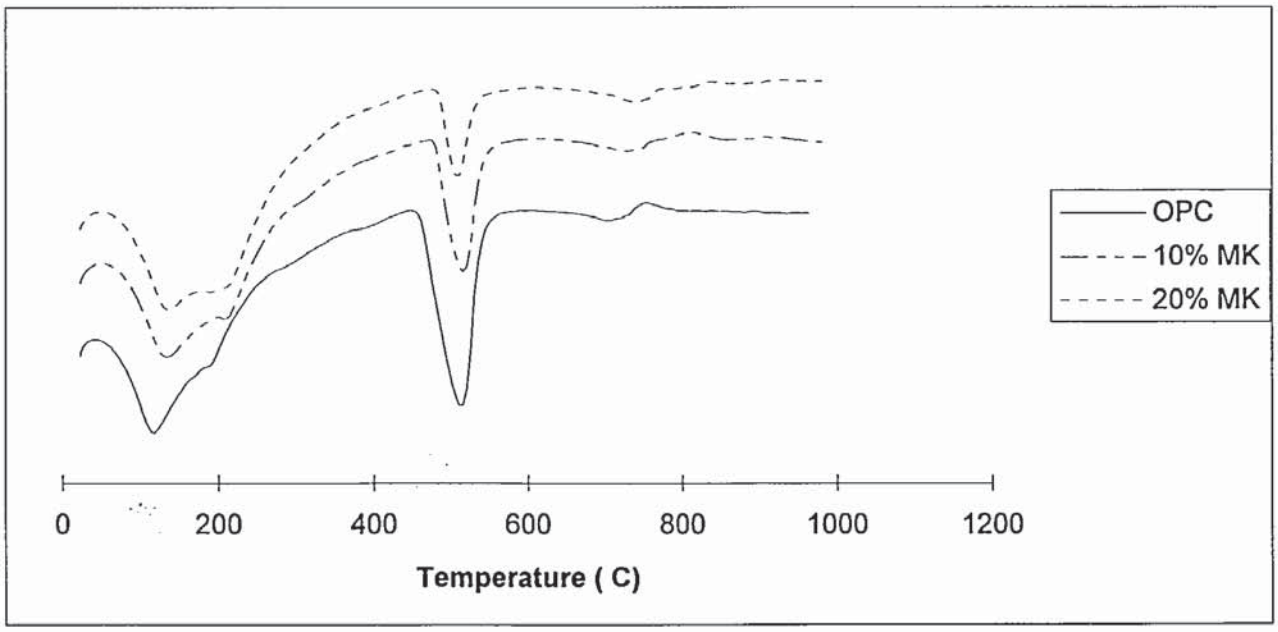

Figure 3.14 D.T.A. thermograms for 31 day old pastes.

CHAPTER 4.

4. CHLORIDE DIFFUSION THROUGH HARDENED CEMENT PASTE

4.1 INTRODUCTION

It is widely recognised that the transport properties, and in particular the diffusion characteristics are important in relation to the durability and service life of concrete structures (Page et al 1981). Depassivation of the steel reinforcement can occur as a result of a reduction in alkalinity of the concrete by carbonation, or by penetration of chloride ions. Subsequently corrosion ensues, the reaction products having a larger volume than the steel, causing cracking of the concrete, and in severe cases spalling, leaving the steel open to further attack. The most common and aggressive form of attack is chloride penetration.

With limitations imposed on the quantity of chlorides incorporated into a concrete mix (BS 8110, 1985), the most significant process by which chlorides enter concrete is by penetration from external sources. Consequently much work (Gjørv and Vennesland 1979, Bamforth 1996, and Ngala 1996) has been carried out on improving the mass transport properties of concrete by incorporating cement replacement materials such as BFS and PFA.

The aim of this investigation is to evaluate the effect of metakaolin as a cement replacement material, and to study its influence on the diffusion of chloride ions into blended matrices. Ternary blends containing PFA and BFS in combination with MK will also be studied. The use of two pozzolans of different reaction rates may lead to the production of very high durability concretes, without the low strength gains associated with traditional formulations containing high levels of cement replacement. Limited results in the published literature indicate metakaolin blended systems to have a good resistance to chloride ingress, although no study has concentrated on the kinetics of diffusion through MK blended pastes (Larbi 1991, Asbridge et al 1996).

4.2 LITERATURE REVIEW

4.2.1 Chloride Ion Penetration into Concrete

Chloride ions can enter concrete either by inclusion in the fresh mix or by penetration from the external environment.

The inclusion of chlorides in the form of admixtures in fresh concrete has been prohibited in BS 8110 since 1977. Prior to this, admixtures such as calcium chloride were used as accelerators. Further restrictions on the chloride content of aggregate were introduced in 1985 (BS 8110). Consequently for the majority of concrete, inclusion of chlorides in the fresh mix is not a consideration. In any case, depending on the concentration, chlorides

included during mixing will be immobilised by reactions with cement hydrates to form products such as Friedel's salt, and so be prevented from attacking the reinforcing steel (Hoffmann 1984, Midgley and Illston 1984). Hence the penetration of chlorides from the surface into the body of the hardened concrete is the prominent source of chloride ions in concrete structures.

One source of chloride ions is sea water. Structures in a marine environment are exposed to very aggressive conditions in terms of chloride penetration and the corrosion of reinforcement, particularly in the splash zone where there is an adequate supply of all reactants (Mangat and Molloy 1991, Liam et al 1992, Bamforth 1994, 1996). With the development of North Sea oil and gas fields, as well as prestigious structures such as the Dartford Crossing and the Second Severn Crossing which are founded in estuarine conditions, construction in severely corrosive environments is becoming common-place (Concrete 1991). Bridges and other highway structures face attack from chlorides spread as de-icing salts during winter months in order to keep roads ice-free in much of the world. The availability and relative cheapness of sodium chloride, means that there are few alternatives as a bulk deicer. Hence in recent years investigations have been carried out to improve the corrosion resistance of concrete by reducing the transport properties of the binder.

The transport of chloride ions through concrete in a natural environment is a complicated process. Penetration takes place through the pore system of the paste although if the concrete is cracked direct access is available for the chlorides to enter the body of the structural element. For submerged structures diffusion is the dominant mechanism responsible for chloride ingress, whereas for elements where the external surface is subject to some form of wetting and drying cycle chloride penetration is supported by capillary absorption and permeation (Kropp 1995). In addition the penetrating chloride ions may also react chemically or be physically absorbed onto the surface of the cement hydrates (Verbeck 1975, Hoffmann 1984).

In general it is assumed that diffusion is the dominant and rate limiting process involved in the penetration of chloride ions into HCP. Hence the apparent diffusion coefficient is the parameter commonly used to assess a concrete's resistance to chloride ingress.

4.2.2 Factors Affecting Chloride Diffusion into Hardened Cement Paste

In the case of ionic diffusion in water the diffusion coefficients are of the order 10^{-9} m^2/s. This can decrease to 10^{-12} m^2/s for diffusion through water saturated porous cementitious materials. One of the factors contributing to the decrease is the smaller area through which the ions may move in a porous matrix. Other contributory factors are pore size distribution,

interconnectivity of pores, tortuosity of capillary spaces and chloride binding capacity of hydrates (Page et al 1981, Li and Roy 1986). In addition temperature, age of the material, immobilisation and interaction of chlorides ions with hydrates and the pore solution chemistry will influence diffusivity (Kumar and Roy 1986). Atkinson and Nickerson (1984) indicated that temperature had a dual effect on diffusion, firstly due to the basic temperature dependence of the diffusion mechanism and secondly to induced changes in pore structure. For diffusion of chloride ions into a semi-permeable material with and without chemical reaction with the medium, a relationship, as shown in Figure 4.1 has been suggested (Schiessl 1983, Verbeck 1975).

In order to maintain electrical neutrality during the diffusion process, the negative charge carried by the penetrating chloride ions must be balanced by a corresponding flow of other ions. The penetrating chloride ion must either be balanced by a positive ion simultaneously moving into the concrete, or a counter diffusion of negative ions, or an ion exchange with hydration products. Thus chloride penetration depends on the cation involved as well as the concrete pore solution and the hydrates present, all of which may change drastically due to concrete additives, blending materials, or environmental factors such as carbonation (Sergi 1986).

Investigators have shown that elevated curing results in a lowering of diffusivity for pozzolanic cement pastes (Dhir et al 1993a). Goto and Roy (1981) found that curing had a negligible effect on diffusion of sodium and chloride ions below a water:cement ratio of 0.45. Gjørv and Vennesland (1979) reported that curing and water:cement ratio had a major influence on cover concrete.

4.2.2.1 Pore Size

Pores are formed from the remnants of water filled space in the fresh paste. During hydration water is consumed forming voids, which are subsequently filled with hydration products that have precipitated out of the pore solution, leaving pores ranging in size from several mm to a few nm. The volume and size distribution of these pores is largely controlled by the amount of water present at mixing. Pores ranging in size from several 100 μm to a 10 nm are termed capillary pores, through which the transport of fluids occurs.

Gel pores are much smaller, less than 10 nm, and are the spaces between CSH structures, and as such are fixed in size by the type of CSH gel. Turriziani (1964) has shown that different types of gel can form with different C:S ratios, depending on the cement replacement. Thus it is probable that gel pores will vary in size between different CSH gel types. Gel pores are virtually impermeable to chloride ion diffusion (Ngala 1995).

Powers (1954, 1958) studied the effect of water:cement ratio on pore size distribution and found that permeability is related to capillary porosity. However when the w/c ratio of the cement paste is less that 0.4, gel pores control the permeability since capillary pores become inter connected by gel pores. For cementitious materials where the capillary porosity is high, a continuous capillary pore network exists throughout the matrix. Consequently even for mature pastes with a w/c ratio greater than 0.5, capillary porosity dominates permeability.

It is generally acknowledged that the diffusion of chloride ions takes place through capillary pores. A reduction in diffusivity can thus be affected by reducing the volume of capillary pores. It is believed this is one of the ways in which pozzolans such as PFA and latent hydraulic binders such as BFS reduce diffusivity. Their slow reactivity means that hydration products are deposited in the pores of the cement matrix, reducing total and capillary pore volume. In addition these hydration products sub-divide the pore structure reducing connectivity (Kumar and Roy 1986).

Ngala et al (1995) also found chloride ion diffusion to be heavily influenced by capillary porosity. For PFA blended and OPC pastes chloride diffusion coefficients tended to zero as capillary porosity approached zero. However for the same capillary porosity PFA pastes have a notably smaller effective chloride diffusion coefficient, suggesting a greater continuity of the capillary pore system in OPC paste, and also possible surface interactions between chloride ions and cement hydrates.

Kumar and Roy (1986) and Li and Roy (1986) found that water permeability and diffusion of ions were more closely related to median pore radius and threshold diameter than total porosity. (The threshold diameter is the pore size at which significant penetration by mercury of the specimen occurs. The median or mean pore radius is the radius which divides the pore volume by 50%).

As hydration progresses capillary transport is reduced due to decreasing capillary pore size, pore volume and interconnectivity. Below a critical capillary porosity all flow must go through CSH gel pores, but flow will be dominated by paths that contain isolated capillary pore regions, and not those made up of pure CSH gel pores.

4.2.2.2 Connectivity

Atkinson and Nickerson (1984) postulated that constrictivity and not tortuosity is the crucial factor in controlling the diffusion of ions through a cement matrix. They regarded the pore structure of cement paste as large caverns interconnected by pores of very small diameter located in the hydrated gel structure.

Several investigations have studied the relationship between diffusion behaviour and pore geometry, and have shown the diffusion of ions and permeability of fluids through a cement matrix is related to the volume of pores, their size and interconnectivity (Kumar and Roy 1986, Li and Roy 1986). These studies have tended to link diffusion behaviour with pore tortuosity and constrictivity measured by mercury intrusion porosimetry. It must be noted that there are some drawbacks intrinsic to the use of this technique especially when dealing with blended cements (Winslow and Diamond 1970, Feldman 1984, Day and Marsh 1988).

Immediately after mixing, the solid phases in a cement system are discontinuous. As hydration progresses, the solid phase is built up through random growth of reaction products, until it is continuous across the sample. The formation of hydration products results in regions of capillary pore space being encapsulated and cut off from the main pore network, reducing the fraction of pores that form a connected pathway for transport. As this process continues the capillary pore space can lose all long range connectivity, so that 'fast' transport through relatively large capillary pore system would end and 'slow' transport would then be regulated by the smaller CSH gel pores. For systems with w/c ratios above 0.6 there will always be some degree of connectivity of the capillary pores as there is not enough cement present to bring the capillary porosity down to the critical level.

Computer modelling by Bentz and Garboczi (1991) shows that connectivity of the pore system through a sample is lost when capillary porosity falls below 18% ± 5% i.e. transport will occur through capillary pores and gel pores, which connect areas of capillary porosity. Thus transport rate through the gel pores will be the controlling factor.

4.2.2.3 Binding and Adsorption

Chlorides occur in hardened cement paste in three forms: chemically bound, physically adsorbed and free chlorides in pore fluid (Figure 4.2). Relative proportions of each, depend on cement type and content, w/c ratio, curing temperature and age.

Chemically bound chlorides are usually found as calcium chloro-aluminate hydrates or Friedel's salt, formed from the reaction of C_3A and chlorides by the mechanism shown below (Midgley and Illston 1980, 1984, Hoffman 1984).

$$Ca(OH)_2 + 2NaCl \rightarrow CaCl_2 + 2NaOH \qquad \text{Eqn. 4.1}$$

$$CaCl_2 + 3CaO.Al_2O_3 + 10H_2O \rightarrow 3CaO.Al_2O_3.CaCl_2.10H_2O \qquad \text{Eqn. 4.2}$$

In addition to C_3A, other compounds contribute towards the binding of chloride ions, since C_3A free cements have been found to show significant binding capacity (Verbeck 1975). Most of the work carried out on binding capacity of cements involved adding chlorides to the mix water and after a given hydration period expressing the pore solution to determine free chloride content. This is generally not what happens in practice where chlorides enter the hardened cement matrix via the pore system. By adding the chlorides with the mix water, chlorides will be immobilised in the hydration products, which would otherwise not occur if chloride ions penetrated from an external source after significant hydration had occurred. Thus there is some doubt over the validity of binding capacity data from specimens where the chlorides were added at the mixing stage. Midgley and Illston (1984) found that chloride ions penetrating a hardened cement matrix, reacted with anhydrous C_3A, but not with complex aluminate hydrates.

Physically adsorbed chloride ions are those adsorbed onto the pore walls and built into the structures of the hydration products (Tuutti 1980). The amount of physically adsorbed chlorides depends on availability of binding sites and nature of the hydration products. Free and adsorbed chlorides are in equilibrium and so their relative proportions depend on concentration of chloride ions in the pore fluid.

A proportion of chlorides entering via the pore system are adsorbed by hydration products. Since free and adsorbed chlorides are in equilibrium, it is not simply a case of all the binding sites being occupied before concentration in the pore solution can build up and allow diffusion. There will always be a small concentration of chlorides in the pore solution even when binding sites are still available. However corrosion of embedded steel only becomes critical above a given free chloride content (Tuutti 1982).

Free chloride ions in the pore solution are the most significant in terms of corrosion of embedded steel. Chemically bound chlorides are unable to affect corrosion. However physically adsorbed chlorides may act as a buffer for the free chloride ion content of the pore solution, as these are in equilibrium (Arya and Newman 1990). Thus when corrosion begins and the pore concentration of free chlorides drops, physically adsorbed chlorides may be released into solution.

It has been reported (Page and Lambert 1986, Dhir 1991) that prolonged exposure of specimens to chloride ions results in a decrease in the rate of chloride ingress, suggesting modifications to the pore structure and binding properties. Hoffmann (1984) noted a decrease in gel pores in chloride exposed cement mortars attributable to Friedel's salt. Kayyali (1989, 1988) concluded that chloride ingress caused a reduction in permeability due to the formation of smaller discontinuous pores.

Chloride binding capacity increases with pH of the pore solution. This is thought to be a consequence of the increased solubility of Friedel's salt in low pH. As pH of the pore solution decreases, for instance due to a pozzolanic reaction or carbonation, dissolution of Friedel's salt occurs releasing chlorides into the pore solution (Page and Vennesland 1983).

4.2.2.4 Surface Charge Effects

Collepardi et al (1972) investigated the non-steady state diffusion of chloride ions into cement pastes. The large differences in chloride diffusivity for OPC and OPC/pozzolana blends could not be explained by porosity alone. The difference was attributed to different interactions between chloride ions and the pore surfaces, and differing mobility of water molecules present in the gel pores of the materials studied.

Atkinson and Nickerson (1984) measured the diffusivity of Cs^+ and I^- ions and found different values, especially at lower water:cement ratios. They concluded that the diffusion mechanism through cement paste cannot be the same as in the free liquid simply constrained by the pore structure.

Goto and Roy (1981) and Kumar and Roy (1986) investigated the diffusion of positively and negatively charged ions through cement pastes and concluded that the hardened cement matrix may be considered to act as an electronegative membrane, as cation diffusion was retarded compared to that of the anion. It is believed that the surface charges on the pore walls and the associated strongly attached liquid known as the electric double layer influence diffusion by attracting ions and causing a reduction in the rate of diffusion.

Page et al (1981) carried out an investigation into steady state diffusion of chloride ions through hardened cement paste. They found that activation energies for the chloride ions were much higher in cement paste than in aqueous solutions. In addition 0.4 and 0.5 w/c ratio pastes were found to have constant activation energy, but 0.6 w/c paste had a significantly lower activation energy. The authors suggested that the rate limiting process governing the diffusion of chloride ions in mature Portland cement involves some form of surface interaction. Variation in activation energy with w/c was explained in terms of the Powers model. The capillary pore network in well cured 0.4 and 0.5 w/c ratio pastes would be subdivided by gel. Hence diffusing ions would be forced into closer contact with pore walls, causing interaction. In 0.6 w/c ratio pastes a residue of capillary pores might be expected to remain unsegmented, these paths would dominate ionic movement, thus interactions are likely to be less common and not as strong.

Goto and Roy (1981) found activation energies for sodium and chloride ions were 20 kcal/mol and 12 respectively, suggesting a strong interaction between ions and surface hydrates. The effect of w/c (0.45-0.3) on effective diffusion coefficients of sodium and chloride ions was found to be relatively small. The authors ascribed this to the probability that ions diffuse on the surface of the hydrates, or that strong interaction of the ions with the surface hydrates occurs during diffusion.

Ngala et al (1995) found that PFA blended cement pastes limit chloride diffusion more effectively than plain Portland cement systems although the lower diffusivities could not be ascribed solely to reductions in capillary pore volume.

4.2.3 Influence of Blending Materials

Cement pastes containing PFA, BFS and SF exhibit substantially lower diffusion rates than corresponding OPC pastes (Page et al 1981, Gjørv and Vennesland 1979, Dhir and Byars 1993). These blending materials enhance the microstructure of hardened cement paste by forming additional CSH gel on reaction with calcium hydroxide, which in turn reduces capillary porosity.

Kumar and Roy (1986) found that addition of PFA results in lower chloride ion diffusion rates at 38°C and 60°C, attributable to a decrease in interconnectivity of the porous matrix. Although total porosity increased, this was offset by an increase in the proportion of finer pores. Therefore any migrating ion would have to traverse these small pores which would limit diffusion rate. Uchikawa et al (1986) also found that mineral admixtures increased total porosity, but decreased the volume of capillary pores.

Ngala (1995) investigated the effect of PFA and BFS replacement on the diffusion properties of Portland cement paste, and concluded that replacement with 65% BFS produced the best resistance followed by 30% PFA. Chloride diffusivity was found to tend to zero as capillary porosity approached zero. As diffusivity approached zero, total porosity approached 35% for all systems. This figure represents the proportion of gel pores which are virtually impermeable to chloride ions. For the same capillary porosity blended systems have a lower effective diffusivity, suggesting that either the capillary pores are more sub-divided and do not form an extensive interconnected network as found in OPC pastes, or that other factors such as surface interactions with the diffusing ions are occurring. The effective diffusion coefficients of blended pastes were found not to vary significantly with w/c ratio, unlike the case of OPC pastes, which led to the inference that pozzolanic hydrates sub-divide the capillary pore structure. OPC pastes of high w/c ratio do not have a sub-divided capillary pore structure and as a result have high diffusivities.

Li and Roy (1986) hypothesised that pozzolanic additives improved diffusion resistance by producing a significant amount of gel, the critical factor being that gel-type hydrates are located to block pores (Figure 4.3). The authors also calculated the concentrations of cations (Ca^{2+}, Al^{3+}, Si^{4+}) in fly ash pastes to be 2.5 times as high, and that of K^{+} to be half as low, as that in normal OPC. The large cations have lower diffusion rates and restrict the mobility of the coexisting chloride ions whereas the K^{+} ion increases mobility. They also postulated that PFA pastes produce tortuous pore channels in which the movement of chloride ions may be inhibited by interaction with other ions. These ions may exist in the pore channel itself or as part of the electric double layer. Thus they assumed that the activation energy for chloride diffusion in blended cements is considerably higher than that in OPC pastes, though this is not found to be so.

4.2.4 Autogenous Shrinkage

The quest for high strength, high durability concrete has highlighted the problem of autogenous shrinkage in the manufacture of high performance concrete (Jensen and Hansen 1995). There are several forms of shrinkage, although the most commonly known is drying shrinkage, which results from the withdrawal of water from concrete stored in unsaturated air, causing a volume change, part of which is irreversible. Loss of free water, which takes place first, causes little or no shrinkage. As drying continues, adsorbed water is removed and a change in the volume of the unrestrained hydrated cement paste occurs. Although shrinkage is a three dimensional phenomenon it is usually expressed as a linear strain, typical values being of the order 4000×10^{-6} (Neville 1995).

Autogenous shrinkage occurs due to continued hydration of the paste after setting has taken place. The withdrawal of water from capillary pores by the hydration of hitherto unhydrated cement results in a volume change and cracking of the paste matrix, a process known as self desiccation. For ordinary portland cement concrete autogenous shrinkage is of the order 100×10^{-6}, and has been ignored for practical purposes. However at very low water:cement ratios (0.17) values of 4000×10^{-6} have been reported for silica fume and metakaolin pastes, even though they have been stored under water (Tazawa and Miyazawa, 1993, 1995, Kjellsen and Jennings, 1996).

Factors suggested by Neville (1995) as increasing autogenous shrinkage are increases in temperature, cement content, pozzolan content, C_3A and C_4AF content. Aggregate particles however, tend to restrain contraction of the cement matrix, so shrinkage of concrete is an order of magnitude smaller than in neat cement paste. An increase in the fineness of cement will increase autogenous shrinkage in pastes. Particles larger than 75μm that tend to hydrate comparatively little, will have a restraining effect similar to aggregate particles.

4.2.5 Methods of Measuring Diffusion Coefficient

Diffusion coefficients of chloride ions through cement pastes are usually obtained by applying Fick's laws of diffusion. There are two methods commonly used to investigate ionic diffusion in cement systems, concentration profile or non steady state diffusion and steady state diffusion.

4.2.5.1 Non-Steady State Diffusion

Ionic diffusion into a concrete or cement paste sample can be monitored by analysing the depth of penetration or chloride profile after a known exposure period (Collepardi et al 1972, Gjørv and Vennesland 1979, Bamforth 1996). The procedure involves sealing all except one surface of a specimen to prevent multi-directional penetration. The specimen is immersed in a chloride solution and after a given exposure period the specimen is removed and the penetration depth or ionic concentration profile established. Assuming Fick's second law is applicable the apparent diffusion coefficient can be calculated. If the pore system is not saturated with water capillary suction and permeation will occur and the assumption of pure diffusion will be manifestly inappropriate. Immersion experiments are time consuming, however this method has the advantage that it can be applied to in situ concrete structures.

4.2.5.2 Steady State Diffusion

The steady state method has conventionally been used as the most appropriate laboratory method for studying rate of diffusion of a particular species through cement paste. Figure 4.4 shows a typical experimental arrangement used to study steady state diffusion. The method has been applied to concrete specimens although the large thickness of these samples needed to avoid aggregate bridging effects results in long experimental durations.

The underlying assumption of the method is that relationships between measured values of steady-state flux and concentration gradient are in accordance with Fick's first law of diffusion to a reasonable approximation. Complications can arise due to interactions between the diffusing species, electrolyte and pore surface interactions. Whilst the values of effective diffusivity have no fundamental significance and are not material constants but a system property, they provide a useful means of comparison which allows the major factors affecting diffusion kinetics to be evaluated.

Buenfeld (1987) pointed out drawbacks of the steady state method such as the need for thin specimens to reduce "edge effects" and insensitivity to changes in effective diffusion coefficient during long term measurements. In contrast MacDonald and Northwood (1995) found that specimen thickness had a minor effect on effective diffusivity, provided the samples were less than 5 mm thick. They also found that the duration of experiments could

be reduced by increasing the concentration of the chloride solution in compartment 1 (Figure 4.4), without affecting measured effective diffusivity. Specimen to specimen variation was noted to increase with increasing water:cement ratio, attributed to higher susceptibility to segregation in these pastes, or a consequence of using relatively thin disk samples which will be affected by the presence of small entrapped air voids.

The movement of chloride ions under a concentration gradient through a water-saturated porous medium has been described by Fick's first law of diffusion. In such a system it is assumed that diffusion only takes place in the aqueous phase and any adsorbed ions can only move by desorption into the liquid with which they are in equilibrium. A thin disk of cement paste was used to separate two reservoirs, one containing a high concentration of chloride ions (compartment 1) and the other chloride free (Figure 4.4). After an initial period during which steady-state diffusion becomes established across the sample, the build up of chlorides in the low concentration reservoir was monitored. Time required to achieve steady state varied from a few days to a several weeks depending on the cement type and specimen thickness. Throughout the experimental period the chloride ion concentration in compartment 1 was assumed to remain constant, since the concentration of diffused chloride ions was comparatively small. Assuming Fick's first law is applicable the diffusion coefficient can be directly calculated.

The flux of chloride ions entering compartment 2 is given by:

$$J = \frac{V}{A}\frac{dC_2}{dt} = \frac{D_{eff}}{l}(C_1 - C_2) \qquad \text{Eqn 4.1}$$

where

J	flux of chloride ions entering compartment 2 ($mol.cm^{-2}s^{-1}$)
D_{eff}	Diffusion coefficient (cm^2/s)
l	Thickness of specimen (cm)
V	Volume of solution in compartment 2 (cm^2)
A	Diffusion area (cm^2)
C_1, C_2	Concentration of chloride ions in compartments 1 and 2 respectively

Integrating both sides between t and t_0 gives

$$\frac{V}{A}C_2 = \frac{D_{eff}}{l}(C_1 - C_2).(t - t_o) \qquad \text{Eqn 4.2}$$

$$\frac{C_2}{C_1 - C_2} = \frac{D_{eff} A}{Vl}(t - t_o) \qquad \text{Eqn 4.3}$$

for $t > t_0$ $C_1 >> C_2$

$$C_2 \approx \frac{DAC_1}{Vl}(t - t_o) \qquad \text{Eqn 4.4}$$

D_{eff} may be calculated from the slope S of C_2 vs. t

$$D_{eff} \approx \frac{VlS}{AC_1} \qquad \text{Eqn 4.5}$$

D_{eff} may be expressed as a function of temperature by the Arrhenius equation.

$$D(T) = D_o e^{-\frac{U}{RT}} \qquad \text{Eqn 4.6}$$

D_0	constant
U	Activation Energy
R	Gas Constant
T	absolute temperature (K)
D(T)	Diffusion coefficient at temperature T.

Taking logs gives

$$\text{In } D(T) = \text{In } D_0 - \frac{U}{RT} \qquad \text{Eqn 4.7}$$

by plotting log D(T) against $\frac{1}{T}$ activation energy can be calculated from the slope.

4.2.6 Resistivity of Cement Systems

Electric current is conducted through concrete by electrolytic means, that is by ions in the pore solution, with electronic conduction through the solid matrix being negligible due to its much higher resistivity (Whittington et al 1981, Hammond and Robson 1975).

Since resistivity is a function of the pore structure and water filling the pores, it has been suggested by Andrade et al (1993) that it can be used to assess the proportion of pores available, for gas or chloride penetration. Buenfeld and Newmann (1984) showed that

electrical resistivity is related to permeability, which in turn influences the strength and durability of a specimen. Hence the electrical resistivity of pastes can be used to assess mass transport properties and variability between samples.

Investigators have also shown that electrical resistivity can be used to assess the severity of corrosion of embedded steel in concrete (Hope et al 1985, Millard et al 1990). Corrosion rate is controlled by the ease with which ions can pass through the concrete from cathodic to anodic regions. Hence a large potential gradient associated with a low concrete resistivity will normally result in high corrosion rates.

4.2.6.1 Measurement of Electrical Resistivity

Resistivity is a fundamental property of a particular material and is defined as the resistance between opposite faces of a unit cube of that material. Resistivity is independent of the volume, whereas resistance depends upon shape and size of the specimen.

$$\rho = \frac{V}{I} \cdot \frac{A}{l} \qquad \text{Eqn 4.8}$$

ρ	Resistivity (Ωcm)
V	Voltage (V)
I	Current (I)
A	Area (cm^2)
l	Thickness of specimen (cm)

The conductivity of a material is defined as the reciprocal of its resistivity.

$$\sigma = \frac{1}{\rho} \qquad \text{siemens } m^{-1} \qquad \text{Eqn 4.9}$$

It is generally acknowledged that measurement of resistivity using direct current produces polarisation of the electrode, with most investigators using alternating current of high frequency (1000 Hz) to eliminate polarisation effects (Whittington et al 1981, McCarter et al 1995).

Measurement techniques involve applying an alternating current through a known volume of specimen. If external plate electrodes are used, conducting media such as agar gel or blotting paper soaked in an electrolyte are included between electrode and sample to facilitate electrical contact, since errors can arise due to non-uniform contact between the concrete and electrode. The choice of electrode arrangement has a significant effect on measured values. The most commonly used technique for insitu site testing is the Wenner 4-

probe technique (Millard et al 1990, Ewins 1990). The probe is placed on the surface of the test concrete and an alternating current passed between the outer two electrodes while voltage across the inner two is recorded. One of the drawbacks of this technique is that the conduction paths are not accurately known, especially if embedded steel is near the surface. The technique can be improved by embedding electrodes of known area in the concrete at known separation distances.

More accurate resistivity values are obtained using external plate electrodes enabling the current to traverse the full area of the specimen (Whittington et al 1981). Errors due to edge effects are further reduced if the area of the specimen is much greater than its thickness.

4.3 EXPERIMENTAL PROCEDURE

4.3.1 Steady State Diffusion

Cement paste cylinders were cast and cured as described in Chapter 2. Discs 2.5 to 3 mm thick were cut from the central regions of each cylinder using a Cambridge Research Microslice, the diamond cutting wheel being lubricated with deionised water. To ensure saturation the discs were kept under curing solution for a further week before their surfaces were lightly ground with 200 grade emery paper to remove any burrs which would prevent a water tight seal in the diffusion cell. Each disc was then measured for bulk density and resistivity to ensure uniformity between specimens before mounting in diffusion cells as shown in Figure 4.4. Greased rubber gaskets and PTFE tape were used to form a water-tight seal, with a layer of PVC tape for additional rigidity. During filling of the cell the paste disk was examined for any sign of leakage due to cracks or imperfections, before being placed in a water bath at 25^{o}C. After steady state had been established, 100 µl aliquots of solution were extracted from compartment 2, on a regular basis, and analysed for chloride concentration using a spectrophotometric technique described in Chapter 2.

4.3.2 Electrical Resistivity

The experimental arrangement is shown in Figure 4.5. A cement paste disc was sandwiched between two compartments, each containing a stainless steel electrode and an electrolyte of 0.035M NaOH. Rubber gaskets were used to provide a water tight seal between electrolyte reservoir and cement disk, and also a known exposure area. The apertures of the rubber gaskets were aligned using bolts, to eliminate spurious end effects.

Using an AC power source, an alternating current of 100 MHz and potential of 10 Volts were applied through the specimen. The current and voltage across the specimen were measured, and knowing the conducting area and thickness of the disc the resistivity of the specimen could be calculated from equation 4.8.

4.4 RESULTS AND DISCUSSION

4.4.1 Preparation Procedure

Initial diffusion experiments with unplasticized hand mixed MK pastes produced inconsistencies between batches, although within a batch the results were similar. A possible reason for these inconsistencies was that hand mixing without the aid of a dispersant was insufficiently vigorous to homogenise the OPC/MK mix. This resulted in a 'plum pudding' arrangement with agglomerates of MK, possibly with an hydrated outer crust, embedded throughout the OPC matrix. As a consequence full pozzolanic hydration was not possible, and the reaction occured to varying degrees dependent on degree of dispersion.

In fact as water:binder ratio increases, dispersion of the MK is aided, resulting in a greater pozzolanic reaction than occurs in a poorly dispersed mix of lower water:binder ratio. As a consequence of the additional pozzolanic hydrate, mixes of high water:binder ratio had lower diffusivities and mass transport properties than similar mixes of lower water content. It should be noted that although MK pastes deviated from expected water:cement ratio and diffusivity relationships, no MK pastes had higher diffusivities than control OPC mixes.

Sellevold et al (1981) reported variations in the properties of silica fume pastes when used without a suitable dispersant . The small particle size of SF resulted in the formation of agglomerations which could not be dispersed by mixing alone.

A series of experiments was carried out to assess the effect of mixing procedure on mass transport properties of MK pastes, and establish a manufacturing procedure to produce consistent samples. The investigation described in Appendix B indicated that preparation procedure has a marked effect on the properties of the resultant hardened cement paste.

The most consistent results were obtained by pre-mixing the MK, water and a type N plasticiser to form a slurry. OPC powder was then gradually added to the slurry whilst continually mixing with an Hobart mechanical mixer. Once all the constituents had been added the paste was mixed for a further 7 minutes.

The formation of a MK slurry may not be necessary for mortars and concretes, as the aggregate may help to break up agglomerates by milling. In addition the small scale nature of these heterogeneities would be masked by the insensitivity of using concrete samples.

4.4.2 Effect of MK on Effective Diffusivity

Effective chloride diffusion coefficients were calculated for OPC, and 5, 10 and 20% MK pastes, and are shown in Tables 4.2 to 4.5 (Appendix C details an example calculation). Capillary and total porosities listed, were obtained using the desorption technique detailed in Chapter 2. Also shown are bulk densities and resistivity values. The correlation and consistency of these results between replicate specimens validate the preparation method employed.

Figure 4.6 shows that the effective diffusion coefficients obtained for MK pastes were lower than those for OPC pastes, especially at high water:binder ratios. Even at a replacement level of 5% MK significant reductions in diffusivity were obtained in comparison to OPC controls. A notable feature of MK blends, is that the diffusivity varies little with water:binder ratio, as highlighted by Figure 4.7. Effective diffusion coefficients for OPC pastes increase by a factor of 10 with an increase in water:cement ratio from 0.4 to 0.65, while in contrast 20% MK pastes increase by a factor of 2. A possible explanation is that MK hydrates are impermeable to chloride ions, and are precipitated, blocking pores and segmenting the capillary network within the cement matrix. Consequently large reductions in diffusivity result from relatively small changes in total and capillary porosity. This mechanism has been proposed for other pozzolanic systems by Feldman (1984), Li and Roy (1986) and Ngala (1995). Figure 4.7 also highlights the similar performance of MK pastes of differing MK dosage at the same water:binder ratio. Again this could be attributed to pore blocking of the capillary network, as opposed to a large reduction in total porosity having a dramatic effect on diffusivity. The relatively low replacement levels of MK necessary to reduce effective diffusivity could also be attributed to the high reactivity of MK, which has been found to react with its own weight of calcium hydroxide in the Chapelle test (Kostuch et al 1993). Pozzolans such as PFA, may require high replacement levels to effect significant reductions in diffusivity, due to its lower reactivity, whereas MK appears to be a very efficient calcium hydroxide "mop".

Interestingly, chloride diffusivity does not decrease with increasing MK replacement level. In theory OPC produces 15% of calcium hydroxide by weight on full hydration (Neville 1995). From Chapelle tests it has been shown that MK reacts with lime on a 1:1 basis by weight (Kostuch et al 1993). Consequently a 10% replacement should consume 80% of the calcium hydroxide available, and a 20% replacement should be sufficient to consume all the lime, even taking into account heterogeneity within the mix, leaving an excess of MK. Any unreacted MK might be expected to act as a very fine inert aggregate, and would certainly not be expected to detrimentally affect diffusivity. Given these factors increasing MK content should reduce diffusivity. This is not the case, so there must be another factor

influencing diffusivity, possibly the production of a lower volume of hydrates due to the reduced quantity of OPC.

Tazawa and Miyazawa (1993,1995) measured autogenous shrinkage in MK and SF pastes stored under water. The high pozzolanic reactivity of these materials resulted in the rapid formation of a matrix with a discontinuous capillary pore network. They postulated that as hydration progressed water in the central regions of the mix was consumed, and could not be replenished quickly enough by migration of water from external areas resulting in cracking. Autogenous shrinkage is likely to become more significant as water:binder ratio decreases, and pozzolanic replacement level increases. Kjellsen and Jennings (1996), using an environmental scanning electron microscope, measured microcracks formed as a result of autogenous shrinkage in silica fume pastes. Crack widths of the order 100 to 500 nm, approximately the size of capillary pores, were observed depending on relative humidity conditions. The results shown in Figure 4.7 could indicate the formation of extra capillary pores as a consequence of autogenous shrinkage.

Figure 4.8 shows that as capillary porosity decreases to zero, chloride diffusivity also reduces to zero, for both OPC and 5, 10, 20% MK systems. This is in agreement with other workers who have shown that chloride diffusion in cement paste takes place through capillary pores, and implies gel pores are virtually impermeable to chloride ions (Powers 1954, Ngala 1995). For a given capillary porosity OPC and MK systems have different diffusivities. Ngala (1995) attributed this to a greater continuity of capillary pores in OPC pastes.

The plot of chloride diffusivity against total porosity (Figure 4.9) indicates that as chloride diffusion coefficient tends to zero, total porosity converges to a value of between 30 and 35% for both OPC and MK systems. Ngala (1995) attributed this pore volume to the proportion of gel pores completely impermeable to chloride ions.

The MK diffusion coefficients are not as low as those reported by Ngala (1995) for PFA and BFS blends, although different curing regimes were employed in the two separate investigations. Ngala concluded that curing at 38°C improved the pore structure of blended cements by promoting pozzolanic hydration and reducing $Ca(OH)_2$ content. It is not known what effect warm moist curing will have on MK blended pastes. OPC pastes are believed to have coarser pore structure after warm curing (Detwiler et al 1991), and Turriziani (1964) reported that one of the hydrates of MK, gehlenite hydrate (strätlingite), becomes unstable above 50°C. However the chloride diffusion rates of MK pastes do compare favourably with results in similar studies listed in Table 4.1.

4.4.3 Activation Energy

From the Arrhenius plots shown in Figure 4.10 activation energies were calculated. OPC and 20% MK pastes of water:binder 0.5 had activation energies of 53.1 and 30.1 kJ/mol respectively.

The different activation energies for chloride ion diffusion through cement paste compared to that for electrolyte solutions (17.6 kJ/mole) led Page et al (1981) to conclude that the rate limiting process governing the diffusion of chloride ions in OPC paste involves some form of surface interaction.

Ionic diffusion through cement paste occurs through the pore solution. Chloride ions adsorbed onto the hydrates can only move by desorption into the pore fluid. A possible explanation for the different activation energies is that the kinetics of the MK and OPC systems are different. Jones et al (1992) have shown that MK absorbs alkali metal ions such as Na^+ and reduces the occurrence of ASR. Larbi (1991) showed that MK reduced the diffusivity of sodium ions much more than for chloride ions. Therefore MK may reduce chloride diffusivity by hindering the progress of the co-diffusing cation.

4.4.4 Resistivity

Resistivities listed in Tables 4.2 to 4.5 for saturated hardened cement pastes containing MK increase with decreasing water binder ratio as expected. As water content decreases the volume of pores decreases, reducing the quantity of evaporable water available through which conduction can take place. Figure 4.11 shows the plot of chloride diffusivity and resistivity for the OPC and MK systems, confirming that there is a relationship between mass transport properties and the electrical resistivity of a hardened cement paste. The plot suggests that there are different factors controlling ionic movement in OPC and MK blended systems.

MK blends have higher resistivities than OPC pastes, indicative of a higher resistance to chloride movement. However it should be pointed out that the current carried through the sample is not carried purely by chloride ions, but by all the ions in the pore fluid.

4.4.5 Ternary Blends

Tables 4.6 and 4.7 list effective diffusivities for ternary blended pastes containing OPC, MK and PFA or BFS. Ternary blends exhibit low effective chloride diffusion coefficients, an order of magnitude smaller than OPC mixes. Comparing the diffusivity values of the ternary blends with those for 10% MK shows that the reduction in diffusivity is not purely due to the MK component (Figure 4.12). The low effective chloride diffusivities must be due to a

symbiotic relationship between the constituents of the binder. Thus there would appear to benefits in combining slow and fast reacting pozzolans to improve durability.

The ternary blends were formulated so that all of the lime produced by hydration of the OPC would be consumed by pozzolanic reaction, thereby maximising the improvements in resistance to chloride ingress. Using Chapelle test data the MK/BFS blends theoretically contain sufficient pozzolan to consume all the lime produced by hydration, whereas the MK/PFA blends contain an excess of pozzolan.

The use of ternary blends containing BFS or PFA and MK shows potential for the economical production of high durability concrete. The high cost of MK may be offset by combining it with a cheaper cement replacement, and a lower cement content. From these results it would appear the benefits in terms of low chloride diffusivities may not be significant when compared to binary systems. However the rapid reaction of MK with calcium hydroxide may go some way to overcoming delayed strength gain associated with common cement replacement materials. Fine tuning of the blend proportions would also be necessary to find an optimum combination in terms of strength and durability, while at the same time ensuring a workable mix.

4.5 CONCLUSIONS

The inclusion of metakaolin as a cement replacement material reduces the diffusion rate of chloride ions through saturated cement pastes, when compared with OPC controls. Significant reductions were obtained even at low replacement levels of 5% MK.

The use of BFS or PFA in combination with MK in ternary blends produced cement pastes with low chloride diffusion coefficients, an order of magnitude smaller than comparable OPC pastes.

For a given capillary porosity MK pastes had lower chloride diffusion rates than OPC pastes, suggesting that the mechanism responsible for improving the diffusivity was segmentation of the pore network by metakaolin hydrates.

The different activation energies for chloride diffusion in OPC and MK pastes suggests that different factors are controlling the mechanisms in each of the cementitious systems.

Aston University
Illustration removed for copyright restrictions

Figure 4.1 Diffusion of chloride ions into a semi-permeable material (modified from Verbeck 1975).

Aston University
Illustration removed for copyright restrictions

Figure 4.2 Occurrence of chlorides in hardened cement paste (Tuutti, 1980).

Figure 4.3 Schematic showing pozzolanic hydrates forming a plug in a pore (Li and Roy, 1986).

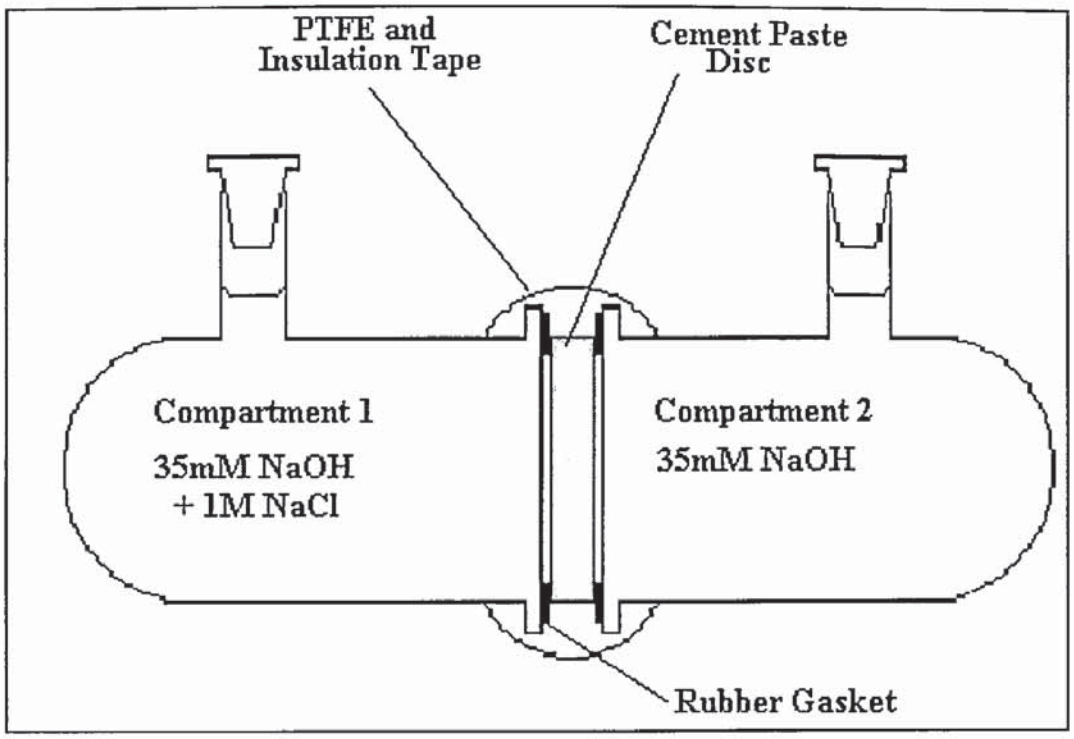

Figure 4.4 Experimental arrangement of a steady state diffusion cell.

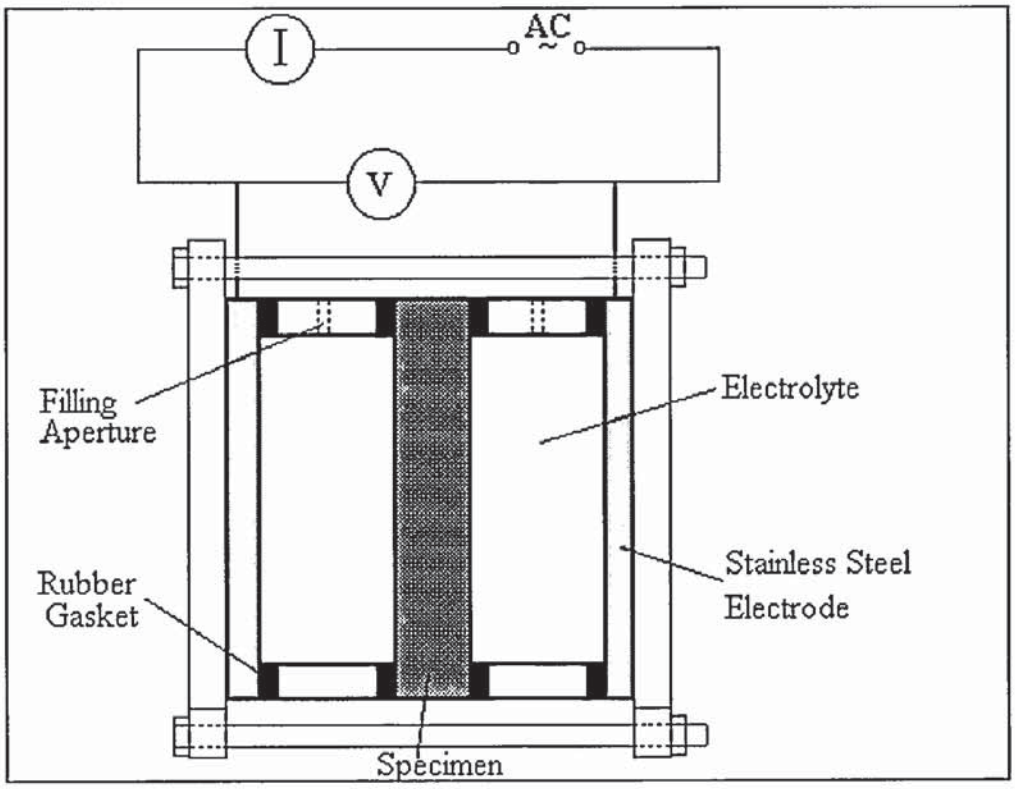

Figure 4.5 Experimental arrangement of resistivity cell.

Source	Mix	Age (Days)	W/B Ratio	Temp. (°C)	D ($x10^{-8}$ cm^2/s)
Page et al (1981)	OPC	60	0.4	25	2.6
		60	0.5	25	4.47
		60	0.6	25	12.35
	30%PFA	60	0.5	25	1.47
	65%BFS	60	0.5	25	0.41
Goto and Roy (1981)	OPC	28	0.4	27	6.9
Kumar & Roy (1981)	OPC	28	0.35	27	7.51
Gautefall (1986)	OPC	180	0.5	20	5.79
			0.7	20	9.28
			0.9	20	19.1
Byfors (1987)	OPC	420	0.4	22	1.8
			0.5		6.8
			0.6		18.7
	15%PFA		0.4		0.63
			0.5		3.2
			0.6		2.6
	40%PFA		0.5		0.32
			0.6		1.7
Larbi (1991)	20% MK Mortar	100	0.4	20	0.01
Tang & Nilsson (1992)	OPC	45	0.4	22	2.9
			0.5	22	9.4
			0.8	22	21.0
Ngala et al (1996)	OPC	90	0.4	25	3.95
		90	0.5	25	7.8
		90	0.6	25	12.6
		90	0.7	25	21.46
	30%PFA	90	0.4	25	0.39
		90	0.5	25	0.43
		90	0.6	25	0.9
		90	0.7	25	1.03

Table 4.1 Summary of steady state diffusion data reported in previous investigations.

Water:Binder	Chloride Diffusivity ($x10^{-8}cm^2/s$)	Resistivity ($k\Omega.cm$)	Bulk Density (g/cm^3)	Capillary Porosity (%)	Total Porosity (%)
0.4	1.69	6.50	2.021	1.96	35.10
	2.06	6.47	2.019	1.95	34.98
	1.88	6.51	2.020	1.96	35.25
	2.13	6.48	2.019	2.05	34.52
		6.52	2.023	2.18	35.03
Average	1.94	6.50	2.020	2.02	34.98
0.5	4.98	4.98	1.908	6.37	40.43
	4.79	4.95	1.906	5.98	41.30
	5.32	5.04	1.911	5.99	41.21
	4.79	5.20	1.909	5.89	41.00
	5.51	5.11	1.910	6.31	41.34
Average	5.08	5.06	1.909	6.11	41.06
0.65	8.05	4.04	1.762	10.52	51.17
	8.51	3.82	1.766	10.38	51.38
	9.09	3.82	1.765	10.42	51.01
	8.59	3.79	1.775	10.39	51.19
	9.99	3.82	1.772	10.74	50.96
Average	8.85	3.86	1.768	10.49	51.14

Table 4.2 Results for OPC pastes cured under 35mM NaOH for 100 days.

Water:Binder	Chloride Diffusivity ($x10^{-8}cm^2/s$)	Bulk Density (g/cm^3)	Capillary Porosity (%)	Total Porosity (%)
0.4	0.71	1.985	1.30	40.097
	0.53	1.972	1.27	39.953
	0.68	1.971	1.40	40.017
	0.58	1.981	1.32	40.005
	0.52	1.982	1.25	41.069
Average	0.60	1.978	1.31	40.228
0.5	1.21	1.872	2.36	45.27
	1.31	1.864	2.62	45.29
	1.25	1.870	2.28	45.24
	1.29	1.868	2.55	45.37
	1.42	1.877	2.58	45.25
Average	1.30	1.870	2.48	45.29
0.65	1.75	1.816		
	2.14	1.803		
	1.66	1.804		
	1.87	1.788		
	1.93	1.774		
Average	1.87	1.797		

Table 4.3 Results for 5% MK pastes cured under 35mM NaOH for 100 days.

Water:Binder	Chloride Diffusivity ($x10^{-8}cm^2/s$)	Resistivity ($k\Omega.cm$)	Bulk Density (g/cm^3)	Capillary Porosity (%)	Total Porosity (%)
0.4	0.59	20.55	1.978	2.33	39.71
	0.69	21.25	1.976	1.90	39.63
	0.59	21.59	1.959	1.43	39.48
	0.46	21.75	1.966	1.40	39.72
	0.41	22.98	1.967	1.36	39.64
Average	0.55	21.62	1.969	1.69	39.64
0.5	1.23	10.97	1.878	2.70	48.81
	1.41	10.79	1.882	2.88	48.85
	1.40	10.68	1.877	2.46	48.53
	1.44	10.86	1.881	2.85	48.94
	1.06	11.08	1.868	2.32	48.86
Average	1.31	10.88	1.877	2.64	48.80
0.65	1.78	8.02	1.728	4.07	52.79
	2.06	8.08	1.722	4.38	52.64
	2.32	8.42	1.717	3.83	52.54
	1.52	8.25	1.718	4.69	52.90
	1.97	8.03	1.722	4.24	52.72
Average	1.93	8.16	1.721	4.24	52.72

Table 4.4 Results for 10% MK pastes cured under 35mM NaOH for 100 days.

Water:Binder	Chloride Diffusivity ($x10^{-8}cm^2/s$)	Resistivity ($k\Omega.cm$)	Bulk Density (g/cm^3)	Capillary Porosity (%)	Total Porosity (%)
0.4	1.10	12.50	1.944	1.16	42.32
	1.00	13.32	1.946	1.27	42.02
	0.95	16.74	1.945	1.23	42.34
	0.66	14.17	1.942	1.12	42.50
	0.90	15.42	1.949	1.20	42.46
Average	0.92	14.43	1.945	1.20	42.33
0.5	1.36	10.87	1.859	2.17	46.25
	1.39	9.63	1.858	2.98	45.50
	1.34	10.16	1.861	2.73	45.64
	1.15	9.53	1.868	2.28	46.48
	1.17	10.14	1.857	2.03	47.12
Average	1.28	10.07	1.861	2.44	46.20
0.65	2.50	9.34	1.738	5.15	53.15
	1.69	8.63	1.736	5.94	52.76
	1.45	8.46	1.742	7.05	53.09
	1.90	9.02	1.745	4.82	53.15
	2.28	8.92	1.738	6.75	53.17
Average	1.96	8.87	1.740	5.94	53.06

Table 4.5 Results for 20% MK pastes cured under 35mM NaOH for 100 days.

Water:Binder	Chloride Diffusivity ($x10^{-8}cm^2/s$)	Resistivity ($k\Omega.cm$)	Bulk Density (g/cm^3)	Capillary Porosity (%)	Total Porosity (%)
0.4	0.59	19.61	1.960	1.76	39.69
	0.53	19.47	1.962	1.38	39.17
	0.59	19.24	1.965	1.36	39.02
	0.41	19.60	1.969	1.22	39.08
		19.73	1.966	1.43	39.05
Average	0.53	19.53	1.964	1.43	39.20
0.5	0.79	13.94	1.841	2.12	45.83
	0.71	13.38	1.843	2.11	46.06
	0.49	13.76	1.844	2.18	46.17
	0.35	13.80	1.845	1.91	43.64
	0.47	13.60	1.838	2.20	45.76
Average	0.56	13.70	1.842	2.10	45.49
0.65	0.55	10.66	1.747	5.32	52.03
	0.79	10.62	1.757	4.42	50.95
	0.53	10.22	1.753	4.77	51.66
	0.41	9.83	1.758	4.47	51.15
	0.70	9.42	1.757		
Average	0.60	10.15	1.754	4.74	51.45

Table 4.6 Results for 8% MK/20%PFA pastes cured under 35mM NaOH for 100 days.

Water:Binder	Chloride Diffusivity ($x10^{-8}cm^2/s$)	Resistivity ($k\Omega.cm$)	Bulk Density (g/cm^3)	Capillary Porosity (%)	Total Porosity (%)
0.4	0.62	26.56	1.948	2.45	42.51
	0.77	26.78	1.956	2.51	42.18
	0.42	26.40	1.952	2.46	42.12
	0.64	27.01	1.955	1.80	41.82
	0.33	26.88	1.961	2.02	41.78
Average	0.56	26.73	1.954	2.25	42.08
0.5	0.63	20.77	1.842	2.04	45.82
	0.79	21.23	1.843	2.11	46.67
	0.52	21.20	1.844	2.19	47.02
	0.69	21.36	1.849	2.32	47.40
	0.33	21.16	1.853	4.53	47.68
Average	0.59	21.14	1.846	2.64	46.92
0.65	0.68	14.20	1.707	6.21	54.53
	0.66	14.70	1.711	5.70	53.94
	0.75	14.40	1.717	5.14	54.13
	1.00	15.04	1.711	5.32	54.37
	0.82	15.07	1.713		
Average	0.79	14.68	1.712	5.59	54.24

Table 4.7 Results for 8%MK/40%BFS pastes cured under 35mM NaOH for 100 days.

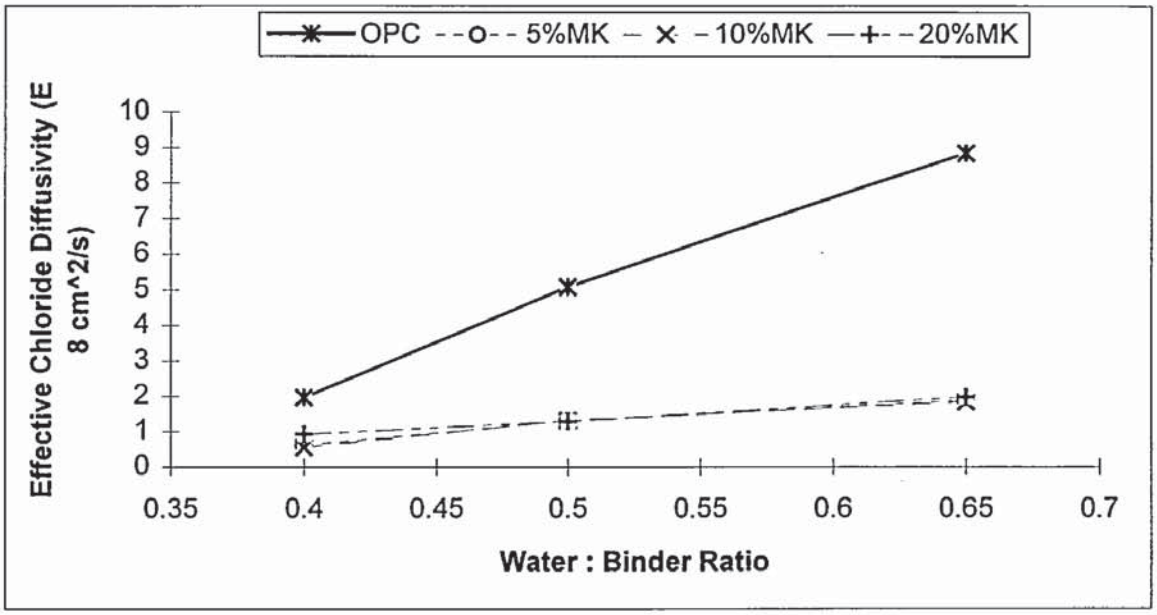

Figure 4.6 Effect of water/binder ratio on effective chloride diffusivity.

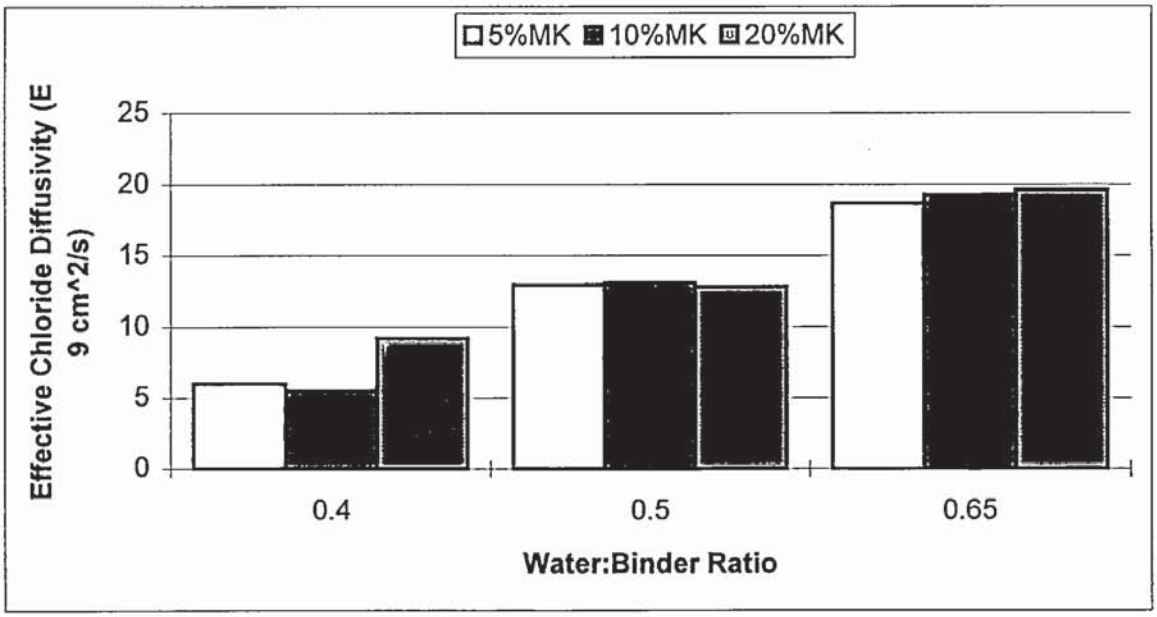

Figure 4.7 Effect of MK replacement level on effective chloride diffusivity.

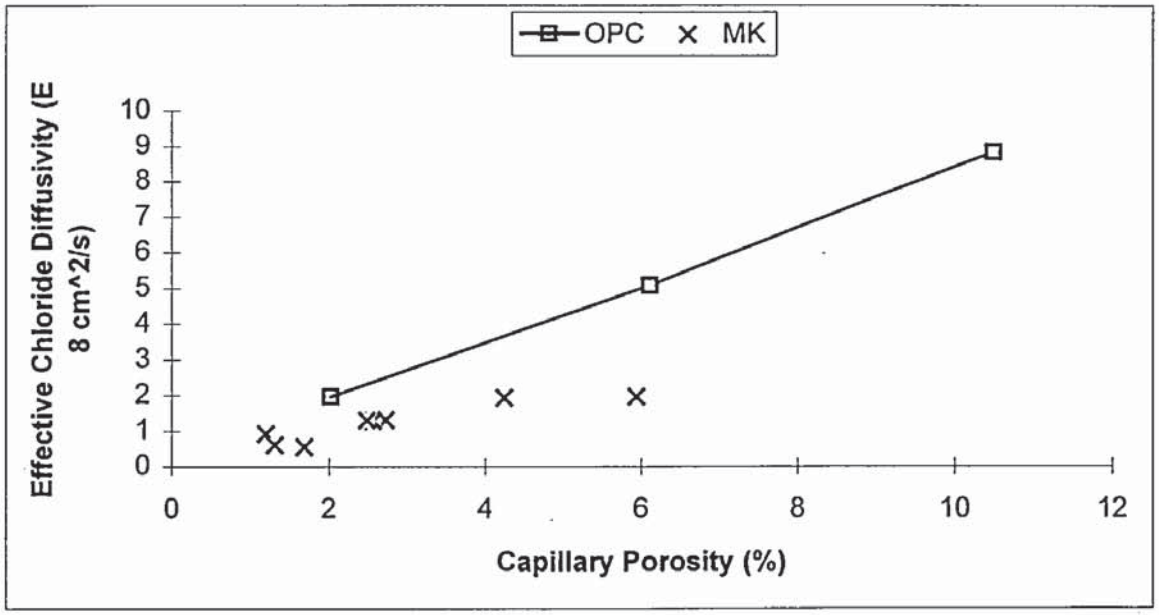

Figure 4.8 Plot of effective chloride diffusivity against capillary porosity.

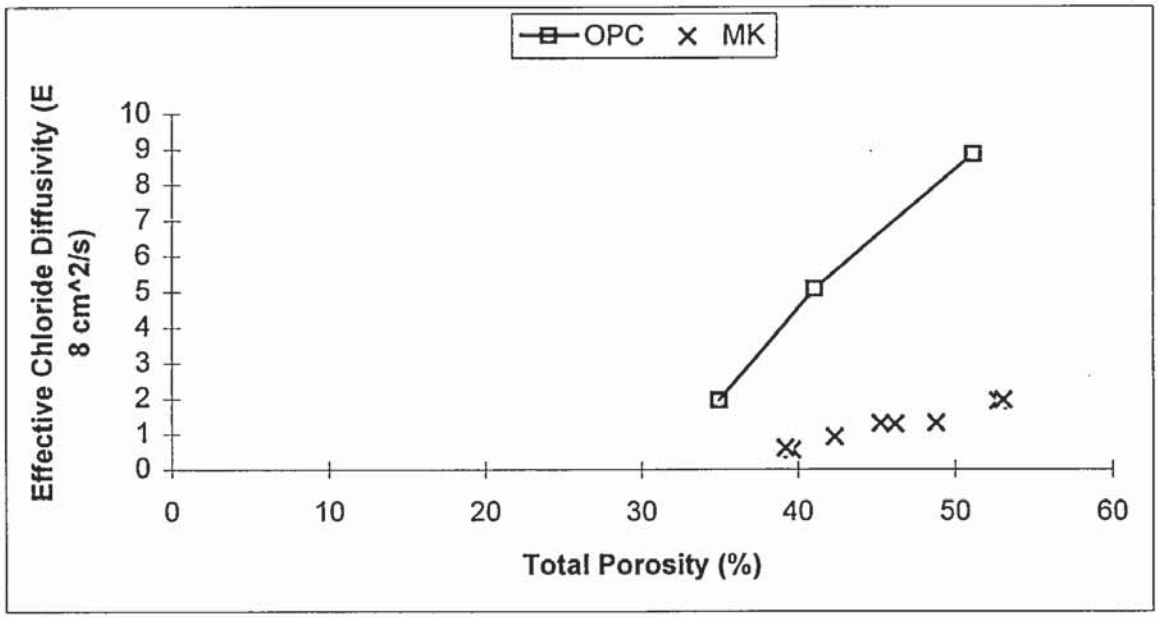

Figure 4.9 Plot of effective chloride diffusivity against total porosity.

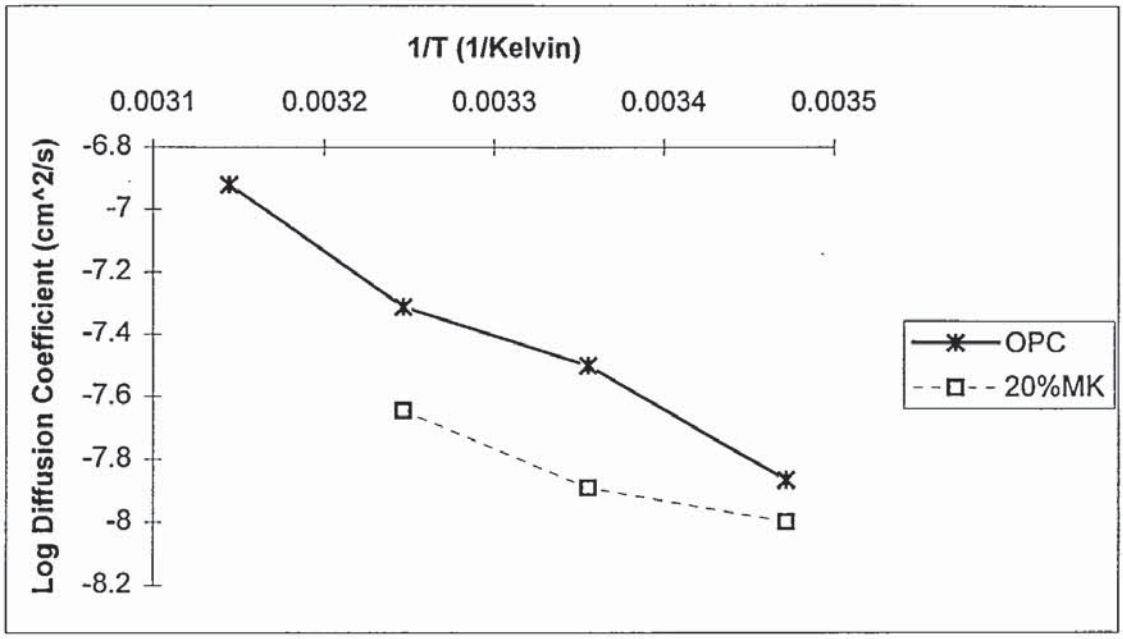

Figure 4.10 Arrhenius plots for OPC and 20% MK pastes of water/binder ratio 0.5.

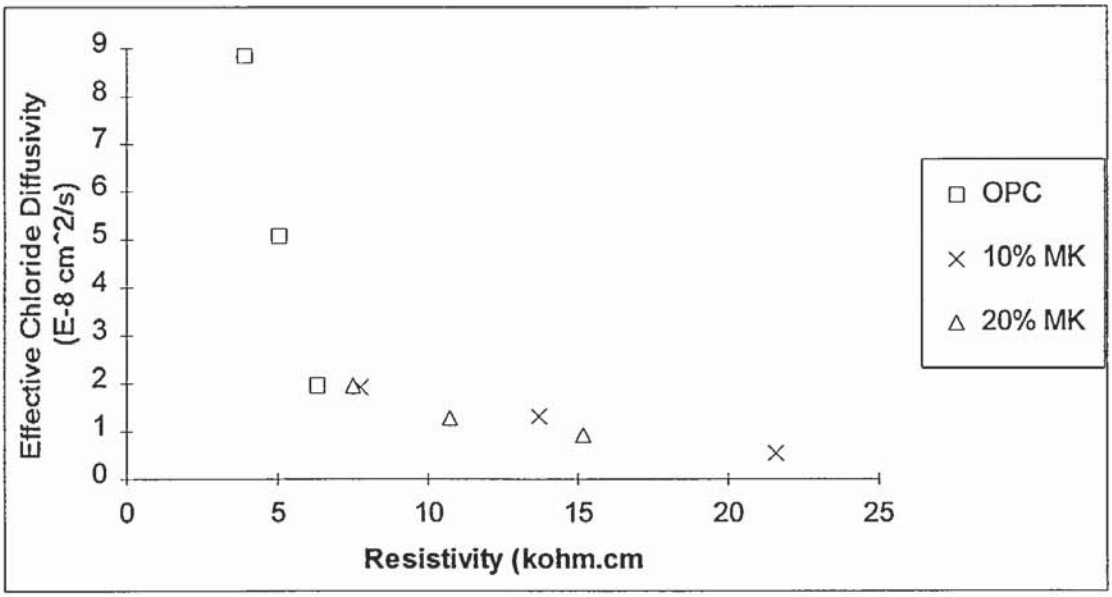

Figure 4.11 Plot of effective chloride diffusivity against resistivity.

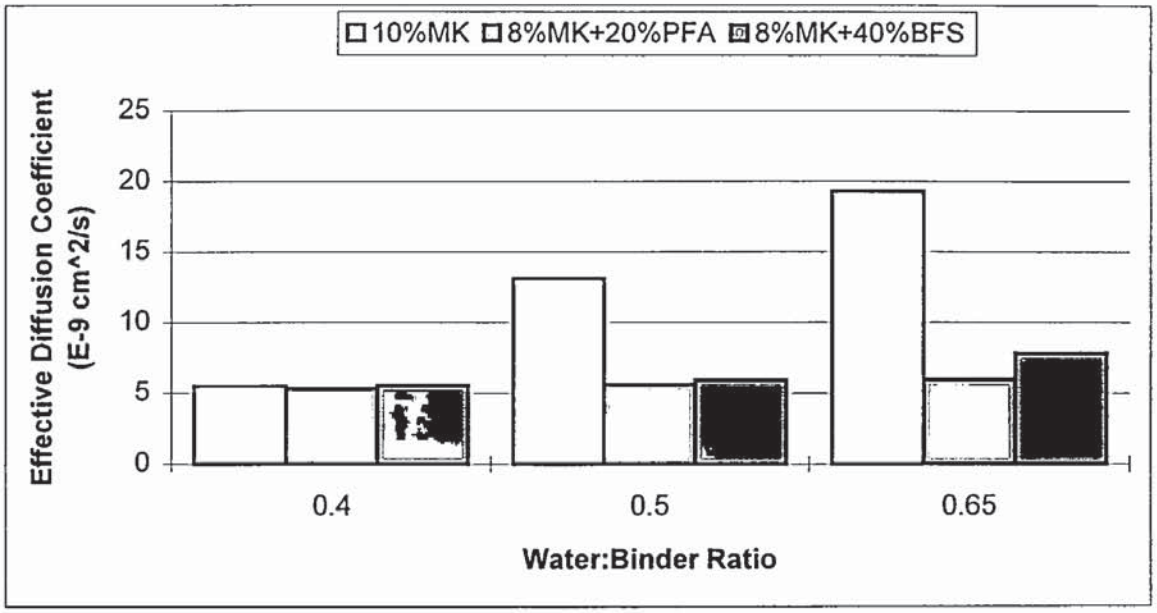

Figure 4.12 Effective diffusion coefficients for ternary blends.

CHAPTER 5

5. OXYGEN DIFFUSION THROUGH HARDENED CEMENT PASTE

5.1 INTRODUCTION

Steel embedded in a cement system is usually protected from significant corrosion by a surface film of γ-Fe_2O_3. The iron oxide forms a passive film around the bar which is thermodynamically stable in alkaline conditions commonly found in cement pore fluid. Breakdown of the passive film can occur by carbonation which reduces pore fluid pH rendering the iron oxide unstable, or through the presence of chloride ions which stimulate local disruption of the film leading to pitting corrosion (Page and Treadaway 1982). In both instances the presence of dissolved oxygen at a corrosion site is essential to perpetuate the process as indicated by the following equations:

Anodic Reaction

$$Fe_{(s)} + \rightarrow Fe^{2+} + 2e^- \qquad \text{Eqn. 5.1}$$

Cathodic Reaction

$$O_2 + 2H_2O + 4e^- \rightarrow 4OH^- \qquad \text{Eqn 5.2}$$

If oxygen is not present, the cathodic reaction cannot proceed and corrosion is halted. This phenomenon is termed "cathodically restrained general dissolution", and most commonly occurs in fully submerged marine structures. If the cathodic reaction becomes controlled by the diffusion rate of oxygen, it may be insufficient to balance the anodic "leakage" current density required to maintain a passive film and cathodically restrained general dissolution ensues. The steel undergoes uniform anodic dissolution at a very low rate, and is generally insignificant except where abnormally long service life is required.

High corrosion rates are more likely to occur in splash zones where the concrete is periodically wet and dry enabling rapid access for both water and oxygen. Several workers have investigated the influence of oxygen diffusivity on progress of corrosion although in this particular investigation, oxygen diffusion through saturated cement paste is studied not for cathodically restrained general dissolution, but to assess the effect of pore surface interactions on diffusion processes.

The diffusion process is an important feature of common forms of degradation, and an understanding of the factors influencing the phenomenon is of interest. It is known that geometrical factors such as tortuosity and pore size distribution play a significant role in diffusion. Less is known of the relationship between pore surfaces and diffusing species interaction.

Oxygen molecules and chloride ions have similar sizes and diffusion coefficients in infinitely dilute solutions, 2.1×10^{-5} and 2.03×10^{-5} cm^2/s at 25°C respectively (Cussler 1984). Thus one might expect similar diffusion coefficients through hardened cement paste for both species if surface interactions played no part. In comparison with diffusion of chloride ions, however, diffusion of oxygen would be considerably less affected by the surface charge or double layer at the pore solution interface, since oxygen is a neutral molecule without dipolar character.

5.2 LITERATURE REVIEW

5.2.1 Measurement of Oxygen Diffusion Through Hardened Cement Paste

Kobayashi and Shuttoh (1991) and Ohama et al (1991) have investigated the diffusion of oxygen gas through mortar specimens preconditioned at several relative humidities, with the aim of evaluating the effect of degree of saturation and cement type on the diffusion of oxygen, the situation being analogous to the splash zone in a marine exposure environment. It was hoped that by covering the splash zone with a protective coating of mortar with a low oxygen diffusivity corrosion could be reduced. The authors found that by using a polymer modified mortar oxygen diffusion coefficients could be reduced to 1/70 of that for concrete.

Gjørv et al (1986) investigated the diffusion of dissolved oxygen through concrete to study the factors controlling rate of corrosion of steel corrosion in submerged marine structures. In high chloride environments it is only a matter of time before detrimental amounts of chloride reach the embedded steel causing disruption of the passive film. The rate controlling factor for corrosion in these circumstances may then be availability of oxygen at the steel surface, which is primarily controlled by diffusion through the cover concrete, or resistivity. Several test methods were employed. One involved a test specimen separating two reservoirs containing oxygenated water and deoxygenated water respectively. The amount of diffused oxygen was measured by potentiodynamic consumption at the cathode. The other technique involved casting an electrode into a sample and measuring the rate of oxygen diffusion through to the electrode. At steady state the amount of oxygen reaching the electrode was equal to that being consumed. This method was found to be particularly suitable for simulation of insitu conditions as it takes into account the cover concrete. Using these methods values of oxygen diffusivity of 2 to 11×10^{-6} cm^2/s through OPC concrete were measured. The authors found that variations in w/c ratio had little effect compared to the influence of the cover concrete which dramatically reduced oxygen diffusivity. Mortars were also found to have much lower diffusivities than concrete.

Page and Lambert (1987) employed an electrochemical cell similar to that used for steady-state chloride diffusion by Page et al (1981), to measure rates of diffusion of oxygen through hardened cement paste. The cell design was later improved by Yu and Page (1991). By comparing oxygen and chloride diffusivities an understanding of the influence of surface charge effects between penetrating charge particles and pore walls on transport properties could be gained.

5.2.2 Electrostatic Effects on Ionic Movement Through Hardened Cement Paste

Measurements of activation energy for chloride diffusion in hydrated OPC pastes have been made by Page et al (1981) and Goto and Roy (1981) and found to be greater than those characteristic of simple aqueous electrolytes, leading the authors to suggest that surface interactions may dominate the movement of ions in hardened cement paste.

The rates of transport of co-diffusing cations such as sodium and potassium are found to be less than chloride and hydroxide ions, leading Goto and Roy (1981) to postulate that HCP acts as a semi-permeable electronegative membrane.

Oxygen being a neutral molecule should not be dominated by electrostatic surface interactions with the electric double layer, developed at the cement-matrix/pore-solution interface. The similar sizes of the oxygen molecule and chloride ions means that purely geometrical restrictions should be constant for oxygen and chloride diffusion, and determination of diffusion rates of the two species should yield insight into the importance of surface charge effects on chloride ion transport.

Yu and Page (1991) compared the steady state diffusion of chloride ions and oxygen molecules through HCP. Comparison of the diffusion rate of the charged chloride ion and the uncharged oxygen molecule yielded information on the effect of surface charge effects. They found that for cement pastes of w/c less than 0.5 surface charge effects were dominant rather than geometric restrictions. Since decreasing w/c increases the volume fraction of micropores the authors concluded that "electrostatic effects on ionic movement at the cement-matrix/pore-solution interface can be significant only in pores no wider than a few times the value of the double layer thickness." The double layer thickness was calculated to be 13 to 3 Å.

Page and Lambert (1987) investigated the kinetics of oxygen diffusion in cement paste. They found that D_O for OPC pastes of w/c ratio 0.4 to 0.6 were of a similar magnitude to values obtained by Page et al (1981) for ionic diffusion. Activation energies were found to be roughly half those of chloride diffusion with values at 0.4 and 0.5 of similar magnitude, but that at w/c 0.6 significantly lower.

Ngala et al (1995) investigated oxygen and chloride diffusion through well cured OPC and OPC/PFA blended pastes. They found that the diffusion rate of chloride ions diminished markedly with reductions in w/b ratio and tended to a very low value as capillary porosity approached zero. For a given w/b ratio or capillary porosity the chloride diffusivities for OPC/30%PFA paste were smaller than those for OPC paste.

The diffusion of dissolved oxygen also diminished with a reduction of w/b ratio but did not tend to low values as capillary porosity approached zero, suggesting that the cement hydrates (CSH) are permeable to oxygen. Oxygen diffusivity through blended pastes was lower than through OPC possibly due to a smaller proportion of coarsely crystalline $Ca(OH)_2$, and discontinuity of the capillary pore system in the blended pastes. The ratio of oxygen to chloride ion diffusion rates, an indication of surface charge effects, increased with decresing capillary porosity, supporting the view that diffusion of chloride ions is retarded by the surface charge of the hydrated cement gel.

Oxygen diffusivity through OPC pastes measured by Ngala (1995) shown in Figure 5.1 indicate that as w/b ratio increases oxygen diffusivity increases with a substantial increase at w/b ratio of 0.7. In contrast PFA and BFS pastes showed very little variation in D_O with w/s. An explanation put forward by Ngala was that there was greater continuity of the pore system in OPC pastes. The author also found differing D_O for the same capillary porosity in different cement systems, suggesting that different factors are controlling movement within a particular cementitious system. The different hydrates produced by OPC, BFS and PFA show different permeabilities to the oxygen molecule. Oxygen diffusivity for BFS pastes appears to be almost independent of capillary porosity.

Collepardi et al (1972) in an investigation of chloride penetration into OPC and pozzolanic mortars found chloride ions diffuse at different rates in pozzolanic and OPC systems, whereas uncharged urea molecules penetrate at the same rate for both systems. This discrepancy was ascribed to surface interactions between the charged particle and the pore walls of the cement paste. The uncharged urea molecule is less likely to be affected by charge effects, and only be influenced by purely geometric considerations.

5.2.3 Oxygen Reduction in Alkaline Solutions at a Platinum Electrode

An electrochemical technique used to measure oxygen diffusion through cement systems has been developed by Page and Lambert (1987), improved by Yu and Page (1991), and Ngala et al (1995).

If an electrochemically active substance is consumed at a constant potential with respect to a reference electrode, the criterion for a virtually complete consumption is the decay of current from a high value initially to a value close to zero. Lingane (1958, 1967) considered such a system where the rate of the electrode process is limited by the diffusion and electro-migration of the reacting species from the bulk solution to the electrode surface. Suppose the current controlling factor is the rate of diffusion through the depleted layer of the solution in contact with the electrode, and the concentration of the reactive species is practically zero. The instantaneous current (I) can be derived from Fick's first law and Faraday's law, assuming that the substance which diffuses through the diffusion layer to the electrode surface is immediately consumed:

$$I = \frac{nFDA_eC}{l} \qquad \text{Eqn. 5.3}$$

n number of electrons transferred per molecule of reactant
F Faraday number
D Diffusivity (cm^2/s)
C Concentration of substance in solution (mol/cm^3)
A_e effective surface area of electrode (cm^2)
l thickness of diffusion layer (cm)

If l is constant $I \propto C$, and from Lingane (1958 and 1967) the decay current resulting from the gradual consumption of the reactant having an initial concentration C_o, in a fixed volume V, is given by:

$$I = I_o.e^{-(\frac{DA_et}{Vl})} \qquad \text{Eqn. 5.4}$$

where t polarisation time (seconds) and I_o is the initial current at t=0. Integrating I over time gives

$$\frac{Q}{Q_o} = 1 - e^{-(\frac{DA_et}{Vl})} \qquad \text{Eqn. 5.5}$$

These equations provide a basis for the choice of experimental conditions to achieve rapid depletion of the reacting species. Yu and Page (1991) improved the efficiency of the cell developed by Page and Lambert (1987) by increasing the ratio of electrode area to solution volume. The diffusion layer thickness was reduced by ensuring adequate stirring of the reactants.

The reduction of oxygen in an alkaline solution is the only significant cathodic reaction at -600 mV SCE and follows the form shown in equation 5.2. If diffusion of oxygen is at steady state it is possible to obtain a stable flux current I_d, since at this flux current, the diffused amount is the same as that being consumed, given by:

$$J_o = \frac{I_d}{nF} \qquad \text{Eqn 5.6}$$

J_O total flux (mmol/sec)

The flux current is related to diffusivity by:

$$I_d = nFDA\frac{dc}{dx} \qquad \text{Eqn. 5.7}$$

$\frac{dc}{dx}$ concentration gradient of oxygen

A Cross-setional area.

Oxygen diffusivity (D_O) is calculated from Fick's first law and Faraday's law using:

$$D_o = \frac{L(\frac{Q_t}{t_d})}{4FAC_o} \qquad \text{Eqn. 5.8}$$

L disc thickness

$\frac{Q_t}{t_d}$ (mA) slope from Qt - td curve

A diffusion area

C_O solubility (1.23×10^{-3} M)

$\frac{C_o}{L}$ assumed concentration gradient.

In order to calculate the diffusivity of oxygen the concentration in the anode compartment must be known. Oxygen solubility in 0.035M NaOH at 25°C has been found experimentally to be 1.27×10^{-3} M by Ngala (1995), compared with the value of 1.23×10^{-3} M for oxygen solubility in water (Dean 1985). Due to the similarity between the two values the solubility in water was used throughout this investigation.

5.3 EXPERIMENTAL PROCEDURE

Cement paste discs used for oxygen diffusion experiments were cast, cured and prepared as described in Chapter 2. The discs were ground with emery paper, and rinsed with deionised

water to remove any burrs and striations inflicted during cutting, enabling a water-tight seal when mounted in the diffusion cell. The discs were kept under 0.035M NaOH and prevented from drying out to ensure saturation as oxygen diffuses faster through air than water. Prior to mounting in the diffusion cell, resistivity and bulk density measurements were made, to provide a check on sample uniformity.

The oxygen diffusion cell is shown schematically in Figure 5.2 and consisted of anodic and cathodic compartments each filled with 0.035 M NaOH to prevent leaching, and separated by the cement paste disc test specimen. To ensure a water-tight seal between the specimen and glass cell, greased neoprene rubber gaskets were used and the whole joint held in place with PTFE tape. Added rigidity was provided by PVC tape.

The cathodic compartment contained a platinum foil and wire electrode and magnetic bar follower to enable mixing by external DC motor, of the solution and ensure thorough consumption of any diffused oxygen. To enable steady-state to be established quickly the cathodic solution was first purged of any dissolved oxygen by bubbling white spot nitrogen through in a de-aeration cell. The anodic side was kept saturated with dissolved oxygen by continuously bubbling oxygen gas through the anolyte for the duration of the experiment. The oxygenation system was arranged such that a cyclic stream was set up whereby anolyte was removed from the body of the anodic compartment, oxygenated and returned to the cell thereby maintaining a saturated solution. The anodic compartment also contained an anodised titanium electrode and a standard calomel electrode (SCE).

Once the diffusion cell was assembled and any air bubbles removed, particularly from the cathodic compartment, the cell was immersed in a water bath at a constant temperature of 25^{o}C.

5.3.1 Polarisation Measurements

For the first 5 days or so until steady state conditions were established, the cells were polarised to remove any diffused oxygen, but the data not recorded. The cathode was polarized at -600 mV SCE, where the only possible reaction is the reduction of oxygen.

The current generated by the consumption of dissolved oxygen was measured every second by computer controlled potentiostats and total charge passed calculated by integrating the current-time decay curve.

The amount of diffused oxygen in the cathodic compartment was determined every 1 to 3 days. Once steady state had been reached six readings were taken in order for Doxy to be

calculated, each polarization lasting 10 000 seconds. A constant ratio of charge passed to diffusion time interval was indicative of a steady state diffusion situation.

The flux can be calculated from Faraday's law from the ratio of $\frac{Q_t}{t_d}$ or $\frac{Q}{t_t}$. The total charge passed was plotted against the total diffusion time, and the slope used to calculate oxygen diffusivity (Do). Refer to Appendix D for example calculation of Do.

5.4 RESULTS AND DISCUSSION

The oxygen diffusion results for OPC and MK pastes are shown in Tables 5.1 to 5.4, along with bulk density and porosity data. The bulk density data is consistent and indicates that there is no problem with mix preparation in terms of segregation or inaccurate batching. Consistency between resistivity measurements for specimens is indicative of homogeneity between discs.

Comparing the values for oxygen diffusivity obtained for OPC pastes with results from other workers reveals that the values obtained in the present study are slightly higher. This could be due to a number of factors such as differences between cement batches or curing conditions.

Diffusion of the uncharged oxygen molecule provides information on the pore structure of HCP available to act as diffusion paths. Figure 5.2 shows that as water:binder ratio increases so does oxygen diffusivity, consistent with an increase in pore volume and a reduction in tortuosity (Powers 1958). The results also indicate that the rate of diffusion of the oxygen molecule through hardened cement paste is much greater than that of the chloride ion found from work in Chapter 4. This could be because the cement hydrates are more permeable to oxygen than chloride ions, or that penetration of the chloride ion is hindered by surface charge interactions.

Ngala (1995) suggested three factors to account for the lower diffusivity of chloride ions compared with oxygen molecules through hardened cement paste; surface charge effects, physical and chemical binding of chloride ions to cement hydrates, and a greater number of diffusion paths for dissolved oxygen.

For chloride ions to have a reduced number of diffusion paths ions could either be repelled from pores open to oxygen diffusion or be prevented from penetrating by blockages in the pores. Goto and Roy (1981), Ushiyama and Goto (1974) postulated that HCP behaves as a semi-permeable electronegative membrane due to the double layer of the surface hydrates.

If this is so chloride ions would be repelled from pores. Only pores large enough for the double layer effect to be negligible would be expected to allow passage of chloride ions.

Chlorides physically adsorbed to the pore surfaces or chemically bound with other hydration products may act as pore blockers reducing the availability of diffusion paths and increasing tortuosity i.e. reduced diffusion path is due to repulsion by electric double layer or pore blocking with chloro aluminate compounds.

5.4.1 Influence of MK on Oxygen Diffusivity

Figure 5.3 illustrates how oxygen diffusivity varies with MK content for 0.4, 0.5 and 0.65 water:binder pastes. The plots indicate that as MK content increases from 5% to 20%, rate of oxygen diffusion increases. However there is no consistent relationship between MK pastes and OPC pastes. At low MK replacements (<10%), the oxygen diffusivity of MK paste is lower than comparable OPC pastes. The reverse is true for 20% MK pastes.

Figure 5.4 confirms that 5% MK pastes have a lower permeability to dissolved oxygen than either OPC or other MK pastes. The relationship between oxygen diffusivity and capillary porosity suggests that the factors controlling diffusivity are different in the 3 different replacement systems, as for the same capillary porosity each binder exhibits a different oxygen diffusivity.

Capillary porosity is known to be the predominant parameter in mass transport, so it might be expected that there would be a direct relationship between capillary porosity and the diffusion of an uncharged particle, which is only likely to be influenced by geometric pore parameters. Clearly this not the case, even for MK systems only differing in the replacement level.

The hydrates produced by MK hydration, namely CSH gel and gehlenite hydrate, would be expected to be identical in composition between pastes of different replacement level. Only the relative quantities of the OPC and pozzolanic hydrates are expected to differ between pastes, depending on the initial proportions of the binder. If this were true porosity and hence oxygen diffusivity would be expected to decrease as pozzolanic content increased, due to an increase in secondary hydrates. The coarsely crystalline and hence porous calcium hydroxide crystals are replaced with CSH gel of lower porosity. It might be expected that porosity and oxygen diffusivity would decrease with increasing replacement level up to a point where insufficient calcium hydroxide was produced by the OPC for complete pozzolanic reaction. Then the OPC content would be too low, resulting in a dramatic increase in porosity due to low production of hydrates. If this were valid all results for MK

pastes irrespective of replacement level should fall on the same trend line for capillary porosity against oxygen diffusivity, except at very high replacement levels necessary to consume all the lime and leave an excess of pozzolan.

A possible, but unlikely explanation for the observed results is inadequate dispersion of MK in paste samples, especially at high replacement levels. As MK content increases there is a greater volume of powder and relatively less water in which to disperse the binder adequately. At low MK contents better dispersion is achieved, than at higher replacement levels, purely due to the lower total surface area of the binder. High MK contents lead to the formation of MK clumps which may act as preferential diffusion sites, through which rapid penetration occurs. If MK pastes were studded with unhydrated MK clumps, it is likely that they would be surrounded by a crust of pozzolanic hydrates. Consequently there is unlikely to be a rapid diffusion path available so, the addition of MK, even if it formed an heterogeneous mix, is unlikely to lead to higher oxygen diffusivities than a comparable OPC paste.

Therefore the increase in oxygen diffusivity associated with pastes of high MK content may be due to higher permeability of the pozzolanic hydrates. Significantly 5% MK pastes have the lowest oxygen diffusivity of all the MK pastes as well as having lower diffusivities than comparable OPC pastes. This suggests that MK hydrates in the 5% MK paste may be different to those in pastes of higher replacement. Murat (1983) investigated the hydration of metakaolin with lime at differing ratios. For MK/CH ratios of 0.5, 0.6 1.0, Murat proposed that CSH gel would be formed in all cases as well as C_4AH_{13}, C_3AH_6 and C_2ASH_8 respectively. Subsequent experiments revealed the presence of CSH gel and gehlenite hydrate but no C_3AH_6. At low MK/CH ratios (0.5) Murat proposed that C_4AH_{13} and CSH gel are produced with little or no gehlenite hydrate. At higher ratios C_2ASH_8, CSH gel and possibly some C_4AH_{13} are formed. Table 5.5 shows the MK:calcium hydroxide ratios calculated for the pastes studied in this investigation. From work by Murat (1983) it would appear that the 5% MK paste is conducive to the production of C_4AH_{13} as opposed to C_2ASH_8. Consequently a proposed explanation for the lower diffusivity of the 5% MK paste is that hydrated gehlenite has a higher oxygen permeability than other hydrates, including calcium hydroxide. Thus MK mixes with high gehlenite hydrate contents will have high oxygen diffusivities.

CSH gel formed from MK is likely to be of slightly different composition than OPC gel. Turriziani (1964) found that gel formed from pozzolans and that formed from OPC differed in composition in terms of C:S ratio. This difference in structure may alter the permeability of the gel to dissolved oxygen.

Cook (1986) found that in calcined kaolin clays, gehlenite hydrate was formed to the detriment of CSH. Thus as MK content increases there is more alumina available for reaction, leading to a higher percentage of gehlenite hydrate and less CSH gel.

The various hydrates produced by MK may depend on the stoichiometry of the reactants present, namely calcium hydroxide, water and MK. Low MK and water contents may lead to the formation of a mix high in CSH gel and low in gehlenite hydrate and possibly some calcium aluminate hydrate (C_4AH_{13}). High MK contents may promote the formation of a higher proportion of C_2ASH_8 to the detriment of CSH gel. This C_2ASH_8 may be more permeable to oxygen molecules and possibly chloride ions than CSH gel, resulting in the high rates of oxygen diffusion noted for 20% MK pastes. Different forms of calcium aluminate hydrate may also form as Cook (1986) suggested that the value of x could vary from 9 to 13 in the compound C_4AH_x.

Notably Figure 5.4 shows for all binder types, oxygen diffusivity does not diminish to very small values as capillary porosity approaches zero, indicating that dissolved oxygen molecules are not limited to capillary pores as are chloride ions.

Linear extrapolation of oxygen diffusion coefficient against total porosity in Figure 5.5 demonstrates that as oxygen diffusion coefficient diminishes to zero for OPC, pore volume decreases to a very low value. This suggests that all pores in OPC pastes are permeable to oxygen molecules. In contrast MK pastes, particularly 5 and 10% appear to converge on a total porosity of approximately 30% as oxygen diffusion coefficient reduces to small values. This indicates that not all pores in MK pastes are available for diffusion of dissolved oxygen, possibly due to the impermeability of hydrates which encapsulates porosity, rendering it isolated from the pore network.

5.4.2 Ratio of Oxygen to Chloride Diffusivity

The ratio of oxygen to chloride diffusion coefficients has been considered to be a measure of surface charge and diffusing species interaction as demonstrated by Yu and Page (1991) and Ngala et al (1995) for OPC and PFA pastes. The ratio of oxygen to chloride diffusivity for MK pastes is listed in Table 5.6. The results show that in all cases chloride diffusion rate is less than oxygen diffusion rate, indicating that the rate controlling factors of diffusion are different for the negatively charged chloride ion and the neutral oxygen molecule. As the pastes become denser and water:binder ratio decreases, they provide a greater resistance to the ingress of chloride ions than oxygen molecules. This is illustrated graphically, together with data from earlier studies (Yu and Page 1991, Ngala et al 1995, Ngala 1995), in Figure 5.6 which shows a plot of oxygen to chloride diffusion ratio against chloride diffusion coefficient. As the MK pastes become less permeable to chloride ions they offer

progressively more resistance to the diffusion of chloride ions than to the diffusion of dissolved oxygen. This is consistent with results obtained for OPC, PFA and BFS by other workers, and comply with their conclusions that ionic diffusion is greatly retarded by interaction with pore surfaces (Yu and Page 1991, Ngala et al 1995, Ngala 1995).

The D_O/D_{Cl} ratio for OPC pastes approaches 1 for high w/c ratios, compliant with the theory of a continuous capillary pore network which offers little resistance to penetration of diffusing species. Ottewill (1983) reported that the influence of the electric field generally extends from the surface to a distance of approximately twice the double layer thickness. Yu and Page (1991) calculated that surface interactions will only be significant in pores smaller in diameter than 0.2 to 2.6 nm, where the surface charge effects of the pore wall extend far enough into the pore to prevent unhindered passage of charged species. In large pores the chloride ion will be able to pass through unaffected by the pore walls due to the limited field of influence exerted by the electric double layer.

The findings in this work are consistent with Goto and Roy (1981) and Ushiyama and Goto (1974), who pointed out cement pastes behave as electronegative semi permeable membranes for temperatures up to 70°C.

5.5 CONCLUSIONS

1) MK pastes exhibit different rates of diffusion of dissolved oxygen molecules, depending on the MK content of the mix.

2) Increasing MK content increases oxygen diffusion coefficient.

3) 5% MK pastes had the lowest oxygen diffusion coefficients of all the mixes investigated.

4) D_O is greater than D_{Cl} for OPC and MK hardened cement pastes supporting the theory that surface interactions between the charged chloride ions and the cement-matrix/pore-fluid interface dominate ionic transport characteristics in hardened cement paste.

5) D_O/D_{Cl} ratios for MK pastes correlate well with relationships for OPC, PFA and BFS pastes.

6) The diffusion of dissolved oxygen through MK and OPC pastes does not reduce to very low values as capillary porosity approaches zero, as is the case for the diffusion of chloride ions, suggesting that OPC and pozzolanic hydrates are permeable to disolved oxygen.

Aston University

Illustration removed for copyright restrictions

Figure 5.1 Plot of oxygen diffusion coefficient against water/binder ratio (Ngala 1995).

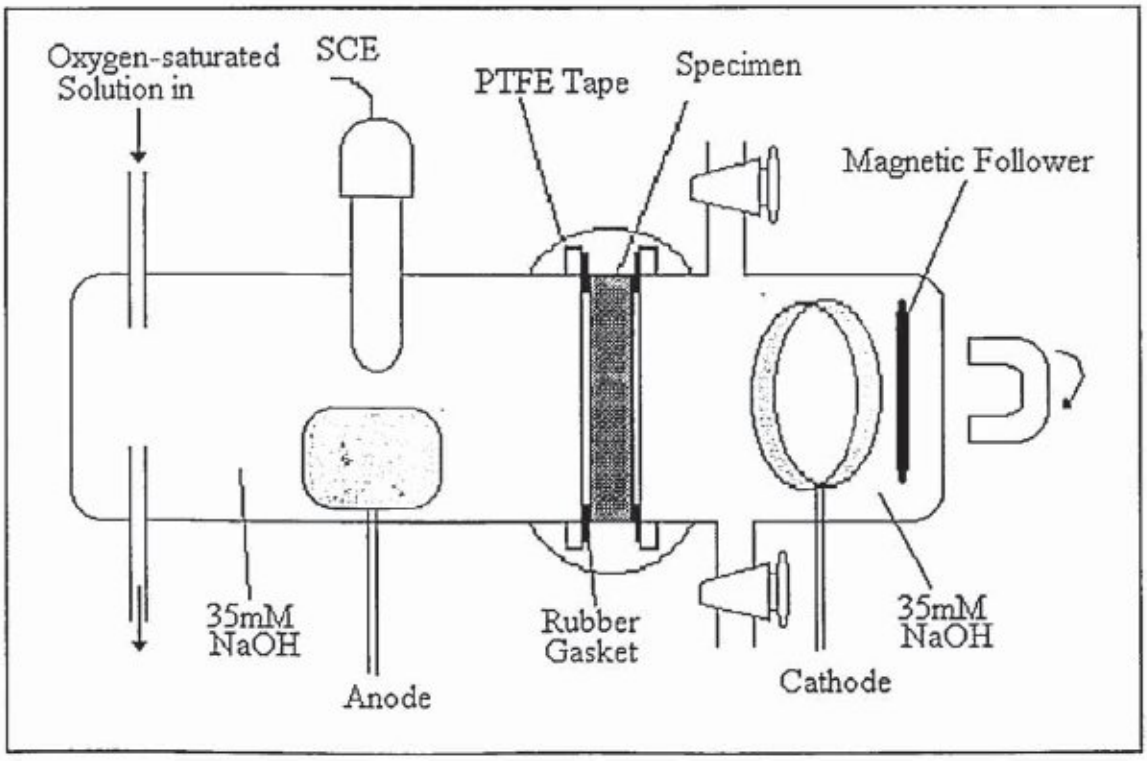

Figure 5.2 Schematic of the electrochemical oxygen difusion cell.

% Replacement with MK	MK:CH (by mass)
5%	0.26
10%	0.56
20%	1.25

Table 5.1 MK:Calcium hydroxide ratios in paste.

Water:Binder	Oxygen Diffusivity ($10^{-7}cm^2/s$)	Resistivity (kΩ.cm)	Bulk Density (g/cm^3)	Capillary Porosity (%)	Total Porosity (%)
0.4	1.262	6.50	2.010	1.96	35.10
	1.331	6.58	2.014	1.95	34.98
	1.480	6.32	2.021	1.96	35.25
	1.093	6.48	2.019	2.05	34.52
	1.152	6.51	2.020	2.18	35.03
Average	1.264	6.48	2.017	2.02	34.98
0.5	1.341	4.89	1.911	6.37	40.43
	1.255	5.13	1.910	5.98	41.30
	1.564	4.98	1.911	5.99	41.21
	1.553	5.20	1.909	6.31	40.99
		5.11	1.908	5.89	41.34
Average	1.361	5.06	1.910	6.11	41.06
0.65	1.505	4.17	1.777	10.52	51.17
	1.607	4.04	1.769	10.38	51.38
	1.579	3.79	1.766	10.42	51.01
	1.948	3.82	1.772	10.39	51.19
		3.91	1.765	10.74	50.96
Average	1.660	3.95	1.770	10.49	51.14

Table 5.2 Results for OPC hardened cement paste.

Water:Binder	Oxygen Diffusivity ($10^{-7}cm^2/s$)	Bulk Density (g/cm^3)	Capillary Porosity (%)	Total Porosity (%)
0.4	0.555	1.985	1.30	40.10
	0.619	1.972	1.27	39.95
	0.604	1.971	1.40	40.02
	0.524	1.981	1.32	40.01
	0.418	1.982	1.25	41.07
Average	0.544	1.978	1.31	40.23
0.5	0.958	1.872	2.36	45.27
	0.971	1.864	2.62	45.29
	0.853	1.870	2.28	45.24
	0.737	1.868	2.55	45.37
	0.763	1.877	2.58	45.25
Average	0.856	1.870	2.48	45.29

Table 5.3 Results for 5% MK hardened cement paste.

Water:Binder	Oxygen Diffusivity ($10^{-7}cm^2/s$)	Resistivity (kΩ.cm)	Bulk Density (g/cm^3)	Capillary Porosity (%)	Total Porosity (%)
0.4	0.948	19.85	1.978	1.33	39.71
	0.502	20.55	1.976	1.90	39.63
	0.353	21.25	1.959	1.43	39.48
	0.635	21.59	1.966	1.40	39.72
	0.840	21.75	1.967	1.36	39.64
Average	0.656	21.00	1.969	1.69	39.64
0.5	1.313	10.97	1.878	2.70	48.81
	1.262	10.79	1.882	2.88	48.85
	1.208	10.68	1.877	2.46	48.53
	1.194	11.08	1.868	2.85	48.94
	1.259	11.19	1.880	2.32	48.86
Average	1.247	10.94	1.877	2.64	48.80
0.65	1.660	8.02	1.728	4.07	52.79
	1.650	8.08	1.722	4.38	52.64
	1.867	8.03	1.718	4.69	52.54
	1.416	7.99	1.722	3.83	52.90
	1.369	7.97	1.724	4.24	52.72
Average	1.592	8.02	1.723	4.24	52.72

Table 5.4 Results for 10% MK hardened cement paste.

Water:Binder	Oxygen Diffusivity ($10^{-7}cm^2/s$)	Resistivity (kΩ.cm)	Bulk Density (g/cm^3)	Capillary Porosity (%)	Total Porosity (%)
0.4	1.284	14.17	1.941	1.16	42.32
	1.068	11.48	1.949	1.27	42.02
	1.231	11.63	1.945	1.23	42.34
	1.382	12.60	1.943	1.12	42.50
	1.415	10.91	1.956	1.19	42.46
Average	1.276	12.16	1.947	1.20	42.33
0.5	1.553	9.13	1.864	2.17	46.25
	1.418	9.06	1.868	2.98	45.50
	1.651	11.25	1.856	2.73	45.64
	1.460	13.45	1.884	2.28	46.48
	1.461	9.41	1.860	2.03	47.12
Average	1.509	10.46	1.866	2.44	46.20
0.65	1.832	7.49	1.724	5.15	53.15
	1.695	9.34	1.736	5.94	52.76
	1.588	9.01	1.735	7.05	53.09
	1.504	7.77	1.766	4.82	53.15
	1.785	7.89	1.732	6.75	53.17
Average	1.681	8.30	1.739	5.94	53.06

Table 5.5 Results for 20% MK hardened cement paste.

W:B Ratio	MK Replacement Level (%)	Oxygen Diffusivity (Do) ($x10^{-7}$ cm^2/s)	Chloride Diffusivity (Dcl) ($x10^{-8}$ cm^2/s)	Do/Dcl
0.4	0	1.264	1.94	6.51
0.5	0	1.361	5.08	2.68
0.65	0	1.660	8.85	1.88
0.4	5	0.544	0.60	9.04
0.5	5	0.856	1.30	6.61
0.4	10	0.656	0.55	11.95
0.5	10	1.247	1.31	9.54
0.65	10	1.592	1.93	8.26
0.4	20	1.276	0.92	13.84
0.5	20	1.509	1.28	11.76
0.65	20	1.681	1.96	8.57

Table 5.6 Ratio of oxygen to chloride diffusion coefficient for hardened cement pastes.

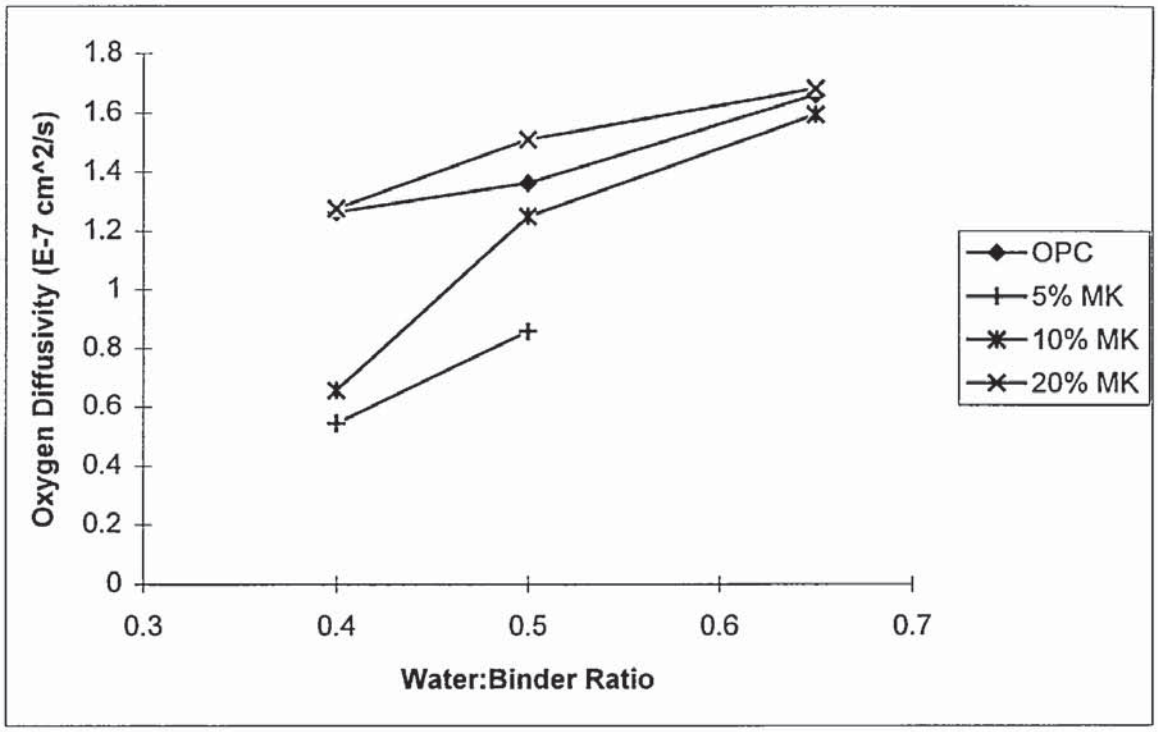

Figure 5.2 Plot of oxygen diffusivity against water/binder ratio.

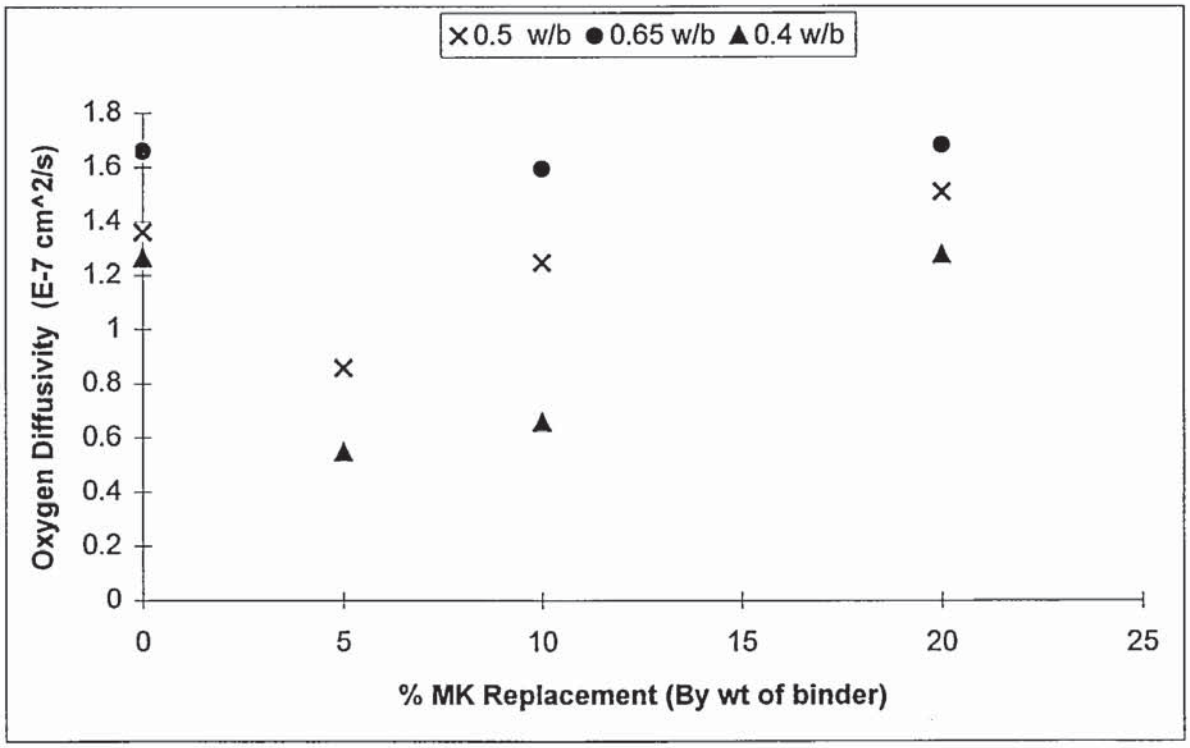

Figure 5.3 Plot of oxygen diffusivity against MK content.

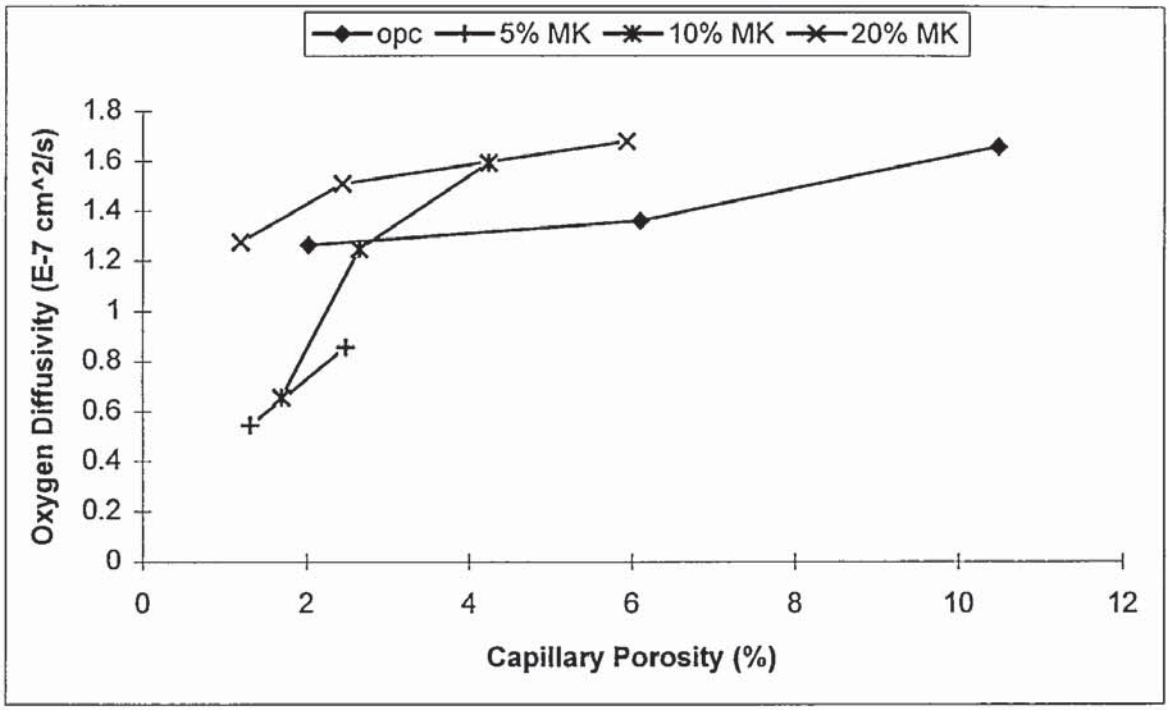

Figure 5.4 Plot of oxygen diffusivity against capillary porosity.

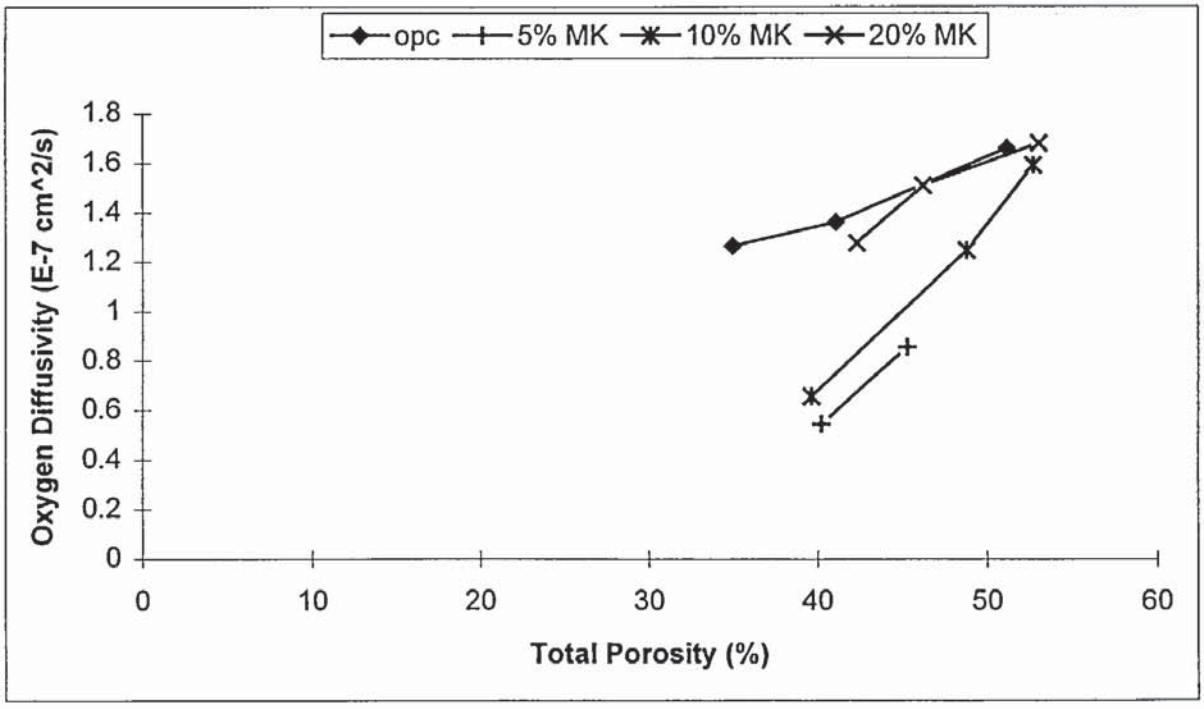

Figure 5.5 Plot of oxygen diffusivity against total porosity.

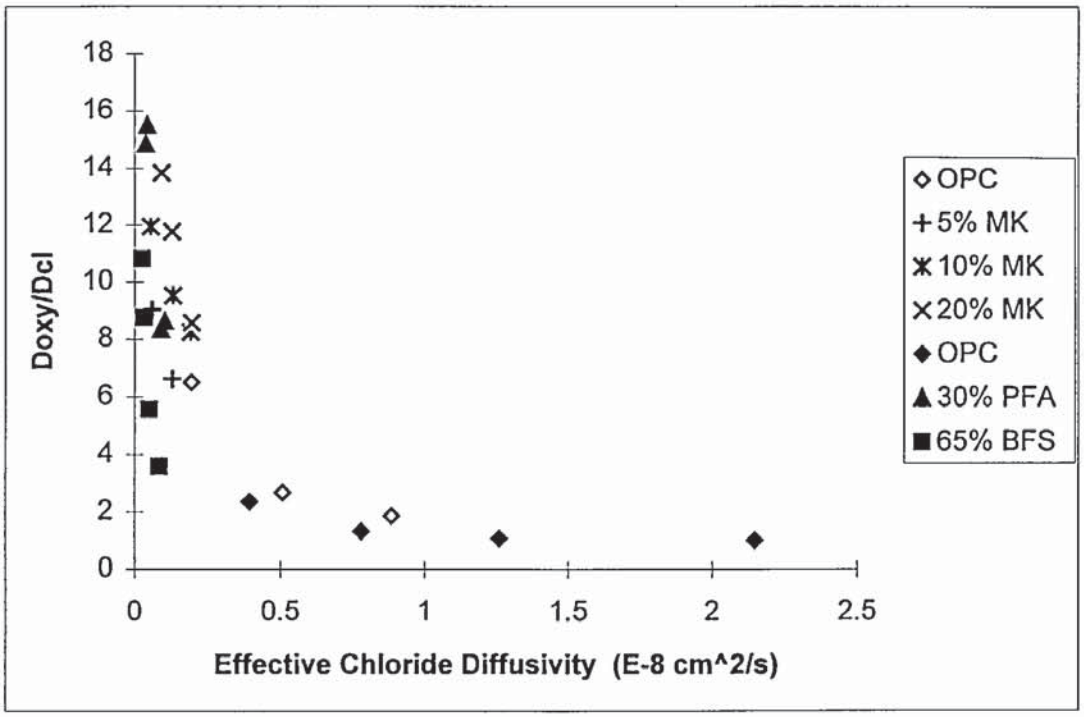

Figure 5.6 Graphical representation of the interaction between charged species and pore walls (Data from Ngala 1995 shown by dark points).

CHAPTER 6

6. INFLUENCE OF METAKAOLIN ON THE DIFFUSION PROPERTIES OF THE PASTE-AGGREGATE INTERFACIAL ZONE

6.1 INTRODUCTION

The pore structure of Portland cement has been studied extensively with the assumption that the knowledge gained about plain paste is applicable to paste in mortar and concrete. That is, the pore structure of paste when it forms in the presence of aggregate is the same as that in the absence of aggregate. However, research has indicated that paste that forms near the interface with an aggregate has a different microstructure (Barnes et al 1978).

Unlike the bulk matrix, the microstructure of the interfacial zone (IZ) is characterised by less cement paste, more capillary pores and coarse preferentially orientated calcium hydroxide crystals. The effect of the interfacial zone on transport properties is not fully understood. Some studies suggest the IZ does not play a major role, while others show contrary findings (Kayyali 1987, Winslow et al 1994). Work by Larbi (1991) has postulated a theory that the bulk paste characteristics are of more influence than the IZ. In typical mortars and concretes the interfacial zone cement paste comprises 20 to 30% of the total cement paste volume, and will presumably have an influence on the behaviour of the material. This would be true even if the phase were discontinuous, although work by Winslow et al (1994) has shown that even if the IZ thickness is taken to be as small as 10 μ m the interfacial cement paste can form a continuous percolating channel, with an influence on transport properties. Thus no investigation of the performance of a new pozzolan would be complete without a study of the impact of the IZ on diffusion characteristics.

The work in this study investigated the influence of the IZ on diffusion characteristics of MK mortars. The techniques used were similar to those employed by Ngala (1995), who studied chloride diffusion in mortars, with glass beads as model aggregate. The single size aggregate enabled the influence of the interfacial zone on transport phenomena to be evaluated by employing Maxwell's theory for diffusion through a periodic composite.

6.2 LITERATURE REVIEW

6.2.1 The Interfacial Zone

According to Diamond (1987) paste in concrete consists of narrow ribbons 80 to 150 μm separating aggregate particles, interrupted by air voids. Paste can be further categorised as paste in the bulk matrix and paste formed in the vicinity of aggregate termed interfacial zone (IZ) cement paste. Microbleeding may also cause variation in microstructure, due to the build-up of water beneath aggregate particles (Ollivier et al, 1995).

Differences in the microstructure between the cement paste in the interfacial zone and the bulk paste arise from the "wall effect" and the "one-sided growth effect"(Neville 1995, Garboczi 1995b).

6.2.1.1 Wall Effect

At the paste/aggregate interface the formation of a dense matrix is hindered by the aggregate which prevents the most efficient spatial arrangement of cement grains. Aggregate is many times larger than typical cement particles, hence on a μm scale the aggregate edge appears flat, preventing the particles packing together as well as is possible in free space. As a result the microstructure of the cement paste in the immediate vicinity of aggregate particles differs in several respects from the microstructure of the cement matrix. The concentration of cement grains is lower around aggregates compared to the bulk, resulting in a higher porosity and water content which persists even after hydration.

6.2.1.2 One-Sided Growth Effect

Although the "wall-effect" is the main contributory factor to interfacial zone microstructure, one-sided growth does play a small part. Capillary pore space in the bulk paste will be filled with reaction product from all directions since cement particles are located randomly and isotropically. If an aggregate particle is located adjacent to the capillary pore space, reaction products can only be deposited on the cement paste side.

6.2.1.3 Effect of Aggregate Type

Farran (1956) was one of the first workers to study the microstructure of the paste-aggregate interfacial zone for different minerals. The paste-calcite bond strength was found to be higher than the rest of the minerals examined and the author concluded that this effect was due to "corrosion" of the calcite surfaces as a result of the dissolution of calcite. The product formed a bridge across the paste-calcite interface increasing bond strength.

Buck and Dolch (1966) performed similar work on limestone and concluded that alkali solutions in the cement paste attacked the calcite "transforming" it into calcium hydroxide which precipitated with a definite orientation to the aggregate surface.

6.2.2 Microstructure of the Interfacial Zone

Hadley (1972) and Barnes et al (1978, 1979) studied the paste aggregate interface using SEM and EDAX. They reported the formation of a two-part, or duplex film, 1 to 1.5 μm thick. The film was predominantly composed of calcium hydroxide which formed a layer nearest the aggregate, topped with a layer of CSH gel arranged like "the bristles of a hair brush". The presence of "Hadley grains" was noted in the vicinity of the aggregate.

Hadley grains form through the surface hydration of cement particles forming a shell of CSH gel, and are associated with rapid hydration. The inner core of the grain later dissolves away leaving an empty shell, or one with a residual cement grain diminished in size.

Following work by Barnes et al (1978, 1979) the microstructure of the paste-aggregate interfacial zone was detailed by Diamond (1987);

i) In the immediate vicinity of the aggregate surface is a "duplex film" of calcium hydroxide topped by or occasionally intermixed with CSH. Sometimes this duplex film occurs in close intimacy with the aggregate. At early ages the film modifies into a dense layer, sometimes bonding within the surrounding cement paste. The side of the film in contact with the aggregate is a layer of crystalline calcium hydroxide ~0.5 μm thick. Following this layer is a thin deposit of CSH gel, in the form of short fibres, that extend into cement paste. Total extent of duplex film is ~1.0 μm.

ii) Next to the "duplex film" is the "transition zone". This region is relatively larger ~50 μm wide, including the "duplex film". Generally this zone contains a large number of hollow-shell hydration grains (Hadley grains) and enriched in larger calcium hydroxide crystals and ettringite.

The occurrence of a large number of hollow shell hydration grains suggests that cement hydration is accelerated at the IZ. This is presumably because of the availability of excess water in the vicinity of the aggregate particles. Also since the growth of large crystals of calcium hydroxide is enhanced in a more open system, the occurrence of such large crystals at the interfacial zone is an indication of the existence of higher porosity.

The paste-aggregate interfacial zone has also been characterised by Zimbelmann (1978), who carried out bond strength tests and SEM studies on paste-rock interfaces (Figure 6.1). According to Zimbelmann the paste in the vicinity of aggregate could be classified into three layers as described below;

i) Directly at the surface of the aggregate is a dense layer 2-3 μm thick and composed essentially of calcium hydroxide covering a network of ettringite crystals. This layer may be equivalent to the "duplex film " found by Barnes et al (1978). According to Zimbelmann, this layer is formed during early ages of hydration, that is up to 10 hours old. After about 12 hours the calcium hydroxide forms a continuous closed layer which he referred to as the "contact layer".

ii) Directly adjacent to the contact layer is a zone ~5-10 μm thick the "intermediate layer". This layer consisted for the most part of needle shaped ettringite crystals, leaf or flake-like calcium hydroxide, sporadic needle-shaped calcium silicate hydrate and big "hexagonal" calcium hydroxide crystals aligned steeply with respect to aggregate surface.

iii) The "Transition zone" ~10 μm thick is characterised by dense paste which merged into the bulk cement paste.

Zimbelmann attributed the origin of the interfacial zone to the formation of thin films of water ~10 μm thick on cement grains and around large aggregate particles in fresh concrete. The formation of water films on the aggregate particles seems quite likely, although the formation of such films on cement grains appears doubtful since mixing, handling and compaction are likely to destroy such films.

Scrivener and Pratt (1986) agreed with previous workers in that there is a high proportion of larger and better crystallised hydrates, predominantly calcium hydroxide and ettringite in the interfacial zone, as well as higher porosity than the bulk matrix. In addition the calcium hydroxide crystals in the IZ have preferential orientation such that their Basal cleavage planes are nearly perpendicular to the aggregate surface (Figure 6.2).

6.2.3 Porosity of the Interfacial Zone

The aggregate-paste interface has a definite effect on the pore size distribution due to its considerably higher porosity and larger pores. Winslow and Liu (1990) compared the porosity of neat cement pastes to that of pastes in mortar and concrete using MIP and observed higher porosities in mortars attributable to the interfacial zone. Much of the additional pore volume is found in pores with diameters greater than the threshold diameter of the plain paste and is therefore likely to influence transport properties. Kayyali (1987) performed a similar study but concluded that the interfacial zone was lower in porosity.

Scrivener et al (1988) using back scattered electron imaging and quantitative image analysis studied the particulates at the interfacial zone in plain and mineral addition concretes. Figure 6.3 is a summary of their results, showing that the concentration of anhydrous cement grains is lowest in the vicinity of the aggregate, increasing towards the bulk. Porosity is highest at the interface and decreases towards the bulk paste.

The relationship between transport processes in cement systems and pore structure can be described in terms of pore size and connectivity. Large pores have higher transport rates than small diameter pores, and blocked pores have negligible transport rates. Following on from these concepts ionic diffusivity and permeability depend on pore size in different ways

although both will depend on pore connectivity in the same manner (Garboczi 1995). Consequently workers have used percolation theory to describe the transport characteristics of mortar and concrete systems in terms of the porous interfacial zone (Garboczi et al 1990, 1992,1995, Winslow et al 1994)

6.2.4 Percolation Theory

Immediately after mixing the cement paste in a mortar is a viscous liquid. As hydration progresses, and reaction products form, regions of water filled capillary space will become cut off from the main pore network, reducing the volume of pores that form a continuously connected transport pathway. As this process continues capillary pore space can become segmented by smaller CSH gel pores resulting in the loss of long range connectivity. The point just before the pathway ceases to span the whole system is termed the percolation threshold. Thus the percolation threshold will be influenced by the degree of hydration and water:cement ratio. Garboczi et al (1995) have shown that for OPC systems with w/c ratios of 0.6 and above there will be a continuous (or percolated) capillary pore system.

Percolation of a system via the higher porosity of the interfacial zone will be influenced by the thickness of the zone, and the volume fraction of aggregate. When more aggregate particles are present there is less space between them enabling percolation to occur for smaller IZ thicknesses. If the interfacial zones do not percolate, then their effect on transport properties will be negligible, as any transport path through the concrete would have to go through the lower porosity of the bulk paste.

6.2.5 Influence of the Cement Paste-Aggregate Interface on Compressive Strength

Hsu and Slate (1963) indicated that the interfacial bond between coarse aggregate and cement paste is the "weakest link" in concrete with respect to strength. "Bond cracks" at the aggregate interface were shown to exist even when the concrete was kept in continuously wet conditions, and before the application of a load. Sha and Slate (1968) found that failure of concrete was characterised by bond failure within the interfacial layer.

Mindness and Diamond (1982) reported that cracking in mortars and concretes tends to initiate at the interfacial region, and that the crack path generally ran within the interfacial zone at a distance of a few microns from the surface of the aggregate particles. Bentur and Mindness (1986) observed that for high strength cement systems cracks go around aggregate particles, while Regourd (1985) found cracks passed through the interfacial layer. Other studies have shown that by increasing the paste-aggregate bond strength, compressive strength of concrete tends to increase (Bentur et al 1988, Detwiler and Mehta 1989, Mindness 1986).

According to Mehta (1986) strength between hydration products and aggregate particles is the force of adhesion resulting from Van der Waals force of attraction. Strength therefore depends on volume and size of voids present. Where there is crystallisation of new products in the voids of the IZ adhesive strength between paste and aggregate could increase, for instance as a result of the pozzolanic reaction with calcium hydroxide to form CSH gel.

Marchese (1983) believes large calcium hydroxide crystals in the IZ tend to possess less adhesion capacity, due to their lower specific surface and correspondingly weak Van der Waals forces of attraction. Also because of their oriented structure in the transition zone, the large calcium hydroxide plates serve as preferred cleavage sites allowing cracks to occur preferentially along their weakly bonded Basal cleavage planes.

Larbi(1991) studied the effect of MK on the strength of mortars and pastes. MK was found to increase the compressive strength of mortar, and also accelerate strength gain at early ages compared to an OPC control. The author attributed this to the improved adhesive strength of the paste to aggregate bond, as a direct result of better particle packing and the pozzolanic reaction densifying the interfacial zone. Improvements to the bulk matrix could not be responsible for increased mortar strength as both OPC and MK pastes had similar compressive strengths. The thinner denser IZ also led to better stress transfer from matrix to aggregate particles.

Goldman and Bentur (1989) suggested other causes for the lower paste strength in silica fume blended systems than in mortars. Ultrafine cementitious additions such as silica fume and metakaolin (> 5% by wt of cement) are not effectively dispersed, even in the presence of superplasticizers and after prolonged mixing. The pozzolan exists as "clumps" within the paste which are not completely broken up for subsequent pozzolanic reaction. In mortars the tumbling and shearing of the aggregate particles with the MK and silica fume tends to result in the break up of any clumps. Thus the performance of these additions in pastes is limited by heterogeneous mixing.

6.2.6 Effect of IZ on Durability

Most work on the influence of the IZ on durability has concentrated on permeability of the IZ. Malek and Roy (1988) reported that the paste-aggregate IZ does not seem to play any major role in determining permeability of concrete and hence may not influence durability. In contrast Tognon and Cangiano (1980) found that IZ contributed significantly to permeability and durability, as did Nyame (1985) who concluded that increasing aggregate volume increased the permeability due to interfacial effects.

Halamickova et al (1985) postulated that the effects of the transition zone on transport properties should depend on the aggregate content. When the transition zones are isolated by a less porous bulk paste, the rate of transport should be significantly lower than if the transition zones overlap, which would create a continuous path of low resistance to penetration. This interconnection has been referred to as "percolation". Winslow et al (1994) calculated that a 20 μm IZ thick would result in percolation in most typical construction concrete mixes, with an adverse effect on long term durability performance (Figure 6.4).

Work by Halamickova et al (1995) showed that the introduction of inert sand particles into Portland cement paste resulted in higher diffusivities measured by electrical migration and permeabilities even though sand particles are impenetrable compared with cement paste. As hydration proceeded, the difference became more pronounced, leading to the conclusion that the differences in transport phenomena are due to different pore structure developed in the presence of sand. Percolation was found to occur between 35 and 45% sand for 0.4 w/c ratio systems.

Winslow et al (1994) in a MIP study of OPC mortars found a sudden increase in "pro-threshold" volume as sand content increased from 44.8 to 48.6% suggesting the occurrence of a critical percolation phenomena. Little evidence of percolation was found for silica fume mortars with an aggregate volume of 40%. The authors concluded that SF reduced the thickness of the IZ reducing the likelihood of percolation. Consequently increases in transport properties would be subtle because non-porous aggregate replaces porous cement paste, all be it that there is an increase in the volume of the very porous interfacial zone paste. Percolation in the IZ of SF mortars was suggested to be a consequence of dissolved calcium hydroxide crystals forming pores as opposed to the presence of Hadley grains. Rapid formation of calcium hydroxide crystals at early ages in the IZ followed by dissolution as the pozzolanic reaction progressed led to an interconnected percolation pathway.

Larbi (1991) found that the IZ in OPC mortars increased the capillary porosity, relative to pure Portland cement pastes, but had a small effect on mass transport. It was suggested that the cement matrix as the continuous phase, controlled the transport processes in concrete, presumably because the large pores in the IZ are not interconnected with each other, but rather through the small pores of the matrix.

6.2.7 Effect of Mineral Additives on IZ

Several studies have shown that the inclusion of cement replacement materials improves the paste-aggregate interface by reducing its thickness and increasing its density (Detwiler, 1986, Bentur et al 1988, Mehta and Monteiro 1988). The inclusion of SF has been found to

improve particle packing around aggregates due to its small particle size (figure 6.5). Reduced microbleeding has also been highlighted as a factor for improved strength of the IZ (Goldman and Bentur 1989).

Larbi (1991), in an investigation of the diffusion characteristics of the IZ, showed that the addition of SF, PFA or MK lowered the capillary pore volume of the interfacial zone resulting in a densification, attributable to improved particle packing and the replacement of calcium hydroxide crystals with secondary hydrates in an "elimination-by-substitution" reaction. The author also noted that MK reduced the thickness of the interfacial zone from 43 μm in OPC mortars to 9.8 μm in 20% MK mortars. This decrease means that the volume of the more permeable region, which may be used as a preferential diffusion path, is reduced. However the author concluded that the increased resistance to penetration of aggressive ions is in part due to the improvement in microstructure of the IZ, "but more importantly, to the marked improvement of the matrix of blended mixes."

6.2.7 Resistivity Measurements of the IZ

The resistance of a material can readily be calculated from Ohm's law knowing the applied potential difference and current. However the resistance depends upon the size and shape of the sample being tested whereas resistivity is independent of the volume of material. Several studies have investigated the resistivity of cement systems, and these are discussed in more detail in Chapters 2 and 4.

The electrical resistivity of a mortar is important as a means of probing the structure of the material, as well as a measure of ionic diffusivity. However the relationship is complicated by the presence of aggregate and accompanying interfacial zone, which have different resistivities to the bulk matrix. The pore fluid in the cement matrix is responsible for the conduction of current, while the aggregate particles act simply as inert obstacles to the flow of current. Tumidajski (1996) described electrical conduction through mortar as a compromise between the insulating effects of the aggregate which lowers conductivity and the transition zone, which being more porous, increases conductivity.

Whittington et al (1981) carried out resistivity measurements on cement pastes and concretes to investigate the mechanisms of conduction of electricity. They concluded that factors such as water:cement ratio, temperature and degree of hydration influenced the resistivity, and that the resistivity of the concrete is almost entirely dependent upon the resistivity of the paste within the concrete.

Garboczi et al (1995) modelled the effect of the interfacial zone on the electrical conductivity of mortar, and found that the presence of the interfacial zone cement paste

influences the overall conductivity of the mortar. They viewed mortar as a three-phase composite of bulk cement paste, aggregate and interfacial zone cement paste. An analysis of work by Halamickova et al (1995) showed that the ratio of IZ conductivity to that of the bulk paste, for OPC mortars, was between 10 and 20, indicating that the IZ is much more porous that the bulk paste. As the interfacial zone cement paste occupies a significant fraction of the total cement paste phase, and is percolated in typical mortars and concretes, the higher conductivity of this phase will cause the overall conductivity of the mortar or concrete to be higher than expected for just a simple bulk cement paste plus aggregate composite.

6.3 EXPERIMENTAL PROCEDURE

6.3.1 Model Aggregate System

Glass beads of diameter range 0.925-1.292 mm with 80% in the range 1.01-1.275 mm were used as model aggregate. Although the use of single size aggregate particles is not a true reflection of the packing in actual mortars or concretes, it enables the volume fraction of beads to be calculated accurately. In addition the system follows the model of diffusion in a periodic composite proposed by Maxwell (1873) and discussed in Cussler (1985). The author considered a solid consisting of periodically spaced spheres, where diffusion takes place through the interstitial spaces and the spheres themselves. If the volume fraction of the spheres, the diffusivities of the spheres and matrix are known the effective diffusivity through the composite can be evaluated exactly from:

$$\frac{D_{eff}}{D} = \frac{\frac{2}{D_s} + \frac{1}{D} - 2\Phi_s\left(\frac{1}{D_s} - \frac{1}{D}\right)}{\frac{2}{D_s} + \frac{1}{D} + \Phi_s\left(\frac{1}{D_s} - \frac{1}{D}\right)} \qquad \text{Eqn. 6.1}$$

where D Diffusivity in interstitial pores.

D_s Diffusivity in spheres.

Φ_s Volume fraction of sphere.

If the spheres are impenetrable diffusion takes place through the cramped and tortuous pores of the interstitial spaces, effectively reducing the diffusion cross-sectional area and increasing the diffusion path length. These effects alter the diffusivity and the resultant value termed effective diffusivity. Thus the composite material situation is analogous to mortar, with the paste pores forming the interstitial space pores and the glass beads the spheres. Since the spheres are impermeable Ds = 0 the relationship simplifies to:

$$\frac{D_{eff}}{D} = \frac{2(1-\Phi_s)}{2+\Phi_s} \qquad \text{Eqn. 6.2}$$

This relationship is applicable if the composite consists of one continuous phase and one discontinuous phase, as is the case with cement paste and the glass beads

6.3.2 Sample Preparation and Experimental Set-Up

An initial study was carried out on 20% MK unplasticized paste. Due to the cohesive characteristics of high MK content pastes, a water:binder ratio of 0.5 was used without segregation occurring during placement and compaction. However, in the light of the dispersion problems encountered in the preparation of MK paste samples, the work was repeated using a lower MK content and 1% superplasticizer by weight of binder. Due to the lower MK content and the dispersive property of the plasticizer, a mix of water:binder ratio 0.35 had to be used to restrict segregation on compaction. For each of the regimes investigated five volume fractions of aggregate were studied, ranging from 15 to 55%.

6.3.2.1 Preparation of Unplasticized Mix

The materials for each mix were proportioned by mass. The MK was preblended dry with the OPC in an Hobart laboratory mixer for 2 minutes. Deionised water was then added and the paste mixed for 5 minutes, followed by the glass beads, and mixing for a further two minutes. The mortar was then placed and compacted in PVC cylindrical moulds and cured as described in Chapter 2.

6.3.2.2 Preparation of Plasticized Mix

The 10% MK plasticized mixes were manufactured by first blending the deionised water, MK and plasticizer in an Hobart mixer for 2 minutes. The superplasticizer used was a sulphonated naphthalene formaldehyde condensate (Type N), proportioned in accordance with the manufacturers instructions at 1% by weight of binder. OPC powder was gradually added to the MK slurry, and mixing continued for a further 5 minutes. Finally the glass beads were added and the same casting and curing procedure followed as described above.

After 12 weeks of moist curing under 35 mM NaOH at 22°C, discs approximately 3.5 mm thick were cut from the cylinders as described in Chapter 2. The experimental set-up was identical to that for steady state diffusion using the diaphragm cell described in Chapter 4. In addition bulk density, capillary porosity, total porosity and resistivity measurements were taken, using the procedures outlined in Chapter 4.

6.4 RESULTS AND DISCUSSION

Tables 6.1 to 6.3 list the diffusion data for 20% and 10% MK mortar samples. Equation 6.2 was used to calculate the diffusivity of the pastes from the measured effective diffusivities, assuming the beads to be impermeable.

The results for the unplasticized 20% MK mortar mixes listed in Table 6.1 show reasonable consistency, suggesting that the preparation problems associated with neat pastes are not as significant a factor in mortars. Presumably the inclusion of aggregate aids dispersion by "milling" the paste particles, breaking agglomerations and improving homogeneity.

The results for the 10% MK plasticized mix are listed in Tables 6.2 to 6.3. The close correlation among bulk density and resistivity results, validate the preparation method, and show that segregation of the mixes was not a significant problem.

Notably, the results for specimens of differing aggregate content show overlap probably because the differences in diffusivity between each aggregate fraction are quite small. Consequently any variation between discs due to the presence of heterogeneities will result in a relatively significant variation.

6.4.1 Diffusivity

Figures 6.6 and 6.7 show the effective diffusivities for 20% and 10% MK mortars respectively. The general trend in both cases is for a decrease in effective diffusion coefficient as the volume fraction of aggregate increases. As the aggregate volume increases the proportion of paste in the sample (which contains the pores) decreases. Since the glass beads are impermeable, the voids content decreases, by virtue of the lower paste volume. Hence transport properties are reduced due to a reduced diffusion cross-sectional area. In order to meaningfully evaluate results for mortars of differing paste volume fractions, Equation 6.2 was used to correct the data, enabling the paste component of each mortar to be compared directly.

Figures 6.8 and 6.9 show the diffusion coefficients for the paste fraction of the mortars, calculated using Equation 6.2. The diffusivity of the "mortar-paste" (paste component of mortar) does not alter significantly with aggregate content. Although the results are scattered they indicate that the diffusivity of mortar-paste is approximately the same as that for plain paste. This is in contrast to Ngala (1995) who found that the diffusivity of the mortar-paste in OPC mortars increased steadily with increasing aggregate content. At high aggregate contents the paste in OPC mortar was up to twice as permeable as paste in the absence of aggregate, indicative of an overlapping of the interfacial zones, which in turn created a preferential diffusion pathway. However the author noted that although diffusivity

of the mortar-paste increased with aggregate content, the effective diffusivity of the mortar remained constant. The conclusion was that the paste matrix is the continuous phase in mortars and is responsible for chloride ion transport. This is in agreement with Larbi (1991) who studied the effect of the interfacial zone on permeability, diffusivity and pore structure.

As the volume of aggregate in the mortar increases, there will be a gradual predominance of the microstructural characteristics of the IZ over those of the bulk paste. Thus if the IZ is more permeable, then it follows that, with increasing aggregate content, the mortar paste will be more permeable. These results suggest that the interfacial zone in MK mortars does not play a significant role in the diffusion of chloride ions at the aggregate volume fractions investigated. This may be because the interfacial zone is reduced to such an extent that pore structure in MK mortars is identical to that in plain pastes, or that the interfacial zones are not percolated, ensuring diffusion must take place through the smaller pores of the bulk matrix. Hence the properties of the bulk matrix will be the controlling parameters.

Larbi (1991) found that interfacial zones are reduced in thickness and porosity by pozzolanic additives, reducing the incidence of percolation. The improvements to the IZ were attributed to more effective packing around aggregates as a direct result of the small particle size of pozzolans. Secondly, pozzolanic hydrates deposited in place of calcium hydroxide in an "elimination-by-substitution" reaction was thought to reduce the thickness and increase the density of the region.

Winslow et al (1994) found evidence of percolation of an OPC mortar occurring at an aggregate volume fraction of 45%. If MK mortar behaved in a similar manner to OPC one might expect a similar phenomenon to be observed. However no evidence of percolation was found in the diffusion result for percolation even at aggregate volume fractions of 55%.

6.4.2 Desorption

Figure 6.10 shows the influence of aggregate volume fraction on total porosity. As expected the total porosity decreases as the volume of aggregate increases due to the lower paste fraction. If the data is corrected for the proportion of "mortar-paste" the total porosity remains constant irrespective of aggregate content. This is to be expected as pore space is the remnant of water filled space, and as each mix had the same water:cement ratio and curing conditions the evaporable water and hence total porosities for the paste components should be the same.

Figure 6.11 shows that capillary porosity of mortar-paste decreases with addition of 15% aggregate. Presumably the decrease in capillary porosity is due to the milling effect which produces a more homogenous sample than the plain paste. Hence a more thorough

pozzolanic reaction can take place in the mortars reducing capillary porosity. This postulation would seem to be supported by data for 30 and 40% aggregate mortar, whose paste components have the same capillary porosity. The constant capillary porosity for aggregate contents up to 40% is reflected in the diffusion data for the mortar-pastes. In contrast the capillary porosities of mortars with aggregate contents higher than 50% increases, suggesting that percolation is occurring in certain regions of the sample. Diffusion data does not support the conclusion that there is percolation as there is no corresponding increase in diffusivity. A possible explanation is that an increase in the aggregate content, and hence the volume of porous interfacial zone paste, is accompanied by an increase in interconnectivity of these regions. Since the interfacial zones are no longer as isolated, as at lower aggregate contents, capillary porosity increases. However transport properties are still dominated by the smaller pores in the bulk paste as the specimens are not fully percolated, preventing any increase in diffusivity.

6.4.3 Resistivity

The resistivity data in Figure 6.12 shows that as aggregate content increases so does resistivity of the mortar, consistent with a reduction in paths available for the migration of ions. The resistivity of the component paste of the mortar, calculated using Maxwell's composite theory discussed by Whittington et al (1981) is constant irrespective of aggregate volume fraction. There is no reduction in resistivity at high aggregate contents as one might expect if percolation had occurred. Presumably percolation did not occur either because the porosity of the IZ is not significantly different from that of the matrix, or the resistivity was controlled by the gel pores which are interconnecting the more permeable regions. If the former is the case then the IZ thickness must be significantly reduced to prevent percolation, especially at high aggregate contents.

Figure 6.13 shows a graph produced by Garboczi et al (1995) from a computer simulation of conductivity through an OPC mortar. Each of the lines represents a system with an interfacial zone of conductivity higher than the bulk paste. E.g. 20 refers to a mortar in which the interfacial zone paste is 20 times more conductive than the bulk. Conductivity data for 10% MK mortar is plotted on this graph, and agrees closely with the simulation for a mortar where interfacial zone paste and bulk paste have the same conductivity. This indicates that the transport properties of the matrix and the interfacial zone in MK mortars are similar.

6.5 CONCLUSIONS

Chloride ion transport in MK mortars reduces with increasing aggregate content.

Chloride diffusivity in MK "mortar-paste" is similar to that in a corresponding cement paste containing no aggregate and is independent of aggregate content. This suggests that the inclusion of MK reduces the percolation effects of the interfacial zone associated with OPC mortars. The results agree with Larbi's (1991) conclusions that the diffusion of chloride ions is controlled by the bulk cement paste matrix.

Improvements in the microstructure are likely to be a result of more efficient particle packing around aggregates, and a densifying of the interface due to the replacement of calcium hydroxide with pozzolanic hydrates.

The production of homogenous MK samples is aided by the use of aggregate, which appears to improve dispersion by breaking up agglomerates through the tumbling and milling that occurs during mixing.

Aston University

Illustration removed for copyright restrictions

Figure 6.1 Schematic of the transition zone (Zimbelmann 1978)

Aston University

Illustration removed for copyright restrictions

Figure 6.2 Schematic of the transition zone (Mehta 1986)

Aston University
Illustration removed for copyright restrictions

Figure 6.3 Variation of porosity and anhydrous material across interfacial zone (Scrivener et al 1988).

Aston University
Illustration removed for copyright restrictions

Figure 6.4 Percolation of interfacial zones in mortar and concrete systems (Winslow et al 1994)

Aston University
Illustration removed for copyright restrictions

Figure 6.5 Packing arrangement in the interfacial zone in concrete with and without silica fume (Goldman and Bentur 1989)

Volume Fraction Beads (%)	Effective Diffusivity D_{eff} ($x10^{-9}$ cm^2/s)	"Mortar-Paste" Diffusivity D ($x10^{-9}$ cm^2/s)
0	1.36	1.36
	1.39	1.39
	1.34	1.34
	1.15	1.15
	1.17	1.17
Average	1.28	1.28
15	1.09	1.38
	1.22	1.54
	1.35	1.71
	1.52	1.93
	1.35	1.71
Average	1.31	1.65
30	0.76	1.25
	1.65	2.71
	1.07	1.76
	1.73	2.84
	1.49	2.45
Average	1.34	2.20
40	0.32	0.64
	0.58	1.15
	0.84	1.68
	1.07	2.14
	0.45	0.89
Average	0.65	1.30
50	0.53	1.32
	0.42	1.05
	0.74	1.84
	0.20	0.50
	0.19	0.470
Average	0.42	1.04
55	0.38	1.08
	0.63	1.79
	1.14	3.22
	0.84	2.38
	0.58	1.64
Average	0.71	2.02

Table 6.1 Diffusion results for 20% MK "model mortars" of w/b 0.5.

Volume Fraction Beads (%)	Effective Diffusivity D_{eff} ($x10^{-9}$ cm^2/s)	"Mortar-Paste" Diffusivity D ($x10^{-9}$ cm^2/s)	Capillary Porosity (%)	Total Porosity (%)
0	2.57	2.57	2.50	38.45
	4.70	4.70	2.30	38.66
	5.73	5.73	2.05	38.42
	4.17	4.17	2.13	38.63
	2.75	2.75	1.74	38.44
Average	3.99	3.99	2.14	38.52
15	3.49	4.41	1.06	30.52
	3.54	4.48	1.19	30.55
	3.59	4.54	1.30	30.65
	3.38	4.27	1.17	30.70
			1.21	30.15
Average	3.50	4.43	1.19	30.51
30	2.97	4.87	0.91	24.57
	3.28	5.39	1.00	24.52
	2.13	3.51	0.98	24.42
	2.88	4.73	0.98	24.37
			0.81	24.06
			0.91	24.31
Average	2.82	4.63	0.93	24.37
40	2.84	5.69	0.70	19.87
	2.21	4.43	0.88	20.16
	2.13	4.27	0.64	19.61
	2.43	4.87	0.62	20.06
			0.83	20.32
			0.81	20.11
Average	2.41	4.81	0.75	20.02
50	1.77	4.42	0.76	16.19
	1.60	4.01	0.84	16.56
	1.88	4.69	1.02	16.80
	1.43	3.59	0.93	16.68
Average	1.67	4.18	0.89	16.56
55	1.22	3.45	0.75	14.10
	2.01	5.69	0.98	14.37
	1.15	3.25	0.94	14.04
	1.06	3.01	0.83	14.62
	0.88	2.48	0.74	14.76
			0.88	14.05
Average	1.26	3.58	0.85	14.33

Table 6.2 Diffusion results for 10% MK "model mortars" of water:binder ratio 0.35

Volume Fraction Beads (%)	Bulk Density of Mortar (g/cm^3)	Resistivity of Mortar (kΩ.cm)	Resistivity of "Mortar-Paste" (kΩ.cm)
0	2.069	24.44	24.44
	2.058	25.03	25.03
	2.072	24.00	24.00
	2.063	25.15	25.15
	2.067	24.64	24.64
Average	2.066	24.65	24.65
15	2.219	24.75	19.57
	2.231	25.17	19.90
	2.233	23.64	18.69
	2.230	24.21	19.14
	2.229	23.60	18.66
Average	2.228	24.27	19.19
30	2.366	32.64	19.87
	2.364	31.98	19.46
	2.356	32.16	19.57
	2.369	31.79	19.35
	2.349	31.75	19.32
Average	2.361	32.06	19.51
40	2.453	42.53	21.27
	2.451	41.96	20.98
	2.450	43.13	21.57
	2.451	42.29	21.15
	2.454	41.11	20.56
Average	2.371	42.20	21.10
50	2.514	50.67	20.27
	2.518	52.02	20.81
	2.512	48.22	19.29
	2.518	52.20	20.88
	2.522	46.94	18.78
Average	2.517	50.01	20.00
55	2.569	61.56	21.73
	2.561	60.25	21.27
	2.557	60.35	21.30
	2.563	60.89	21.49
	2.562	60.00	21.18
Average	2.562	60.61	21.39

Table 6.3 Results for 10% MK "model mortars" of water:binder ratio 0.35.

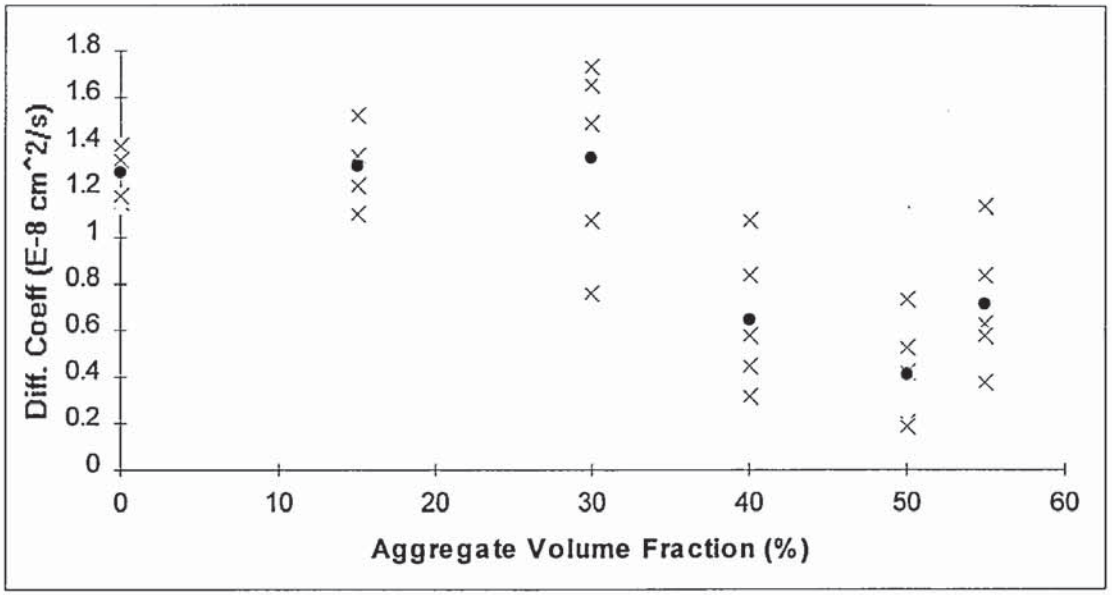

Figure 6.6 Effective diffusivity against aggregate volume fraction for 20% MK mortar.

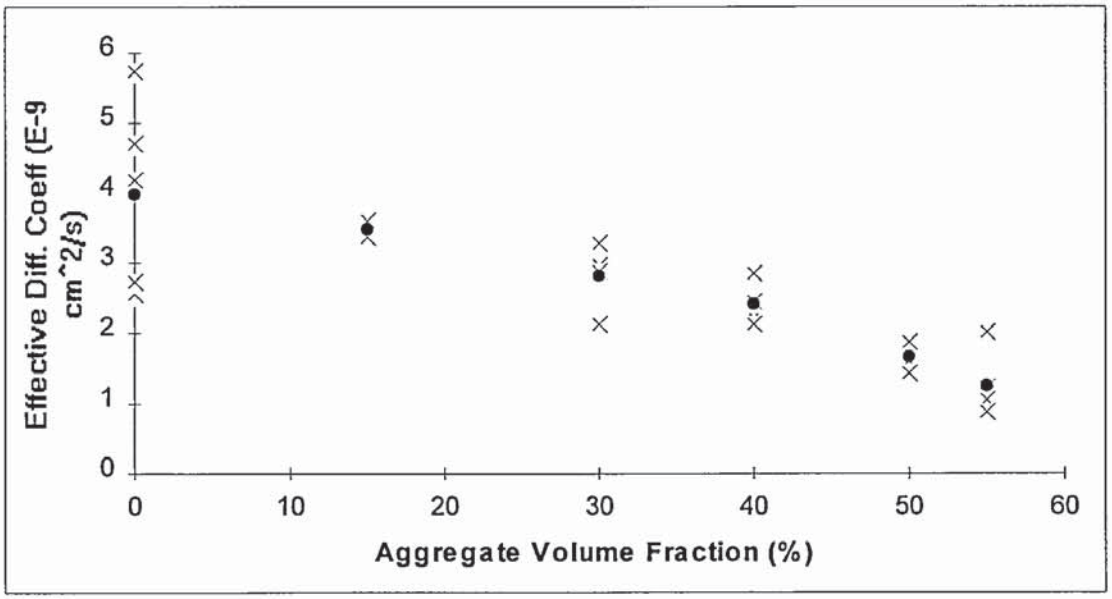

Figure 6.7 Effective diffusivity against aggregate volume fraction for 10% MK mortar.

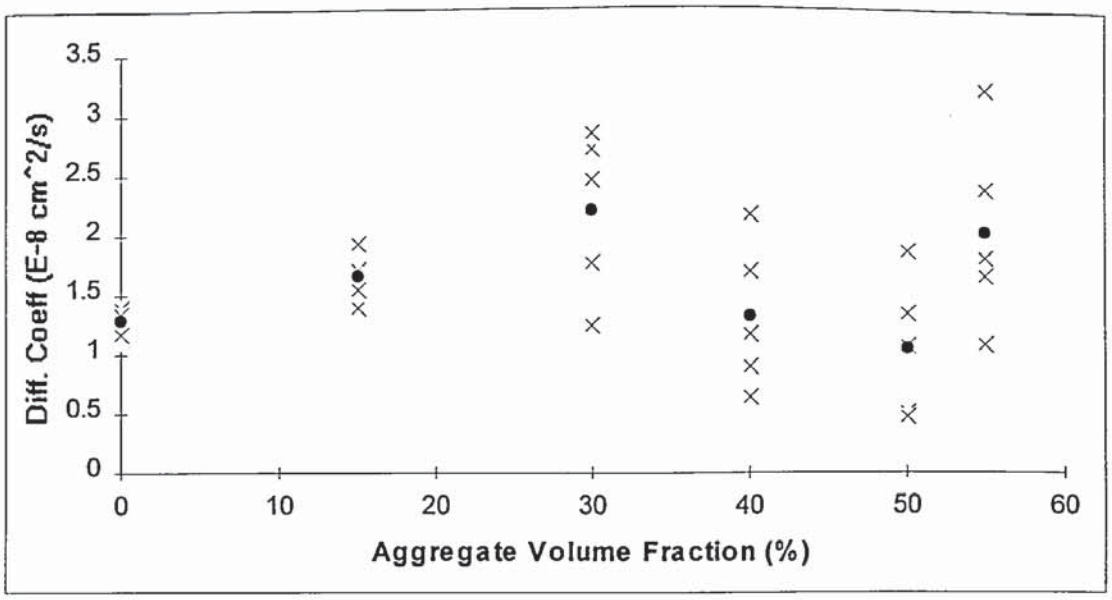

Figure 6.8 Paste diffusivity against aggregate volume fraction for 20% MK mortar.

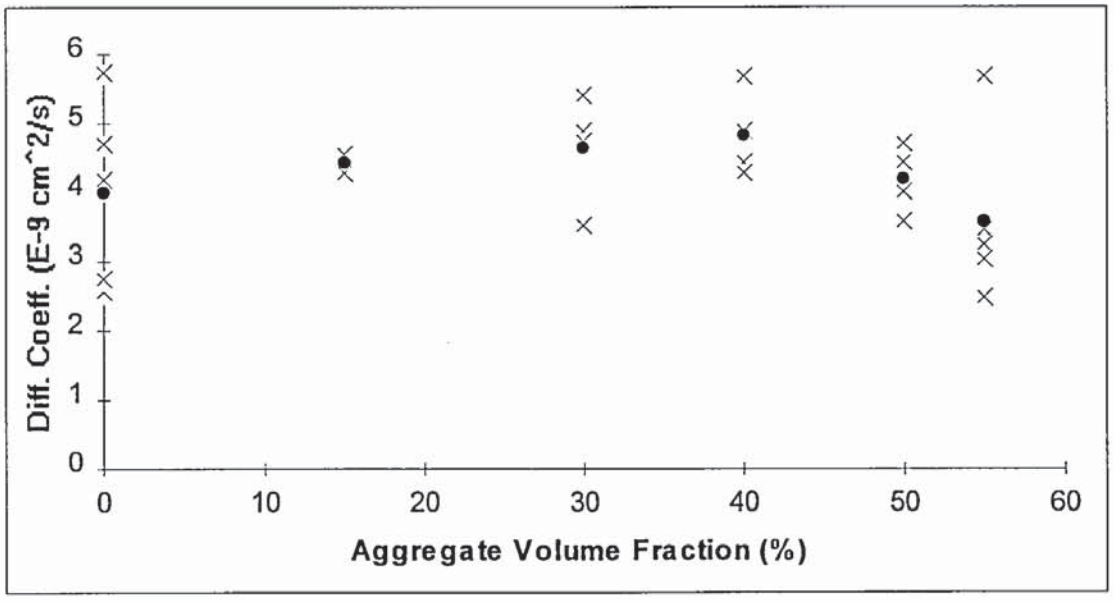

Figure 6.9 Paste diffusivity against aggregate volume fraction for 10% MK mortar.

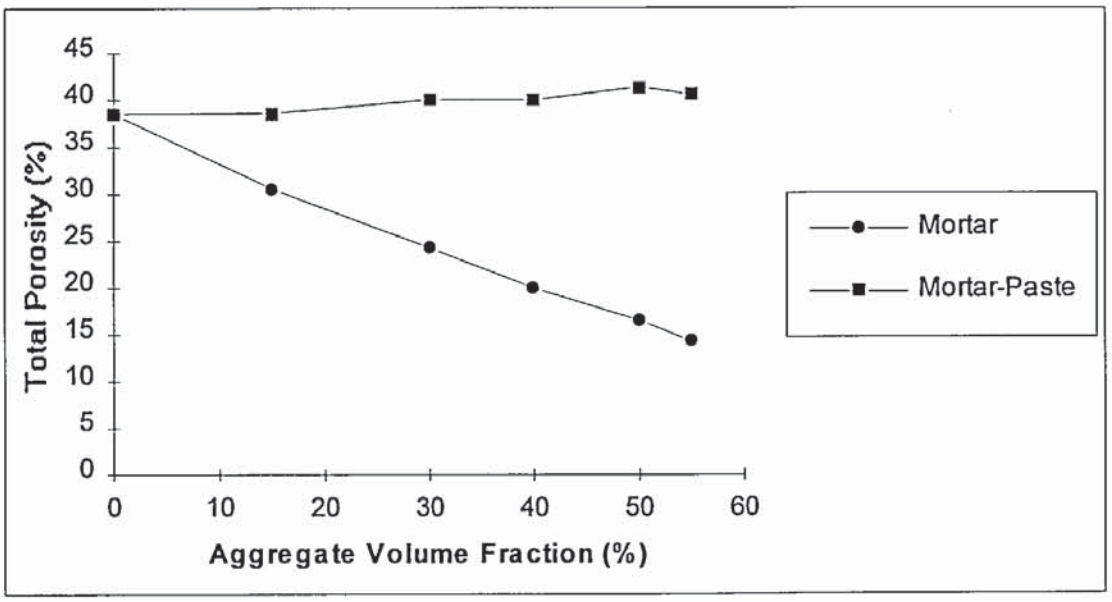

Figure 6.10 Total porosity against aggregate volume fraction for 10% MK mortar.

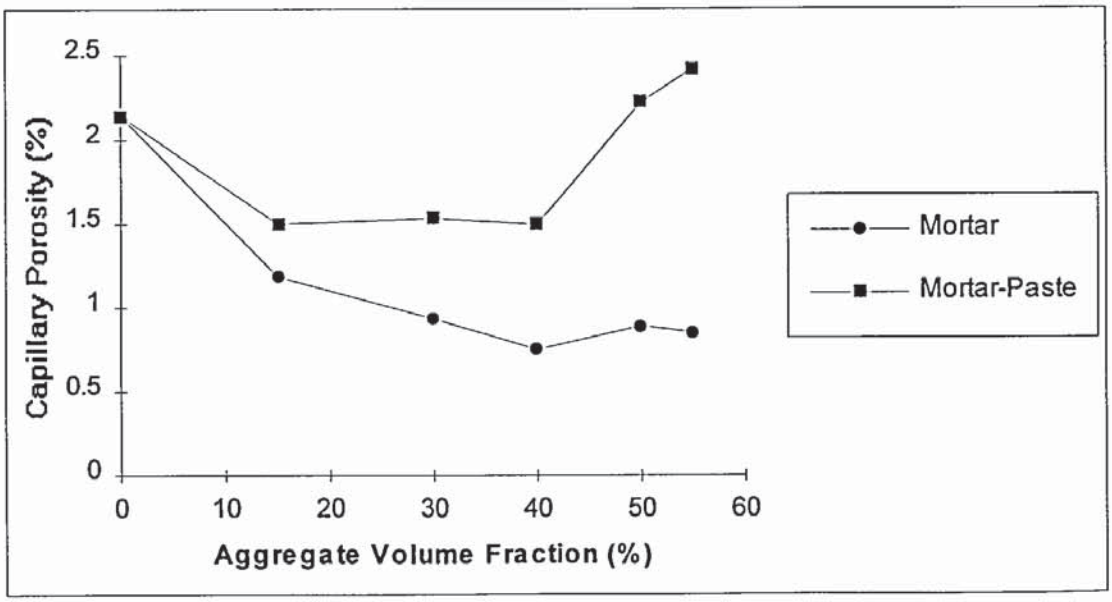

Figure 6.11 Capillary porosity against aggregate volume fraction for 10% MK mortar.

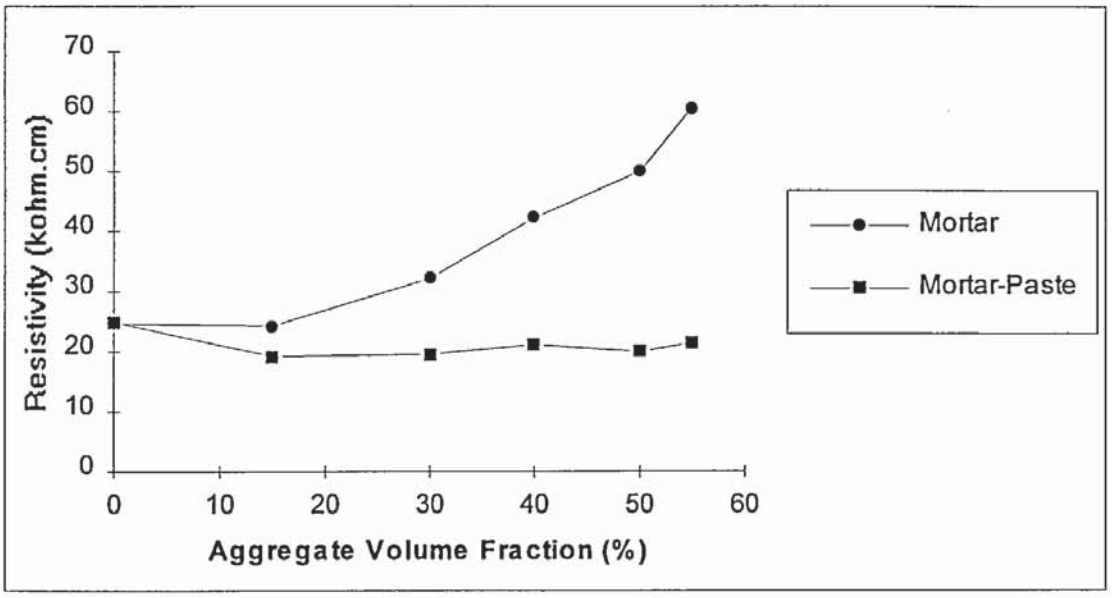

Figure 6.12 Resistivity against aggregate volume fraction for 10% MK mortar.

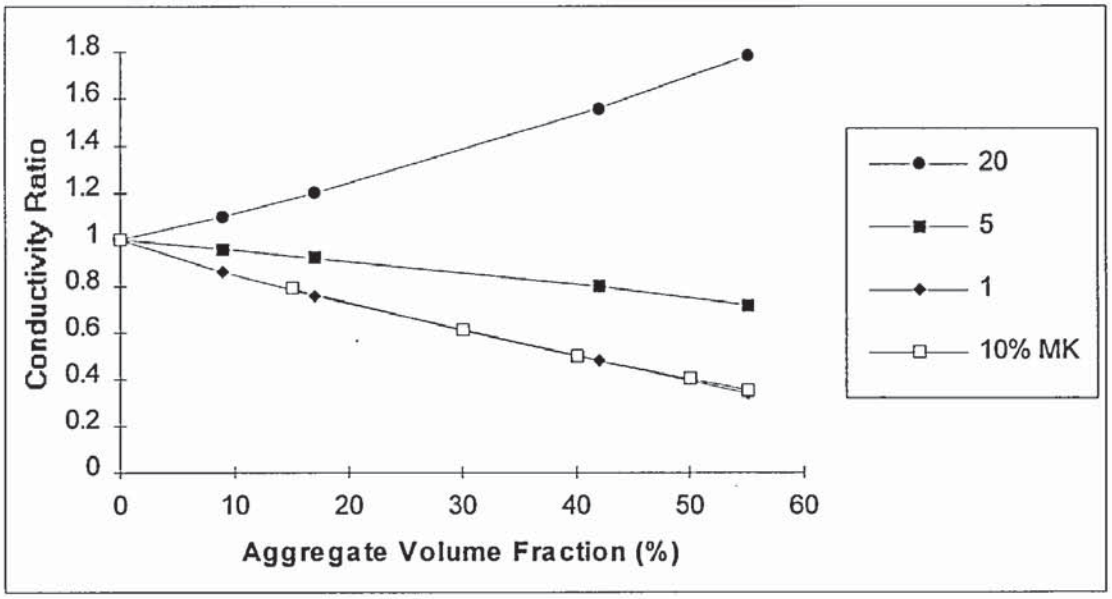

Figure 6.13 Mortar to paste conductance ratio against aggregate volume fraction (replotted data from Garboczi et al 1995).

CHAPTER 7

7. CHLORIDE PENETRATION AND CORROSION OF REINFORCEMENT IN CONCRETE

7.1 INTRODUCTION

Steel reinforcement embedded in concrete is usually prevented from corroding by the impermeability of the concrete, and the formation of a passive ferric oxide film on the steel surface which is stabilised by the alkalinity of the system. Ingress of chloride ions can lead to attack and subsequent disruption of the passive film followed by pitting corrosion of the steel, even if the cement matrix remains alkaline.

During pitting corrosion, the steel is attacked over a small area and, the largely passive remainder of the steel act as cathodic sites leading to very high corrosion activity at the smaller anodic sites, causing rapid loss of steel cross sectional area. Corrosion resistance of the system may also be reduced by a reduction in the alkalinity and consequently stability of the passive film. This usually occurs through carbonation, whereby atmospheric carbon dioxide forms an acidic solution in the pore water, neutralising the alkalinity of the matrix. Although studies have shown supplementary blending materials to reduce mass transport rates, the consumption of calcium hydroxide by pozzolans may reduce the buffering capacity of the matrix or the stability of the passive film. Thus a high diffusion resistance may be offset by a poor corrosion resistance, either through reduced alkalinity of the pore solution to such an extent that anodic dissolution takes place, or by reducing the threshold level of chlorides needed to initiate corrosion.

For MK to be a viable pozzolanic cement replacement for structural concrete it was important to investigate its performance in terms of corrosion resistance of embedded steel. The present study aims to compare the performance of MK concrete with OPC and more common blended systems in terms of both chloride ion diffusion and corrosion behaviour of the embedded steel exposed to a severe chloride environment, and is presented in two parts. Part 1 of the study concentrates on the chloride ion ingress into OPC and several blended cement concrete cylinders exposed to a high concentration of sodium chloride solution.

The corrosion behaviour of mild steel bars embedded in OPC and several blended cement concrete specimens exposed to a severe chloride environment by ponding was investigated in the second part of the study.

PART I. NON-STEADY STATE DIFFUSION OF CHLORIDE IONS INTO CONCRETE.

7.2 LITERATURE REVIEW

A model for the lifetime of a structure was proposed by Browne (1982), whereby the life span was divided into two periods, initiation and propagation (Figure 7.1). The first or initiation period t_0, refers to the time taken for chloride ions to penetrate from the surface through cover concrete to reach the level of the steel. During this period the steel is passive until the threshold value is reached for corrosion and t_1 begins. The propagation period (t_1) is the time taken for the build up of stress due to corrosion products to cause failure of the concrete. The rate of corrosion of steel is determined by the availability of oxygen, water and the resistivity of the concrete. Generally the initiation period is much larger than the propagation period, so workers take this as being a conservative estimate of the life span of the structure (Bamforth 1993). The initiation period is largely a function of the transport properties of the concrete. This has led to a considerable interest in assessing the transport properties and in particular the diffusion properties of concretes to prolong service life. A number of studies (Gjørv and Vennesland 1979, Dhir 1991, Bamforth et al 1993, 1994) have looked at the factors involved in increasing the initiation period, and concluded that the inclusion of supplementary cementing materials such as PFA, SF and BFS can be beneficial.

7.2.1 Non-Steady State Diffusion

The penetration or immersion test has been used by a number of workers to describe the ingress of chloride ions into concrete test specimens exposed to a saline environment (Sergi et al 1992, Gjørv et al 1994, Polder 1996). The test involves sealing all except one exposure surface of the specimen to prevent multi-directional penetration and immersing the specimen in a solution containing a high concentration of chloride ions. After a period of exposure the specimen is removed and the penetration depth or concentration profile of the chloride ion measured. By assuming Fick's second law of diffusion to be applicable (equation 7.1) the apparent diffusion coefficient can be calculated.

$$\frac{\partial C}{\partial t} = D\frac{\partial^2 C}{\partial x^2} \qquad \text{Eqn 7.1}$$

Collepardi et al (1972) calculated diffusion coefficients by measuring the maximum penetration depth of the ion after a known exposure period and applying equation 7.2. A solution to Fick's second law, described by Crank (1975), commonly adopted to model chloride penetration into concrete is given by equation 7.3 for the stipulated boundary conditions.

$$X_d = 4\sqrt{DT} \qquad \text{Eqn. 7.2}$$

$$\frac{C_x}{C_s} = 1 - erf\left(\frac{x}{2\sqrt{DT}}\right) \qquad \text{Eqn 7.3}$$

For $C = 0$, at $t = 0$ $\quad 0<x<\infty$

$C_X = C_S$ at $x = 0$ $\quad 0<t<\infty$

where X_d -penetration depth (cm)
C_X -Chloride content at depth x (g/cm^3)
C_S -Surface chloride concentration (g/cm^3)
x -Depth (cm)
T -Exposure duration (s)
D -Apparent diffusion coefficient (cm^2/s)
erf -Gaussian error function

The application of Fick's second law to chloride penetration into concrete structures entails several assumptions, some of which may not be valid. Pure diffusion is assumed through permanently saturated concrete, none of the chloride is considered to be immobilised, the diffusion coefficient remains constant throughout the exposure period, the external chloride source remains constant.

In reality few, if any of these assumptions are valid especially where the specimen is exposed to wetting and drying cycles. For diffusion alone to take place the concrete pore system must be saturated, otherwise absorption will occur. Absorption enables the penetration of chlorides to a much greater depth over a shorter period than would otherwise occur by diffusion.

The assumption that the diffusion coefficient remains constant throughout the exposure period is unlikely to be valid, especially if the concrete is exposed to chlorides from an early age. As hydration progresses the pore structure will develop and become more refined, reducing the diffusivity of the concrete. In addition the diffusivity of the material may not be constant throughout the element since concrete is a heterogeneous material. This variability is likely to be greatest between the bulk and cover zone concrete which are exposed to different curing and environmental conditions, as highlighted by Gjørv and Vennesland (1979).

In field exposure conditions Roy et al (1993) have noted that the surface chloride level has seasonal variations. This will not only alter the rate of diffusion, but also affect calculation of the apparent diffusion coefficient. If sampling is undertaken when surface chloride levels are high, D will appear to be lower than if a low surface chloride level was used.

As the chlorides penetrate the concrete they react with or are adsorbed on to the surface of hydrates preventing further ingress. This binding effect is temperature dependent, as well as being influenced by carbonation, blending materials and pore fluid composition (Sergi 1986).

However despite these limitations the penetration test is still widely accepted throughout the industry as providing information on performance in terms of durability and service life.

7.2.2 Influence of Blending Materials

Gjørv and Vennesland (1979) in a study of the durability performance of concretes concluded that OPC concrete of high quality and low water/cement ratio was incapable of offering long term protection to embedded steel in severe salt exposure conditions. The addition of supplementary cementing materials such as PFA, SF and BFS were shown to improve resistance to chloride ingress. Similar findings were reported by Thomas (1991), Dhir (1991) and Bamforth (1993). Table 7.1 lists diffusion coefficients obtained by applying Fick's second law to chloride profiles. Although these results are for different concrete mixes and exposure conditions a general observation is that under similar test regimes OPC concretes have higher diffusion coefficients than blended mixes.

Thomas (1991) and Bamforth (1994) have noted a decrease in diffusion coefficient for PFA and BFS blends with time (Table 7.1). Both authors attributed this behaviour to high initial absorption of chloride containing solution into the unsaturated concrete. Once the concrete reached saturation, diffusion predominated. Thomas (1991) found negligible increase in chloride concentration profiles between 1 and 2 years of exposure for PFA concretes, suggesting that the initial high ingress of chloride ions is due to absorption, resulting in an over estimate of the diffusion coefficient. However a reduction in apparent diffusion coefficient was noted by Seneviratne (1991) for PFA and OPC concretes saturated prior to exposure to a chloride containing environment. Absorption could not be responsible in this instance, although it is likely that continued hydration during exposure resulted in a refining of the pore structure. Work by Bamforth (1994) showed that BFS and PFA continue to reduce diffusivity values several years after casting, whereas OPC and Silica fume mixes did not exhibit this continued improvement to the same extent.

Some workers (Seneviratne 1991, Liam et al 1992, Roy et al 1993, Gjørv et al 1994) have found evidence that diffusion coefficients for chloride ions through pastes obtained by steady state methods, are comparable with those obtained by concentration profile solution to Fick's second law of diffusion for concrete exposed to long term insitu conditions. This

would negate the need for time consuming tests on concrete specimens, as data from the much shorter diffusion through thin paste specimens could be used to compare performance.

Larbi (1991) in an investigation of the aggregate-paste interfacial zone (IZ) found that although the interfacial zone was more porous than the bulk paste, it was the bulk paste which governed diffusion characteristics. The porosity in the IZ was isolated and diffusion mainly occurred through the bulk HCP, which is the only continuous phase in concrete. Therefore diffusion through the bulk paste is the rate limiting factor. However other workers have proposed percolation theories whereby aggressive species are able to rapidly penetrate the cement matrix via interconnected aggregate-paste interfacial zones (Garboczi et al 1990, 1992, 1995, Winslow et al 1994). Thus, due to the uncertainty concerning diffusion paths in concrete it is not safe to predict durability performance of concrete solely from experiments on hardened cement paste.

There is a paucity of data on the performance of MK concrete in severe salt exposure conditions. In terms of the practical application of MK, comparative tests on concrete containing blended cement need to be carried out to provide an indication of the service life performance of MK concrete. Diffusion data obtained from this study will not provide "material constants" that will be applicable to all situations to enable service life predictions of structures knowing the surface concentration of chlorides. The resistance of a particular concrete to chloride ingress will not only depend on the factors mentioned already such as binder composition but also on curing and environmental conditions. Hence diffusivity data obtained for mixes manufactured cured and exposed to the same regimes can only be used to provide relative information of the performance of comparable mixes to aggressive chloride environments. MK concrete was compared with plain OPC, PFA and BFS concrete to elucidate whether the inclusion of MK could improve resistance to chloride ion penetration. The use of ternary blends was also investigated. By using two pozzolans with different rates of hydration and hydration products, improvements may be possible in terms of workability, strength and durability.

7.3 EXPERIMENTAL PROCEDURE

Concrete mixes listed in Table 7.2 were prepared as described in Chapter 2. The mixes used in this test programme were not based on standard mixes for severe exposure conditions, since this would require strength to be constant necessitating different binder and water contents. Mix proportions were kept constant to enable evaluation of the effect of binder type. Studies using PFA and BFS often reach favourable conclusions, where strength is kept at the same level as the control mix, as invariably a lower water/binder ratio is used for the blended mix. Although such studies provide important information on the type of mixes used in practice, they do not identify clearly the extent to which improved performance is

caused by reduced water/binder ratio or by the blending material itself. Such information is necessary when comparing the relative performance of different cement replacement materials and when assessing the relative merits of other direct water-reducing admixtures.

The composition of the ternary blends were arbitrarily chosen. No previous testing was undertaken to evaluate the optimum proportions of pozzolan. Rough estimates of pozzolanic content were made on lime consumption data from Chapelle test data.

Concrete cylinders 100 mm in diameter by 150 mm were cast, demoulded after 24 hours and cured under water at 20°C for 28 days. At the end of the curing period the cylinders were coated with two layers of paraffin wax on all surfaces except the exposure face. The cast end face was used as the exposure surface as it was thought it would be subject to less variation during manufacture than the trowelled face. The cylinders were then submerged in a tank containing a large volume of 0.5M NaCl solution. This solution was changed every 3 months to maintain a constant concentration. After 12 to 14 months the cylinders were analysed, at incremental depths from the exposed face, for total chloride content.

The cylinders were removed from the tank immediately prior to testing to avoid possible false chloride profiles, due to the movement of chlorides as a consequence of drying. The paraffin wax was removed and the cylinder located firmly in the jaws of a lathe. By using the lathe at low rotation speed and a hardened steel bit, concrete samples were ground off the cylinder in increments of 2 mm from the exposure face. The powder was collected on a clean sheet of paper, transferred to air-tight plastic bags, and taken for total chloride analysis. Slow rotation of the sample was necessary to prevent the grindings being scattered and to minimise aggregate plucking.

There are several advantages of using this technique over traditional methods of saw cutting at consecutive depths. Firstly no water is used to lubricate the cutting process which may result in washout of some chlorides. Secondly specimens can be sampled at small depth increments enabling accurate profiling. As concrete is heterogeneous too small a sample would not be representative and would also require a large number of slices to establish a profile. Bigger slices would reduce the accuracy of the profile as well as causing severe aggregate pull out. Thus 2 mm was adopted as the slice thickness.

The concrete powder samples were placed in an oven at 105°C over night, then ground to pass a 150μm sieve. The sample was thoroughly mixed and 5 grams weighed out accurately. Chloride analysis using titration with silver nitrate solution was performed as described in Chapter 2.

7.4 RESULTS AND DISCUSSION

The chloride profiles obtained for each mix are shown in Figures E.1 to E.7 of Appendix E, along with theoretical chloride profiles established from calculated values of apparent diffusion coefficient and surface chloride concentration. The similarity between theoretical and experimental profiles validates the calculation procedure.

Form Figure E.1 it can be seen that the OPC mix has the lowest surface chloride content, but the highest penetration depth. This seems anomalous at first as a higher chloride content near the surface would result in a large driving force for diffusion causing greater penetration. However Bamforth (1993) explained this phenomenon in terms of binding capacity whereby chlorides are incorporated in the cement hydrates or adsorbed on their surfaces, and are not available for diffusion. OPC mixes are believed to have lower binding capacities (Arya 1995) than PFA and BFS mixes and combined with a more open pore structure enables significant chloride penetration.

All the profiles except the OPC mix show the maximum chloride content a few mm into the specimen, and not at the surface as expected . A possible explanation is initial absorption of chloride solution. This is unlikely as the specimens were saturated prior to exposure. In addition the length of exposure would tend to lead to a diffusion mechanism masking any absorption that had occurred. More likely is that the surface concrete is not representative of the bulk. Since the exposure face is a cast face it is more likely to be affected by short term curing and production procedures than the internal bulk concrete. Notably the mixes containing a high replacement content seem worst affected. This probably meant that these concretes were more susceptible to initial curing, and consequently did not develop a refined pore structure even after 28 days. To a certain extent this is reflected in the compressive strength results (Figure 7.2), which show blended mixes to generally have lower strengths than the control mix. The surface layers also show low total chloride content indicating a low binding capacity and possibly inadequate hydration. This suggests that blended mixes containing high levels of cement replacement material will require more curing than an OPC concrete. In order to obtain profiles more representative of the bulk it may be necessary to remove the first 5 mm or so of the sample prior to exposure. However the profiles obtained in this study include the effects of the surface zone, and are more likely to be representative of insitu concrete.

7.4.1 Binary Blends

The apparent diffusion coefficients for each mix calculated using the error function solution (Eqn 7.3) to Fick's second law of diffusion are listed in Table 7.3. The partial replacement of cement with MK improves the chloride diffusion properties of concrete. 10% and 20%

MK concrete have apparent diffusion coefficients 70% and 90% smaller than corresponding OPC concrete. The higher resistance provided by MK concrete to chloride ingress can be attributed to a number of factors. Firstly work on pore structure reported in Chapter 3 indicates that the addition of MK modifies the pore structure and reduces the capillary porosity of the matrix. Work described in Chapter 6 shows that MK blended mortars are not as greatly effected by the paste-aggregate interfacial zone as OPC mortars (Page and Ngala 1997).

The lower apparent diffusivities of MK blends may be due to the co-diffusing alkali ions being absorbed and immobilised by the pozzolanic CSH gel, slowing the ingress of the co-diffusing chloride ion. Walters and Jones (1991) found that MK suppressed alkali silica reaction by immobilising alkali metal ions. A similar mechanism was proposed by Gjørv et al (1994) for Silica fume (SF) concrete. SF reduces alkali metal and hydroxyl ions in the pore solution, reducing the ion exchange capacity of the system reducing the chemical diffusion potential.

The PFA and BFS binary blends represent typical mix formulations for these replacement materials. The MK concrete mixes compare favourably with the PFA and BFS mixes. The 70% BFS mix has an unexpectedly high apparent diffusion coefficient. This may be because BFS mixes are more susceptible to poor curing, especially at high replacement levels. It was noted during manufacture of the samples that the BFS mix had poor strength gain. Consequently to prevent cracking, demoulding of the specimens had to be delayed from the usual 24 hours to 3 days. The low diffusivities reported in the literature (Table 7.1) for BFS mixes tend to be for long exposure durations. Bamforth (1993), in an extensive review of site exposed concrete highlighted a trend of decreasing diffusivity with age for blended mixes. This may be a manifestation of high early chloride ingress through the immature pore structure which is significantly reduced over subsequent years by continued hydration. The relatively short curing and exposure regime in this study may not be have revealed long term benefit of BFS and PFA mixes. Owing to the high pozzolanic reactivity and rapid pore structure development MK may be better at preventing initial ingress of chloride ions than BFS mixes, which may have better long term microstructural improvements.

7.4.2 Ternary Blends

All the ternary blends performed significantly better than plain OPC concrete in terms of reducing chloride ion diffusion. Comparing 20%PFA/10%MK with 25% PFA and 10% MK mixes it can be seen that the ternary blend has a lower apparent diffusivity than the constituent binary blends. Thus one component alone is not responsible for the improvement, it must be a combination of both. The improvement in resistance to chloride

ion penetration might be a consequence of the higher blending component of the mix or there may be a symbiotic relationship between the PFA and MK.

The 60%BFS/10%MK ternary blend shows improvement over the 70% BFS blend. Notably this mix did not suffer retarded strength gain associated with the BFS binary blend although both contained equivalent weights of cement replacement. These mixes contain the same total replacement levels so improvements in diffusivity must be due to the combined effect of both pozzolans being better than BFS alone.

Comparison of these results with other workers (Table 7.1) is difficult due to the variations of the mix proportions and test regimes used which will influence mass transport properties. Bearing in mind the water/binder ratio (0.55) and the relatively short exposure period the results from this investigation compare favourably with the published data, and the blended mixes perform significantly better than OPC mixes. The apparent chloride diffusion coefficients obtained from this study are not exceedingly low, possibly due to insufficient curing and the high cement replacement levels employed, which may have resulted in retarded or incomplete hydration. However within the test regime employed MK mixes performed significantly better than the control OPC concrete, and slightly better than PFA and BFS blends.

7.4.3 Compressive Strengths

With the exception of the 10% MK mix all the blended concretes showed lower compressive strength than the control at 7 days (Figure E8). The phenomenon is more pronounced in blends containing high replacement levels. The higher strength of 10% MK may be due to accelerated hydration associated with the filler effect discussed in Chapter 3. A reduced lime content may also have reduced the size of the paste-aggregate interfacial zone promoting more efficient stress transfer between the matrix and aggregate.

7.5 CONCLUSIONS

These results show that MK when used as a partial cement replacement can reduce the ingress of chloride ions into concrete when compared to a plain OPC mix. The MK blends also performed better than the more common PFA and BFS mixes under the particular curing and exposure conditions. The relatively short exposure period of one year may highlight the benefits of a highly reactive pozzolan, but mask the long term benefits of slower reacting blending materials such as PFA and BFS. Consequently although the ternary blends investigated showed lower apparent diffusion coefficients than the OPC control, the long term benefits may not have been realised.

SOURCE	EXPOSURE CONDITION	MIX	W/B RATIO	D cm^2/s ($x10^{-8}$)
Page et al (1991)	Submerged	OPC	0.5	14.5
Thomas (1991)	Tidal Zone	OPC 15-50% PFA	0.68-0.49 0.61-0.39	15.06-2.09 1.13-3.73
Thomas (1990)	Tidal Zone	OPC 30% PFA	0.68-0.49 0.61-0.39	15.52-5.56 7.70-2.17
Liam et al (1992)	Tidal Zone Splash Zone	OPC	0.5 (Assumed)	2.13 5.50
Collepardi (1972)	Submerged	OPC Natural Pozzolan	0.4 0.4	1.65 1.05
Bamforth (1993)	Splash Zone	OPC 30% PFA 70% BFS 8% SF	0.66 0.54 0.48 0.72	6.57 2.20 3.30 4.08
Bamforth (1994)	Splash zone	OPC 30% PFA 70% BFS 8% SF	0.66 0.54 0.48 0.72	12.2 0.414 0.796 8.21
Polder (1996)	Submerged	5% SF 5%SF/10%PFA OPC 70% BFS	0.43 0.43 0.43 0.43	3.0 1.0 2.5 0.8
Seneviratne (1991)	Submerged	OPC 26% PFA	0.57 0.47	3.54 2.10
Roy et al (1993)	Splash Splash Submerged Submerged	OPC OPC OPC OPC	0.7 0.4 0.7 0.4	21.3 10.0 32.5 7.8
Gjørv (1994)	Submerged	9% SF OPC	0.28-0.44	0.27-0.56 1.4

Table 7.1 Diffusion coefficients for concrete exposed to saline environments published in literature.

	OPC	MK	BFS	PFA	10mm	Sand	Water	W/B
	kg/m^3							
A	420	-	-	-	985	710	231	0.55
B	126	42 (10%)	252 (60%)	-	985	710	231	0.55
C	294	42 (10%)	-	84 (20%)	985	710	231	0.55
D	315	-	-	105 (25%)	985	710	231	0.55
E	126	-	294 (70%)	-	985	710	231	0.55
F	378	42 (10%)	-	-	985	710	231	0.55
G	336	84 (20%)	-	-	985	710	231	0.55

Table 7.2 Mix designs for non-steady diffusion samples.

	Mix	Surface Chloride Content (%Cl/g Binder)	Apparent Diffusion Coefficient (x10^{-8} cm^2/s)
A	OPC	1.80	7.73
B	60%BFS/10%MK	2.66	3.81
C	20%PFA/10%MK	2.92	1.95
D	25% PFA	3.05	3.02
E	70% BFS	2.63	4.81
F	10% MK	2.13	2.37
G	20% MK	3.13	0.789

Table 7.3 Apparent diffusion coefficients and surface chloride concentrations.

Aston University

Illustration removed for copyright restrictions

Figure 7.1 Time from exposure to significant deterioration for concrete due to steel corrosion (modified from Browne 1982).

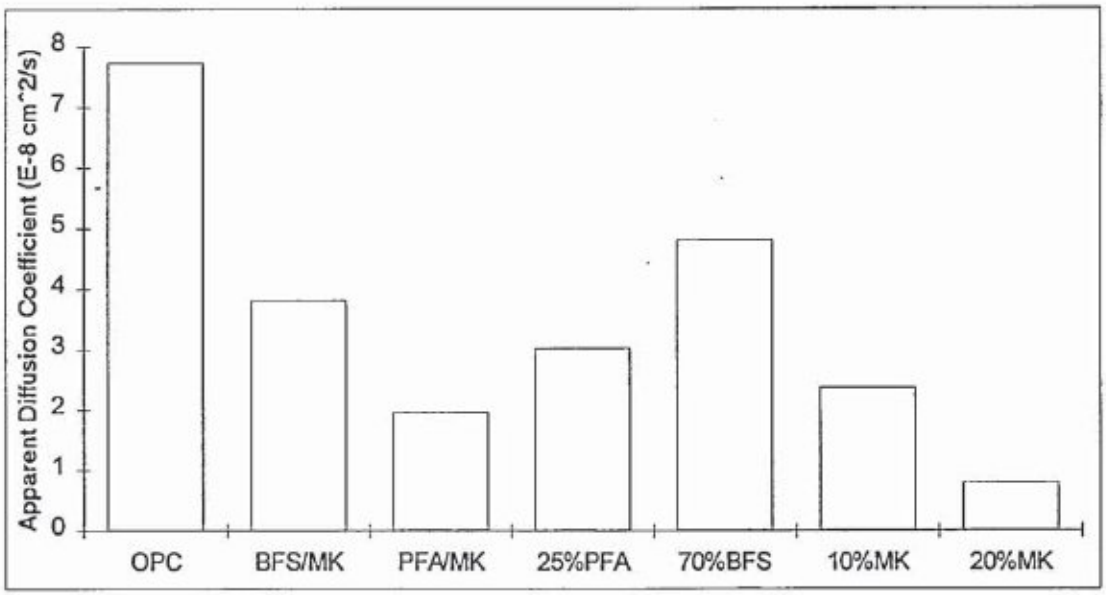

Figure 7.2 Apparent chloride diffusion coefficients for concrete specimens.

PART II. CORROSION OF STEEL EMBEDDED IN CONCRETE

7.6 LITERATURE REVIEW

As with any new material there are questions concerning long-term behaviour that must be assessed on the basis of investigations of relatively short duration. This work aims to investigate possible effects of MK on durability of reinforcing steel in concrete exposed to chloride containing environments.

In most practical situations penetration of chloride ions will be a combination of permeation, absorption and diffusion. Pure permeation or diffusion can only occur in saturated concrete where no capillary forces can be active. If dry or non-saturated concrete is exposed to a chloride solution, absorption is the dominant mechanism. Cyclic wetting and drying not only provide ideal conditions for corrosion to propagate, but also promotes chloride ingress into concrete (Lambert et al 1991). During wetting periods the near-surface concrete layers readily absorb the chloride solution. Upon drying the water will evaporate, leaving the salt in the pore system of the near-surface region. Successive wetting re-saturates the surface zone, dissolving precipitated chloride as well as carrying more chlorides into the concrete. Repeated wetting and drying cycles increase the salt concentration in the pore system, to levels higher than the source, or that which would result from diffusion alone. This type of exposure regime mirrors that of insitu concrete structures such as bridges and carparks, where repeated ponding of salt solutions result in high chloride concentrations and localised steel corrosion.

7.6.1 Corrosion of Steel in Concrete

Steel embedded in concrete is protected from corrosion by a passive γ-Fe_2O_3 film that forms a protective layer on the surface of the metal. High concentrations of hydroxyl ions found in the concrete pore solution stabilise the film and enable the layer to be continuously repaired, effectively stifling the anodic dissolution of ferrous ions so that corrosion rate remains negligibly small. While carbonation encourages corrosion by neutralisation of the hydration products around the steel so that the passive layer becomes unstable, free chloride ions will locally destroy the passive film forming sites of intense local anodic activity known as pits, even in a highly alkaline environment. With the pits acting as anodes and the large, unaffected areas of passivated steel acting as cathodes, pits can rapidly penetrate the thickness of the steel, since cathodic and anodic currents must be equal enabling high anodic current densities to develop. In the electrochemical corrosion reactions, chlorides ions are not consumed but may form intermediate corrosion products such as $FeCl_2$. Subsequent hydrolysis liberates the chloride ion, releasing hydrogen ions, which reduce the pH at anodic sites, forming conditions more favourable for corrosion.

Anodic Reaction

$$Fe \rightarrow Fe^{2+} + 2e^{-} \quad \text{Eqn. 7.4}$$

$$Fe^{2+} + 2(OH^{-}) \rightarrow Fe(OH)_2 \quad \text{Eqn. 7.5}$$

$$Fe(OH)_2 + 2H_2O + O_2 \rightarrow 4Fe(OH)_3 \quad \text{Eqn. 7.6}$$

Cathodic Reaction

$$4e^{-} + 2H_2O + O_2 \rightarrow 4(OH^{-}) \quad \text{Eqn. 7.7}$$

Several studies (Bamforth et al 1993,1994, Mangat and Molloy 1991, Dhir et al 1991) have concentrated on corrosion of steel in concrete exposed to chloride containing environments. It has been shown that most blending materials improve corrosion resistance. Coleman and Page (1997) reported that the addition of MK reduces the alkalinity of the pore solution to around pH 13. This is not low enough to cause corrosion as steel is expected to remain passive at pH 11.5 or above, although it may reduce the effectiveness of the buffering capacity of the system, and reduce the threshold value necessary to cause corrosion.

7.8.2 Threshold Value

Depassivation of the steel surface requires a chloride ion concentration exceeding a threshold value, which is often referred to as the critical chloride concentration. Critical chloride concentration is not constant for any concrete or exposure condition but depends on pore solution composition, cement type and w/c ratio which determine the free chloride content in the pore fluid, and how much is chemically bound (Hansson 1984). For example the chloride threshold level in water saturated concrete is higher than in concrete subject to wetting and drying. This has led to reported threshold levels of between 0.2 and 2.5% total chloride by weight of binder.

There is some debate as to how to specify threshold value. It has been suggested that $\frac{Cl^-}{OH^-}$ ratio of the pore solution is critical (Page et al 1991, Kayyali and Haque 1995, Hussain et al 1991). In OPC systems a high $\frac{Cl^-}{OH^-}$ ratio increases the risk of corrosion. However PFA, SF and BFS blends tend to exhibit high $\frac{Cl^-}{OH^-}$ ratios due to the lower lime contents of these mixes, although this is not reflected in high corrosion activity (Mangat and Molloy 1991). It is thought that low ionic mobility due to pore blocking may be a factor.

Free chloride content of the pore solution is thought to be a more reliable indicator of corrosion risk, although samples are difficult to obtain, especially from insitu specimens. The process requires taking a concrete sample and crushing it at high pressures in a sealed chamber to express the pore fluid. This has led to investigations on indirect methods of assessing free chloride contents, using solvents and distilled water to remove chlorides from

the sample (Arya et al 1987, Dhir et al 1990). The reported accuracy of these tests is poor with different solvents required depending on the concentration of free chloride present.

For practical situations the total or acid soluble chloride content is often used to assess corrosion risk. Free and bound chloride contents are thought to be in equilibrium and so bound chloride content will be directly related to free chloride content and hence corrosion risk (Mangat 1994). There is no consensus on the permissible levels of chloride in concrete between national standards. The BRE has proposed a classification for assessing risk of corrosion in terms of acid soluble chloride content by wt of cement (Everett and Treadaway 1980). Total chloride contents less than 0.4% by weight of cement represent a low risk, and 1% chloride by weight of cement or above represent a high risk of corrosion. Bamforth (1994) reported that cement replacement materials have no effect on chloride threshold level. Conversely Thomas (1996) in an extensive field study of PFA concrete found that threshold level was reduced as PFA content increased, although this did not adversely effect corrosion behaviour. The lower threshold level was offset by the lower penetrability of chloride ions. Total chloride content, as an indicator of corrosion risk, has been adopted in this work as the basis for threshold level, as this seems to be the predominant method of specification in current UK codes of practice (BS8110).

7.6.3 Methods for measuring Reinforcement Corrosion in Concrete

The corrosion of steel in concrete can be studied by exposing samples to known environments for long periods, then removing the cover concrete and weighing the steel to determine the amount of corroded material. Obviously these type of experiments are destructive and cannot give an indication of instantaneous corrosion rate. Electrochemical methods have been developed that enable corrosion rates to be measured.

In order for corrosion to proceed, there must be a complete "electrical circuit" between anodic and cathodic areas of the steel, that is ions and electrons must flow between these areas. The magnitude of the corrosion current is a direct measure of the rate of corrosion of the steel. As in any electrical circuit, corrosion current is limited by resistance of the circuit i.e. the electrical resistance of concrete.

7.6.3.1 Corrosion Potential (Ecorr)

Electrical resistance of the concrete is one of the factors controlling how fast corrosion can occur, electrochemical potential is one of the parameters which determine whether corrosion is possible. Electrochemical potential or corrosion potential is a measure of the ease of electron charge transfer between steel and the cement pore water solution, and is thus a property of the steel/concrete interface. It is not possible to determine the absolute value of the potential and therefore the potential difference between the steel surface and a reference

electrode , such as a saturated calomel electrode (SCE), is taken as a measure of the actual potential.

The simple and most frequently used method of potential mapping using a reference electrode in contact with the surface of the concrete, reveals the areas most likely to undergo corrosion. The two major limitations of the use of such measurements are their purely qualitative character and the difficulty of interpretation. Corrosion Potential (Ecorr) depends on moisture content of the concrete, oxygen availability and occurrence of galvanic macrocouples, and hence only gives an indication of the likelihood of corrosion. Passive steel in well oxygenated concrete usually has an Ecorr more noble than -250 mV on the saturated calomel electrode scale (SCE). More negative values can be obtained if oxygen supply is restricted, giving a false indication of corrosion. Steel undergoing pitting has an Ecorr typically in the range -350 mV to -500 mV SCE.

7.6.3.2 Linear Polarisation

Developed by Stern and Geary (1957) linear polarisation has been successfully used by many investigators (Andrade et al 1986, Lambert et al 1991, Page and Havdahl 1985) to monitor corrosion of steel in concrete. The equipment and procedure used to measure the corrosion rate, by linear polarisation, of steel bars in this investigation is described in Chapter 2.

EXPERIMENTAL PROCEDURE

Mild steel bars 7 mm in diameter were used to simulate reinforcement in concrete slabs. The bars were prepared by removing the oxide film and any surface staining by sand blasting. Acetone was used to degrease the bars before they were wiped with tissue paper and placed in a desiccator for 1 week, to enable the formation of a passive oxide film. To prevent spurious end effects the ends of the bars were masked as described in Chapter 2. The length of the coating was such as to ensure that shortest distance between the exposed steel and the external environment was through the exposure face.

The concrete mixes detailed in Table 7.4 were prepared as described in Chapter 2. For each mix a series of slabs 300 x 200 x 130 mm were produced. A 30 mm deep pond was cast into each slab to allow application of 1 molar sodium chloride solution. The corrosion slabs were cast exposure face down in resin coated wooden moulds, with the bars positioned at cover depths of 10, 25 and 40 mm. Three bars per slab were embedded at each depth, with each mix consisting of three reinforced and one unreinforced slab (giving a total of 9 bars at each depth for each mix). By using a cast face as the exposure surface variations between samples due to bleeding and finishing could be eliminated.

Immediately after casting the specimens were transferred to a curing room at 22°C, and covered with damp hessian cloth and polythene to prevent evaporation and plastic shrinkage. After 24 hours the specimens were demoulded, wrapped in polythene and returned to the curing room for 28 days. Prior to exposure the corrosion blocks were painted with two coats of a waterproof bituminous paint. This was to prevent chloride penetration from directions other than the exposure face.

In order to promote rapid chloride ingress and high corrosion activity, the slabs were subject to a monthly wetting and drying cycle. A litre of one molar sodium chloride solution was ponded on the slabs, and left for three weeks. After this period, any remaining salt solution was poured off, and the slabs moved to a 38°C curing room. One week later the slabs were returned to the lab, and the cycle repeated. Approximately 10 days into each wetting cycle corrosion potential measurements were taken, and every three months linear polarisation measurements were taken.

To give an indication as to the effect of blending materials on threshold values, the unreinforced slab was periodically sampled at depths corresponding to embedded bars, using a 5 mm diameter masonry drill. To prevent contamination the slabs were washed to remove any surface chloride prior to drilling. Samples were taken by drilling horizontal holes in the sides of the slab using a bench mounted drill. Dust from the first 10 mm was discarded as being unrepresentative. After sampling at each depth the slab was cleaned with compressed air before other holes were drilled. The holes were filled with repair concrete, the slabs repainted and exposure continued. The powder obtained was analysed for total chloride by titration with silver nitrate as described in Chapter 2.

7.8 RESULTS AND DISCUSSION

The slabs were exposed to the wetting and drying regime for approximately two years, with potential readings being taken every month, and corrosion current readings every quarter. As with all corrosion measurements there is some degree of scatter, although it was found that Ecorr measurements mirrored the onset of corrosion activity in the bars. Figure 7.3 is a plot of Ecorr against Icorr for all bars. It can be seen that for potentials more noble than -250 mV (SCE), Icorr is less than 0.1$\mu A/cm^2$ i.e. negligible corrosion is occurring. At potentials more negative than -300 mV (SCE) significant corrosion occurs, consequently this potential was taken as an indication of corrosion activity.

Figures 7.4 to 7.11 show the variation of corrosion potential of the bars with time. Potential readings were taken more regularly than Icorr, so these plots highlight the onset of significant corrosion activity more clearly.

7.8.1 Initiation Period

The time to initiation of corrosion of the bars provides a convenient means of ranking the durability performance of each mix. The longer the time to the start of corrosion the more durable the mix. The wetting and drying exposure regime not only ensures rapid chloride ingress and high corrosion activity it mirrors the type of environment in which marine structures and highway structures are found. Chloride penetration of the surface layers is accelerated by a partial drying out of the concrete and subsequent capillary absorption of chloride solution. The corrosion rate after depassivation is high because the concrete remains wet so the concrete resistivity is relatively low and furthermore, sufficient oxygen is available for corrosion to occur. Therefore wetting and drying test regimes are effective ways of simulating real exposure environments over relatively short time periods.

Table 7.5 summarises the time to corrosion initiation (t_1) of bars embedded in each concrete mix. Unfortunately in the time scale not all of the bars have started to corrode, so that separation of the more durable mixes is not possible. However it can be seen that OPC and 15% PFA mixes perform similarly, which is some way short of the other mixes. Of the remaining mixes only the 10 mm bar is showing corrosive activity. Although it must be borne in mind that any surface imperfections in the concrete are likely to be exacerbated, promoting early corrosion. The wet/dry cyclic exposure regime means that this bar is most likely to undergo absorption enabling rapid chloride penetration, as opposed to a combined absorption and diffusion mechanism as is likely to be the case with the deeper bars.

The OPC mix exhibited poor resistance to chloride ingress with the 10 mm cover bar starting to corrode almost immediately. Even the 40 mm cover bar showed corrosion activity after only 9 months. This is in general agreement with Gjørv and Vennesland (1979) who stated that even in good quality low w/c ratio concrete, OPC could not provide adequate resistance to chloride attack.

The 15% PFA mix does not appear to improve durability, and in fact performed slightly worse than the OPC control. A possible explanation is the curing of the specimens which were only wrapped in polythene to keep them moist. Work by Mangat and Molloy (1991) has shown inferior performance of PFA concrete when air cured. Additionally the low level of PFA used may have been insufficient to produce significant improvement in the microstructure to have been of benefit.

The ternary blend containing MK and PFA shows considerable improvements in durability over the 6% MK and 15% PFA mixes. The improved durability could be a result of combining fast and slow reacting blending materials, or a greater weight of cement replacement, although the binder contents are the same. The MK and BFS ternary blend

shows a high level of resistance to corrosion when compared to the OPC control, with initiation times to corrosion of the 10 and 25 mm cover bars double those of the OPC mix. However it is notable that the MK/BFS ternary blend has a lower durability than the binary BFS mix. Both mixes have similar quantities of replacement material, although in this case it appears that the ternary blend is not as effective at reducing corrosion of bars exposed to a saline environment. The 50% BFS mix exhibits high resistance to corrosion of embedded steel exposed to a chloride environment, as the 25 mm cover bars do not show significant corrosive activity even after 660 days of exposure. The 10 mm cover bars have an initiation time to corrosion of 250 days, more than 3 times as long as that of the OPC control.

Bearing in mind the drawbacks, mentioned earlier, of using the time to corrosion of the 10 mm cover bar, there are several notable points. Firstly the 50% BFS mix has approximately the same time to initiation as the 10% MK concrete. Slag mixes are commonly used in structure exposed to aggressive marine environments, such as the Second Severn Crossing (Concrete 1996) and the Dartford Crossing (Concrete 1991) and represent the best available option in terms of durability. These mixes take three times as long to initiation of corrosion of the 10 mm bar as the OPC control. Notably the 20% MK mix does not appear as durable as the 10% MK mix. Since absorption takes place through capillary pores and assuming that all slabs are dried to an equal degree, the initiation time of the 10 mm bar gives an indication of the improvements in capillary porosity due to inclusion of blending materials. Consequently it would be expected that the 20% MK mix would perform better than the 10% MK mix. However this is not the case and suggests that the better initial curing is required to obtain full hydration at higher replacement levels.

7.8.2 Total Chloride Threshold Level

Figure 7.12 shows a plot of corrosion potential against total chloride content. Potentials less than -250 mV (SCE), indicative of a low risk of corrosion, correspond to total chloride contents of 0.5% by weight of binder or less. Potentials of -300 mV (SCE) or more correspond to chloride contents greater than 0.6%Cl/g binder (by wt). Results for OPC and all MK blends are similar suggesting that lower levels of chloride are not necessary to initiate corrosion in MK blends. This however gives no indication of free chloride contents and $\frac{Cl^-}{OH^-}$ ratios of the pore solution.

7.9 CONCLUSIONS

MK does appear to improve corrosion resistance of concrete over OPC mixes exposed to chloride environment, as does the use of ternary blends containing MK and PFA or BFS. The higher resistance of blended mixes are probably due to improved microstructure and hence high resistance to chloride ingress.

From the limited number of data points th total chloride contents of MK concrete mixes at the initiation of significant corrosion are similar to those of OPC concrete suggesting that lower calcium hydroxide contents do not reduce threshold values.

10% MK concrete appears to have a higher resistance to corrosion of embedded steel. Although it is too early to draw any firm conclusions a possible explanation was than the short curing period affected the performance to the higher replacement mix.

This work has highlighted the potential of ternary blends containing MK and other more common and cheaper cement replacements BFS and PFA. However the particular proportions chosen in this investigation may not be the optimum in terms of high durability.

	Kg/m^3							
MIX	OPC	MK	PFA	BFS	10 mm	Sand	Water	W/B Ratio
OPC	420				985	710	223	0.53
6% MK	395	25			985	710	223	0.53
10% MK	378	42			985	710	223	0.53
20% MK	336	84			985	710	223	0.53
15% PFA	357		63		985	710	223	0.53
50% BFS	210			210	985	710	223	0.53
6%MK/15%PFA	332	25	63		985	710	223	0.53
6%MK/45%BFS	214	25		189	985	710	223	0.53

Table 7.4 Mix proportions for corrosion slabs.

	Initiation Period t_1 (Days)		
MIX	10 mm	25 mm	40 mm
OPC	75	175	270
15% PFA	70	185	200
6% MK	130	350	>675
6%MK/15%PFA	175	>660	>660
50% BFS	250	>660	>660
6%MK/45%BFS	125	660	>660
10% MK	270	>420	>420
20% MK	135	>420	>420

Table 7.5 Corrosion Initiation times for steel bars embedded in concrete.

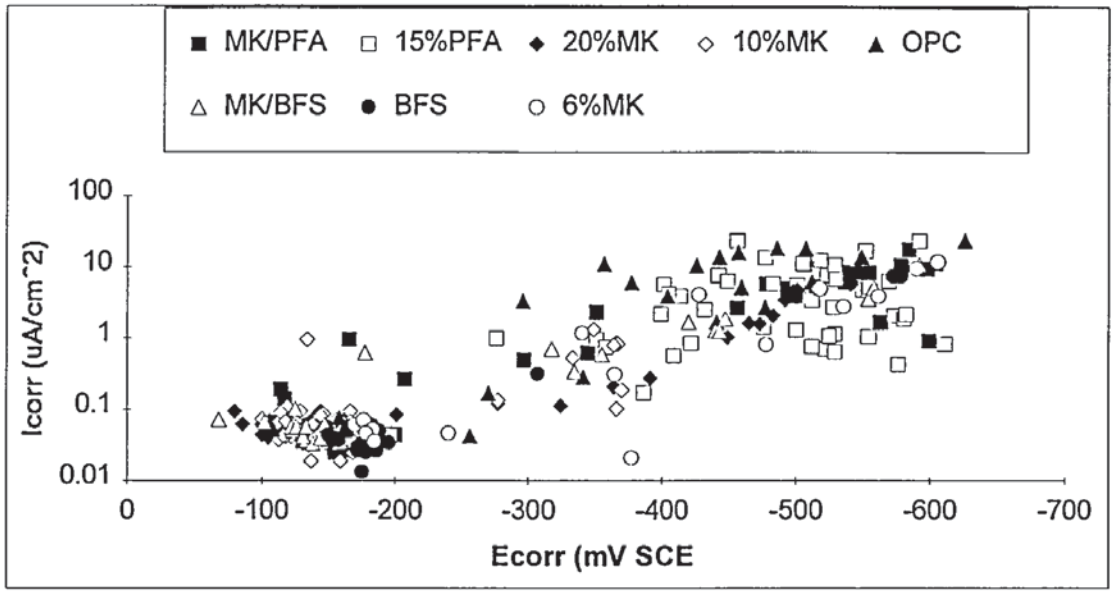

Figure 7.3 Corrosion potential against corrosion rate measurements

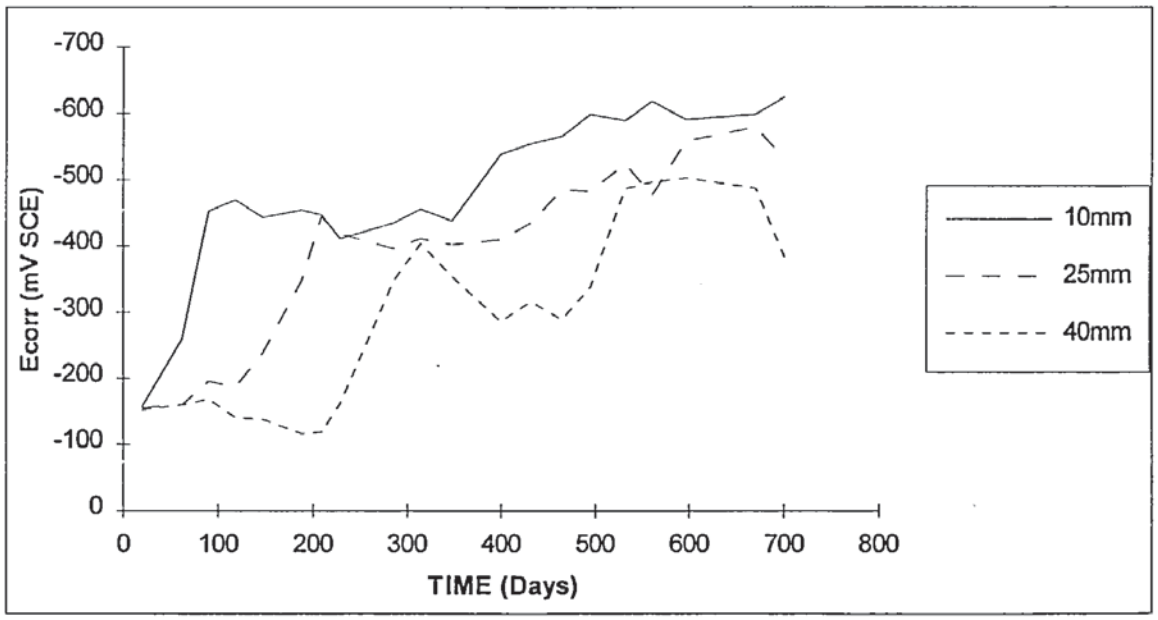

Figure 7.4 Change in corrosion potential with time for OPC concrete

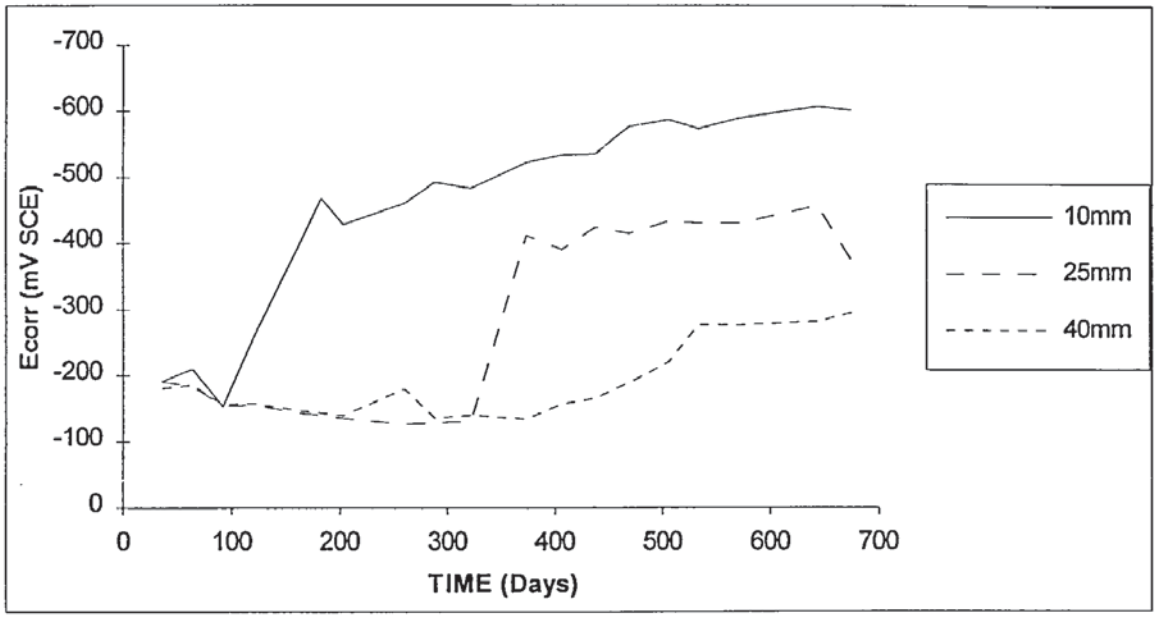

Figure 7.5 Change in corrosion potential with time for 6% MK concrete

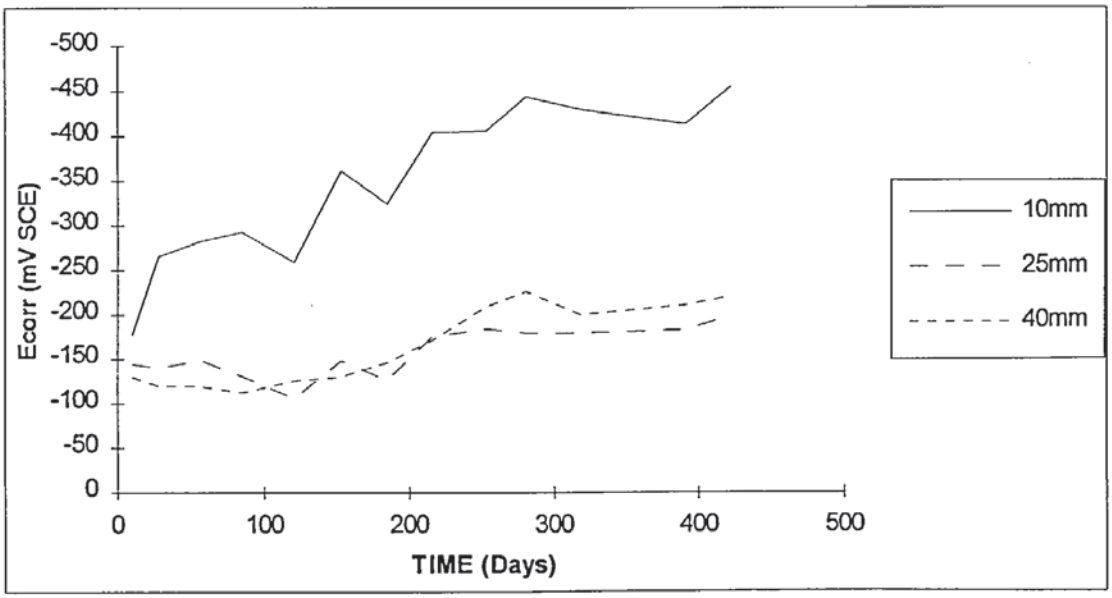

Figure 7.6 Change in corrosion potential with time for 20% MK concrete

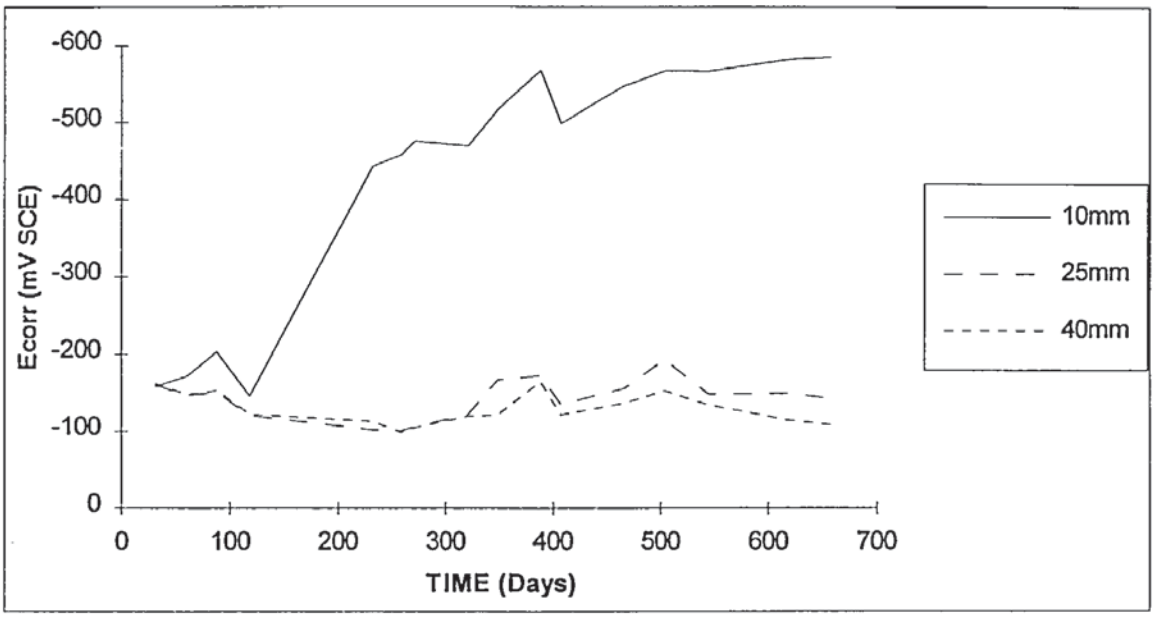

Figure 7.7 Change in corrosion potential with time for 6%MK/15%PFA concrete

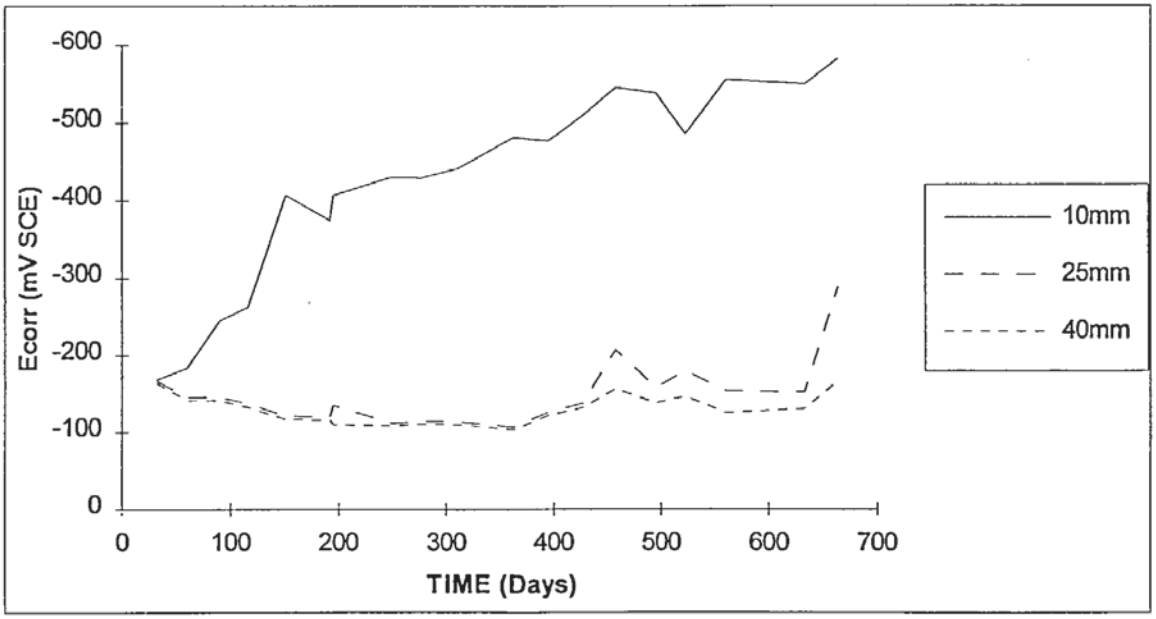

Figure 7.8 Change in corrosion potential with time for 6%MK/45%BFS concrete

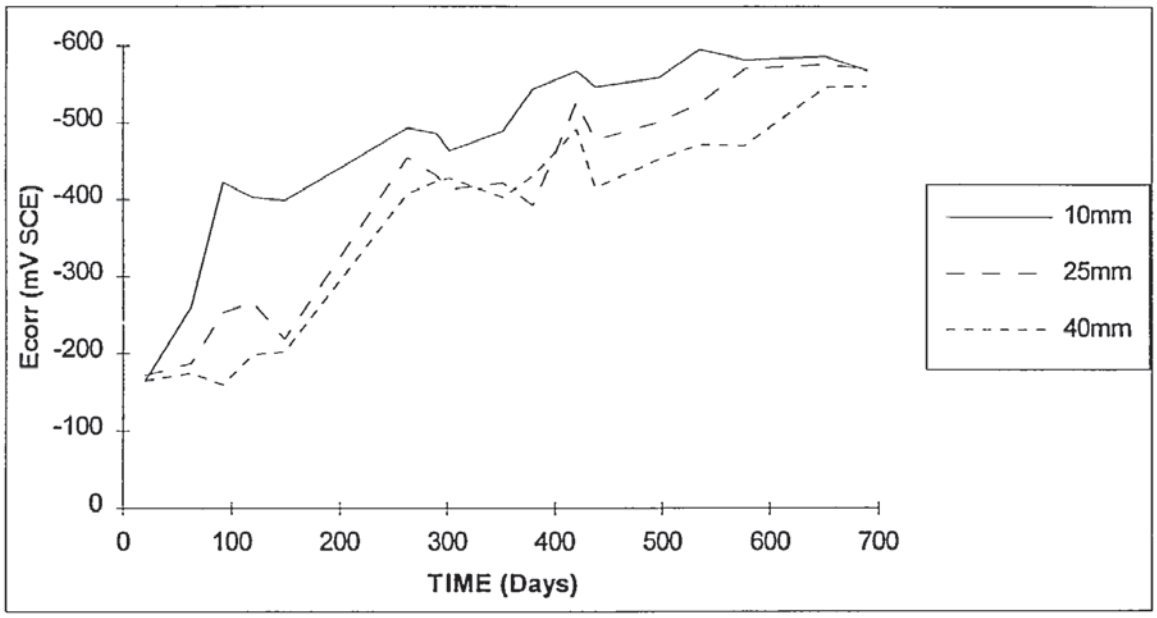

Figure 7.9 Change in corrosion potential with time for 15% PFA concrete

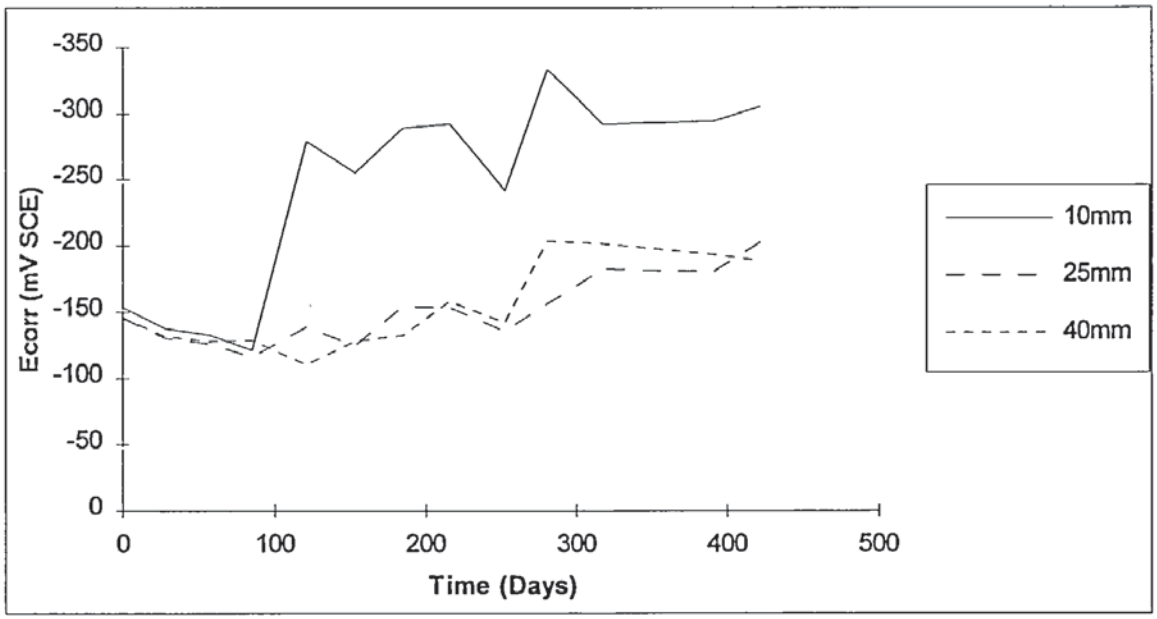

Figure 7.10 Change in corrosion potential with time for 10% MK concrete

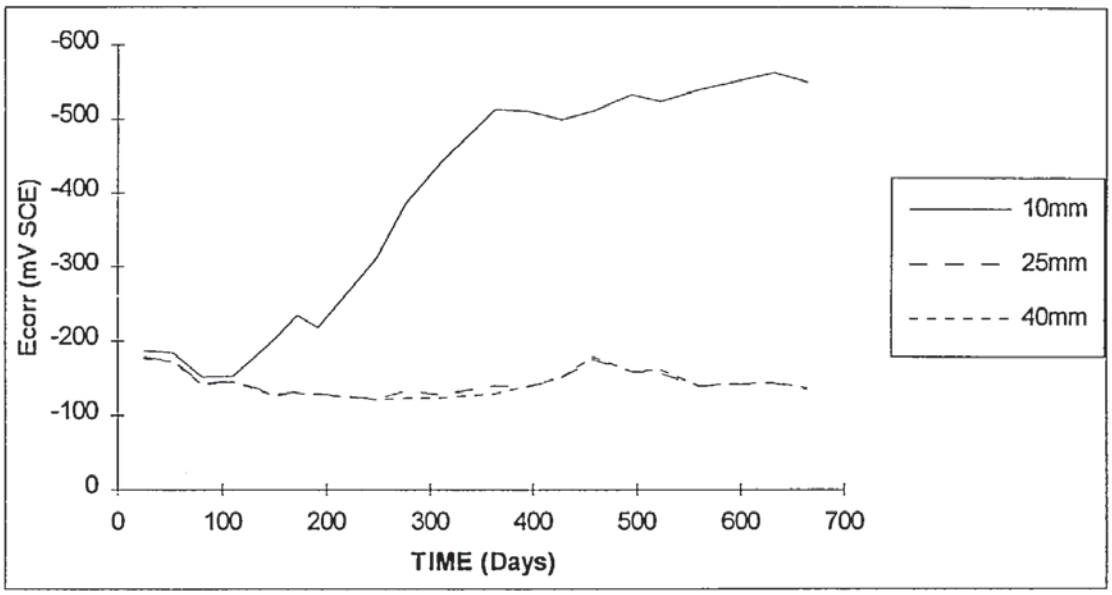

Figure 7.11 Change in corrosion potential with time for 50% BFS concrete

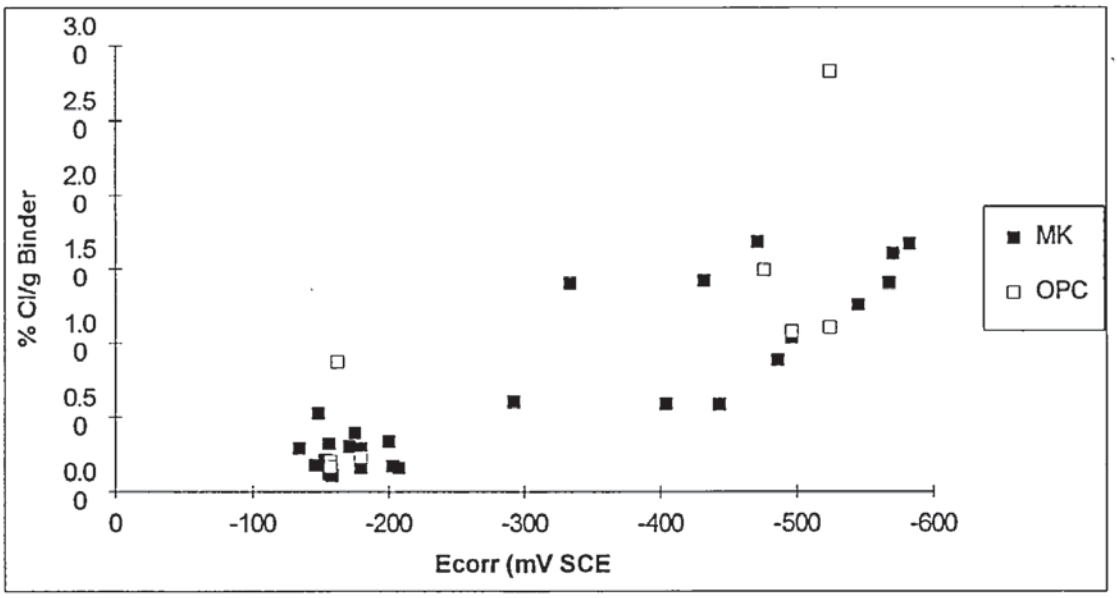

Figure 7.12 Total chloride threshold value against corrosion potential.

CHAPTER 8

RHEOLOGY OF CEMENT PASTES AND MORTARS CONTAINING METAKAOLIN

8.1 INTRODUCTION

An intrinsic part of producing a high performance concrete is the ability to transport, place and compact the material satisfactorily, so that a homogeneous mix with the minimum air voids content as efficiently possible is attained. A concrete that cannot adequately undergo these processes, will not achieve the desired strength and durability in the finished structural element, irrespective of its constituents.

Consequently the rheological behaviour of the fresh concrete has a significant influence on the performance of the hardened material. This investigation aims to establish the effects of MK, when used as a partial cement replacement, on the workability of concrete. The rheology of cement pastes and mortars were studied to provide an understanding of the factors controlling concrete workability. Banfill (1991) considered mortars containing sand particles less than 2 mm in size as model concrete, and suggested that an understanding of their rheology may enable the properties of the concrete to be predicted from small-scale tests on mortar. In addition the rheology of mortar is important for determining the ease of use of the material for bricklaying and repairing damaged concrete.

8.2 WORKABILITY

For complete hydration of ordinary Portland cement, a theoretical water/cement ratio of the order of 0.25 is required (Neville 1995). However practical unplasticized concretes use much higher water cement ratios, the extra water being necessary to lubricate the particles and facilitate placement and compaction. This higher water content, and the associated higher capillary porosity, hinders concrete durability and strength. Too much water leads to segregation and honeycombing, and too little can lead to a stiff mix which cannot be adequately compacted. Thus a balance must be struck between adding enough water to enable compaction but not so much as to affect performance detrimentally.

Despite the influence of fresh concrete properties on the long term performance of hardened concrete, there is no single definition of workability, or a single method of measurement. BS1881 describes numerous tests for assessing workability and quality control. However no test is able to be used in all situations and results from different tests are not directly comparable.

Neville (1995) described a workable mix as one that "can be transported, placed and finished sufficiently easily and without segregation". Thus a mix that might be deemed workable for one application, such as a floor slab, may not be suitable for a column congested with reinforcement, and so may be described as workable in one instance and not in another. More specific definitions have been given by Tattersall (1986) and Domone (1994), who described workability in terms of the concrete meeting manufacturing and finished requirements. A workable concrete is one that can be transported, handled, compacted and finished by the available techniques, without segregation or excessive bleeding to obtain a satisfactorily strong, durable and homogenous product. However this definition is still open to subjective interpretation as to what is a workable concrete. A more precise definition was proposed by Tattersall (1991) who defined workability in terms of satisfying certain criteria. "Workability is the property of the concrete alone. Workability will be expressed quantitatively in terms of one or more physical constants. All constants should be expressible in fundamental units. The constants must together provide a sufficiently complete description".

Tattersall and Banfill (1983) proposed that the workability of a cement system be specified in terms of its plastic viscosity and yield stress. Although this system has not been adopted by national standards, it is generally acknowledged that the standard tests available do not indicate the insitu performance of fresh concrete. The present investigation utilised plastic viscosity and yield stress to characterise the flow behaviour of pastes and mortars.

Concrete consists of aggregates, cement and water and may be regarded as either a suspension of inert particles in a matrix of cement paste, or as inert particles coated with cement paste. In either case it is reasonable to suppose the paste phase has a significant effect on the rheological properties of concrete. A manifestation of this relationship is the influence of blending materials such as PFA and BFS on the flow properties of concrete.

8.3 THE RHEOLOGY OF CEMENT SYSTEMS

8.3.1 Newtonian and Bingham Materials

The flow behaviour of materials can be classified into several models, the simplest being Newtonian. A Newtonian fluid is one where the applied shear rate is directly proportional to the shear stress with the constant of proportionality termed the viscosity (Figure 8.1). The flow curve of a Newtonian material will obey equation 8.1, so that a minimum of one point on the curve is needed to define the relationship, and evaluate C.

$$\tau = \mu\gamma \qquad \text{Eqn. 8.1}$$

where τ = Shear Stress

μ = Shear Rate

γ = Viscosity

However concrete does not behave as a Newtonian fluid. It requires a minimum force to move it which means its flow curve cannot pass through the origin. Much of the initial rheology work on concrete involved overly simplistic empirical tests to rank mixes in terms of workability, and most assumed Newtonian behaviour. Subsequent work by Tattersall (1973) and Banfill and Tattersall (1983) has shown the principal rheological features of cement systems conform closely to Bingham behaviour, with shear thinning at high shear rates. The equation and typical flow curve for a Bingham material are given in Equation 8.2 and Figure 8.1 respectively. Some authors have claimed decrease in shear stress between up and down curves during cyclic loading to be evidence of thixotropy in cement pastes. However, this is not the case as the structure does not reform on standing (Banfill 1981). Subsequent cycles reveal lower shear stresses indicating time dependent structural breakdown.

$$\tau = \tau_0 + \mu\gamma \qquad \text{Eqn. 8.2}$$

τ	shear stress
γ	shear rate
τ_0	yield stress
μ	plastic viscosity

To characterise the rheological behaviour of concrete and cement systems a minimum of two workability measurements at two different shear rates are required.

Helmuth (1980) and Banfill and Saunders (1981) reviewed the flow behaviour of cement systems and found that, depending on testing regimes, any of the trends shown in Figure 8.1 could be exhibited by cement systems except Newtonian. This was attributed to two simultaneous and irreversible processes, namely shear induced structural break down during mixing and structural build up due to hydration. Reduced fluidity resulting from build up could simply be a consequence of the removal of water due to chemical reaction with cement, or physical immobilisation of water in the spaces between developing outgrowths from the surface or increased contact between particles as a result of outgrowth formation.

Existence of a yield value in concrete is indicative of a structure within the mix, resulting from interactions between cement particles in the paste and aggregate particles. These

interactions can take the form of electrostatic or Van der Waals forces in the case of cement particles and friction in the case of aggregate. Tattersall and Banfill (1983) suggested that links between cement particles are due to a skin forming around particles which are touching when they first come in contact with water. For flow to occur sufficient energy must be expended to overcome viscous forces and break linkages. If a paste is subject to a constant continuous shear rate, the torque exerted by the paste will decrease to a minimum with time, as these links are broken, and subsequently increase due to structural build up as a consequence of hydration.

Mixing and preparation procedures were one of the reasons put forward by Banfill and Gill (1986) for large variations in plastic viscosity and yield values quoted by workers. Banfill and Sanders (1981) found that the time taken over testing a sample in a viscometer, had a significant effect on results, largely due to hydration effects. Consistent results were only obtained for cycle times of 2 minutes or less, where hydration effects are small. Similar discrepancies between flow behaviour of cement pastes were noted by Lapasin et al (1983) who employed different preparation procedures and measuring instruments. A coaxial cylinders viscometer with profiled surfaces was recommended for measurement of cement paste rheology. Asaga and Roy (1979, 1980) studied the effect of preparation and mixing methods on rheology, and found increasingly vigorously mixing procedures reduced yield values but had little effect on plastic viscosity.

8.3.2 Plasticizing Admixtures

The use of admixtures to improve workability characteristics has become common-place over recent years. Although there are several brands of admixture commercially available there are essentially two types of superplasticizer and one type of plasticiser. The superplasticizers are based on sulphonated naphthalene formaldehyde condensates or sulphonated melamine formaldehyde condensates, subsequently referred to in this work as type N and type M respectively. Superplasticizers are synthetically produced and consequently have a high purity unlike the majority of plasticisers which are lignosulphate based (type L) and manufactured from wood pulp. Although high purity lignosulphate admixtures are available they are not as common as superplasticizers, their main use being in conjunction with silica fume mixes. Impurities tend to retard set, although no long term detrimental effects have been reported.

Plasticizing admixtures are used for two purposes, the production of high strength concrete of normal workability made with less water, and the manufacture of standard strength concrete with very high workability. As a consequence of the first application plasticizing admixtures are often referred to as water reducing agents.

Superplasticizers are believed to work by being adsorbed onto the surfaces of cement grains, and forming a net negative charge on the particle (Bonen and Sarkar 1995). This induces interparticle repulsion promoting dispersion and the break-up of agglomerates into individual particles. This not only leads to a reduction in particle interaction and a lowering of consistency, but releases water trapped in cement flocs and inhibits surface hydration of the cement particles which may augment fluidity.

Banfill (1980,1981) investigated the effect of plasticisers on concrete and paste systems. A direct relationship between the yield value in paste and concrete was found. Yield values in pastes could be reduced to a very small value "experimentally indistinguishable from zero" by adding high levels of plasticizer. A similar relationship could be found for concrete although zero was not reached due to the presence of aggregate. Similar observations were made by Petrie (1976) who measured flow curves of cement pastes containing plasticisers. As admixture concentration increased flow behaviour changed from Bingham, with structural breakdown towards reversible Newtonian.

No casual relationship could be elucidated for viscosity. Plastic viscosity increased to a maximum then decreased with increasing plasticiser dosage for the concrete system. Notably the maximum viscosity occurred with the minimum yield value. In the paste system the reverse was found, with viscosity decreasing before increasing at higher dosage levels. These observations were attributed to a reduction in attractive forces between cement particles reducing resistance to flow of the paste. In concrete the role of the paste may be to lubricate aggregate particles such that large agglomerates of paste may improve separation. However when admixtures are used agglomerates are dispersed allowing aggregate particles to approach each other more closely increasing plastic viscosity.

Al-Shakhshir (1988) investigated the effects of a lignosulphonate plasticizer on concrete mixes and concluded that adding the admixture to the mix water or separately at the same time as the mix water made no difference to workability. If the addition was made at the same time as the mix water, yield value was 70% above the value obtained if addition was after one minute of mixing. An explanation put forward attributes preferential adsorption of plasticizer molecules on to tricalcium aluminate. If the admixture is added with the mix water, substantial amounts are rigidly attached to the unreacted tricalcium aluminate, so that only small amounts are available to disperse the silicate phases. If addition is delayed the aluminate phase has time to develop a protective layer of ettringite, so adsorption is reduced. Yield values were also found to be slightly higher for rapid hardening cement than for OPC, attributable to either the high specific surface area or higher sulphate content.

8.3.3 Cement Replacement Materials

The effect of cement replacement materials on properties of fresh concrete are largely a function of particle shape and particle size distribution.

8.3.3.1 Pulverised Fuel Ash

PFA consists of spherical glassy particles ranging from 1 to 150 μm in diameter of which the bulk pass a 45 μm sieve. (Surface area 500 m^2/kg). Work by Ellis (1981) and Banfill (1991) on concretes and mortars containing PFA partial replacements found that plastic viscosity and yield stress were reduced, primarily due to the effect of the spherical shape of PFA particles.

8.3.3.2 Blast Furnace Slag

The effects of BFS on the workability of concrete are much less dramatic than for PFA largely because its physical properties are similar to those of OPC, both being granular. Wu and Roy (1984) investigated the effect of slag on rheology and concluded that slag reduced yield and plastic viscosity values of pastes, explaining the improved slump performance of concrete.

8.3.3.3 Silica Fume

Silica fume (SF) consists of microspheres of very pure glassy silica with a specific surface of about 18 000 m^2/kg. Owing to its high surface area and low bulk density SF is difficult to transport and handle and so is often prepared in the form of a 50% water slurry. SF has a marked effect on workability. Mixes are very cohesive so much so that negative slumps can occur when the concrete sticks to the cone as it is removed. Work by Munn (1986) found that SF increased yield and plastic viscosity by up to 540% and 180% respectively.

8.3.3.4 Metakaolin

Studies on the workability characteristics of MK concretes have been limited to standard tests, and no fundamental analyses of the factors controlling workability have been published. From a knowledge of MK's particle shape and size one would expect its inclusion in a concrete mix to have significant effects on rheological properties. Metakaolin particles are platey in shape, ranging in size from 10 μm to less than 0.5 μm, and consequently have a high surface area of about 12 000 m^2/kg. Thus one would expect MK mixes to be very cohesive with high yield values as is found with silica fume. The fact that

the particles are platey as opposed to granular or spherical is also likely to be detrimental in terms of rheology. Work by Sabir et al (1996) on concrete containing MK at replacement levels 5, 10 and 15% by weight OPC, concluded that metakaolin increases water demand, preventing an accurate assessment of workability by standard tests. MK concretes at low w/b ratios appeared to be dry, however on vibration the concretes exhibited good cohesiveness and good compaction was achieved, such that strength was improved when compared to control mixes. Asbridge et al (1996) in field trials of MK concrete found that the addition of plasticizers improved workability such that no practical problems in terms of handling, placing and compacting were experienced. In fact the "thixotropic" behaviour of MK concrete was an advantage in the laying of an inclined slipway.

8.3.3.5 High Alumina Cements

High alumina cement pastes undergoing steady shear show a double minimum in torque time plots similar to that shown in Figure 8.2 (Banfill and Gill 1986). The general features are rapid initial decrease to a minimum point A, followed by a small peak and another minimum, after which torque steadily rises. The authors noted that changes in water/binder ratio had no effect on times to reach these points. If the peaks were due to hydration, time after contact with water would be critical. This was found not to be the case, the critical time being that from the start of shearing in the viscometer, the changes in rheology due to physical and flocculation changes. MK may exhibit similar characteristics due to its relatively high alumina content, which in turn would mean special attention would have to be paid to preparation.

8.4 WORKABILITY TESTS FOR CONCRETE

8.4.1 Single-Point WorkabilityTests

The most commonly used standard tests are the slump, compacting factor, Vebe and flow table. Detailed descriptions of the test procedures and types of concrete for which each test is applicable are given in BS1881. All the aforementioned tests measure the consistency or mobility of concrete after a standard amount of work has been done, whether that work is self weight in the case of the slump test or vibration in the case of the Vebe test. However a criticism of all standard tests is that they are capable of classifying as identical in properties two concretes that subsequently behave differently in practice i.e. two concretes of the same slump may behave differently on the job. One of the reasons for this is the assumption that concrete is a Newtonian fluid, which it is not.

A Newtonian fluid can be fully described by obtaining one measure of shear stress at a given shear rate. As concrete, cement pastes and mortars are Bingham materials at least two measurements at different shear rates are necessary to describe their workability (Tattersall 1986, Banfill and Gill 1986, Banfill 1990). Consequently it is possible to obtain a similar value, from a single point test, for two separate concretes that subsequently perform differently in situ at a different shear rate. Another drawback of these tests is that they are sensitive to operator technique, enabling different measurements to be made for the same concrete.

Despite these limitations these tests provide a check on the variation in the water content of a given mix, provided this is the only variable, and all other parameters remain constant. Thus the tests can be used for crude quality control.

8.4.2 Two-Point Workability Tests

Two-point workability tests require shear stresses to be measured at a number of different shear rates. Tests of this type tend to be variable speed viscometers, which measure the energy required to move the material at a given speed, or the resistance to flow. Tattersall's two point workability test and the ViscoCorder are two such instruments for measuring the workability of concrete and mortar respectively.

8.4.2.1 Tattersall's Two-Point Workability Test for Concrete

Tattersall's equipment (1973,1986) consists of a steel bucket into which is placed the test concrete and a motor driven impeller (Figure 8.3). The test entails mixing the concrete at several different speeds and measuring the resistance to flow, at various speeds, as a torque, which is proportional to the oil pressure in the hydraulic transmission. Practical problems of torque oscillation arising due to aggregate trapping has led to the development of other measurement procedures. Cabrera and Hopkins (1984) used strain gauges and slip rings fixed to the drive shaft. Wallevik and Gjørv (1990) found that dirt and mechanical vibration interfered with readings, if slip rings were used, and so adopted a pressure transducer in the hydraulic line. An 'H' impeller on a planetary motion spindle is used to measure low workability mixes, and a helical impeller for high workability mixes.

8.4.2.2 Viscocorder

The rheology of cement mortars was investigated using a modified ViscoCorder similar to that described by Banfill (1990) and Hornung (1990). The experimental arrangement is shown in Figures 8.4 and 8.5 and consisted of a smooth sided cylinder, mounted on a

turntable, and a concentric paddle linked to a pressure sensor. Mortar was placed in the cylinder to a specific level, and rotated at various speeds. As the cylinder rotates, the viscous resistance of the mortar flowing through the blades of the paddle forces a lever arm against the pressure sensor, from which torque can be calculated. Work by Banfill (1990) confirmed that the ViscoCorder can be used as a two point workability test for mortars, and that Portland cement mortars conform to the Bingham model on the down flow curves.

8.4.2.3 Co-Axial Cylinders Viscometer

The experimental arrangement for the co-axial cylinders viscometer is shown in Figure 8.6 and is used to measure workability of pastes. Cement paste is trapped between the vertical faces of the two cylinders. The outer cylinder is kept stationary and the inner one rotated at various speeds. The resistance to this movement on the inner cylinder is measured. The underside of the inner cylinder is concave to form an air bubble on assembly, thus no spurious end effects can occur and only the sample between the vertical faces of the cylinders is subject to shearing.

8.4.3 Drawbacks of Two-Point Workability Tests

A problem with all variable speed consistometers when used to test concrete, mortars or pastes is the occurrence of plug flow. Plug flow occurs when the yield stress is not exceeded across the whole of the specimen. In a co-axial cylinders viscometer the yield stress will be reached first at the boundary, and at low shear rates may result in a slip plane forming near the interface. The phenomenon is assumed to be overcome by profiling the surface of the cylinders, but this has not been conclusively proved (Lapasin et al 1983). Plug flow in a coaxial cylinders viscometer was investigated by Tattersall and Dimond (1976), who found during the course of a break down experiment a stationary plug of material formed which produced discontinuities in the breakdown behaviour. If smooth cylinders were used the plug moved around at lower speed than the inner cylinder or disintegrated. When serrated cylinders were used the plug was always stationary, the authors assuming that the only consequence was to reduce the geometry of the system (shear occurring at a single interface). They consequently recommended that serrated cylinders be used in all paste work.

Work by Banfill (1981) on cement paste with a co-axial cylinders viscometer with serrated cups found variation in geometry of the system had a dramatic effect on viscosity and a lesser effect on yield value. Examination of the paste revealed two distinct zones of paste, a runny inner zone and a thicker outer zone indicative of plug flow. Further investigation showed that variations in values could not be due to structural break down as the pastes

were fully broken down by mixing prior to testing. Centrifugal separation was also discounted, although no explanation was put forward to account for the findings.

As cement systems are effectively suspensions in water, segregation can be another problem. Wallevik and Gjørv (1990) have found concrete in prolonged workability tests to separate into distinct layers, with the coarser aggregate concentrating at the bottom. Tattersall (1986) suggested that the phenomenon could be alleviated by using a helical impeller which causes movement of the sample from the bottom to the top of the pan, although Wallevik and Gjørv (1990) found that segregation still occurred and may in fact be exacerbated especially in tests of long duration.

8.5 EXPERIMENTAL PROCEDURE

8.5.1 Mortar Preparation

Mortars were mixed and prepared using a two speed Hobart food mixer, which had an open shield blade rotating in planetary motion. Water, and superplasticizer if used, were preblended in accordance with the manufacturer's instructions, and placed in the bowl of the mixer. Cement was gradually added by hand over a period of 30 seconds, while continuously mixing, followed by the sand over a further 30 seconds. The speed was then increased to the higher setting and the mortar mixed for 60 seconds, giving a total mixing time of 2 minutes. This procedure is similar to that used by Banfill (1990) to ensure full structural break down prior to testing. Test duration was also kept to a minimum in accordance with Banfill and Sanders (1981) to prevent errors occurring due to segregation. The mix proportions of all mortars were 2:1 sand cement, the sand grading given in Table 8.1.

8.5.2 Paste Preparation

Pastes were mixed by hand using a spatula. Water and plasticizer were preblended, after which the MK was added and mixed for 1 minute to ensure dispersion. Next the cement was gradually added and mixing was continued for a further 2 minutes, before the paste was transferred to the viscometer for testing, which commenced 6 minutes after the cement and water came into contact. This period was kept constant to reduce variation due to structural build-up.

The plasticizers used were proprietary brands supplied by Fosroc under the trade names Conplast C430, M1 and P211, and included one admixture from each generic group. Conplast C430 was a sulphonated naphthalene formaldehyde condensate (type N), M1 a

sulphonated melamine formaldehyde condensate (type M), and P211 a lignosulphate plasticiser (type L).

Except where stated the metakaolin used was PoleStar 505. Two other types of MK were used, the main difference being in surface area, to study the effect of particle characteristics on workability. The chemical analyses and grading of metakaolins used in these experiments are given in Table 8.2.

8.5.3 Viscocorder

The ViscoCorder was run at several speeds ranging from 25 to 250 rev/min. Speeds were manually controlled, and measured using a hand held tachometer. A cycle involved incrementally increasing the speed to a maximum followed by a reduction to zero. At each increment the speed was held constant for 10 seconds with the reaction reading at the end of this period being recorded. This procedure was repeated for each specimen, with a two minute recovery time between cycles. The down flow curve from the second cycle was used in calculations, as it was found that full structural break-down had occurred by this stage. For each condition two replicates were carried out, with additional tests only if there was significant discrepancy.

8.5.4 Haake Rotovisco

An Haake rotovisco RV20 coaxial cylinders viscometer with M10 measuring system was used to study paste rheology. Banfill (1986) suggested that differences in viscosities and yield values between workers were a consequence of slip planes forming in the paste. By using profiled surfaces it is believed that these problems can be overcome. Hence the MVP and MVIIP profiled cup and cylinder were used with the Haake system. The system geometry is shown in Figure 8.6. The temperature of the experiment was controlled by a water jacket, through which circulated a supply of water kept at a constant temperature of $25^{o}C \pm 0.2^{o}C$.

Pastes were prepared as described in section 8.5.2, and placed in the pot of the viscometer to a prescribed level. The Haake speed programmer was used, so that shear rates were increased in 9 steps between 7.92 and 527.1 s^{-1}. The speed was maintained for 5 seconds at each increment and the shear stress reading recorded. Up and down cycles were measured to enable flow curves to be constructed. Two tests were carried out on each specimen with a recovery time of 2 minutes between cycles. Duplicate readings were taken on freshly prepared samples to assess reproducibility.

8.6 RESULTS AND DISCUSSION

All calculations of yield value and plastic viscosity were carried out on the down curves of the second cycle, after sufficient mixing had taken place ensuring structural breakdown had occurred. The time between adding water and testing was kept to a minimum to prevent structural build-up effects, as was test duration to prevent segregation. During and after testing the specimens were checked for evidence of plug flow or segregation. Segregation did not seem to be a problem with any of the MK mortars even at longed test times. OPC mortars at high water/cement ratios did show signs of segregation after prolonged testing. At low shear rates and low workability mixes plug flow appeared to occur in MK pastes. However as the speed increased this was eliminated, as the yield value was exceeded throughout the specimen.

8.6.1 Experiments on Mortars using the Viscocorder

The results from viscocorder experiments are not given in fundamental units as they are only used for comparative purposes.

8.6.1.1 Influence of MK on Mortar Rheology

Figure 8.7 shows flow curves for 0.5 water/binder ratio mortars. The curves show that MK mortars behave similarly to OPC mortars, in that they exhibit a yield value and are consequently non-Newtonian. In fact both types of mortar conform to the Bingham model. Figure 8.8 shows that the inclusion of MK has a dramatic effect on yield value and a much smaller influence on plastic viscosity, relative to the OPC control.

Figure 8.9 shows apparent viscosity decreases as speed (shear rate) increases. This may go some way to explaining the apparent thixotropic behaviour reported by Sabir et al (1996) for MK concretes. Thixotropy is defined in BS 5168:1975 as, "a decrease in apparent viscosity under shear stress, followed by gradual recovery when stress is removed". The behaviour exhibited in Figure 8.9 is not thixotropy as the structure does not reform on resting as indicated by Figure 8.10 which shows two up and down cycles, with a two minute rest between tests, for a 20% MK paste and an OPC mortar. The up and down curves for the OPC mortar for both up and down cycles coincide. The first up curve of the MK paste on the other hand, is significantly higher than subsequent cycles. This is a consequence of incomplete structural breakdown during mixing. Once this has occurred flow curves are almost identical. Therefore throughout this work the down curve for the second cycle is reported, to ensure structural break down effects do not distort the results. The large difference between up and down flow curves in the first cycle is indicative of an extensive

structure within the MK mortar which is not broken down by mixing alone. This difference between up and down curves is exacerbated as MK content increases indicating that MK must be increasing particle interaction or that the interactions are stronger.

It might be expected MK would exhibit a degree of thixotropy since it is derived from clay. However it has been shown that although MK retains the physical shape of the clay particles from which it was formed, calcination removes any surface charge, eliminating thixotropic behaviour. The stiffness of MK concrete, which becomes more fluid on application of vibration as observed by Sabir et al (1996), is a direct result of the high yield value associated with MK mixes. Energy is required to start the concrete moving, but once this energy input is stopped or reduced the MK concrete ceases to move giving the impression of a reforming structure.

Compared with OPC mortars, MK systems have higher yield stresses and plastic viscosities which increase with increasing replacement level. These increases must be a consequence of the particle shape and size of MK. Approximately 40% of MK particles are less than 2 μm, resulting in a highly cohesive mix. Combined with their platey structure this means that they have a high surface area to volume ratio. The high surface area ensures that much more water is needed to coat all the particles in a mix, reducing the volume of free water available for lubrication and hence increasing viscosity. Yield value is increased because the particles in an MK mix are able to come into closer contact for a given water content than in an OPC mix, increasing the strength and number of interparticle forces. As MK replacement level increases, the average surface area of the mix particles increases absorbing water that would normally be available for lubrication. Consequently MK mixes will have a higher water demand than an OPC control.

The low density of MK means that replacement of cement by mass not only substitutes platey for angular particles, but also increases the proportion of fine particles, effectively increasing the volume of the binder, resulting in a stiffer mix.

8.6.1.2 Effect of MK Type on Mortar Rheology

Results in the previous section have shown MK to have a dramatic effect on the rheology of mortars. By altering the size of the MK particles it was believed that improvements in the rheological performance could be obtained without reducing pozzolanic reactivity. To this end the influence on rheology of three types of MK were investigated, their particle size distributions being given in Table 8.2.

The influences of MK type on yield value and plastic viscosity are shown in Figures 8.11 and 8.12. M500 particles have a higher surface area than P505 and M401 particles, so it would be expected for M500 mixes to have higher yield and viscosity values, due to an increased water demand. However the results are inconclusive in that the MK with the lowest surface area had the highest yield and plastic viscosity values. Thus surface area cannot be the sole factor influencing rheology.

Figures 8.13 and 8.14 show that although yield values increase with increasing MK replacement level, the viscosities of 20% MK mortars are less than corresponding OPC and 10% MK mixes. Metakaolin may therefore help to lubricate the mix once the initial yield stress has been overcome. The reason for the reduction in viscosity may be that put forward by Banfill (1981), who suggested that agglomerates of binder may prevent close interaction of sand particles, lubricating the mix. Therefore as surface area of the binder increases agglomeration becomes more likely for a given water/binder ratio, improving the viscosity of the mortar.

The graph of yield value against surface area shows a general trend of increasing yield with surface area, for a given type of MK (Figure 8.14). As surface area increases more water is required to disperse the particles. If water content remains constant, the particles are able to stay closer together creating more numerous and stronger interparticle interactions and hence increasing yield value. However as mentioned previously surface area cannot be the sole factor influencing yield value, since for a given surface area the coarser MK has a higher yield value, contrary to expectation. The particle size distribution of the MK batch is likely to influence rheology, particularly the fraction of particles greater than 10 μm in size.

8.6.1.3 Effect of Plasticizer on 10% MK Mortar

Figures 8.15 and 8.16 show the influence of plasticizer type and dosage on mortar rheology. Plasticizer addition decreases yield value to a limiting value close to zero, but has a smaller effect on plastic viscosity. A possible explanation is that the superplasticizer disperses the MK and cement particles by repulsion hence eliminating surface interaction. Yield value can therefore be reduced to a limiting value by adding more plasticizer, as sufficient additive is required to cover all the particles. The yield value cannot be reduced to zero due to the sand fraction in the mortar which will require energy to overcome friction, irrespective of admixture content.

This may also explain the insensitivity of plastic viscosity to plasticizer, as energy will be necessary to overcome aggregate interactions which are not electrostatic in nature. Sand particles are coated in cement paste so their interactions would be lubricated by cement

paste. Plasticizer will not have a dramatic effect on this lubrication except to produce a more uniform coating. Another factor may be that viscosity of mortars is dominated by particle size and shape of the aggregate, which are not dramatically influenced by plasticizer. The findings of this investigation are similar to those of Banfill (1991) for the influence of a lignosulphate plasticizer on OPC mortar.

From figure 8.15 plot of yield value against superplasticizer addition, the steepest gradient is obtained for the type N admixture followed by type L and type M, indicating that type N and L are more efficient than type M at reducing yield value.

In terms of compacting concrete, yield value is the critical parameter, as this must be overcome before flow can occur. The plastic viscosity controls the rate at which flow takes place. Plasticizers dramatically affect the yield stress, and leave the plastic viscosity largely unaltered, while water on the other hand, affects both parameters. Consequently it is not possible to obtain mixes of the same workability that differ only in plasticiser and water content. This is contrary to that believed by those who use plasticizers to obtain the same workability at a lower water content to gain improvements in strength.

It should be noted that the findings in terms of compatibility of superplasticizers with MK are limited. Aitchin and Neville (1993) noted that the interaction between a cement and admixture depends on C_3A, C_4AF and calcium sulphate content. Water/cement ratio will also play an important role as this influences the distance between cement particles as well as the number of ions in solution. Thus the kinetics of hydration and rheology at 0.35 w/c will be different to those at 0.5 w/c.

8.6.2 Experiments on Cement Paste using a Co-Axial Cylinders Viscometer

No evidence of segregation was found in any of the mixes tested over short cycle times. Plug flow did occur in some of the stiffer mixes, with the plug remaining stationary. It was assumed a situation similar to that described by Tattersall and Dimond (1976) had occurred, with shear taking place next to the serrations, the only consequence being to reduce apparatus geometry.

8.6.2.1 Effect of MK on Paste Rheology

Figure 8.17 for OPC and MK pastes show that both types of mixes have similar shaped flow curves and thus exhibit essentially the same Bingham behaviour.

Figures 8.18 and 8.19 show that as water/binder ratio decreases plastic viscosity and yield values increase. This is a direct consequence of the closer proximity of particles and their resultant stronger attractive forces. At 20% replacement level the effects are quite dramatic with a 290% increase in plastic viscosity at 0.4 w/b and a 570% increase in yield value over the control OPC paste.

The relationship between MK replacement level and yield value in pastes is similar to that observed for mortars. However the relationship between plastic viscosity and MK content is not as straight forward. Mortar plastic viscosity is slightly reduced by MK addition, whereas plastic viscosity in pastes is increased. As mentioned earlier in the case of mortars, the paste fraction may help to lubricate aggregate interactions. In the paste system, water is needed to lubricate the particles. As water content increases particle interactions become weaker. By adding MK with its high surface area the free water available for lubrication is reduced. The platey shape of the MK particles in contrast to the angular OPC particles may also hinder flow past each other.

For lower replacement levels and water/binder ratios higher than 0.5 the plastic viscosity and yield values are not significantly different from OPC. This may be attributed to the large surface area and hence water demand of MK particles, the effects of which are exacerbated at low water contents and high replacement levels.

8.6.2.2 Effect of Superplasticizer on Paste

One of the ways in which the workability of concretes can be improved is by the addition of a plasticiser. Figures 8.20 and 8.21 show the effect on plastic viscosity and yield stress of increasing dosages of a type N superplasticizer. Relatively small dosages have a dramatic effect on yield value, and much less so on plastic viscosity. The decrease in yield stress with addition of plasticizer is in agreement with findings by Banfill (1981). However the reduction in plastic viscosity seen in this investigation was not mirrored in Banfill's work.

Even at 1.5% admixture dosage the 20% MK paste has a higher viscosity than the unplasticized OPC paste. At 1.5% admixture content the yield stress of the 20% MK paste is zero, indicative of a neutralisation of particle interaction. However the plastic viscosity of the 20% MK paste is still high, suggesting that it is not solely influenced by particle attraction, but possibly particle size and shape as well.

8.6.2.3 Effect of MK Type on Rheology of Paste

Essentially the difference between M401 and M500 are that M500 has finer particles, and a higher iron oxide content giving a pink appearance. Thus one would expect M500 to be more cohesive and hence have a higher yield value and plastic viscosity. This in fact occurs, as shown in Figures 8.22 and 8.23, which shows that as surface area of the binder particles increases, yield and plastic viscosities increase.

At 0.5 w/b ratio plastic viscosity is constant, while at 0.4 w/b ratio it increases with average surface area of the particles. This may be a result of an increase in the water content increasing separation of the particles and reducing interaction.

8.6.2.4 Constant Shear Rate

Cement pastes of water/binder ratio 0.5 were hand mixed for 4 minutes and tested over 30 minutes at a constant shear rate of 66.88 /s (Figure 8.24).

MK pastes behave similar to OPC and do not exhibit the double minima found with HAC pastes. A significant difference between the MK and OPC pastes is the time taken to reach a minimum shear stress, indicative of full structural break down. OPC has a minimum after 2.5 minutes, 10% MK after 4.5 and 20% MK at 6 minutes. This indicates that MK requires longer mixing than OPC to ensure structural breakdown dispersion and the production of a homogeneous mix.

An increase in shear stress was noted for OPC paste after 10 minutes, possibly due to hydration. A similar increase was not noted for either MK paste at any time during the test. This may indicate that initial set is retarded by MK addition.

8.7 CONCLUSIONS

MK pastes and mortars behave as Bingham bodies in common with Portland cement systems. The addition of MK is accompanied by an increase in yield value which is related to the amount of MK added. This may go some way to explaining the apparent thixotropy of MK concretes, since more energy is needed to overcome the yield stress and start the mix flowing than for a control, although once flowing the concretes will behave similarly. Changes in viscosity are not as straight forward, with different effects being observed in pastes and mortars.

The changes in rheological properties are related to the high surface area of MK and its particle size distribution, resulting in a higher water demand for MK systems. Possible benefits include reduced bleeding , a more cohesive mix, necessary for pumped concrete or highly plasticizer flowing concrete.

The differences in the viscosity behaviour of pastes and mortars, indicates that results obtained for these systems are not necessarily directly applicable to concrete systems. However this study has provided information on the effect of MK on rheology and ways in which these characteristics can be improved.

1. MK pastes and mortars conform to Bingham behaviour, and at high shear rates undergo shear thinning.

2. The addition of MK to paste and mortar increases the yield stress. The increase appears to be linked to the high surface area of MK particles and the particle size distribution.

3. Yield stress of mortars and pastes can be reduced significantly by the addition of superplasticizers.

4. MK increases the viscosity of pastes systems, and decreases the viscosity in mortars. Plasticizing admixtures slightly reduce the viscosity of pastes. The effect of plasticizers is more complex for mortars.

5. Of the three admixtures tested, the sulphonated naphthalene formaldehyde condensate based superplasticizer was the most efficient, followed by the lignosulphate and the sulphonated melamine condensate, for plasticizing MK systems.

Size	2.36 mm	1.18 mm	600 μm	300 μm	150 μm	75 μm
%	100	99.4	66.7	4.6	0.3	0.15

Table 8.1 Sand Grading. % passing BS sieve size.

	MetaStar 401	MetaStar 500	PoleStar 505
> 10 μm (wt. %)	24	12	10
> 5μm (wt. %)	45	33	
< 2 μm (wt. %)	30	37	50
< 1 μm (wt. %)	21	21	
< 0.5 μm (wt. %)		12	
Colour	White	Pink	Pink
Surface area (m^2/g)	10	14	12
SiO_2 (wt. %)	53	52	51.8
Al_2O_3 (wt. %)	42	41	42.3
Fe_2O_3 (wt. %)	1.0	4.6	2.99
CaO (wt. %)	0.1	0.1	<0.1
MgO (wt. %)	0.3	0.2	0.13
K_2O(wt. %)	2.0	0.6	0.61
Na_2O(wt. %)	<0.1	<0.1	<0.1
Pozzolanic reactivity (mg $Ca(OH)_2$ /g)	1000	1050	772

Table 8.2 Metakaolin compositions (information supplied by ECCI).

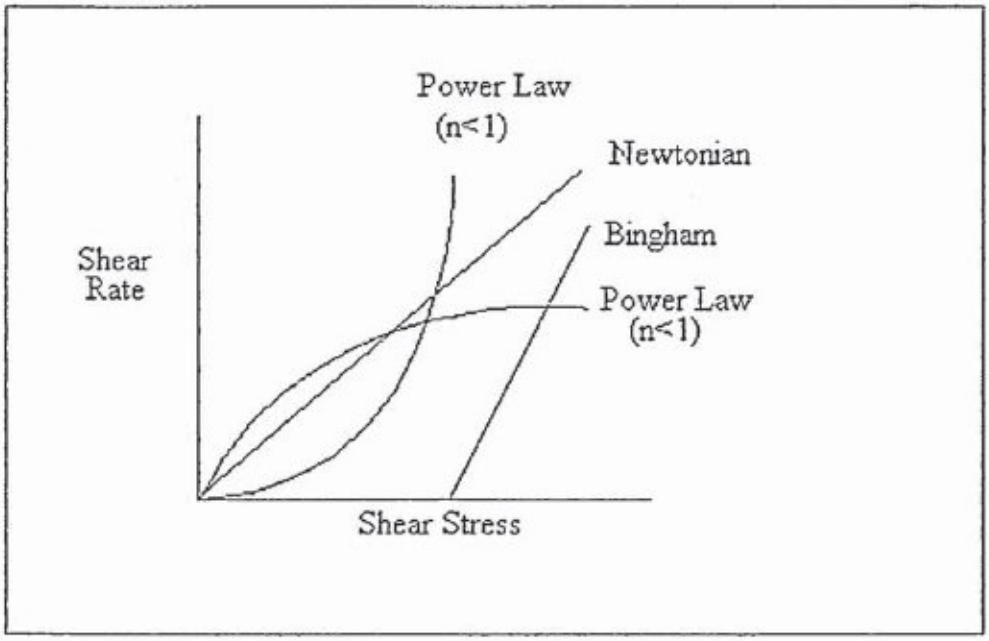

Figure 8.1 Flow curves for rheology models.

Aston University

Illustration removed for copyright restrictions

Figure 8.2 Torque time plot for high alumina cement paste (Redrawn from Banfill and Gill 1986).

Aston University

Illustration removed for copyright restrictions

Figure 8.3 Tattersall's two point workability apparatus (Tattersall 1973).

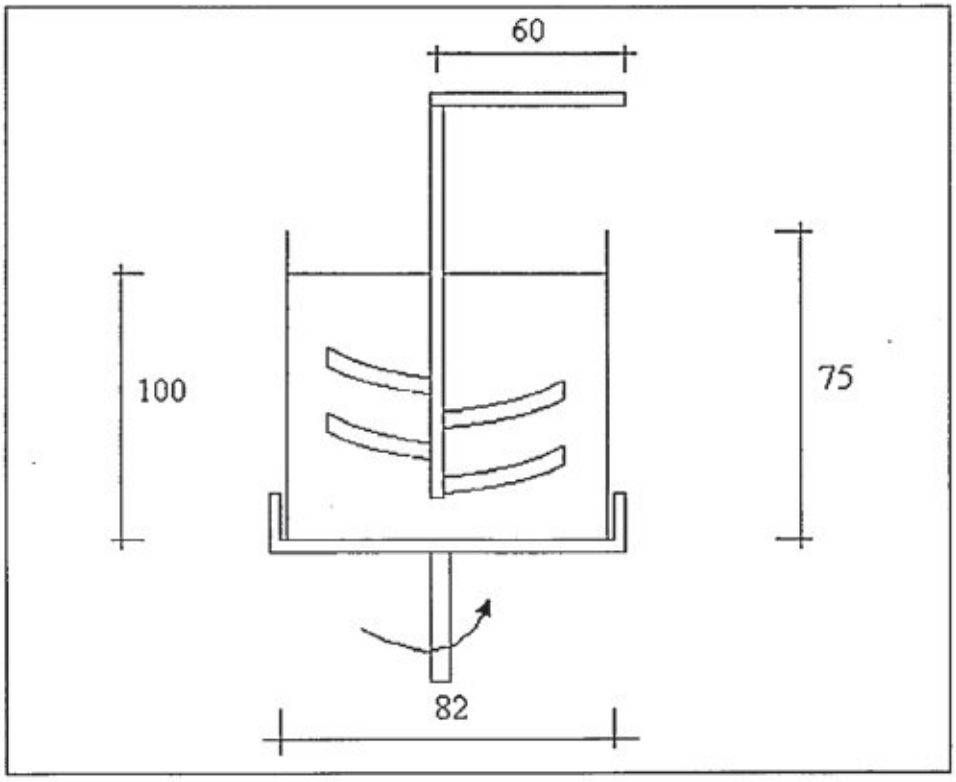

Figure 8.4 Schematic of the Viscocorder.

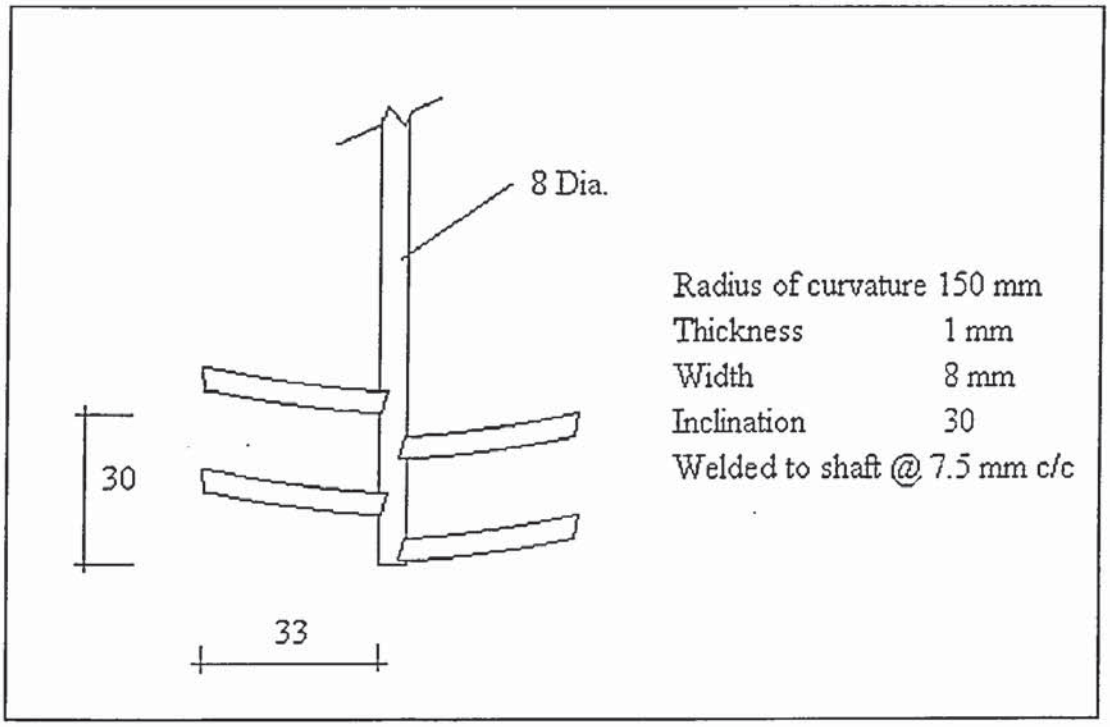

Figure 8.5 Schematic of viscocorder paddle.

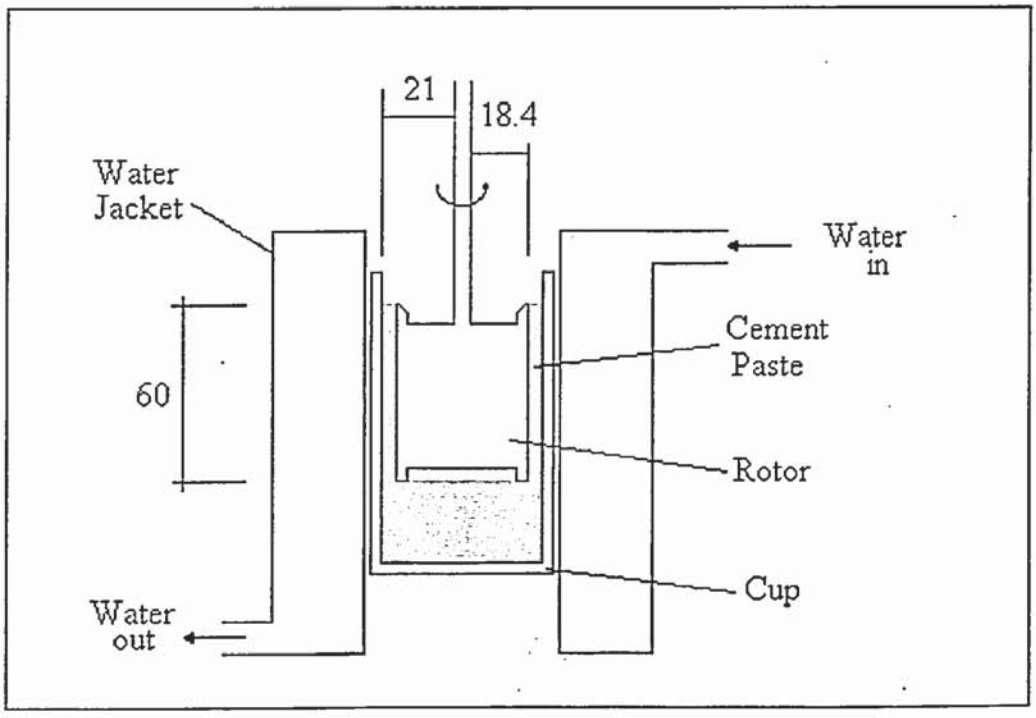

Figure 8.6 Haake rotovisco co-axial cylinders viscometer.

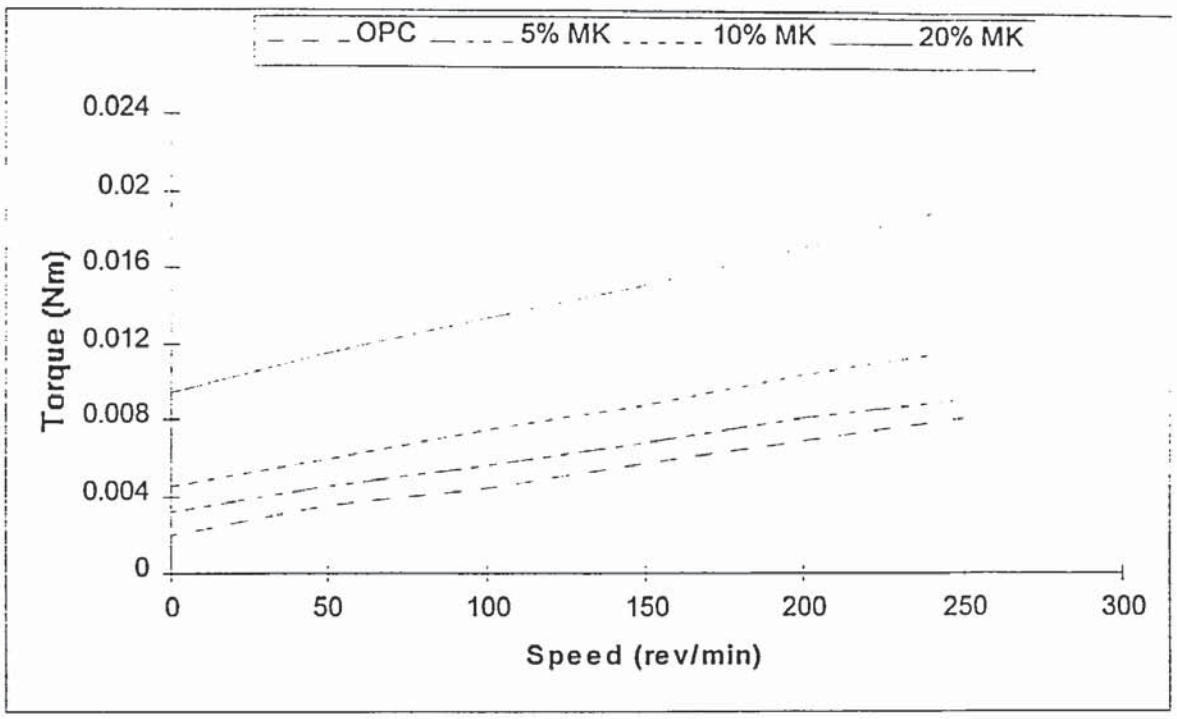

Figure 8.7 Effect of MK replacement level on mortar flow curves.

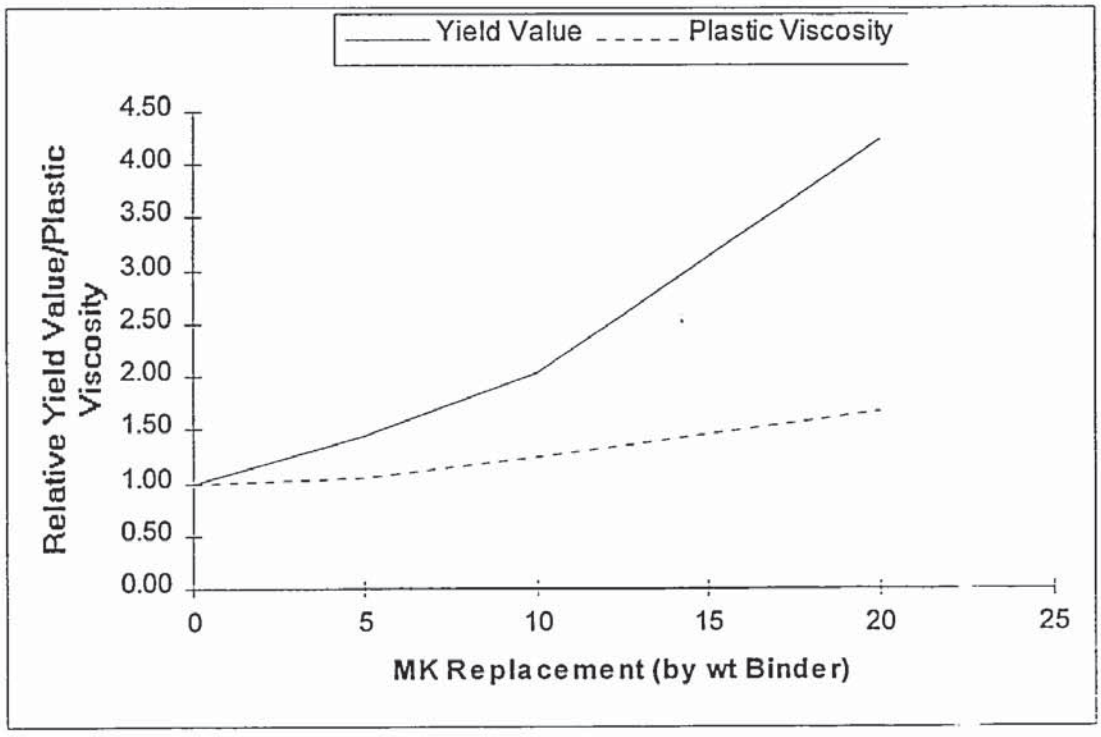

Figure 8.8 Influence of MK on relative yield stress and plastic viscosity.

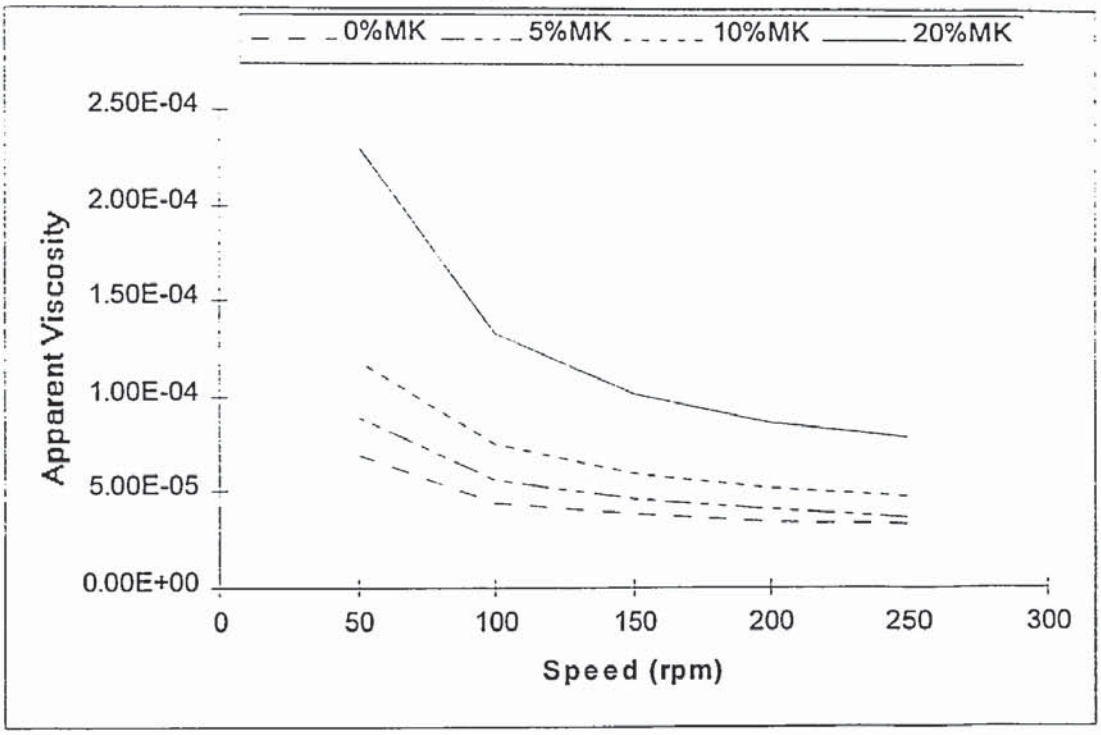

Figure 8.9 Apparent viscosity for 0.5 water/binder mortars.

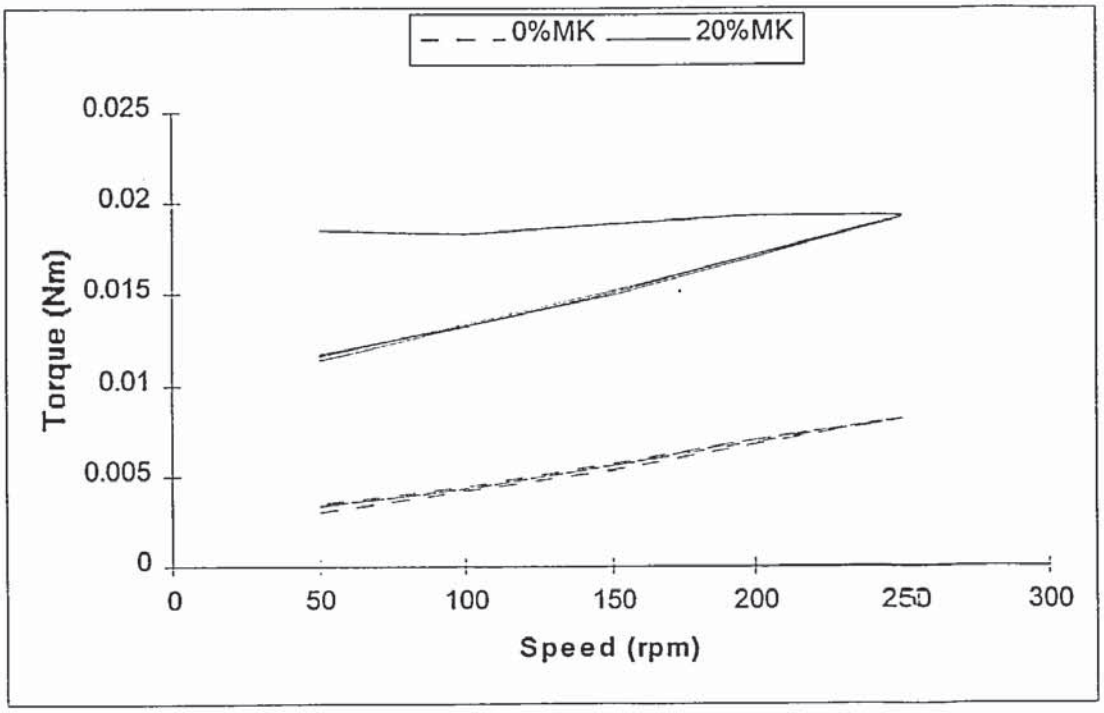

Figure 8.10 Up and down flow curves for 20% MK and OPC mortars.

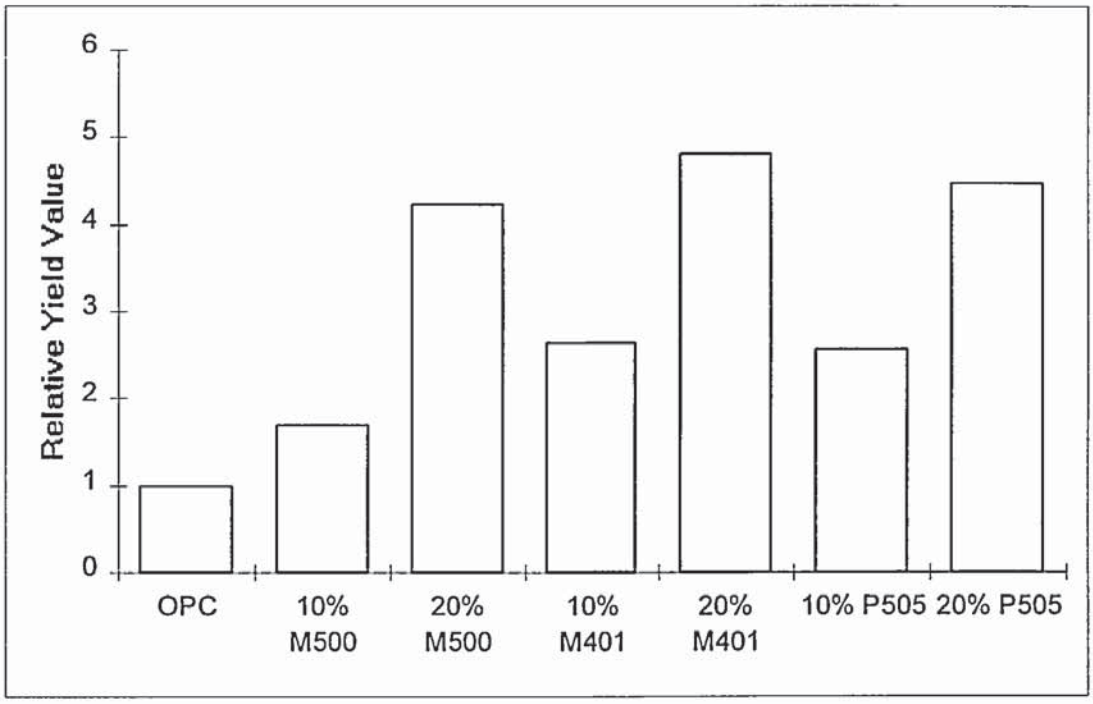

Figure 8.11 Effect of MK type on relative yield value of 0.5 water/binder mortars.

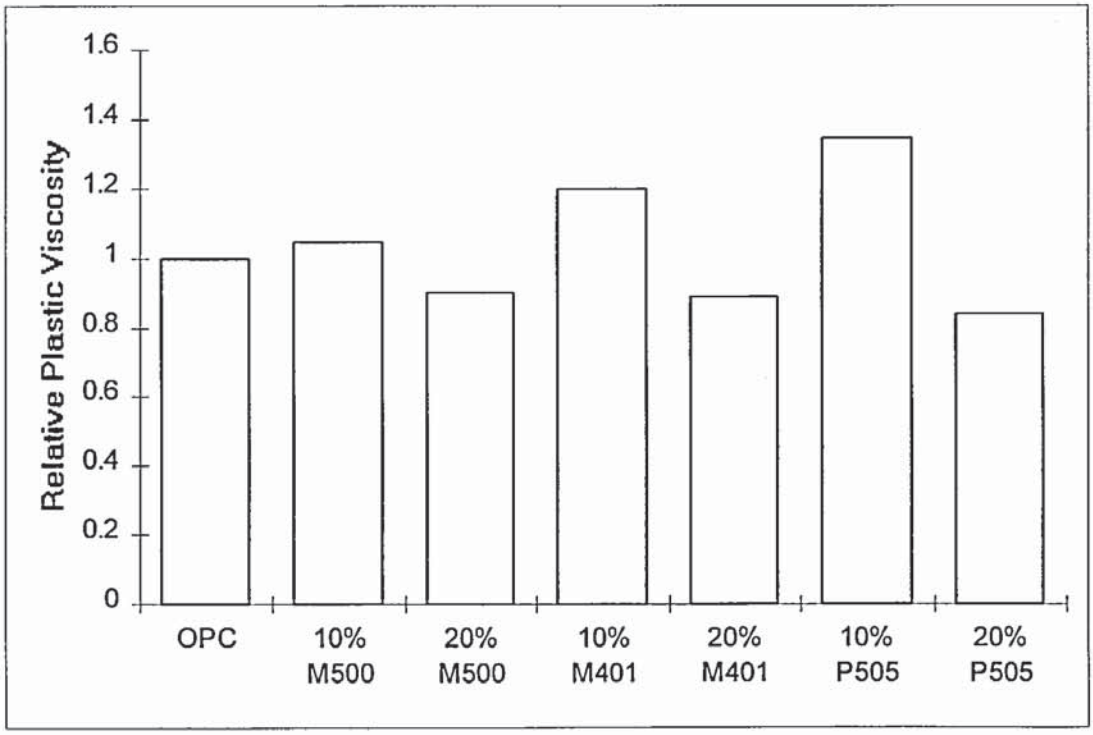

Figure 8.12 Effect of MK type on relative plastic viscosity of 0.5 water/binder mortars.

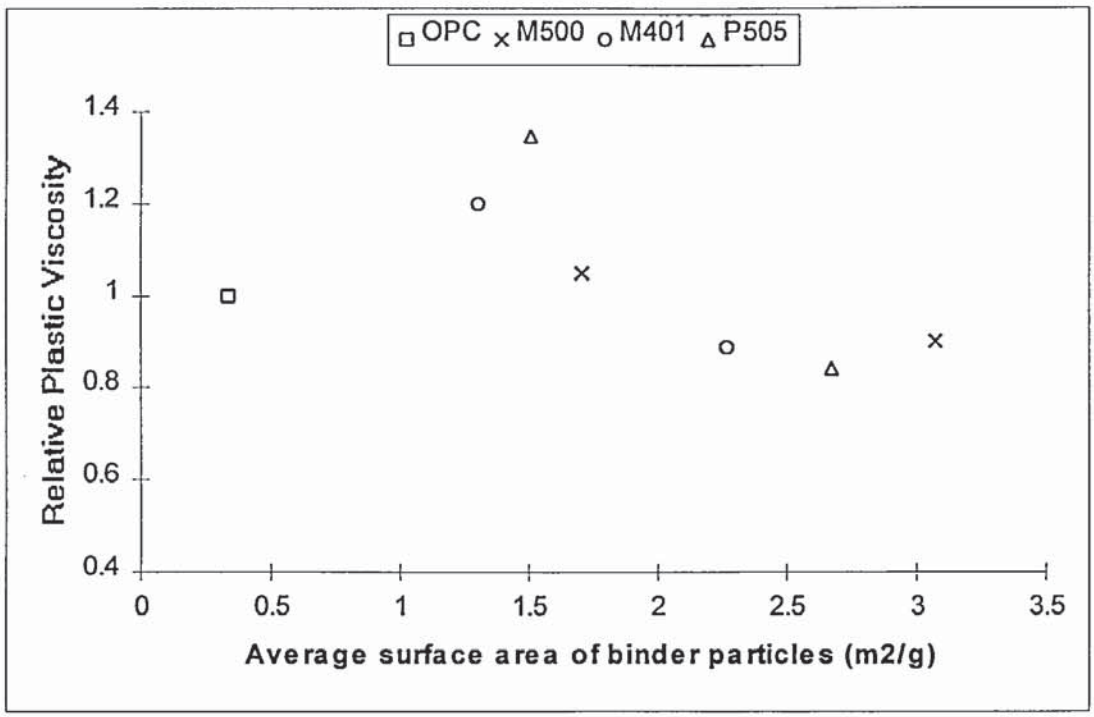

Figure 8.13 Relationship between average surface area of binder particles and relative plastic viscosity of mortar.

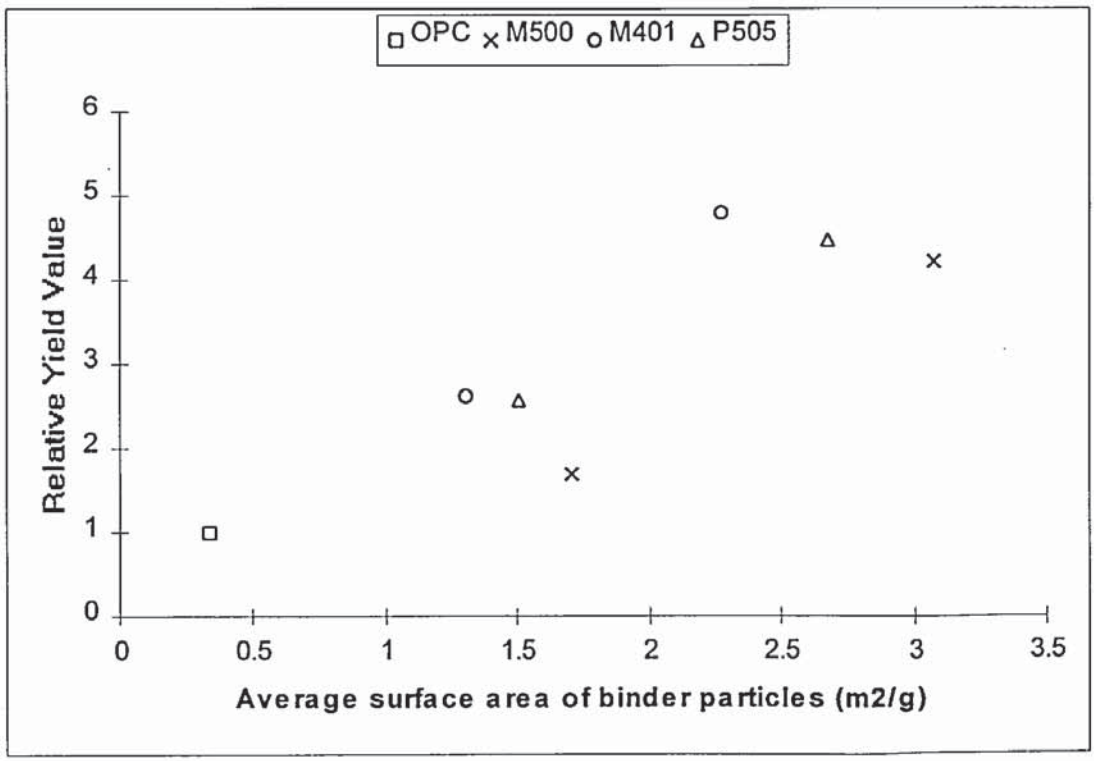

Figure 8.14 Relationship between average surface area of binder particles and relative yield value of mortar.

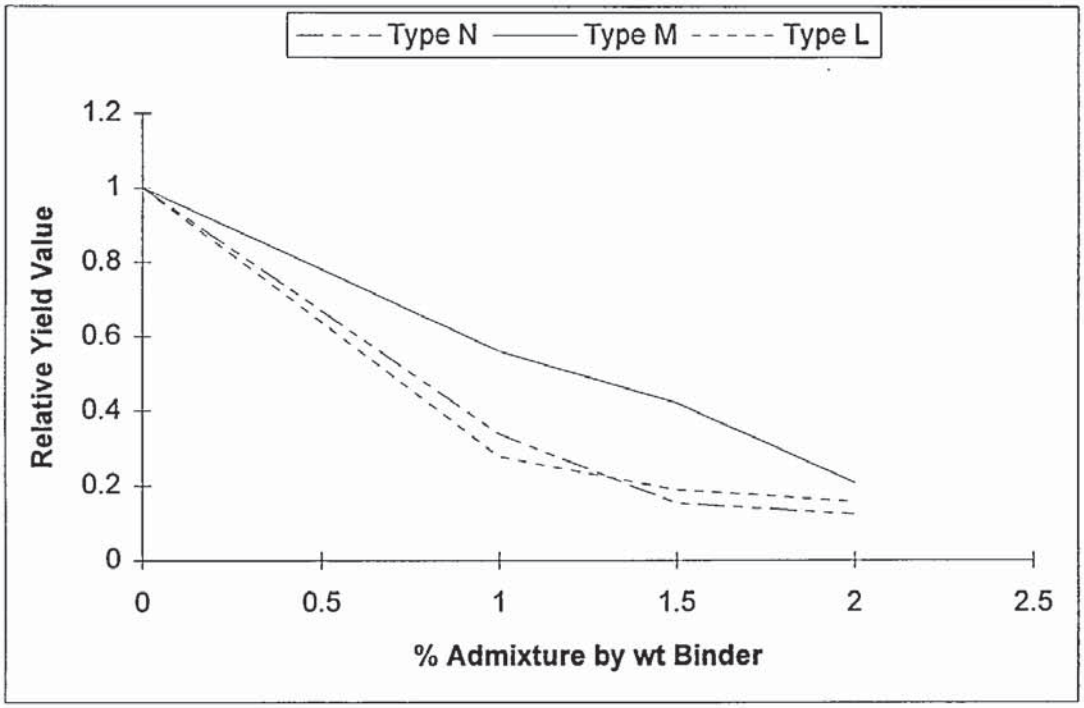

Figure 8.15 Effect of plasticizing admixtures on relative yield value for 10% MK mortar.

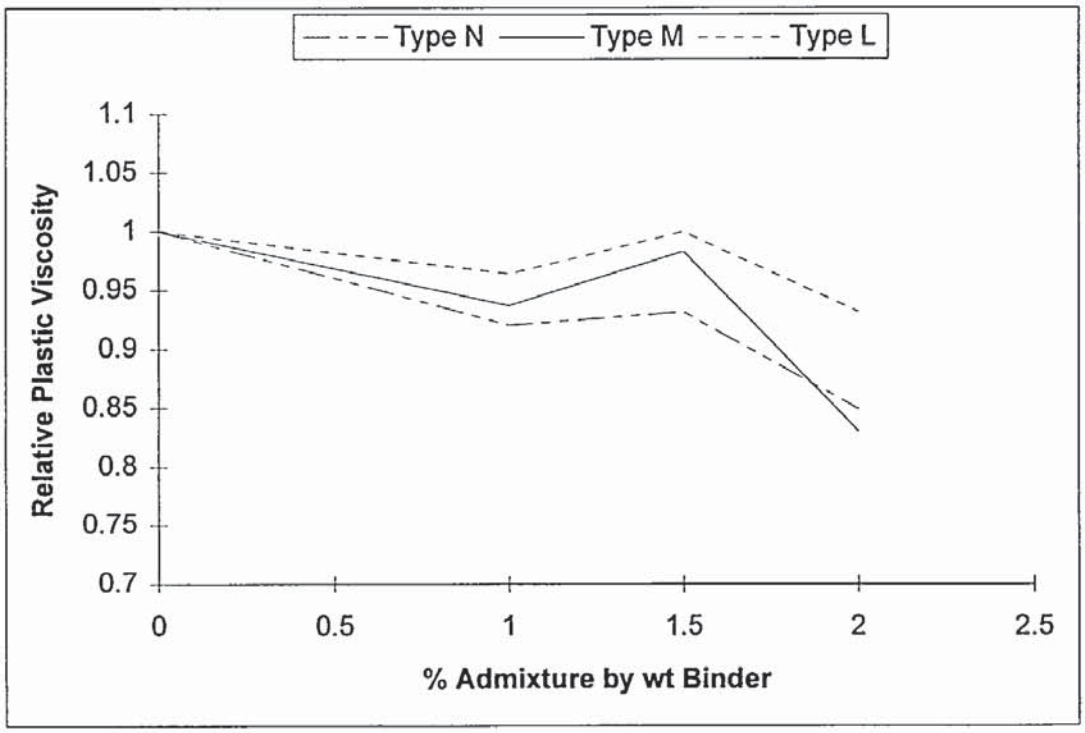

Figure 8.16 Effect of admixtures on plastic viscosity of 10% MK mortar.

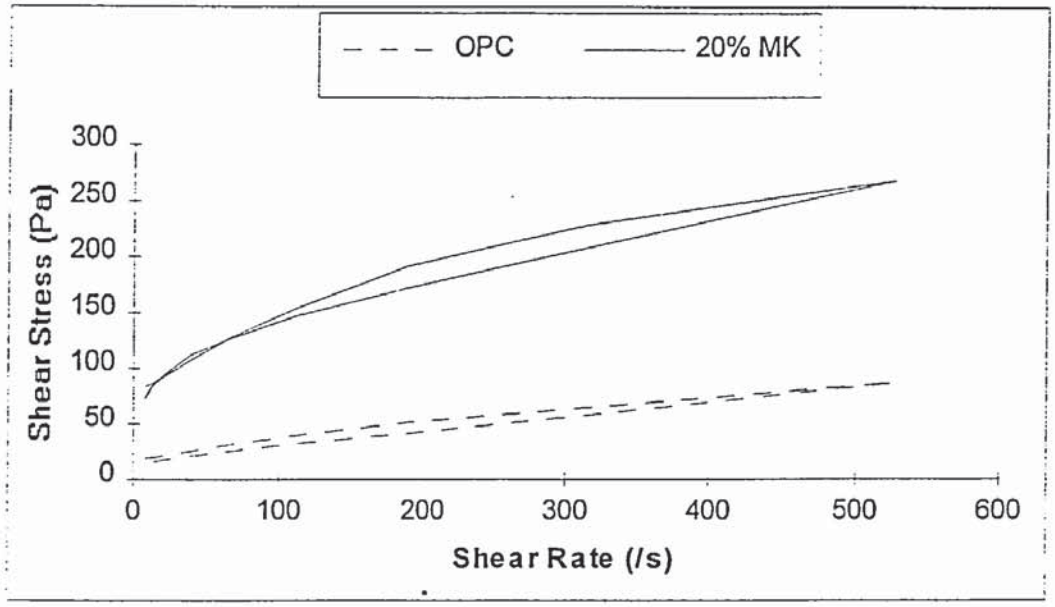

Figure 8.17 Flow curves for OPC and 20% MK pastes.

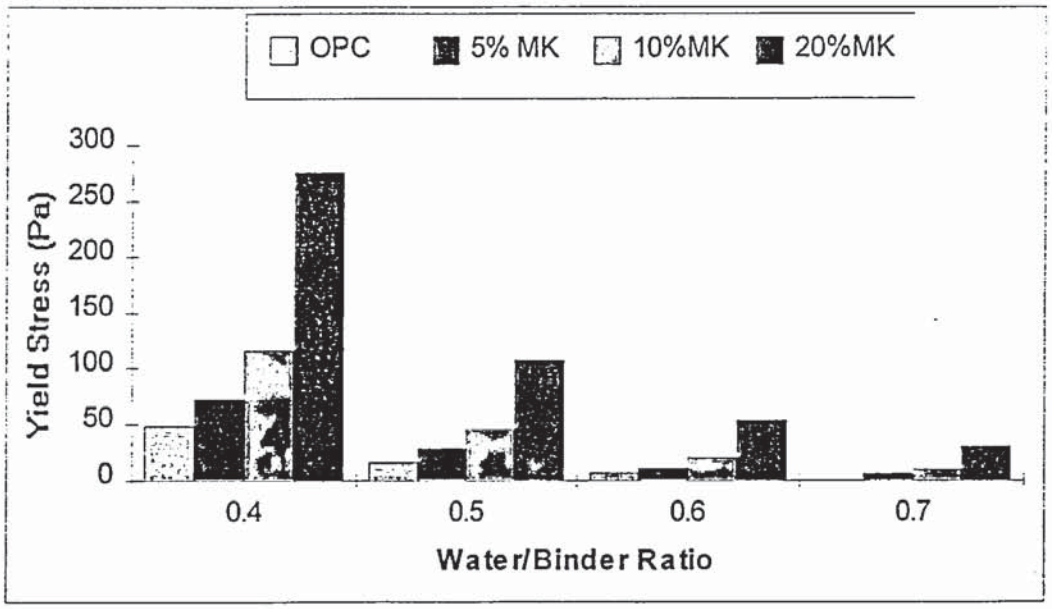

Figure 8.18 Effect of MK on plastic viscosity of cement pastes.

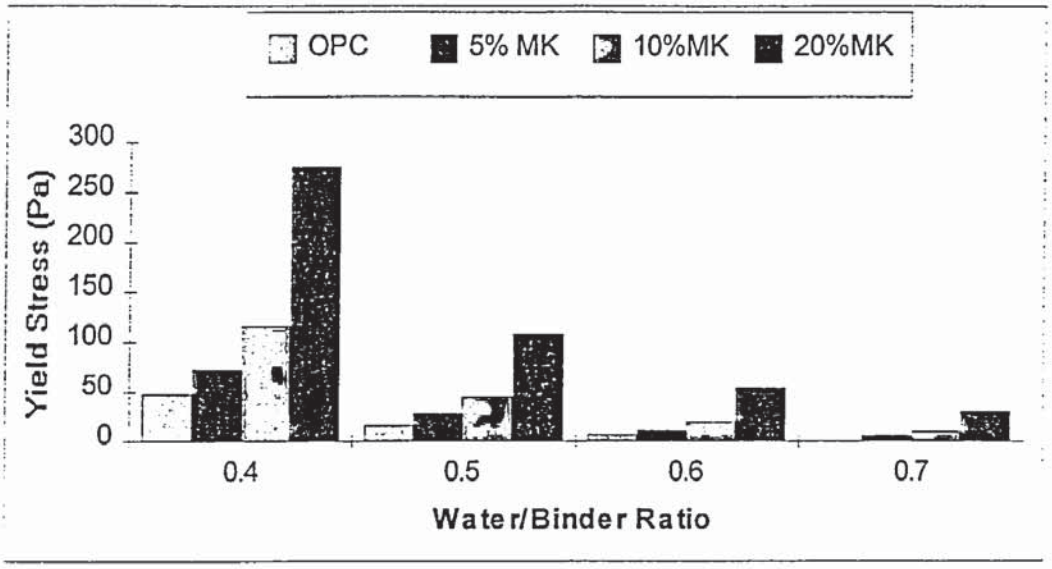

Figure 8.19 Effect of MK on yield stress of cement pastes.

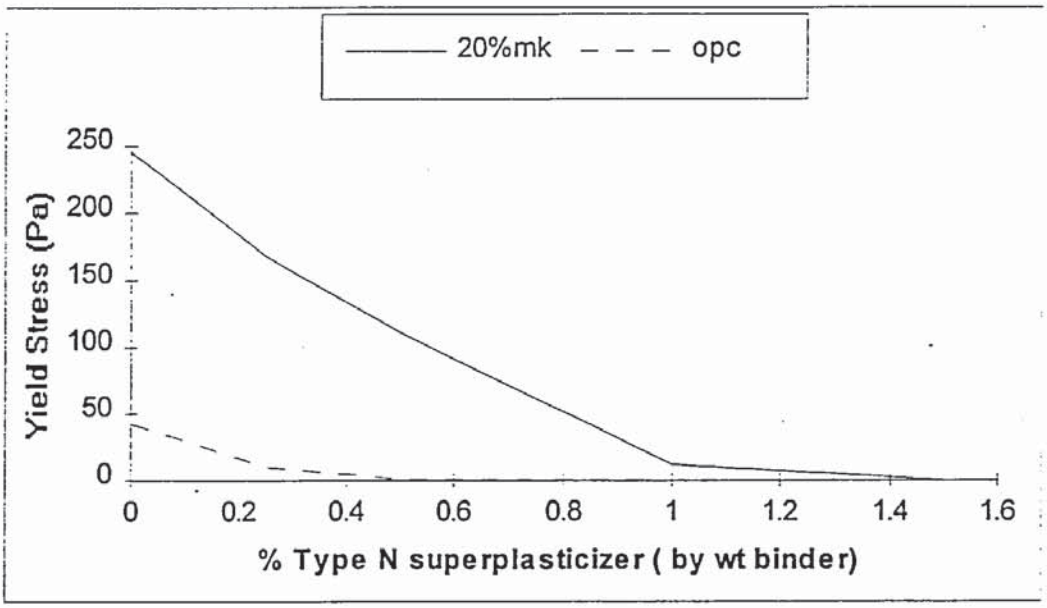

Figure 8.20 Effect of type N superplasticizer on yield value of cement pastes.

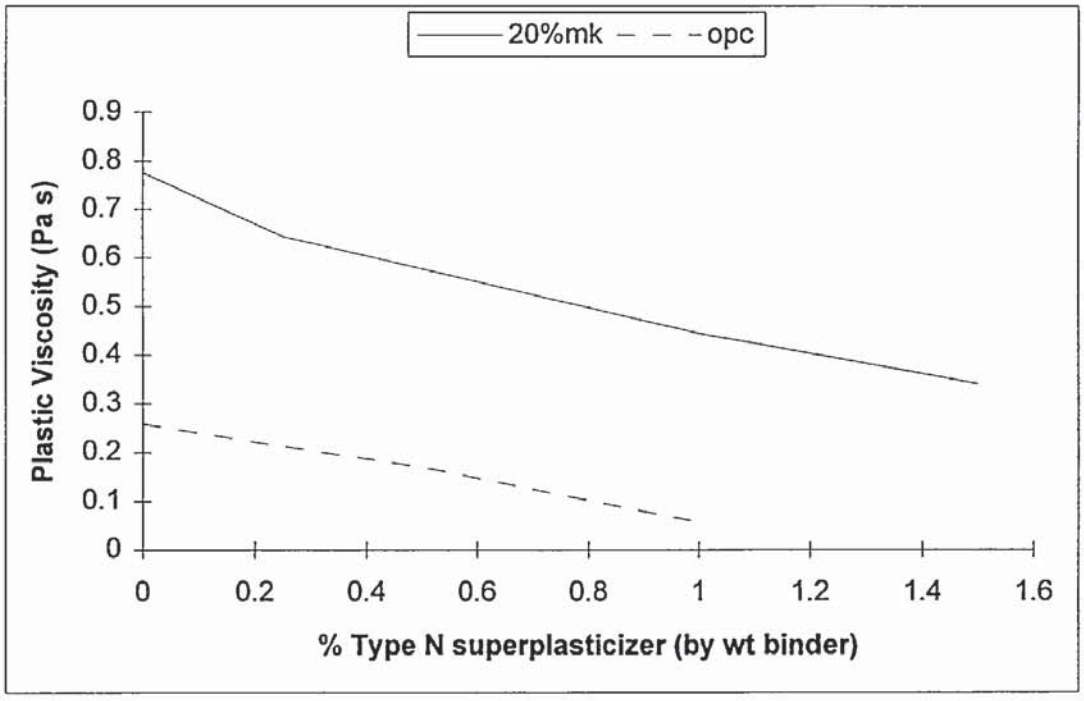

Figure 8.21 Effect of type N superplasticizer on plastic viscosity of cement pastes.

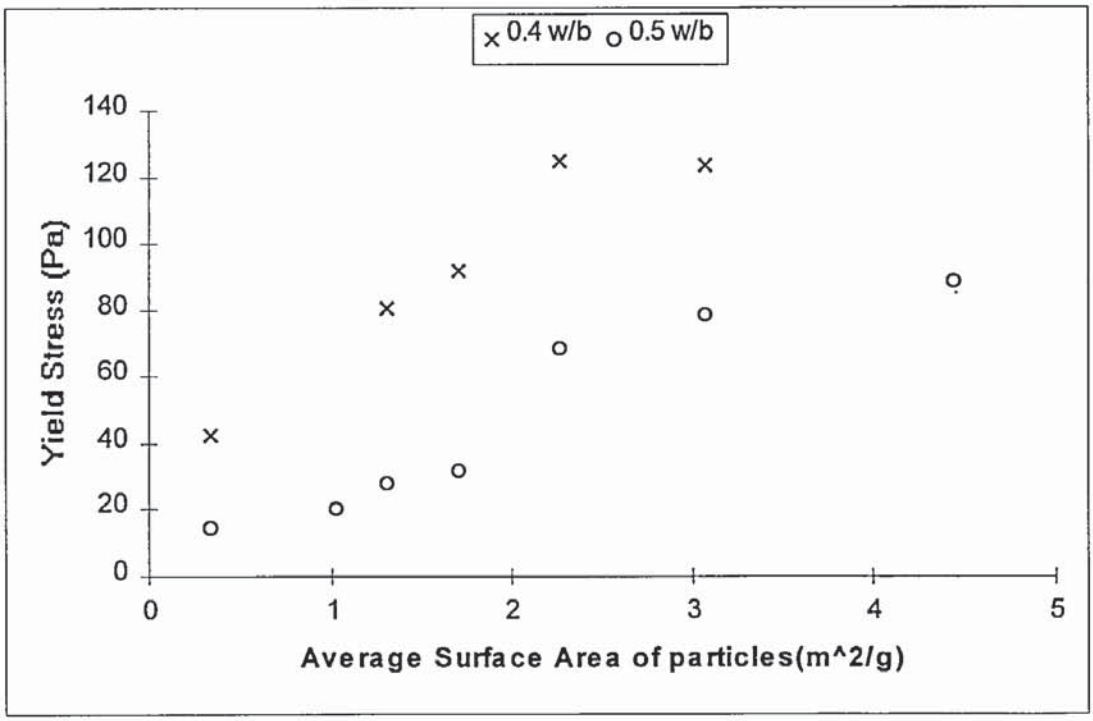

Figure 8.22 Relationship between surface area and yield stress of paste.

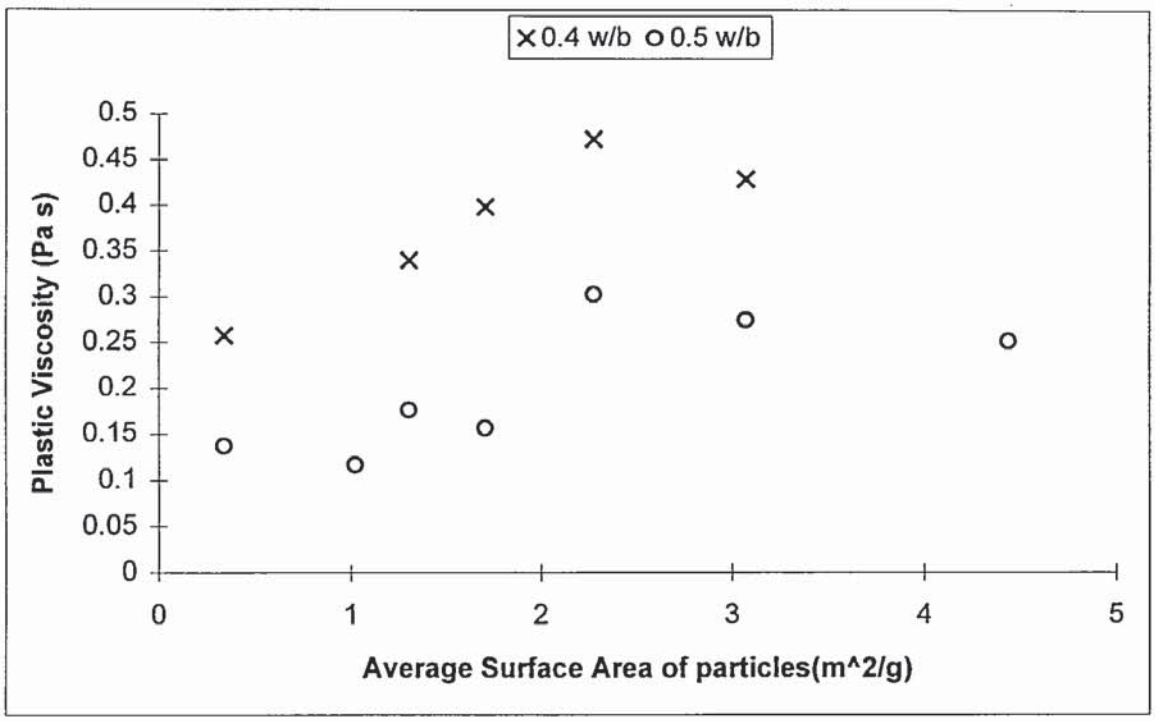

Figure 8.23 Relationship between surface area and plastic viscosity of cement pastes.

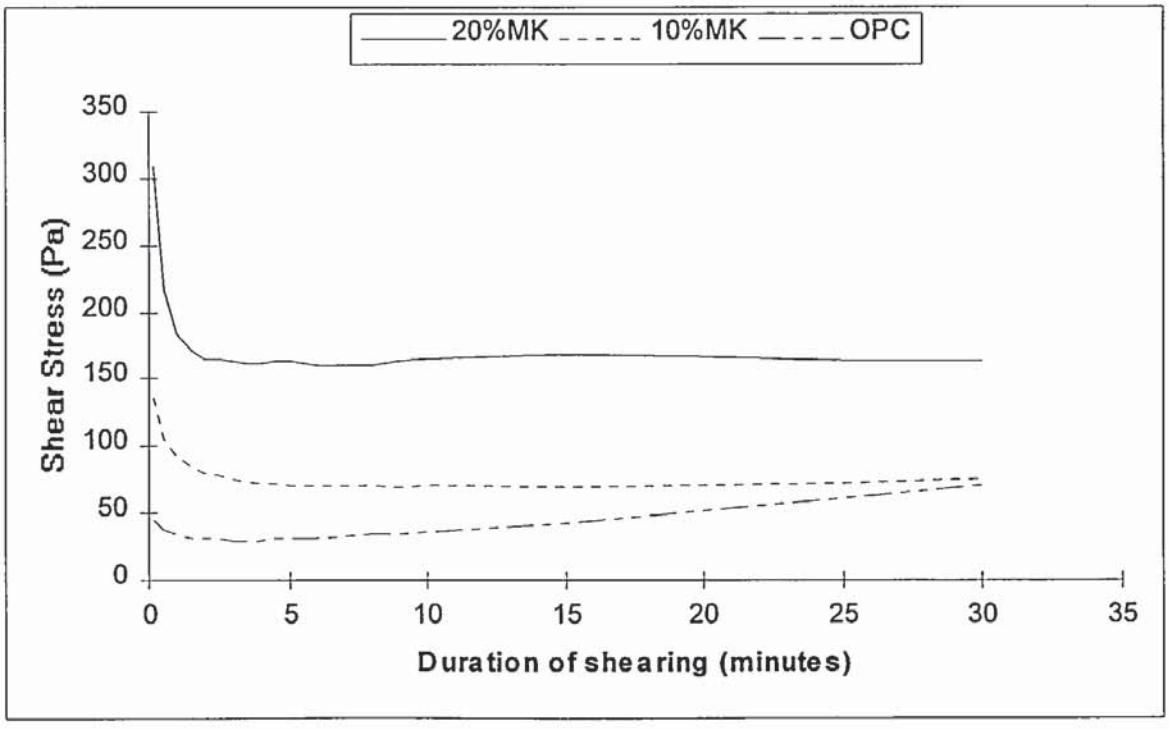

Figure 8.24 Constant shear rate plot for cement pastes.

CHAPTER 9

9. GENERAL CONCLUSIONS AND RECOMMENDATIONS FOR FURTHER WORK

Detailed conclusions have been presented at the end of each chapter and need not be repeated. General conclusions drawn from the study and recommendations for future investigations are presented.

9.1 CONCLUSIONS

The study has shown that inclusion of MK as a partial cement replacement can reduce the ingress of chloride ions into hardened cement paste and concrete, an important factor in reducing the incidence of steel corrosion due to accumulation of chlorides derived from external sources. Careful selection of replacement levels can also lead to increased compressive strength.

Owing to the small particle size and high surface area, metakaolin requires more water than an OPC mix to lubricate particle interaction. A low water content may cause inadequate dispersion of metakaolin particularly in cement pastes, although the phenomenon may not be as noticeable in concrete due to the milling effect of aggregate mixing and the heterogeneity of concrete.

The high surface area of metakaolin particles leads to apparent thixotropic behaviour. However this is a direct consequence of higher yield stress, which requires a higher energy input than OPC concrete to start flow. This is not generally a problem when the concrete is mechanically compacted, although the addition of a superplasticizer can lower yield stresses and improve workability.

The cohesive nature of MK concrete make it suitable for placing by pump. Cohesiveness may also lead to shrinkage cracking if curing is inadequate. Water evaporates from the surface of fresh concrete, and if it is not replaced with water from the body of the concrete quickly enough cracks will form. Cohesiveness can be reduce by reducing the fines content of MK concrete mixes.

a) When used as a partial cement replacement at levels up to 20% by weight of binder, MK improves the pore structure of hardened cement paste by reducing the volume of capillary pores and the threshold diameter. Capillary pores in particular are important in terms of improving durability and mass transport characteristics, as well as influencing other physical properties. Reductions in capillary porosity were attributed to the formation of pozzolanic

hydrates, mainly CSH gel and hydrated gehlenite (strätlingite), and a reduction in calcium hydroxide content. The threshold diameter has been described as being indicative of the largest pore size that penetrates the whole cement matrix. As a result it has a major influence on mass transport properties such as permeability.

b) Even at doses of 20% MK not all the calcium hydroxide is eliminated, enabling the pore fluid concentration of hydroxide ions to be buffered. This is of particular concern in terms of corrosion of reinforcing steel by pitting attack, and resistance to carbonation.

c) Care must be exercised in the manufacture of paste containing MK, due to the possibility of inadequate dispersion of MK particles. A method of preblending MK in water with a superplasticizer was found to produce consistent samples.

d) The partial replacement of OPC with MK reduces the diffusion rate of chloride ions into hardened cement pates when compared to that through plain OPC systems. The lower diffusion rates result from a reduction in capillary porosity, and a subdivision of the pore structure. The reduction in connectivity of the capillary pore network is believed to be not as extensive as in the slow reacting pozzolans such as PFA and BFS, were the secondary hydrates are deposited within a pre-formed cement matrix. Since MK hydrates are produced at an early age, they are unable to partition the larger capillary pores, even though capillary pore volume may be less than a PFA or BFS blended paste.

e) The interaction between penetrating charged species and pore surface charge was found to play a significant role in the diffusion of charged species through hardened cement paste. The ratio of oxygen molecule to chloride ion effective diffusion coefficients (Do/Dcl) was used as a numerical measure of the influence of pore-wall/charged-particle interaction, low values being indicative of highly permeable matrices. This work supports the view that diffusion of chloride ions through hardened cement paste is retarded by interaction with the cement-matrix/pore-fluid interface. MK pastes had Do/Dcl ratios of 14, which compares favourably with PFA which has been found to have values of 15.

f) In general MK pastes had lower oxygen diffusivities than comparable plain OPC pastes, indicating that MK pastes have a lower porosity and MK hydrates are less permeable to dissolved oxygen.

g) The diffusion of chloride ions through model mortars has been shown to decrease with increasing aggregate content, as expected due to the decreasing proportion of permeable paste available. Diffusivity of chloride ions through the mortar-paste fraction remains fairly constant irrespective of aggregate content. This suggests that the paste-aggregate interfacial zone in

MK mortars is not a continuous phase and diffusion rates in mortars are controlled by the diffusivity of the bulk paste. No evidence was found for a percolation path through mortars even at aggregate volume fractions of 55%. The total porosity of the mortar-paste remained constant for differing aggregate contents, suggesting that the interfacial zone in MK systems is not a significant factor in transport processes.

h) Non-steady state diffusion data for concretes immersed in chloride solution for one year showed that MK concrete had better resistance to chloride ingress than OPC, PFA and BFS blended cement concretes exposed to the same curing regime and environment.

i) The corrosion rate of steel embedded in MK concrete exposed to a cyclic wetting and drying saline environment is lower than OPC concrete. Over the short duration of the test MK concrete (10% and 20% MK) performed comparably with the 60% BFS mix, which is a typical replacement level used in structures exposed to aggressive chloride containing environments. There was also good durability shown by the ternary blend containing MK/OPC/PFA. It was concluded that the combination of a slow and fast reacting pozzolan improved durability performance, as well as reducing the cost compared to a binary MK/OPC mix.

j) The flow behaviour of MK fresh pastes and mortars approximates to that of a Bingham plastic, as do OPC cementitious systems. MK systems have much higher yield stresses than comparable OPC mixes, largely due to the high surface area of the MK particle. The high yield stresses associated with MK concrete have led to the conclusion that these mixes are thixotropic. This was found not to be the case. MK concrete will generally not collapse and move as a result of self weight but requires a higher energy input than OPC to initiate flow, giving the appearance of thixotropy.

k) The high yield stresses of MK pastes and mortars can be significantly reduced by the addition of a plasticizing admixture, to aid placement and compaction.

These investigations have shown that MK when used as a partial cement replacement can improve the durability performance of concrete over that of plain OPC concrete. However due to its high cost, MK is unlikely to challenge PFA or BFS as a common cement replacement material, although it has advantages over these materials in terms of its purity and reactivity which may make it a competitive in the high performance concrete sector, where high strength and durability are necessary. In addition the need to use a superplasticizer with MK concretes would not be a disadvantage as water reducing admixtures are commonly used to achieve workability at the low w/c ratios required.

9.2 SUGGESTIONS FOR FUTURE WORK

This work has concentrated on one aspect of durability, namely chloride ingress. Other aspects such as resistance to carbonation will need to be studied, particularly since calcium hydroxide content is a factor controlling carbonation rate. However the low calcium hydroxide content of MK binders might be offset by the low capillary porosity through which the penetration of aggressive species will take place, and thus may be no more susceptible to carbonation than OPC concrete.

Expansion resulting from sulphate attack is another cause of premature failure of concrete, which may be reduced by the inclusion of MK. As well as studying the chemical attack of concrete by each of the above mechanisms individually, combined attacks involving two or more of these processes in combination needs to be studied. Sulphate resisting cement concrete has a low resistance to chloride attack, a particular problem in the Middle East where groundwater containing high concentrations of both these deleterious agents commonly occurs.

The production of hydrated gehlenite is an important factor in the prevention of the conversion reaction in BRECEM. MK may be used in a similar manner to reduce or prevent the conversion reaction occurring in high alumina cements.

The influence of curing on MK systems needs to be investigated, particularly from a practical view point. Examination in terms of strength gain and microstructure of specimens exposed to poor and good curing regimes will provide information on whether MK hydration is as sensitive to early age curing as other pozzolans, and provide information for "good site practice". A review of the literature indicated that hydrated gehlenite was unstable at high temperatures. This needs to be investigated, as changes in microstructure could be detrimental for durability and strength.

Diffusion through mortars needs to be further investigated. The controlling factor of diffusion through MK mortar appears to be the diffusivity of the bulk paste. An investigation of the influence of MK on the paste-aggregate interfacial zone to elucidate whether it is eliminated, or only reduced in size would add to the understanding of diffusion through concrete.

As with all concrete long term behaviour is estimated from data obtained from relatively short term tests. Data is needed from long term exposure to insitu conditions, only then can a true indication of service life performance be gauged.

It was found in this work that combining two pozzolans with OPC, to form a ternary blend, produced favourable durability properties. It appeared that by combining MK with a slower

reacting cement replacement a more refined pore system could be achieved than by binary blending alone. However, in this investigation the proportions of these mixes were arbitrarily chosen. Further work in this area may reveal optimum proportions for very high durability mixes. In addition the relatively high cost of MK could be offset by using it in combination with a cheaper cement replacement.

Autogenous shrinkage of MK systems of low water/binder ratio needs to be considered. The evidence gathered in this work was inconclusive. However if water/binder ratios lower than 0.4 were used, as is common in high durability applications, the high water requirement of MK hydration may lead to microcracking due to self desiccation.

REFERENCES

Aïtcin, P. C. and Neville, A. (1993). High Performance Concrete Demystified. Concrete International, Jan., pp. 21-26.

Al-Shakhshir, (1988). Workability of Plasticized Concrete. In Workability and Quality Control of Concrete, Tattersall, G. H. 1991, E & FN Spon, London.

Ambroise, J., Murat, M. and Pera, J. (1985a). Hydration Reaction and Hardening of Calcined Clays and Related Minerals: IV Experimental Conditions for Strength Improvement on Metakaolinite Minicylinders. Cement and Concrete Research, Vol.15, pp. 83-88.

Ambroise, J., Murat, M. and Pera, J. (1985b). Hydration Reaction and Hardening of Calcined Clays and Related Minerals: V Extension of the Research and General Conclusions. Cement and Concrete Research, Vol.15, pp. 261-268.

Andrade, C. and Gonzalez, J. A. (1978). Quantitative Measurements of Corrosion Rate of Reinforcing Steels Embedded in Concrete using Polarization Resistance Measurements. Werkstoffe und Korrosion, 29, pp. 515-519.

Andrade, C., Castelo, V., Alonso, C. and Gonzalez, J. A. (1986). The Determination of the Corrosion Rate of Steel Embedded in Concrete by the Polarization Resistance and AC Impedance Methods. Corrosion Effects of Stray Currents and the Techniques for Evaluating Corrosion of Rebars in Concrete. ASTM STP 906, pp.43-63.

Andrade, C., Alonso, C. and Goñi, S. (1993). Possibilities for Electrical Resistivity to Universally Characterise Mass Transport Processes in Concrete. Int. Conf. Concrete 2000, Univ. Dundee, 7-9 Sept., pp. 1639-1652.

Andrade, C., Alonso, C. and Acha, M. (1994). Chloride Diffusion Coefficient of Concrete Containing Fly Ash Calculated from Migration Tests. Int. Conf. on Corrosion Protection of Steel in Concrete. Ed. Swarmy, R. N., Sheffield, 24-28 July, Sheffield Academic Press.

Arya, C., Buenfeld, N. R. and Newman, J. B. (1987). Assessment of Simple Methods of Determining the Free Chloride Ion Content of Cement Paste. Cement and Concrete Research, Vol.17, pp. 907-918.

Arya, C. and Newman, J. B. (1990). An Assessment of Four Methods of Determining the Free Chloride Content of Concrete. Materials and Structures, No.25, pp. 319-330.

Arya, C. and Xu, Y. (1995). Effect of Cement Type on Chloride Binding and Corrosion of Steel in Concrete. Cement and Concrete Research, Vol.25, No.4, pp. 893-902.

Asaga, K. and Roy, D. M. (1980). Rheological Properties of Cement Mixes IV: Effects of Superplasticizers on Viscosity and Yield Stress. Cement and Concrete Research, Vol.10, No.2, pp. 287-295.

Asbridge, A. H., Jones, T. R. and Osborne, G. J. (1996). High Performance Metakaolin Concrete: Results of Large Scale Trials in Aggressive Environments. Proc. Int. Conf. "Concrete in the Service of Mankind." Dundee Univ. U.K. 24-26 June 1996.

Atkinson, A. and Nickerson, A. K. (1984). The Diffusion of Ions Through Water-Saturated Cement. Journal of Materials Science, Vol.19, pp. 3068-3078.

Bamforth, P. B. and Pocock, D. C. (1990). Minimising the risk of Chloride induced Corrosion by Selection of Concrete Materials. Proc. 3rd Int. Symp. "Corrosion of Reinforcement in Concrete Construction". SCI 21-24 May, pp. 119-131.

Bamforth, P. B. (1993). Concrete Classifications for RC Structures exposed to Marine and other Salt-Laden Environments. Structural Faults and Repair, 29 June -1 July, Edinburgh.

Bamforth, P. B. and Price, W. F. (1993). Factors Influencing Chloride Ingress into Marine Structures. Economic and Durable Construction through Excellence, Concrete 2000, Dundee 7-9 Sept.

Bamforth, P. B. and Chapman-Andrews, J. F. (1994). Long Term Performance of RC elements under UK Coastal Exposure Conditions. Int Conf. on Corrosion oand Protection of Steel in Concrete. Univ. Sheffield, 24-28 July, Sheffield Academic Press, pp. 395-419.

Bamforth, P. B. (1994). Admitting that Chlorides are Admitted. Concrete, Nov./Dec. pp. 18-21.

Bamforth, P. B. (1996). Definition of Exposure Classes and Concrete Mix Requirements for Chloride Contaminated Environments. 4th Int. Symp. on "Corrosion of Reinforcement in Concrete Construction." Cambridge U.K. 1-4 July.

Banfill, P. F. G. (1980). Workability of Flowing concrete. Magazine of Concrete Research, Vol.32, No.110, March.

Banfill, P. F. G. (1981). A Viscometric Study of Cement Pastes Containing Superplasticizers with a Note on Experimental Techniques. Magazine of Concrete Research, Vol.33, No.114, March.

Banfill, P. F. G. and Saunders, D. C. (1981). On the Viscometric Examination of Cement Pastes. Cement and Concrete Research, Vol.11, No.3, pp. 363-370.

Banfill, P. F. G. and Gill, S. M. (1986). The Rheology of Aluminous Cement Pastes. 8th Int. Congress on the Chemistry of Cement. Rio de Janeiro, 22-27 Sept., Vol.VI, pp. 223-227.

Banfill, P. F. G. (1990a). A Coaxial Cylinders Viscometer for Mortar: Design and Experimental Validation. Proc. Int. Conf. on Rheology of Cement and Concrete, London, pp. 217-226.

Banfill, P. F. G. (1990b). Use of the ViscoCorder to Study the Rheology of Fresh Mortar. Magazine of Concrete Research, Vol.42, No.153, Dec., pp. 213-221.

Banfill, P. F. G. (1991). The Rheology of Fresh Mortar. Magazine of Concrete Research, Vol.43, No.154, March, pp. 13-21.

Barnes, B. D., Diamond, S. and Dolch, W. L. (1978). The Contact Zone Between Portland Cement Paste and Glass "Aggregate" Surfaces. Cement and Concrete Research Vol.8, pp. 233-244.

Barnes, B. D., Diamond, S. and Dolch, W. L. (1979). Micromorphology of the Interfacial Zone Around Aggregate in Portland Cement Mortar. Jr. Am. Ceram. Soc., Vol. 62, No.1-2, pp. 21-24.

Bentur, A. and Mindess, S. (1986). The Effect of Concrete Strength on Crack Patterns. Cement and Concrete Research, Vol.16, pp. 59-66.

Bentur, A., Goldman, A. and Cohen, M. D. (1988). The Contribution of the Transition Zone to the Strength of High Quality Silica Fume Concretes. Mats. Res. Soc. Symp. Proc. Vol.114, pp. 97-103.

Bentz, D. P. and Garboczi, E. J. (1991). Percolation of Phases in a three Dimensional Cement Paste Microstructural Model. Cement and Concrete Research, Vol.21, No.2/3, pp. 325-344.

Bijen, J. M. and Larbi, J. A. (1990). Metakaolinite, a Potential Superior Pozzolan in Concrete. Conf on The Microstructure of Cement and Concrete, Inst. Mat., Oxford 19-20 Sept.

Bonen, D. and Sarkar, S. L. (1995). The Superplasticizer Adsorption Capacity of Cement Pastes, Pore Solution Composition and Parameters Affecting Flow Loss. Cement and Concrete Research, Vol. 25, No.7, pp. 1423-1434.

BRE Digest 392 (1994). Assessment of Existing High Alumina Cement Concrete Construction in the UK. March

Bredy, P., Chabannet, M. and Pera, J. (1989). Microstructure and Porosity of Metakaolin Blended Cements. Mats. Res. Symp. Proc., Vol.137.

British Standards Institution (1991). 12: Part 2, Portland Cement (Ordinary and Rapid-Hardening). HMSO, London.

British Standards Institution (1983). 882: Part 2, Coarse and Fine Aggregates from Natural Sources. HMSO, London.

British Standards Institution (1970). 1881: Part 1, Preparation of Concrete. HMSO, London.

British Standards Institution (1971). 1881: Part 6, Analysis of Hardened Concrete. HMSO, London.

British Standards Institution (1970). 1881: Part 124, Analysis of Hardened Concrete. HMSO, London.

British Standards Institution (1982). 3892: Part 1, Pulverised-Fuel Ash: Specification for PFA for Use as Cementitious Component in Structural Concrete. HMSO, London.

British Standards Institution (1982). 5075: Part 1, Concrete Admixtures. HMSO, London.

British Standards Institution (1985). 8110: Part 1, Structural Use of Concrete Code of Practice for Design and Construction. HMSO, London.

Browne, R. D. (1982). Design Prediction of the Life of Reinforced Concrete in Marine and other Chloride Environments. Durability of Building Materials, Vol.3. Elsevier Science, Amsterdam.

Buck, A. D. and Dolch, W. L. (1966). Investigation of a Reaction Involving Non-Dolomitic Limestone Aggregate in Concrete. Jr. Am. Conc. Inst., Vol.63, No.7, pp. 755-763.

Buenfeld, N. R. and Newman, J. B. (1987). Examination of Three Methods for Studying Ion Diffusion in Cement Pastes, Mortars and Concrete. Materials and Structures, Vol.20, pp. 3-10.

Cabrera, J. G. and Hopkins, C. J. (1984). A Modification of Tattersall's Two-Point Test Apparatus for Measuring Concrete Workability. Magazine of Concrete Research, Vol.36, No.129, pp. 237-240.

Coleman, N. J. (1997). Metakaolin as a Cement Extender. Ph.D. Thesis, Aston University, Birmingham, U.K.

Coleman, N. J. and Page, C. L. (1997). Aspects of the Pore Solution Chemistry of Hydrated Cement Pastes Containing Metakaolin. Cement and Concrete Research Vol.27, No.1, pp. 147-154.

Collepardi, M., Marcialis, A. and Turriziani, R. (1970). The Kinetics of Penetration of Chloride Ions into the Concrete. Il Cemento, 4, pp. 157-163.

Collepardi, M., Marcialis, A. and Turriziani, R. (1972). The Penetration of Deicing Agents in Cement Pastes. Il Cemento, 3, pp. 143-149.

Concrete (1996). Developments in the use of ggbs. Jan./Feb., Vol.30, No.1, pp. 18-20.

Cook, D. J. (1986). Calcined Clay, Shale and Other Soils. Cement Technology and Design. Vol. 3. Cement Replacement Materials. Ed. R. N. Swarmy. Surrey Univ. Press (London).

Cook, R. A. and Hover, K. C. (1993). Mercury Porosimetry of Cement-Based Materials and Associated Correction Factors. ACI Materials Journal, Vol.90, No.2, pp. 152-161.

Crank, J. (1975). The Mathematics of Diffusion. 2nd Edition, Clarendon Press, Oxford.

Cussler, E. L. (1985). Diffusion: Mass Transfer in Fluid Systems. Cambridge University Press, New York.

Damidot, D. and Glasser, F. P. (1995). Investigation of the $CaO-Al_2O_3-SiO_2-H_2O$ System at 25°C by Thermodynamic Calculations. Cement and Concrete Research Vol.25, No.1, pp. 22-28.

Day, R. L. (1981). Reactions Between Methanol and Portland Cement Paste. Cement and Concrete Research Vol.11, pp. 341-349.

Day, R. L. and Marsh, B. (1988). Measurement of Porosity in Blended Cement Pastes. Cement and Concrete Research Vol.18, pp. 63-73.

Dean, J. A. (1985). Lange's Handbook of Electrochemistry, 13th edition, McGraw-Hill, New York, p.10.

Detwiler, R., Krishnan, K. and Mehta, P. (1986). Effect of Blast Furnace Slag on the Transition Zone in Concrete. Proc. Bryant and Katherine Mather Int. Symp. on Durability of Concrete, Atlanta. ACI SP 100-6, Vol.1, pp. 63-72.

Detwiler, R. J. and Mehta, P. K. (1989). Chemical and Physical Effects of Silica Fume on the Mechanical Behaviour of Concrete. ACI Materials Jr., No.86, pp. 609-614.

Dhir, R. K. (1986). Pulverised Fuel Ash. In Concrete Technology and Design, Vol.3, Cement Replacement Materials. Ed. Swarmy, R. N., Surrey University Press, London, pp. 197-255.

Dhir, R. K., Jones, M. R. and Ahmed, H. E. H. (1991). Concrete Durability: Estimation of Chloride Concentration During Design Life. Magazine of Concrete Research, 43, No.154.

Dhir, R. K., Jones, M. R., Ahmed, H. E. H. and Seneviratne, A. M. G. (1993). Rapid Estimation of Chloride Diffusion Coefficient in Concrete. Magazine of Concrete Research, 42, No.152, Sept., pp. 177-185.

Dhir, R. K., Jones, M. R. and Elghaly, A. E. (1993). PFA Concrete: Exposure Temperature Effects on Chloride Diffusion. Cement and Concrete Research, Vol.23, pp. 1105-1114.

Dhir, R. K. and Byars (1993). PFA Concrete: Chloride Diffusion Rates. Magazine of Concrete Research, 45, No.162, March, pp. 1-9.

Diamond, S. (1971). Pore-distribution, Measurement and Comparison. Cement and Concrete Research, Vol.1, No.5, pp. 532-545.

Diamond, S. (1987). Cement Paste Microstructure in Concrete. Mats. Res. Soc. Symp. Proc. Vol.85, pp. 21-31.

Dimond, C. R. and Tattersall, G. H. (1976). The Use of the Coaxial Cylinders Viscometer to Measure the Rheological Properties of Cement Pastes. Proc. Conf. Hydraulic Cement Pastes: Their Structure and Properties, Sheffield, U.K., pp. 118-133.

Domone, (1994). Construction Materials their Nature and Behaviour. 2nd edition, Ed. Illston, J. M., E & FN Spon.

Engineering News Record, (1977). One in Six US Highway Bridges is Deficient. 10 Mar., pp. 18-21.

Ellis, C. (1981). Magazine of Concrete Research, Vol.33, No.117, pp. 233-235.

Everett, L. H. and Treadaway, K. W. J. (1980). Deterioration due to corrosion in Reinforced Concrete. BRE Information Paper, IP12/80, BRE, Garston.

Ewins, A. J. (1990). Resitivity Measurements in Concrete. British Journal of Non Destructive Testing, Vol.32, No.3, March, pp. 120-126.

Farran, J. (1956). Contribution Mineralogique a L'Etude de L'Adherence Entre Les Constituants Hydrates Des Ciments et Les Materiaux Enrobes. Rev. Mater. Const. Trav. Publics. Ed. C. 490-491, pp. 155-172.

Feldman, R. F. and Sereda, P. J. (1970). A New Model for Hydrated Portland Cement and its Practical Implications. Eng. Journal Canada, Vol.53, pp. 53-59.

Feldman, R. F. and Beaudoin, J. J. (1991). Pretreatment of Hardened Hydrated Cement Pastes for Mercury Intrusion Measurements. Cement and Concrete Research Vol.21, No.2/3, pp. 297-308.

Feldman, R. F. (1984). Pore Structure Damage in Blended Cements Caused by Mercury Intrusion. Jour. Am. Ceram. Soc. Vol.67, No.1, pp. 30-33.

Garboczi, E. J. (1990). Permeability, Diffusivity and Microstructural Parameters: A Critical Review. Cement and Concrete Research, Vol.20, pp. 591-601.

Garboczi, E. J. and Bentz, D. P. (1992). Computer Simulation of the Diffusivity of Cement-Based Materials. Journal of Materials Science, Vol.27, pp. 2083-2092.

Garboczi, E. J., Schwartz, L. M. and Bentz, D. P. (1995). Modelling the Influence of the Interfacial Zone on the D.C. Electrical Conductivity of Mortar. Advances in Cement Based Materials, Vol.2, pp. 169-181.

Gjørv, O. E. and Vennesland, Ø. (1979). Diffusion of Chloride ions From Seawater into Concrete. Cement and Concrete Research, Vol.9, pp. 229-238.

Gjørv, O. E., Vennesland, Ø. and El-Busaidy (1986). Diffusion of Dissolved Oxygen through Concrete. N.A.C.E., Vol.25, Part 12, pp. 39-44.

Gjørv, O. E., Tau, K. and Zhang, M. H. (1994). Diffusivity of Chlorides from Seawater into High Strength Lightweight Concrete. ACI Materials Journal, Vol.91, No.5, Sept.-Oct.

Goldman, A. and Bentur, A. (1989). Bond Effects in High Strength Silica-Fume Concretes. ACI Materials Jr. Vol.86, No.5, pp. 440-447.

Goto, S. and Roy, D. M. (1981a). The Effect of w/c Ratio and Curing Temperature on the Permeability of Hardened Cement Paste. Cement and Concrete Research, Vol.11, pp. 575-579.

Goto, S. and Roy, D. M. (1981b). Diffusion of Ions through Hardened Cement Pastes. Cement and Concrete Research, Vol.11, pp. 751-757.

Hadley, D. (1972). The Nature of the Paste-Aggregate Interface. Ph.D. Thesis, Purdue University, USA.

Halamickova, P. and Detwiler, R. J. (1995). Water Permeability and Chloride Ion Diffusion in Portland Cement Mortars: Relationship to Sand Content and Critical Pore Diameter. Cement and Concrete Research, Vol.25, No.4, pp. 790-802.

Hansson, C. M. (1984). Comments on electrochemical measurements of the rate of Corrosion of Steel in Concrete. Cement and Concrete Research, Vol.14, pp. 574-584.

He, C., Osbaeck, B. and Makovicky, E. (1995). Pozzolanic Reactions of Six Principal Clay Minerals. Activation, Reactivity Assessments and Technological Effects. Cement and Concrete Research, Vol.25, No.8, pp. 1691-1702.

Helmuth, R. A. (1980). 7th Int. Congress on the Chemistry of Cement, Paris, Vol.III, V1-0/1.

Hoffmann, D. W. (1984). Changes in Structure and Chemistry of Cement Mortars Stressed by a Sodium Chloride Solution. Cement and Concrete Research, Vol.14, pp. 44-56.

Hope, B. B., Ip, A. K. and Manning, D. G. (1985). Corrosion of Electrical Impedance in Concrete. Cement and Concrete Research, Vol.15, pp. 525-534.

Hornung, F. (1990). The Use of the Brabender Viscocorder to Study the Consistency of Fresh Mortar by Two-Point Tests. Int. Conf. on Rheology of Fresh Cement and Concrete, London, pp. 227-237.

Hsu, T. T. C. and Slate, F. O. (1963). Tensile Bond Strength Between Aggregate and Cement Paste or Mortar. Jr. Am. Conc. Inst. Proc. Vol.60, No.4, pp. 465-486.

Jensen, O. M. and Hansen, P. F. (1995). A Dilatometer for Measuring Autogenous Deformation in Hardening Portland Cement Paste. Materials and Structures, 28, pp. 406-409.

Kayyali, O. A. (1987). Porosity of Concrete in Relation to the Nature of the Paste-Aggregate Interface. Materials and Structures, Vol.20, pp. 19-26.

Kayyali, O. A. and Haque, M. N. (1988). Chloride Penetration and the Ratio of Cl^-/OH^- in the Pores of Cement Paste. Cement and Concrete Research, Vol.18, pp. 895-900.

Kayyali, O. A. (1989). Porosity and Compressive Strength of Cement Pastes in Sulphate Solution. Cement and Concrete Research, Vol.19, pp. 423-433.

Khatib, J. M. and Wild, S. (1996). Pore Size Distribution of Metakaolin Paste. Cement and Concrete Research, Vol.26, No.10, pp. 1545-1553.

Kjellsen, K. O. and Jennings, H. M. (1996). Observations of Microcracking in Cement Paste upon Drying and Rewetting by Environmental Scanning Electron Microscope. Advances in Cement Based Materials, No.3, pp. 14-19.

Kjellsen, K. O., Detwiler, R. J. and Gjørv, O. E. (1991). Developments of Microstructure in Plain Cement Pastes Hydrated at Different Temperatures. Cement and Concrete Research, Vol.21, No.1, pp. 179-189.

Kobayashi, K. and Shuttoh, K. (1991). Oxygen Diffusivity of Various Cementitious Materials. Cement and Concrete Research, Vol.21, No.2/3, pp. 273-284.

Kostuch, J. A., Walters, G. V. and Jones, T. R. (1993). High Performance Concretes Incorporating Metakaolin - A Review. Concrete 2000, University of Dundee, 7-9 Sept.

Kropp, J. and Hilsdorf, H. K. (1995). Performance criteria for Concrete Durability. E & FN Spon, London.

Kumar, A. and Roy, D. M. (1986). Pore Structure and Ionic Diffusion in Admixture Blended Portland Cement Systems.. 8th Int. Congress on the Chemistry of Cement. Rio de Janeiro, 22-27 Sept., Vol.V, pp. 73-79.

Lambert, P., Page, C. L. and Vassie, P. R. W. (1991). Investigations of Reinforcement Corrosion 2. Electrochemical Monitoring of Steel in Chloride-Contaminated Concrete. Materials and Structures, 24, pp. 351-358.

Lapasin, R., Papo, A. and Rajgelj, S. (1983). Flow Behaviour of Fresh Cement Pastes. A comparison of Different Rheological Instruments and Techniques. Cement and Concrete Research, Vol.13, pp. 349-356.

Larbi, J. A. (1991). The Cement Paste-Aggregate Interfacial Zone in Concrete. Ph.D. Thesis, Technical University of Delft, The Netherlands.

Li, S. and Roy, D. M. (1986). Investigation of Relationship between Porosity, Pore Structure and Chloride Diffusion of Fly Ash and Blended Cement Pastes. Cement and Concrete Research, Vol.16, pp. 749-759.

Liam, K. C., Roy, S. K. and Northwood, D. O. (1992). Chloride Ingress Measurements and Corrosion Potential Mapping Study of a 24 Year-Old Reinforced Concrete Jetty

Structure in a Tropical Marine Environment. Magazine of Concrete Research, 44, No.160, Sept. pp. 205-215.

Lingane, J. J. (1958). Electroanalytical Chemistry. Interscience Publishers, New York, pp. 227-229.

Lingane, J. J. (1967). Controlled Potential Electroanalysis. In Coulometry in Analytical Chemistry, Ed. Milner, G. W. C. and Phillips, G. Pergamon Press, Oxford, pp. 172-186.

MacDonald, K. A. and Northwood, D. O. (1995). Experimental Measurements of Chloride Ion Diffusion Rates using a 2 Compartment Diffusion Cell: Effects of Material and Test Variables. Cement and Concrete Research, Vol.25, No.7, pp. 1407-1416.

Malek, R. I. A. and Roy, D. M. (1988). The Permeability of Chloride Ions in Fly-Ash cement Pastes, Mortars and Concrete. Mats. Res. Soc. Symp. Proc. Vol.114, pp. 325-334.

Mangat, P. S. and Molloy, B. T. (1991). Influence of PFA, Slag and Microsilica on Chloride Induced Corrosion of Reinforcement in Concrete. Cement and Concrete Research, Vol.21, No.5, pp. 819-834.

Mangat, P. S. and Molloy, B. T. (1994). Prediction of Free Chloride Concentration in Concrete Using Routine Inspection Data. Magazine of Concrete Research, 46, No.169, Dec., pp. 279-287.

Marchese, B. (1983). Morphology and Composition of Twin Fracture Surfaces of a Crack in Portland Cement Paste. Cement and Concrete Research, Vol.13, pp. 435-440.

Marsh, B. K., Day, R. L., Bonner, D. G. and Illston, J. M. (1983). The effect of Solvent Replacement Upon the Pore Structure Characterisation of Portland Cement Paste. Int. Symp. Principles and Applications of Pore Structural Characterisation, Milan, Italy, pp. 365-374.

Marsh, B. K., Day, R. L. and Bonner, D. G. (1985). Pore Structure Characteristics Affecting the Permeability of Cement Paste Containing Fly Ash. Cement and Concrete Research, Vol.15, pp. 1027-1038.

McCarter, W., Emerson, M. and Ezirim, H. (1995). Properties of Concrete in the Cover Zone- Developments in Monitoring Techniques. Magazine of Concrete Research, Vol.47, No.172, Sept., pp. 243-251.

Mehta, P. K. (1986). Concrete: Structure, Properties and Materials. Prentice-Hall.

Mehta, P. K. and Monteiro, P. J. M. (1988). Effect of Aggregate, Cement and Mineral Admixtures on the Microstructure of the Transition Zone. Mats. Res. Symp. Proc., Vol.114, pp. 65-75.

Midgley, H. G. and Illston, J. M. (1984). Effect of Chloride Penetration on the Properties of Hardened Cement Pastes. Proc. 7th Int. Conf. on the Chemistry of Cement, Paris, Vol.III, VII-101-VII-103.

Midgley, H. G. and Illston, J. M. (1984). The Penetration of Chlorides into Hardened Cement Pastes. Cement and Concrete Research, Vol.14, pp. 546-558.

Millard, S. G., Ghassemi, M. H. and Bungey, J. H. (1990). Assessing the Electrical Resistivity of Concrete Structures for Corrosion Durability Studies. 3rd Int. Symp. on Corrosion of Reinforcement in Concrete Construction. Ed. Page, C. L., Treadaway, K. W. J. and Bamforth, P. B., SCI.

Mindess, S. (1986). Significance to Concrete Performance of Interfaces and Bond: Challenges of the Future. 8th Int. Congress on the Chemistry of Cement. Rio de Janeiro, Vol.1, pp. 151-157.

Mindess, S. and Diamond, S. (1982). A Device for Direct Observation of Cracking of Cement Paste or Mortar Under Compressive Loading Within a Scanning Electron Microscope. Cement and Concrete Research, Vol.12, pp. 569-576.

Moukwa, M. and Aitchin, P. C. (1988). The Effect of Drying on Cement Pastes Pore Structure as Determined by Mercury Porosimetry. Cement and Concrete Research, Vol.18, pp. 745-752.

Munn, C. J. (1986). Compositional Variations between Different Silica Fumes and Their Effect on Early Strength in Cement and Concrete. Project report in Advanced Concrete Technology Course, Cement and Concrete Association.

Murat, M. (1983a). Hydration Reactions and Hardening of Calcined Clays and Related Minerals. I Preliminary Investigation on Metakaolinite. Cement and Concrete Research, Vol.13, pp. 259-266.

Murat, M. (1983b). Hydration Reactions and Hardening of Calcined Clays and Related Minerals. II Influence of Mineralogical Properties of the Raw-Kaolinite on the Reactivity of Metakaolinite. Cement and Concrete Research, Vol.13, pp. 511-518.

Nagano, H. and Naito, T. (1985). Application of Diffusion Theory to Chloride Penetration into Concrete Located in Splashing Zones. Transactions of the Japan Concrete Institute, Vol.7, pp. 157-164.

Neville, A. M. (1995). Properties of Concrete. 4th Edition, Longman (London).

New Civil Engineer. (1991). Heavy Snow Emphasises De-Icing Deficiencies. 14 Feb.

New Civil Engineer. (1996). Colour Supplement: Is Pink Concrete Better? Concrete Engineering Supplement, Nov.

Ngala, V. T. (1995). Pore Structure and Diffusional Properties of Hardened Cement Pastes. Ph.D. Thesis, Aston University, Birmingham, U.K.

Ngala, V. T., Page, C. L., Parrott, L. J. and Yu, S. W. (1995). Diffusion in Cementitious Materials II- Further Investigations of Chloride and Oxygen Diffusion in Well-Cured OPC and OPC/30%PFA Pastes. Cement and Concrete Research, Vol.25, No.4, pp. 819-826

Nyame, B. K. (1985). Permeability of Normal and Lightweight Mortars. Magazine of Concrete Research, Vol.37, No.130, pp. 44-48.

Nyame, B. K. Illston, J. M. (1981). Relationships between Permeability and Pore Structure of Hardened Cement Paste. Magazine of Concrete Research, Vol.33, No.116, pp. 139-146.

Oberholster, R. E. (1986). Proc. 8th Int. Congress on the Chemistry of Cement, Vol.1 pp. 324-335, Brazil.

Ohama, Y., Demura, K., Kobayashi, K., Satoh, Y. and Morikawa, M. (1991). Pore Size Distribution and Oxygen Diffusion Resistance of Polymer Modified Mortars. Cement and Concrete Research, Vol.21, No.2/3, pp. 309-315.

Olivier, J. P., Maso, J. C. and Bourdette, B. (1995). Interfacial Transition Zone in Concrete. Advances in Cement Based Materials, Vol.2, pp. 30-38.

Ottewill, R. H. (1983). Phil. Trans. R. Soc. A310-, pp. 67.

Page, C. L. (1975). Mechanism of Corrosion Protection in Reinforced Concrete Marine Structures. Nature, 258, pp. 514-515.

Page, C. L., Short, N. R. and El Tarras, A. (1981). Diffusion of Chloride Ions in Hardened Cement Pastes. Cement and Concrete Research, Vol.11, pp. 395-406.

Page, C. L. and Treadaway, K. W. J. (1982). Aspects of the Electrochemistry of Steel in Concrete. Nature, Vol.297, No.5862, pp. 109-115.

Page, C. L. and Vennesland, Ø. (1983). Materials and Structures, 16, pp. 19-24.

Page, C. L. and Havdahl, J. (1985). Electrochemical Monitoring of Corrosion of Steel in Microsilica Cement Pastes. Materials and Structures, 18, No.103, pp. 41-47.

Page, C. L. and Lambert, P. (1987). Kinetics of Oxygen Diffusion in Hardened Cement Pastes. Jr. of Materials Science, Vol.22, pp. 942-946.

Page, C. L., Lambert, P. and Vassie, P. R. W. (1991). Investigations of Reinforcement Corrosion 1. The Pore Electrolyte Phase in Chloride-Contaminated Concrete. Materials and Structures, 24, pp. 243-252.

Page, C. L. and Ngala, V. T. (1995). Steady-State Diffusion Characteristics of Cementitious Materials. RILEM international Workshop on Chloride Penetration into Concrete, St. Remy les Chevreuse, France, Oct.

Parrott, L. J. (1987). Measurement and Modelling of Porosity in Drying Cement Paste. Mat. Res. Symp. Proc., Vol.85, pp. 91-104. Mat. Res. Soc.

Parrott, L. J. (1992). Variations of Water Absorption Rate and Porosity with Depth from an Exposed Concrete Surface: Effects of Exposure Conditions and Cement Type. Cement and Concrete Research, Vol.22, pp. 1077-1088.

Petrie, E. M. (1976). Effect of Surfactant on Viscosity of Portland Cement/Water Dispersions. Industrial & Engineering Chemistry, Product Research & Development, Vol.15, pp. 242-249.

Rodriquez, P., Ramirez, E. and Gonzalez, J. A. (1994). Methods for Studying Corrosion in Reinforced Concrete. Magazine of Concrete Research, 46, No.167, June, pp. 81-90.

Polder, R. (1996). Laboratory Testing of Fine Concrete Types for Durability in a Marine Environment. 4th Int. Symp. on Corrosion of Reinforcement in Concrete Construction. Cambridge, U.K., 1-4 July.

Powers, T. C., Copeland, L. E., Hayes, J. C. and Mann, H. M. (1954). Permeability of Portland Cement Paste. Proceedings of American Concrete Research Institute, Vol.51, No.3, pp. 285-298.

Powers, T. C. (1958). Structural and Physical Properties of Hydrated Cement Paste. Jour. Am. Ceramic Soc., Vol.41, No.1, pp. 1-6.

Powers, T. C. and Brownyard, T. L. (1946). Studies of the Physical Properties of Hardened Portland Cement Paste. Proc. Journal of American Concrete Institute. Vol.43.

Regourd, M. (1985). Microstructure of High Strength Cement Paste Systems. Mats Res. Soc. Symp. Proc. Vol.42, pp. 3-17.

Roy, D. M. and Asaga, K. (1979). Rheological Properties of Cement Mixes III: The Effects of Mixing Procedures on Viscometric Properties of Mixes Containing Superplasticizers. Cement and Concrete Research, Vol.9, No.6, pp. 731-739.

Roy, S. K., Chye, L. K. and Northwood, D. O. (1993). Chloride Ingress in Concrete as Measured by Field Exposure tests in the Atmospheric, Tidal and submerged Zones of a Tropical Marine Environment. Cement and Concrete Research, Vol.23, pp. 1289-1306.

Saad, M. N. A., de Andrade, W. P. and Paulon, V. A. (1982). Properties of Mass Concrete Containing an Active Pozzolan made from Clay. Concrete International, July, pp. 59-65.

Sabir, B. B., Wild, S. and Khatib, J. M. (1996). On the Workability and Strength Development of Metakaolin Concrete. Proc. Int. Conf. Concrete in Service of Mankind - Concrete for Environment Enhancement and Protection, Dundee University, U.K. (E & FN Spon).

Schiessl, P. (1983). Corrosion of Reinforcement. CEB International Workshop, Copenhagen, May.

Scrivener, K. L., and Pratt, P. L. (1986). A Preliminary Study of the Microstructure of the Cement-Sand Bond in Mortars. 8th Int. Congress on the Chemistry of Cement. Rio de Janeiro, Vol.III, pp. 466-471.

Scrivener, K. L., Bentur, A. and Pratt, P. L. (1988). Quantitative Characterisation of the Transition Zone in High Strength Concretes. Advances in Cem. Res., Vol.1, No.4, pp. 230-237.

Sellevold, E. J., Bager, D. H., Jensen, E. K. and Knudsen, T. (1981). Silica Fume-Cement Pastes; Hydration and Pore Structure. Nordisk Miniseminar on Silica in Concrete, Dec. 10.

Seneviratne, A. M. G. (1991). Role of PFA Quality on Transportation and Occurrence of Chlorides in Concrete. Ph.D. Thesis, University of Dundee, Scotland.

Sereda, P., Feldman, R. and Ramachandran, V. (1980). Proc. 7th Int. Congress on the Chemistry of Cement, VI-1/3-44 Paris.

Sergi, G. (1986). Corrosion of Steel in Concrete- Cement Matrix Variables. Ph.D. Thesis, Aston University, U.K.

Sergi, G., Yu, S. W. and Page, C. L. (1992). Diffusion of Chloride and Hydroxyl ions in Cementitious Materials Exposed to a Saline Environment. Magazine of Concrete Research, 44, No.158, March, pp. 63-69.

Shah, S. P. and Slate, F. O. (1968). Internal Microcracking, Mortar-Aggregate Bond and Stress-Strain Curve of Concrete. In The Structure of Concrete, Ed. Brooks, A. E. and Newman, K., pp. 82-92.

de Silva, P. S. and Glasser, F. P. (1990). Hydration of Cements Based on Metakaolin: Thermochemistry. Advances in Cement Research, Vol.3, No.12, pp. 167-177.

de Silva, P. S. and Glasser, F. P. (1993). Phase Relations in the System CaO-Al_2O_3-SiO_2-H_2O relevant to Metakaolin-Calcium Hydroxide Hydration. Cement and Concrete Research, Vol.23, pp. 627-639.

Stanley, C. C. (1982). Highlights in the History of Concrete. Cement and Concrete Association. Raithby, Lawrence and Co. Ltd., (London).

Stern, M. and Geary, A. L. (1957). A Theoretical Analysis of the Shape of Polarization Curves. J. of the Electrochemical Society, 104, pp. 56-63.

Stern, M. (1958). A Method for Determining Corrosion Rates From Linear Polarisation Data. Corrosion NACE, 14, 9, pp. 60-64.

Tang, L. and Nilsson, L. O. (1995). A New Approach to the Determination of Pore Distribution by Penetrating Chlorides into Concrete. Cement and Concrete Research, Vol.25, No.4, pp. 695-701.

Tattersall, G. H. (1973). The Principles of Measurement of the Workability of Fresh Concrete and a Proposed Simple Two-Point Test. Proc RILEM Seminar Fresh Concrete: Important Properties and Their Measurement, 22-24 March, Leeds, Vol.1, pp. 2.2-1 to 2.2-33.

Tattersall, G. H. and Banfill, P. F. G. (1983). The Rheology of Fresh Concrete. Pitman, London.

Tattersall, G. H. (1986). Components of Workability and Rheological Measurements on Mortars and Fresh Concrete. 8th Int. Congress on the Chemistry of Cement. Rio de Janeiro, 22-27 Sept., Vol.VI, pp. 228-238.

Tattersall, G. H. (1991). Workability and Quality of Concrete. 1st edition, E & FN Spon, London.

Tazawa, E. and Miyazawa, S. (1992). Autogenous Shrinkage caused by Self Desiccation in Cementitious Material. 9th Int. Congress on the Chemistry of Cement, New Delhi, India, Vol.IV, pp. 712-718.

Tazawa, E. and Miyazawa, S. (1995). Experimental Study on Mechanism of Autogenous Shrinkage of Concrete. Cement and Concrete Research, Vol.25, No.8, pp. 1633-1638.

Teychenné, D. C., Franklin, R. E. and Erntroy, H. C. (1975). Design of Normal Concrete Mixes. HMSO, London.

Thomas, M. D. A., Matthews, J. D. and Haynes, C. A. (1990). Chloride Diffusion and Reinforcement Corrosion in Marine Exposure Concretes Containing Pulverised-Fuel Ash. Int. Conf. Corrosion of Reinforcement in Concrete. Ed. Page et al, Elsevier Applied Science, London, pp. 198-212.

Thomas, M. D. A. (1991). Marine Performance of PFA Concrete. Magazine of Concrete Research, Vol.43, No.156, pp. 171-185.

Thomas, M. D. A. (1996). Chloride Thresholds in Marine Concrete. Cement and Concrete Research, Vol.26, No.4, pp. 513-519.

Tongnon, G. P. and Cangiano, S. (1980). Interface Phenomena and Durability of Concrete. 6th Int. Congress on the Chem. of Cement. Paris, Vol. 111, pp. VII133-VII138.

Tumidajski, P. J. (1996). Electrical Conductivity of Portland Cement Mortars. Cement and Concrete Research, Vol.26, No.4, pp. 529-534.

Turriziani, R. (1964). In The Chemistry of Cements, Vol.2, pp. 69-86. Ed Taylor, H. F. W. Academic Press (London).

Tuutti, K. (1980). Service-Life of Structures with regard to Corrosion of Embedded Steel. ACI Publication, SP-65-13, pp. 223-236.

Tuutti, K. (1982). Corrosion of Steel in Concrete. Swedish Cement and Concrete Research Inst., Stockholm. Research Report F04, pp. 289-292.

Uchikawa, H., Uchida, S. and Ogawa, K. (1986). Influence of Character of Blending Component on the Diffusion of Na and Cl ions in Hardened Blended Cement Paste. 8th Int. Congress on the Chemistry of Cement. Rio de Janeiro, 22-27 Sept., Vol.IV, pp. 251-256.

Ushiyama, H. and Goto, S. (1974). Diffusion of Various Ions in Hardened Portland Cement Paste. 6th Int. Congress on the Chemistry of Cement, Moscow, Vol.II-1, pp. 331-337.

Verbeck, G. J. (1975). Mechanisms of Corrosion of Steel in Concrete. ACI publication, SP-49-3.

Vogel, A. I. (1961). A Text Book of Quantitative Inorganic Analysis. 3rd edition, Longman.

Wallbank, E. J. (1989). The Performance of Concrete in Bridges. A Survey of 200 Highway Bridges. HMSO April.

Wallevik, O. H. and Gjørv, O. E. (1990). Modification of the Two-Point Workability Apparatus. Magazine of Concrete Research, 42, No.152, Sept. pp. 135-142.

Walters, G. V. and Jones, T. R. (1991). Effect of Metakaolin on Alkali-Silica Reaction in Concrete Manufactured with Reactive Aggregate. CANMET ACI SP-126. 2nd Int. Conf. on "Durability of Concrete". Montreal, Canada 1991.

Whittington, H. W., McCarter, J. and Forde, M. C. (1981). The Conductivity of Electricity Through Concrete. Magazine of Concrete Research, Vol.33, No.114.

Wild, S., Khatib, J. M. and Jones, A. (1996). Relative Strength, Pozzolanic Activity and Cement Hydration in Superplasticised Metakaolin Concrete. Cement and Concrete Research, Vol.26, No.10, pp. 1537-1544.

Wild, S. and Khatib, J. M. (1997). Portlandite Consumption in Metakaolin Cement Pastes and Mortars. Cement and Concrete Research, Vol.27, No.1, pp. 137-146.

Winslow, D. N. and Diamond, S. (1970). A Mercury Porosimetry Study of the Evolution of Porosity in Portland Cement. Journal of Materials, Vol.5, No.3, pp. 564-585.

Winslow, D., Cohen, M., Bentz, D., Snyder, K. A. and Garboczi, E. J. (1994). Percolation and Pore Structure in Mortars and Concrete. Cement and Concrete Research, Vol.24, pp. 25-37.

Winslow, D. and Liu, D. (1990). The Pore Structure of Paste in Concrete. Cement and Concrete Research, Vol.20, pp. 227-235.

Wu, X. and Roy, D. M. (1984). Slag Cement Utilization: Rheological Properties and Related Characterization. Cement and Concrete Research, Vol.14, pp. 521-528.

Young, E. (1988). A Review of the Pore Structure of Cement Paste and Concrete and its Influence on Permeability. Am. Conc. Inst. Proc.

Young, J. F. (1967). Humidity Control in the Laboratory using Salt Solutions- A Review. J. Appl. Chem., Vol.17, Sept.

Yu, S. W. and Page, C. L. (1991). Diffusion in Cementitious Materials: Comparative Study of Chloride and Oxygen Diffusion in Hydrated Cement Pastes. Cement and Concrete Research, Vol.21, pp. 581-589.

Zhang, J. Z. and Buenfeld, N. R. (1994). Development of the Accelerated Chloride Ion Diffusion (ACID) Test. Int. Conf. on Corrosion and Corrosion Protection of Steel in Concrete. Univ. Sheffield, 24-28 July, Sheffield Academic Press, pp. 395-419.

Zhang, M. H. and Malhotra, V. M. (1995). Characteristics of a Thermally Activated Alumino-Silicate Pozzolanic Material and its use in Concrete. Cement and Concrete Research, Vol.25, No.8, pp. 1713-1725.

Zheng, L. and Winslow, D. (1995). Sub-Distributions of Pore Size: A New Approach to Correlate Pore Structure with Permeability. Cement and Concrete Research, Vol.25, No.4, pp. 769-778.

Zimbelmann, R. (1978). The Problem of Increasing the Strength of Concrete. Betonwerk + Fertigteil - Technik, Heft 2, pp. 89-96.

PAGINATION ERROR IN

ORIGINAL THESIS

APPENDIX A

IDENTIFICATION OF PHASES FOR D.T.A.

COMPOUND	TEMPERATURE* (°C)
CSH Gel Ettringite Friedel's Salt Calcium Hydroxide Calcium Carbonate (Sergi 1986)	120-130 130-160 320 515-590 750-800
Gehlenite Hydrate (C_2ASH_8) Tetrcalcium Aluminate Hydrate (C_4AH_{13}) (Silva and Glasser 1990)	180-200 260-300
Hydrogarnet (C_3AH_6) (BRE Digest 392)	320-350

*All temperature changes are endothermic.

Table A.1 Characteristic temperature changes for cement paste compounds.

APPENDIX B

B.1 PREPARATION PROCEDURE FOR MK PASTES

In order to evaluate the effect of preparation procedure on the properties of the sample a quick method of assessing mass transport was needed without having to resort to long term steady state diffusion experiments. Resistivity measurements were adopted as being quick and sufficiently accurate, as well as giving an indication of transport properties. Bulk density measurements were used to highlight any variations between specimens, due to inaccurate batching or segregation.

Mixing was carried out either by hand or mechanically, using an Hobart planetary motion mixer. Type N superplasticizer (1% by wt. binder) was also used in some mixes to improve dispersion. Several preparation methods were evaluated, and the procedures are detailed below.

a) OPC and MK powders preblended dry by hand using a steel blade. Water then added and paste hand mixed for 5 minutes using the steel blade.

b) OPC and MK powders preblended dry in the Hobart mechanical mixer. Water then added and paste mixed for a further 7 minutes.

c) OPC and MK powders preblended dry by hand using a steel blade. Water and superplasticizer preblended then added to the powder and the paste hand mixed for 5 minutes using the steel blade.

d) MK, water and superplasticizer preblended by hand using a steel blade, to form a MK slurry. OPC gradually added and paste hand mixed for 5 minutes using the steel blade.

e) OPC and MK powders preblended dry in the Hobart mixer. Water and superplasticizer preblended then added to the powder and the paste mixed for 7 minutes.

f) MK, water and superplasticizer preblended for two minutes in the Hobart mixer to form a MK slurry. OPC gradually added and paste mixed for a further 7 minutes.

The preparation procedures were intended to establish whether mixing, and in particular dispersion of the metakaolin, was the cause of variation within specimens and establish a procedure to enable consistent samples to be manufactured. All mixes contained 20% MK, and were cured for 28 days under 35mM NaOH at 22°C.

B.2 RESULTS

Series	Water:Binder Ratio	Resistivity (kohm.cm)	Bulk Density (g/cm^3)
(a)	0.4	12.02	1.975
Hand mixed	0.4	12.38	1.974
	0.4	6.58	1.966
	0.5	4.19	1.856
	0.5	2.86	1.857
	0.5	3.27	1.866
	0.6	3.32	1.747
	0.6	3.55	1.740
	0.6	3.96	1.750
(c)	0.4	19.65	1.985
Hand mixed	0.4	17.17	1.986
OPC & MK preblended dry	0.4	15.39	1.983
Superplasticizer added with	0.5	27.37	1.874
water	0.5	21.47	1.853
	0.5	22.56	1.860
	0.6	32.23	1.700
	0.6	18.83	1.691
	0.6	15.10	1.702
(d)	0.4	14.92	1.979
Hand mixed	0.4	14.80	1.967
MK, water &	0.4	14.31	1.962
superplastcizer preblended	0.5	16.92	1.865
to form a slurry	0.5	19.50	1.858
	0.5	18.27	1.852
	0.6	9.95	1.715
	0.6	9.40	1.720
	0.6	9.48	1.717

Table B.1 Resistivity and bulk density measurements for hand mixed 20% MK pastes.

Series	Water:Binder Ratio	Resistivity (kohm.cm)	Bulk Density (g/cm^3)
(b)	0.4	19.07	1.993
Mechanically mixed	0.4	17.22	1.983
	0.4	18.28	1.984
	0.5	14.17	1.876
	0.5	15.03	1.871
	0.5	15.98	1.876
	0.6	10.68	1.747
	0.6	10.92	1.744
	0.6	10.18	1.746
(e)	0.4	22.55	1.963
Mechanically mixed	0.4	21.97	1.949
OPC & MK preblended dry	0.4	22.14	1.957
Superplasticizer added with	0.5	19.36	1.852
water	0.5	18.58	1.855
	0.5	19.21	1.860
	0.6	15.74	1.733
	0.6	16.25	1.725
	0.6	16.65	1.727
(f)	0.5	19.86	1.863
Mechanically mixed	0.5	19.83	1.856
MK, water &	0.5	19.05	1.855
superplastcizer preblended			
to form a slurry			

Table B.2 Resistivity and bulk density measurements for mechanically mixed 20% MK pastes.

B3 DISCUSSION

For a given water:binder ratio the bulk densities were consistent irrespective of preparation technique. Since disks were taken from the top middle and bottom regions of a sample compaction and segregation do not appear to be a problem.

The mechanically mixed pastes (series b) gave higher resistivities than hand mixed pastes (series a). This suggests that there is a dispersion problem with the latter which results in lower hydration and hence the lower resistivity. High resistivity values are indicative of a low porosity, and hence provide an indication of the extent of the pozzolanic reaction and hence dispersion. Unplasticized pastes (series a and b) yielded significantly lower resistivities than their plasticized counterparts, indicating that the superplasticizer is promoting dispersion of the MK, and thus greater hydration. The least variation between samples within a batch was for series d.

APPENDIX C

SOLUTION TO FICK'S 1ST LAW OF DIFFUSION

For one-dimensional, Steady-state diffusion the simple linear law known as Fick's first law is applicable, and can be used to evaluate effective chloride diffusivities through hardened cement paste (Crank 1975).

$$J = -D\frac{dC}{dx} \qquad \text{Eqn. C.1}$$

where,

J = Flux or diffusion current density - the amount of material diffusing in a unit time per unit area perpendicular to the x-axis.

D = Diffusion Coefficient.

C = Volume Concentration.

x = Distance along direction of diffusion.

Under steady-state conditions, the above equation can be integrated to:

$$J = -D\frac{C_2 - C_1}{\Delta x} \qquad \text{Eqn. C.2}$$

where C_1 and C_2 are concentrations at the ends of the diffusional length Δx.

For a thin disc of thickness L we have:

$$J = \frac{D}{L}(C_1 - C_2) \qquad \text{Eqn. C.3}$$

For a diffusion cell the flux of ions entering the low concentration compartment is given by:

$$J = \frac{V}{A}\frac{dC_2}{dt} \qquad \text{Eqn. C.4}$$

Combining equations 3 and 4 gives

$$\frac{D}{L}(C_1 - C_2) = \frac{V}{A}\frac{dC_2}{dt} \qquad \text{Eqn. C.5}$$

Assuming the concentration in the "high" compartment (C_1)remains constant,

$$\int_{C_2=k}^{C_2=C_2} -d\frac{(C_1 - C_2)}{(C_1 - C_2)} = \frac{DA}{VL}\int_{t=t_0}^{t=t} dt \qquad \text{Eqn. C.6}$$

$$(-\ln(C_1 - C_2))_k^{C2} = \frac{DA}{VL}(t - t_o) \qquad \text{Eqn. C.7}$$

$$In(\frac{C_1 - k}{C_1 - C_2}) = \frac{DA}{VL}(t - t_o) \qquad \text{Eqn. C.8}$$

$$\ln(1 + \frac{C_2 - k}{C_1 - C_2}) = \frac{DA}{VL}(t - t_o) \qquad \text{Eqn. C.9}$$

For $t > t_O$, $C_2 - k << C_1 - C_2$

i.e. $C_2 << \frac{C_1 + k}{2}$

and:

$$\frac{C_2 - k}{C_1 - C_2} = \frac{DA}{VL}(t - t_o) \qquad \text{Eqn. C.10}$$

if $S = \frac{C_2 - k}{t - t_o}$

thenEqn. C.10 simplifies to $D = \frac{SVL}{A(C_1 - C_2)}$ Eqn. C.11

By plotting a graph of C_2 against t the slope of the graph given by S can be calculated and D, effective chloride diffusivity evaluated.

Worked Example of Calculation of Effective Chloride Diffusion Coefficient

Listed below in Table C.1 are results for the increase in chloride ion concentration in compartment 2 of a diffusion cell for 20% MK w/b 0.65.

Diffusion Time (secs)x10^6	Absorption	Corrected Absorption	Chloride Conc. (mmol/l)
0.59	0.155	0.066	3.74
1.02	0.226	0.137	7.85
1.55	0.305	0.226	13.00
1.80	0.360	0.290	16.71
2.16	0.396	0.330	19.03
2.33	0.410	0.339	19.55
2.49	0.449	0.378	21.81
2.75	0.472	0.396	22.85
3.01	0.518	0.453	26.16
3.36	0.662	0.520	30.04
3.62	0.625	0.545	31.49
4.05	0.673	0.598	34.56

Table C.1 Chloride ion concentration results for 20% MK w/b 0.65 paste.

Figure C.1 show a plot of chloride build up in compartment 2 with time.

Slope (S) = 8.95x10^{-12}mol/cm^3/s

Volume of solution in compartment 2 (V) =84.06 ml
Thickness of Disc (L) =0.2667 cm
Cross-sectional area of disc (A) =8.81 cm^2
Conc. of chloride ions in compartment 1 = 1x10^{-3} mol/cm^3

From $$D = \frac{SVL}{AC_1} = \frac{8.95\times10^{-12}\times84.06\times0.2667}{8.81\times1\times10^{-3}}$$

D = 2.28x$10^{-8}$$cm^2$/s

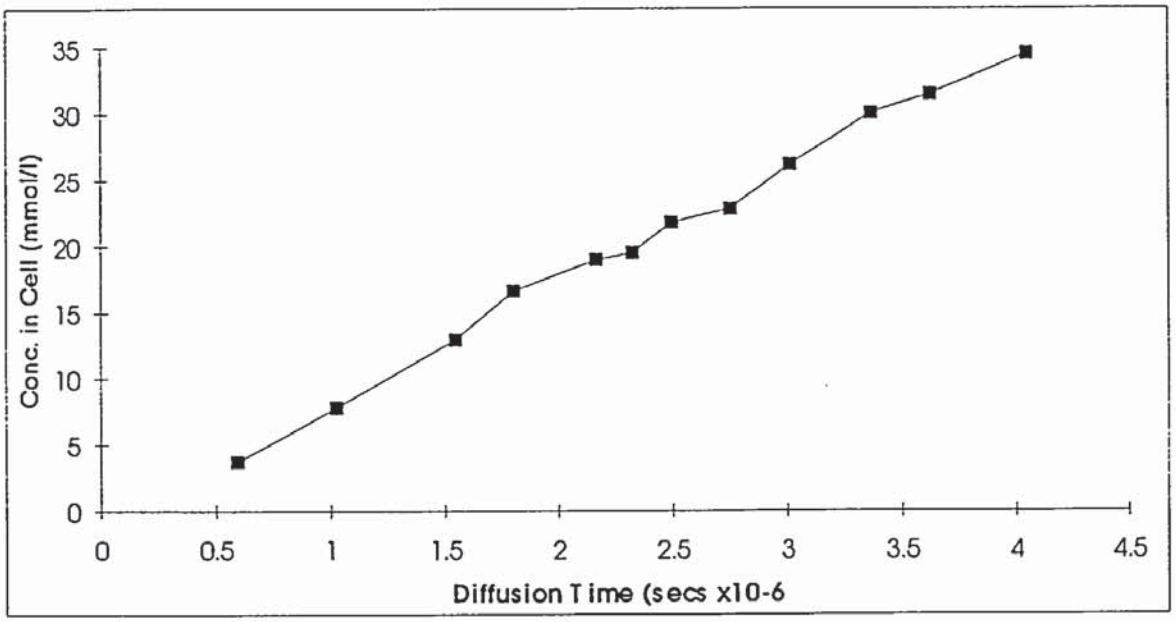

Figure C.1 Increase with time of chloride ion concentration in compartment 2 of ionic diffusion cell, for 20% MK w/b 0.65.

APPENDIX D

CALCULATION OF OXYGEN DIFFUSION COEFFICIENT

Table D.1 shows the experiemntal data for the diffusion of dissolved oxygen through a 10% MK hardened cement paste disc of water/binder ratio 0.65.

The data is plotted in Figure D.1 as cumulative charge passed against time, the slope providing a measure of the steady-sate flux passing through the disc.

Test	Polarization Time tp (sec)	End Current I_e (μA)	Charge Passed Q (C)	Time Interval t_i (Days)	Q/t_i (C/Day)	Total Diffusion Time t_d (Days)	Cumulative Charge Passed Q_t (C)
1	9200	21.6	0.699	3.06	0.229	3.06	0.699
2	9200	19.1	0.407	1.94	0.210	5.00	1.106
3	8000	19.0	0.460	2.23	0.206	7.23	1.567
4	8000	16.4	0.629	2.91	0.216	10.14	2.195
5	8000	12.9	0.376	2.02	0.186	12.16	2.572
6	9000	10.2	0.426	1.91	0.223	14.07	2.998
7	9000	10.8	0.560	3.02	0.185	17.09	3.558
8	8000	9.9	0.490	2.00	0.246	19.09	4.048
9	9000	10.6	0.401	1.93	0.208	21.02	4.450

Table D.1 Oxygen diffusion data for 10% MK hardened cement paste, water/binder ratio 0.65.

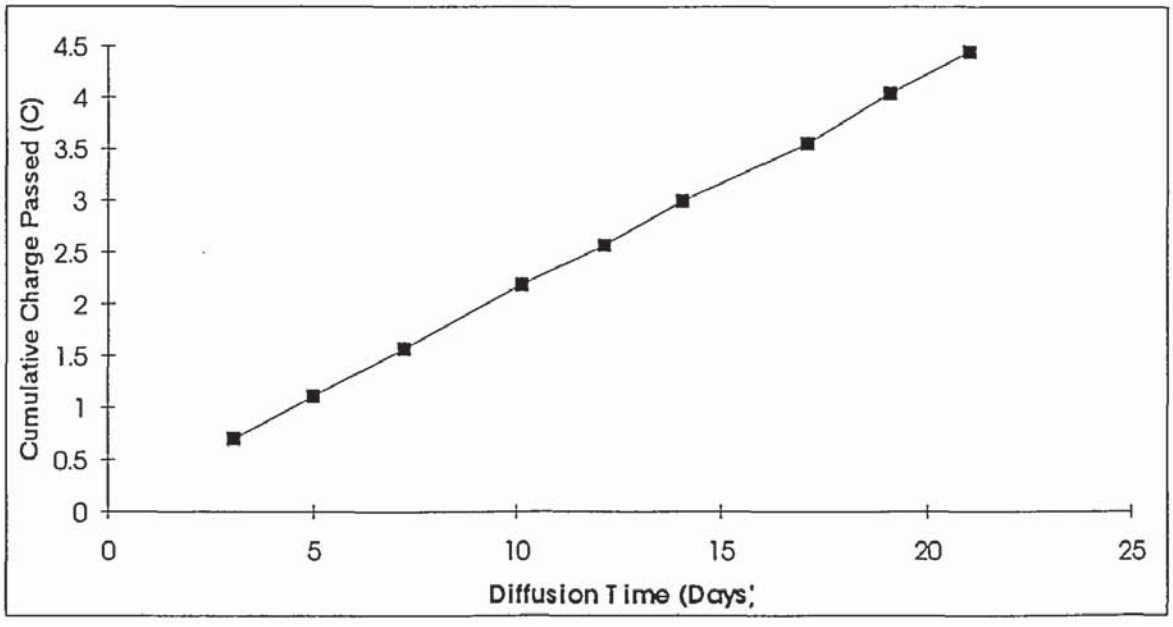

Figure D.1 Plot of cumulative charge against total diffusion time.

Gradient $\frac{Q}{t_d}$=0.208 C/Day (r^2 0.9996)

This is equivalent to 2.403×10^{-6} C/sec

Sample thickness: 0.273 cm

Faraday (F): 96484C

Diffusion area: 9.759 cm^2

From equation 5.8 derived in chapter 5 oxygen diffusivity can be calculated.

$$\text{Oxygen Diffusion Coefficient (Doxy)} = \frac{l \times \frac{Q}{t_d}}{4FAC_o} = \frac{0.273 \times 2.403 \times 10^{-6}}{4 \times 96.48 \times 10^3 \times 9.759 \times 1.23 \times 10^{-6}}$$

Where C_o is the solubility of oxygen in water at 25°C: 1.23×10^{-3} mol/l

Doxy=1.416×10^{-7} cm^2/s

APPENDIX E

CHLORIDE CONCENTRATION PROFILES FOR NON-STEADY STATE DIFFUSION INTO CONCRETE

The dotted line is the profile from experimental data. The solid line is calculated from Fick's second law of diffusion using the apparent diffusion coefficient calculated from experimental data.

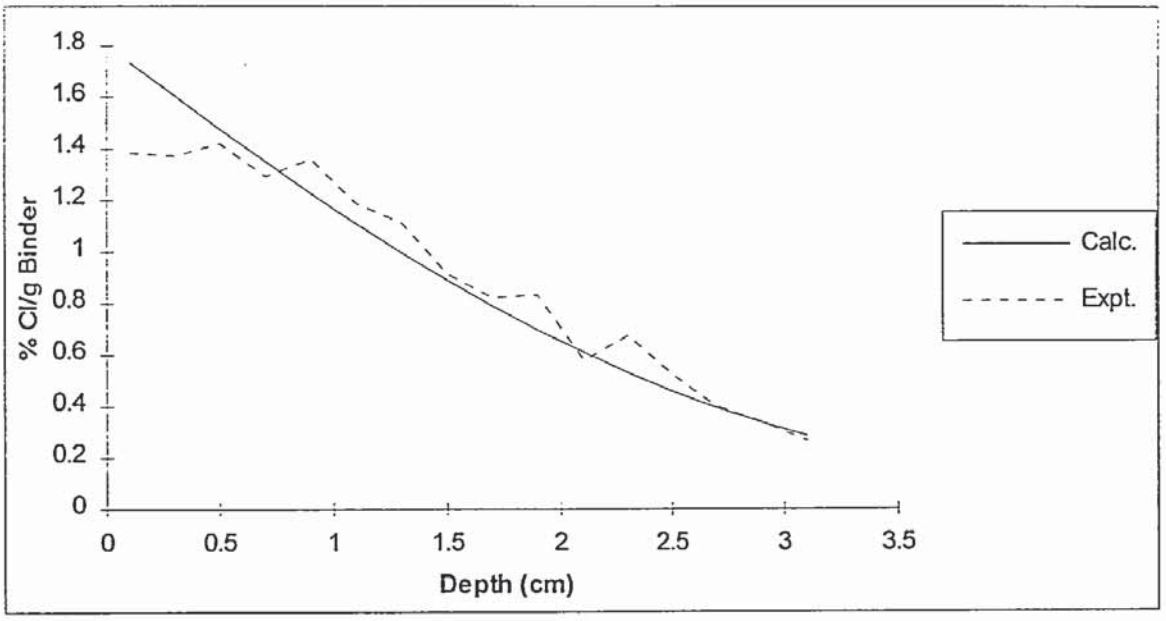

Figure E.1 Chloride concentration profile for OPC concrete

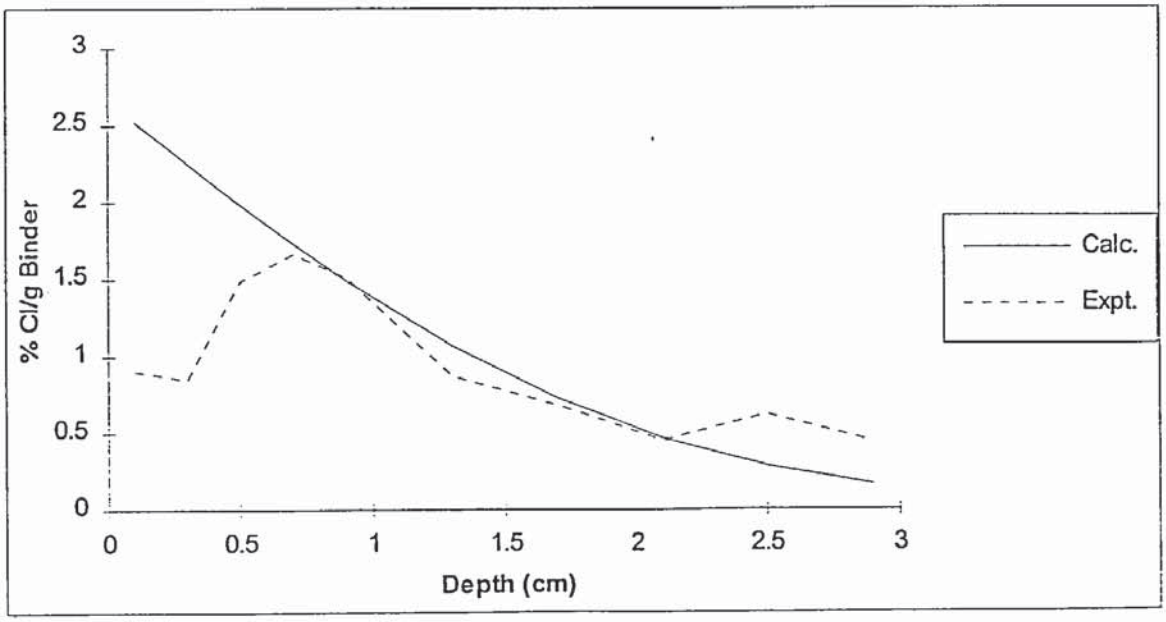

Figure E.2 Chloride concentration profile for 10%MK/60%BFS concrete

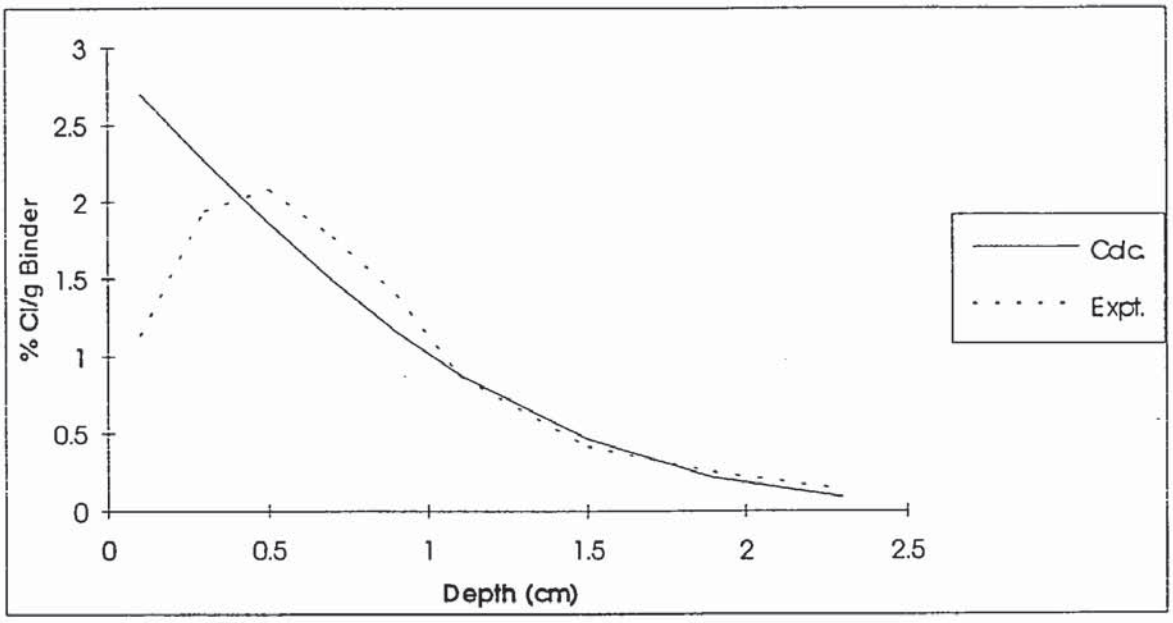

Figure E.3 Chloride concentration profile for 20%PFA/10%MK concrete

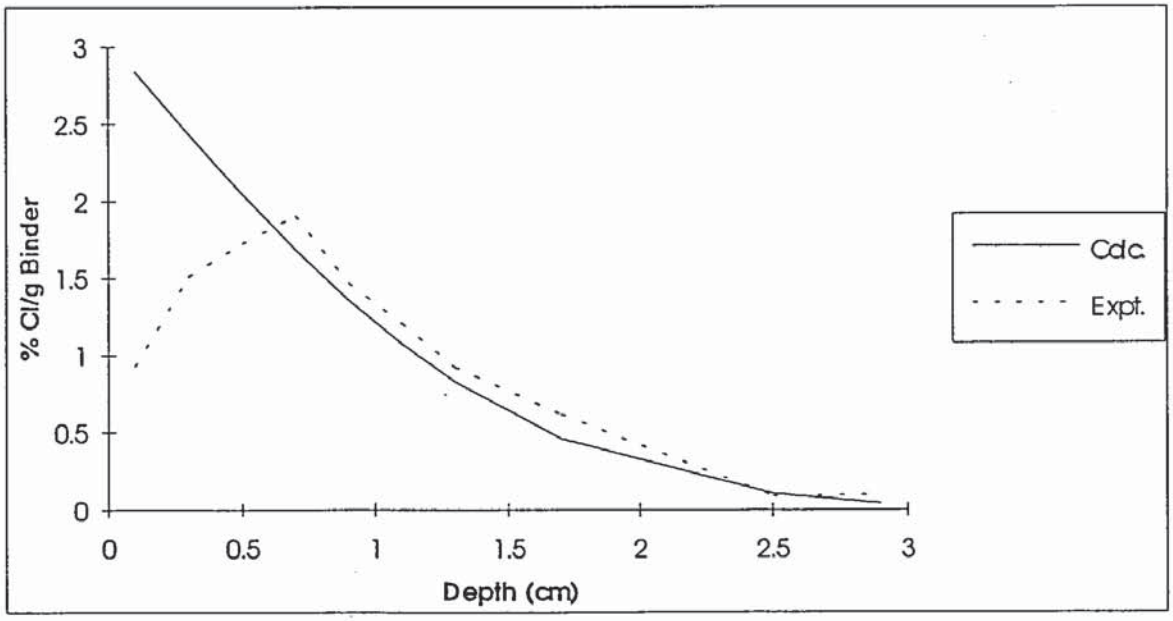

Figure E.4 Chloride concentration profile for 25% PFA concrete

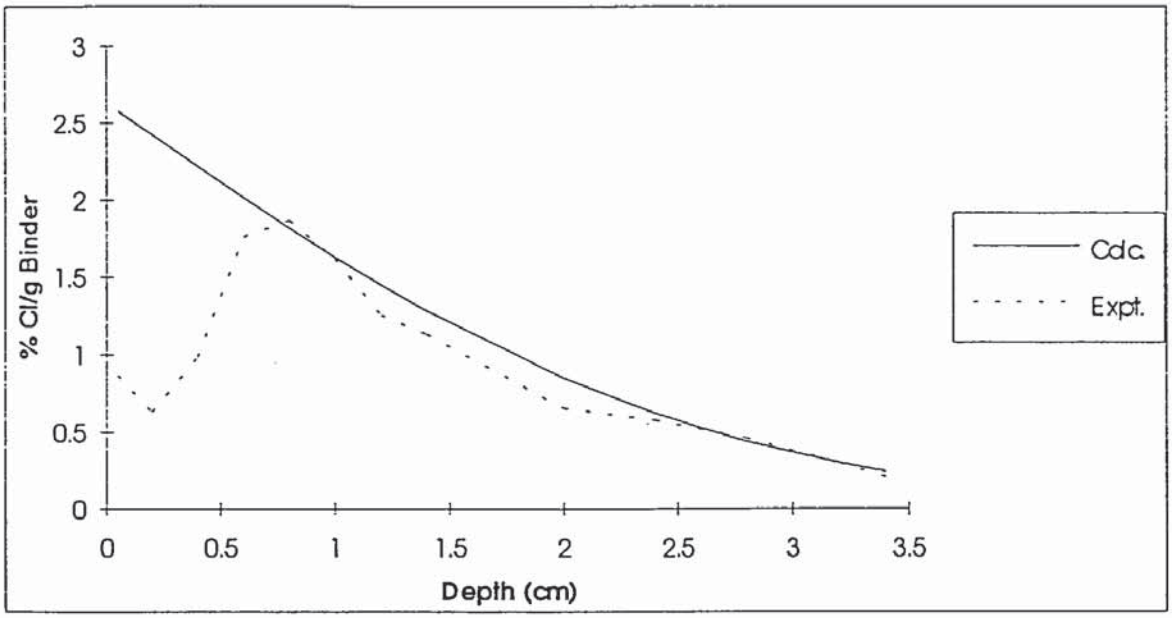

Figure E.5 Chloride concentration profile for 70% BFS concrete

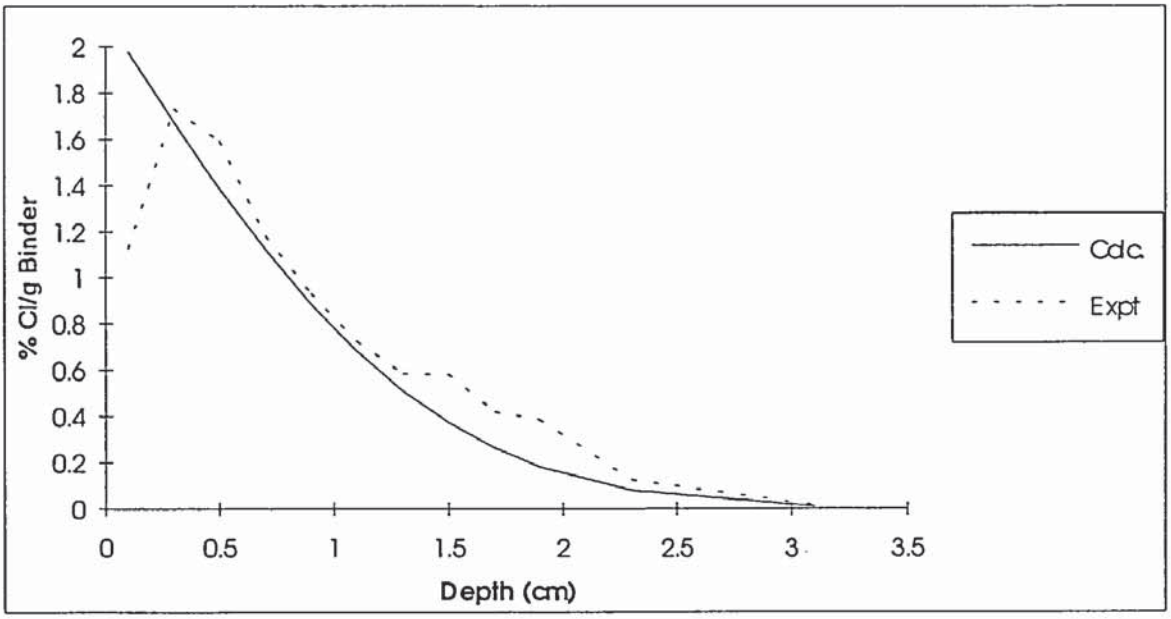

Figure E.6 Chloride concentration profile for 10% MK concrete

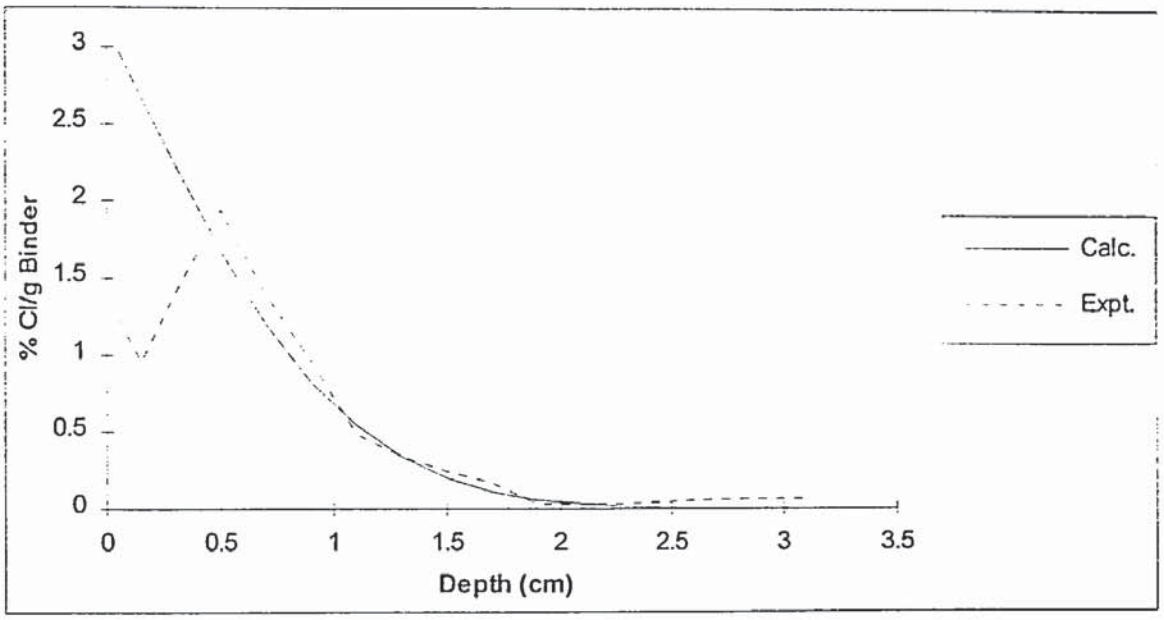

Figure E.7 Chloride concentration profile for 20% MK concrete

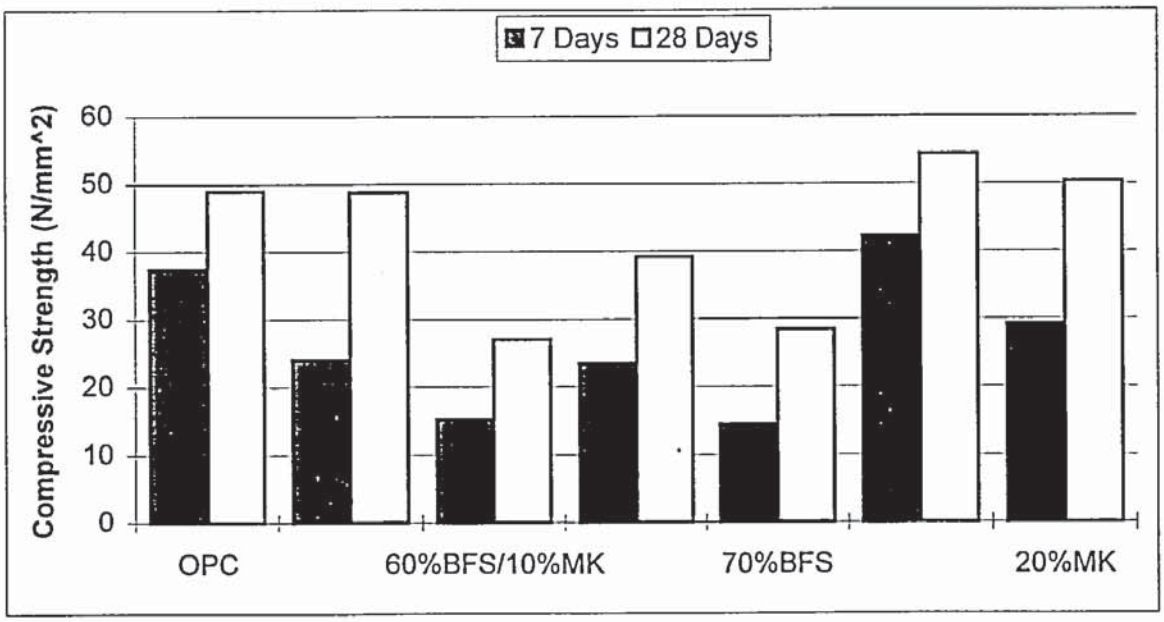

Figure E.8 Compressive strengths at 7 and 28 days for non-steady state diffusion mixes

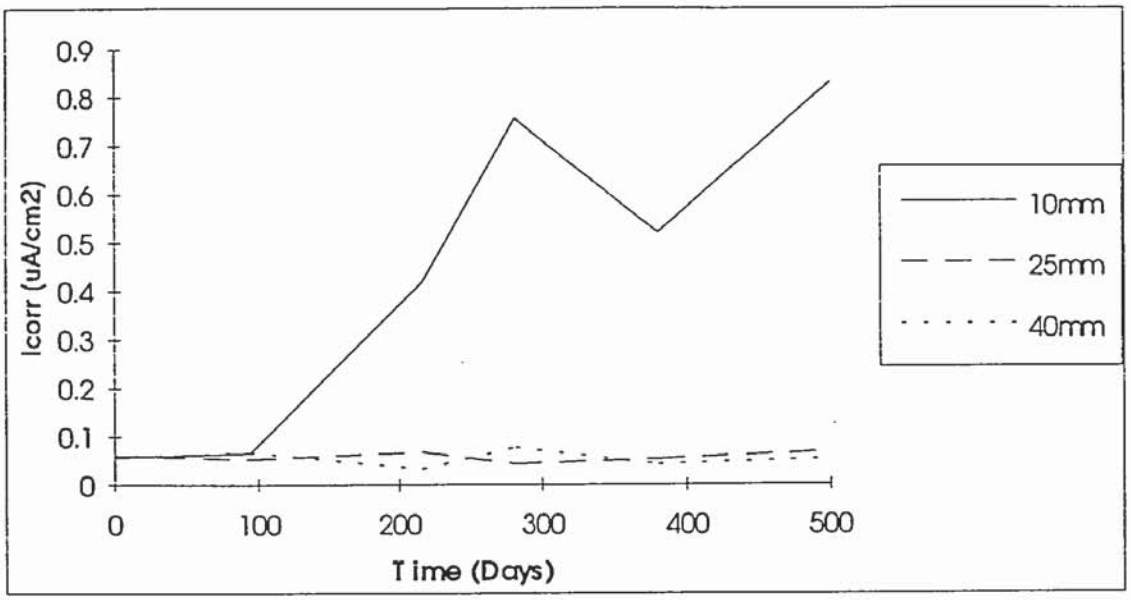

Figure E.9 Corrosion rate against time for steel bars embedded in 10% MK concrete.

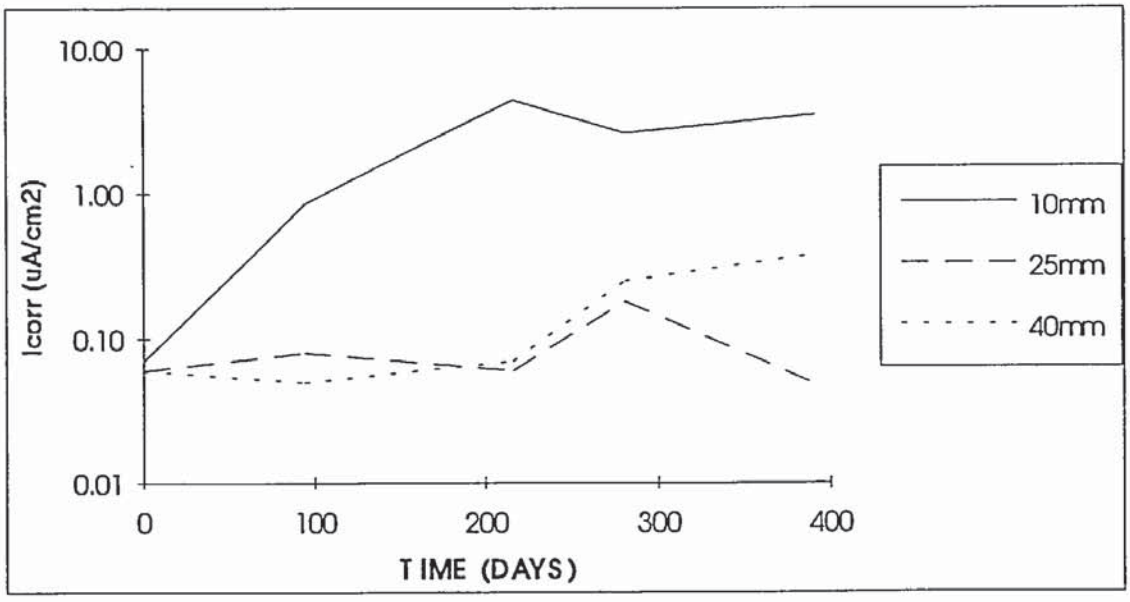

Figure E.10 Corrosion rate against time for steel bars embedded in 20% MK concrete.

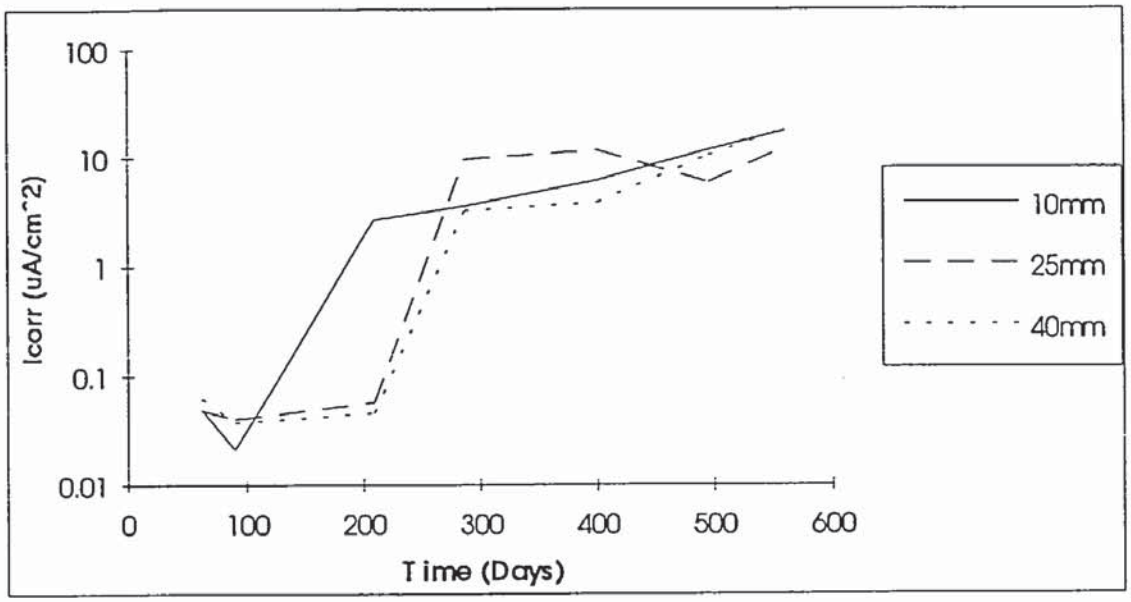

Figure E.11 Corrosion rate against time for steel bars embedded in OPC concrete.

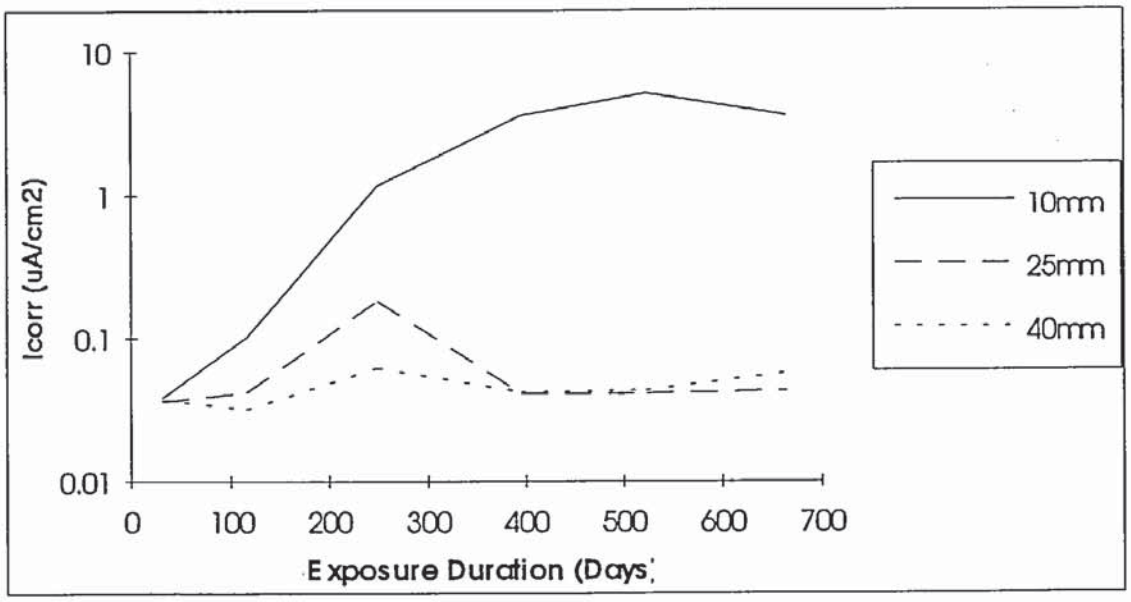

Figure E.12 Corrosion rate against time for steel bars embedded in 6%MK/45%BFS concrete.

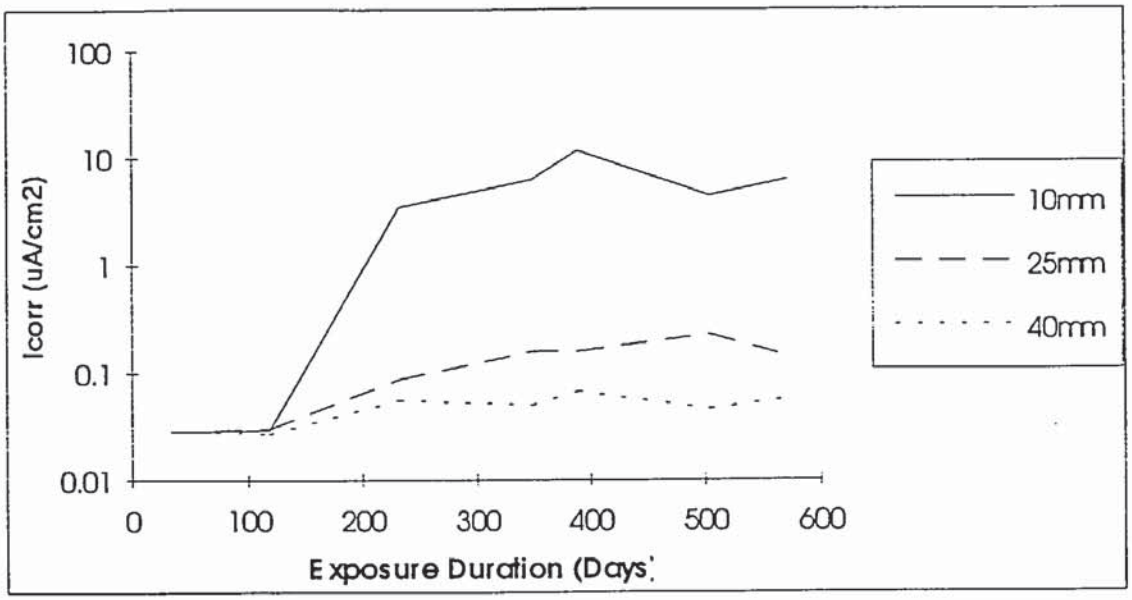

Figure E.13 Corrosion rate against time for steel bars embedded in 6%MK/15%PFA concrete.

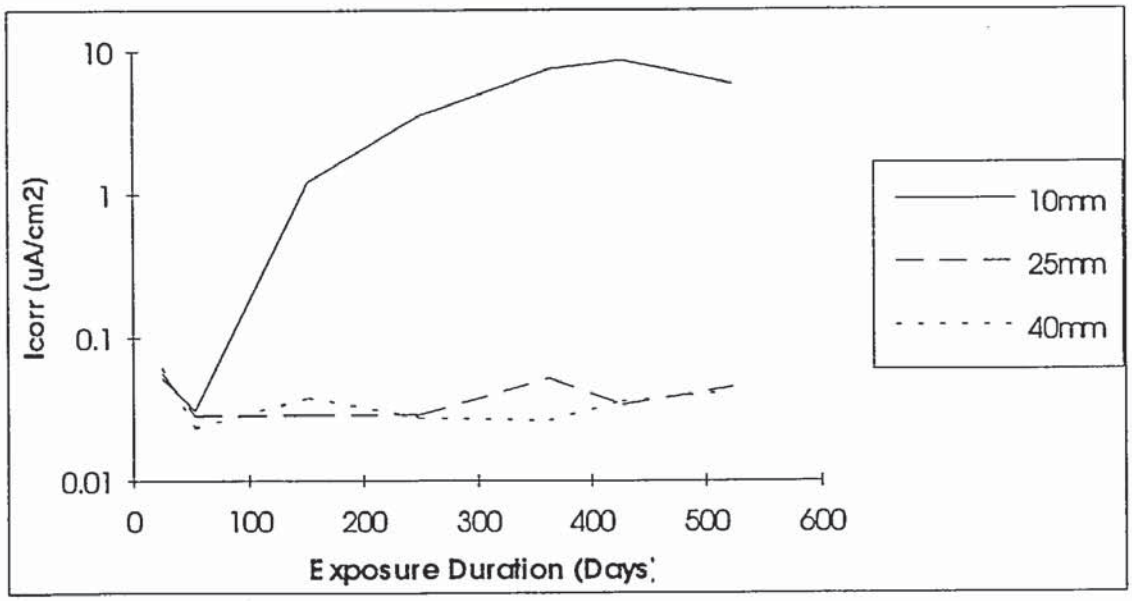

Figure E.14 Corrosion rate against time for steel bars embedded in 50% BFS concrete.

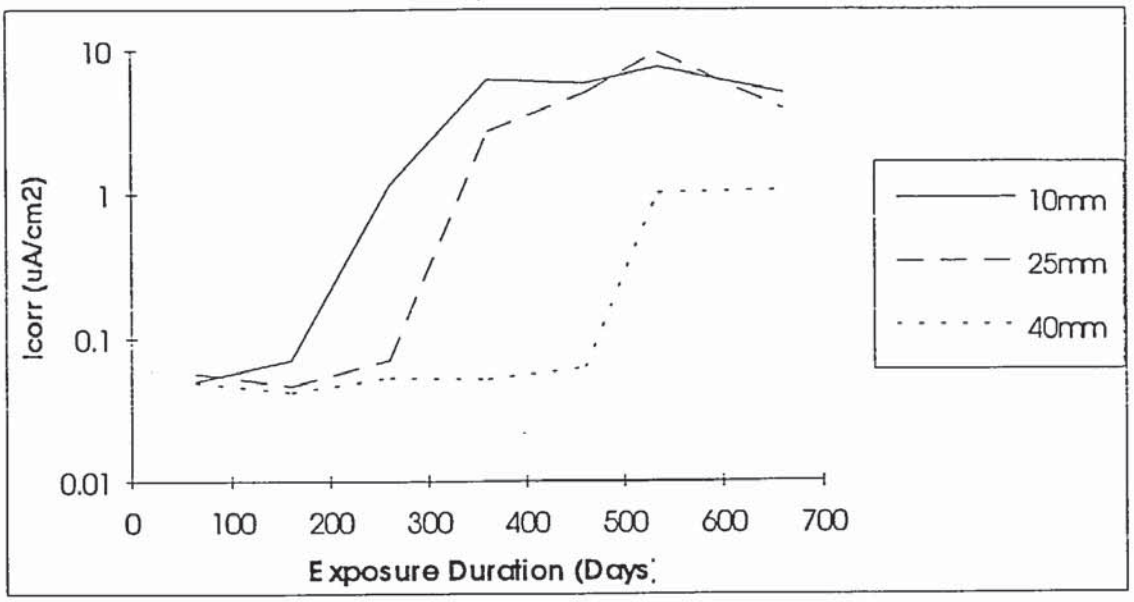

Figure E.15 Corrosion rate against time for steel bars embedded in 6% MK concrete.

APPENDIX F

EXAMPLE CALCULATION OF APPARENT DIFFUSION COEFFICIENT FROM A SOLUTION OF FICK'S SECOND LAW OF DIFFUSION

Solution to Fick's second law given by (Crank 1975)

$$\frac{C_s}{C_x} = 1 - erf\frac{x}{2\sqrt{Dt}} \qquad \text{Eqn. F.1}$$

$$erf(\frac{x}{2\sqrt{Dt}}) = \frac{c_s - c_x}{c_s} \qquad \text{Eqn. F.2}$$

$$\frac{x}{2\sqrt{Dt}} = erf^{-1}(\frac{c_s - c_x}{c_s}) \qquad \text{Eqn. F.3}$$

Let $y = erf^{-1}(\frac{c_s - c_x}{c_s})$ gives

$$y = \frac{x}{2\sqrt{Dt}} \qquad \text{Eqn. F.4}$$

Rearranging gives $D = \frac{1}{4t}(\frac{x}{y})^2$ Eqn. F.5

Shown below is a worked example of the calculation of apparent diffusion coefficient for 20% MK concrete

Figure F.1 shows the chloride concentration profile. Extrapolation of the graph back to the y-axis yields the surface concentration C_S.

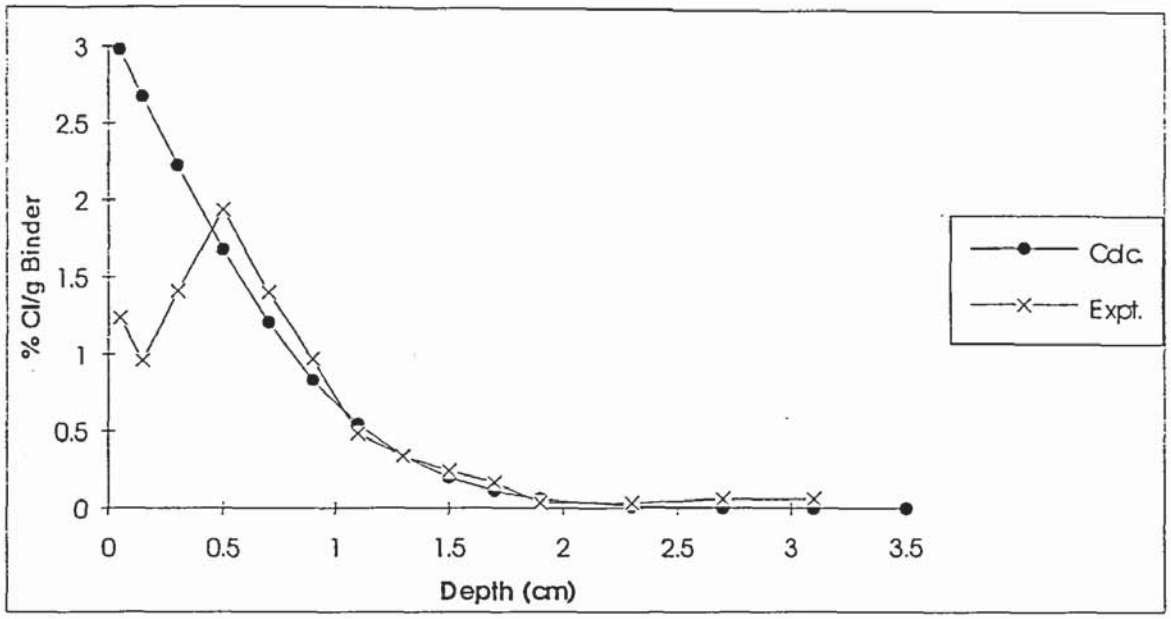

Figure F.1 Chloride concentration profile for 20% MK concrete.

Depth x (cm)	C_x	$\frac{c_s - c_x}{c_s}$	y	$(\frac{x}{y})^2$	$Dx10^{-9}$ cm^2/s
0.05	1.239	0.686	0.71	0.00496	
0.15	0.960	0.539	0.52	0.0832	
0.3	1.411	0.366	0.34	0.779	6.26
0.5	1.939	0.542	0.53	0.890	7.15
0.7	1.401	0.683	0.71	0.972	7.81
0.9	0.970	0.842	1.00	0.81	6.51
1.1	0.483	0.890	1.13	1.947	7.62
1.3	0.336	0.921	1.24	1.099	8.83
1.5	0.243	0.945	1.36	1.216	9.78
1.7	0.167	0.989	1.61	1.112	8.94

Table F.1 Calculation of apparent diffusion coefficient for 20% MK concrete for $t=31x10^6$ seconds.

Average apparent diffuion coefficient= $7.89x10^{-9}$, and standard deviation $1.24x10^{-9}$ 95% confidence limits mean ± 2 x standard deviation which gives

$D=5.39\text{-}10.3 \times 10^{-9}$ cm^2/s